LATVIJAS UNIVERSITĀTES RAKSTI

745. SĒJUMS

Bioloģija

ACTA UNIVERSITATIS LATVIENSIS

VOLUME 745

Biology

ACTA UNIVERSITATIS LATVIENSIS

VOLUME 745

Biology

UNIVERSITY OF LATVIA

LATVIJAS UNIVERSITĀTES RAKSTI

745. SĒJUMS

Bioloģija

LATVIJAS UNIVERSITĀTE

UDK 57(082)
Bi 664

Visi krājumā ievietotie zinātniskie raksti ir recenzēti
Pārpublicēšanas gadījumā nepieciešama Latvijas Universitātes atļauja
Citējot atsauce uz izdevumu obligāta

All the scientific papers published in the present volume have been rewieved

ISSN 1407-2157
ISBN 978-9984-45-049-0

Contents

Acta Universitatis Latviensis, 2008, Vol. 745, Biology, pp. 7–15

Subcellular localization of Hepatitis B virus core protein expressed from two different constructs in the Semliki Forest virus expression system

Sabine Braun[1,2], Ruta Bruvere[3], Anna Zajakina[3]*, Ekaterina Alekseeva[3], Tatyana Kozlovska[3]

[1]Institut für Virologie, Charité, Humboldt-Universität, Universitätsklinikum Charité, Schumannstraße 20/21, 10117 Berlin, Germany
[2]Present address: Klinikum Augsburg, Institut für Laboratoriums-medizin, Mikrobiologie und Umwelthygiene, Stenglinstraße 2, 86156 Augsburg, Germany
[3]Department of Protein Engineering, Latvian Biomedical Research and Study Centre, Ratsupites 1, Riga LV-1067, Latvia

*Corresponding author, E-mail: anna@biomed.lu.lv

Abstract

The subcellular localization of Hepatitis B virus (HBV) core protein in eukaryotic cells was studied by an immunocytochemical method following expression of the HBV core (HBc) gene in the Semliki Forest virus expression system from two different constructs. HBc protein showed cytoplasmic and nuclear localization when it was expressed from a construct that encoded the HBV pregenome, whereas HBc protein that was expressed from a construct encoding the HBc gene alone was found only in the cytoplasm. The possible reasons for this phenomenon are discussed.

Key words: HBV core protein, HBV pregenome, Hepatitis B virus, Semliki Forest virus, subcellular localization.

Introduction

Hepatitis B virus (HBV) core (HBc) protein is the structural material of viral capsids. HBV viral particles consist of an enveloped capsid that contains a 3.2 kb partially double stranded DNA genome and the viral polymerase. The viral relaxed circular DNA is completed to covalently closed circular DNA, which serves as the template for the transcription of the viral RNAs: pregenomic RNA (pgRNA) and three subgenomic RNAs that serve as mRNAs for the viral proteins; pgRNA also serves as a template for reverse transcription. Viral polymerase and pgRNA are packaged into nucleocapsids followed by synthesis of a DNA minus strand, which is converted into the rcDNA genome (reviewed in Seeger, Mason 2000).

HBc protein is composed of two domains, an amino-terminal self-assembly domain (amino acid residues 1 to 150) and a carboxy-terminal protamine-like arginine-rich domain, which contains a nuclear localization signal (Eckhardt et al. 1991). Three serine residues in the C terminal domain overlapping the nuclear localization signal may be phosphorylated and play a role in both regulation of HBV replication (Melegari et al.

2005) and in nuclear localization (Liao, Ou 1995), as only phosphorylated HBc protein binds to the nuclear pore complex (Kann et al. 1999).

In previous research the subcellular localization of internally deleted HBc gene variants was studied (Bruvere et al. 2004). These variants were isolated from renal transplant recipients, where their presence was associated with a severe course of illness leading to end stage liver disease (Guenther et al. 1996; Preikschat et al. 2002; Guenther et al. 2000). Variant HBc protein was localized in the cytoplasm and to a lower extent also in the nucleus of the infected cells. Wild type HBc protein however showed a strictly cytoplasmic localization when synthesized from a plasmid that encoded the HBc gene alone. Surprisingly, wild type protein was found in both nucleus and cytoplasm when expressed in the context of the HBV pregenome.

The strictly nuclear localization of wild type HBc protein could be a consequence of its assembly into stable core particles whereas unassembled HBc protein is transported to the host cell's nucleus. The present study further investigates the reasons for the nuclear and cytoplasmic localization of wild type HBc protein that is expressed in the context of the HBV pregenome.

Materials and methods

Plasmid construction

A wild type Hepatitis B virus core gene of genotype A was amplified by PCR using the following primers: 5'-GCGGATCCATGGACATTGACCCTTATA-3' and 5'-CGCC CGGGTAAAGTTTCCCACCTTATG-3' and ligated into restriction sites *Sma*I and *Bam*HI of vector pSFV1 (Liljestroem, Garoff 1991). A Hepatitis B virus pregenome (gene bank accession number: NCBI: 329640) of genotype D was cloned into the *Sma*I site of pSFVdelStNruI (pSFV1/pg) after PCR amplification with primers 3'-CCGGA AAGCTT GAGCTCTTC TTTTTCACCTCTGCCTAATCA-5', and 5'-CCGGA AAGCTT GAGCTCTTC AAAAAGTTGCATGGTGCTGG-3', restriction with *Hind*III and reconstruction of blunt ends by T4 polymerase.

Cell cultures, RNA transcription, generation of recombinant virus and cell infection

Cell cultures, RNA transcription, generation of recombinant virus and cell infection were performed as described previously (Zajakina et al. 2004).

Immunocytochemical detection of intracellular Hepatitis B virus core protein by monoclonal antibodies

Immunocytochemical detection of intracellular Hepatitis B virus core protein by monoclonal antibodies was performed as described in Zajakina et al. (2004). Anti-HBc monoclonal antibody 10C-6 (epitope aa 134 to 140; Bichko et al. 1993) was used at a dilution of 1 : 200 (in PBS + 0.25 % Triton X-100 + 0.25 % BSA).

Cell lysis

Cell monolayers were lysed in buffer containing 1 % Nonidet P-40 (NP-40), 50 mM Tris-HCl pH 7.6, 150 mM NaCl, 2 mM EDTA, 1 μg mL^{-1} PMSF. After 10 min on ice cell nuclei were removed by centrifugation. Supernatants were used for the isolation of DNA.

Isolation of DNA

DNase I was added to cell lysates at a final concentration of 200 μg mL^{-1} and $MgCl_2$ at a final concentration of 20 mM and incubated at 37 °C for 30 min. DNase was subsequently inactivated by adding EDTA at a final concentration of 50 mM.

To disintegrate capsids, proteinase K (final concentration 1 mg mL^{-1}) and SDS (final concentration 2 %) were added and incubation was performed for 2 h at 37 °C. The suspension was cleared from proteins by adding an equal volume of phenol; after centrifugation DNA was precipitated in the supernatant by adding an equal volume of isopropanol and NaCl to a final concentration of 0.3 M. Precipitation was performed at –20 °C overnight. After centrifugation at 11 000 rpm at 4 °C the pellets were washed in 75 % ethanol, dried and resuspended in water.

Southern blot

The samples were run on a 1 % agarose gel and transferred overnight to a nylon membrane (Boehringer) by capillary blot. After transfer the DNA was immobilized on the membrane by exposing it to ultra violet light for 3 min in a transilluminator.

Detection

The immobilized DNA was hybridised with a Dig labelled probe (random primed with pregenome of genotype A as a template, Roche) overnight at 58 °C. The DIG luminescent detection kit (Roche) and CDP (Tropix) were used for the detection as described by the manufacturers. The blot was developed by exposition to X-ray film.

Analysis of intracellular RNA

The *in vitro* transcribed RNA was transfected into BHK cells by lipofection with Oligofectamine (Invitrogen) according to the manufacturer's instruction. At 24-h post-transfection the total cellular RNA was isolated from cells by TRIzol RNA isolation method (Sigma). Then RNA samples were separated in denaturing conditions on a 1.2 % agarose gel containing 0.65 % formaldehyde and transferred to a positively charged Nylon membrane (Boehringer) by capillary transfer. A digoxigenin-labelled probe (random primed, Roche) directed against the HBV genome, genotype A, was used to detect specific RNAs. For detection the membrane was incubated with anti-digoxigenin alkaline phosphatase (Roche). The CDP – chemiluminescence substrate (Tropix) was used to develop the signal that was detected by a CCD camera.

Results and discussion

The subcellular localization of HBV core protein (HBc) was analyzed by an immunocytochemical method following infection of mammalian cells. Intracellular localization of wild type HBc protein expressed from a construct that encoded the HBc gene alone was compared to the localization of HBc protein expressed from a construct that encoded the entire HBV pregenome. To this purpose a wild type (wt) HBc gene of genotype A was cloned into the Semliki forest virus (SFV) derived expression vector pSFV1 (Liljestroem, Garoff 1991); a complete HBV pregenome of genotype D (HBVpg) was cloned into vector pSFV1delStNruI. Baby hamster kidney cells (BHK-21) were transfected with recombinant RNA, which was transcribed *in vitro* from the SP6 promoter or alternatively, infected

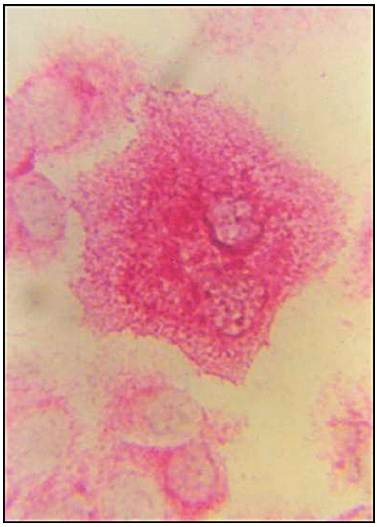

Fig. 1. Immunocytochemical analysis of HBc protein in BHK-21 cells. Cells were infected with recombinant pSFV1/HBVpg particles expressing the HBV pregenome. HBc protein (red staining) was detected by monoclonal antibody 10c/6 in both cytoplasm and nucleus of the cells (magnification × 270).

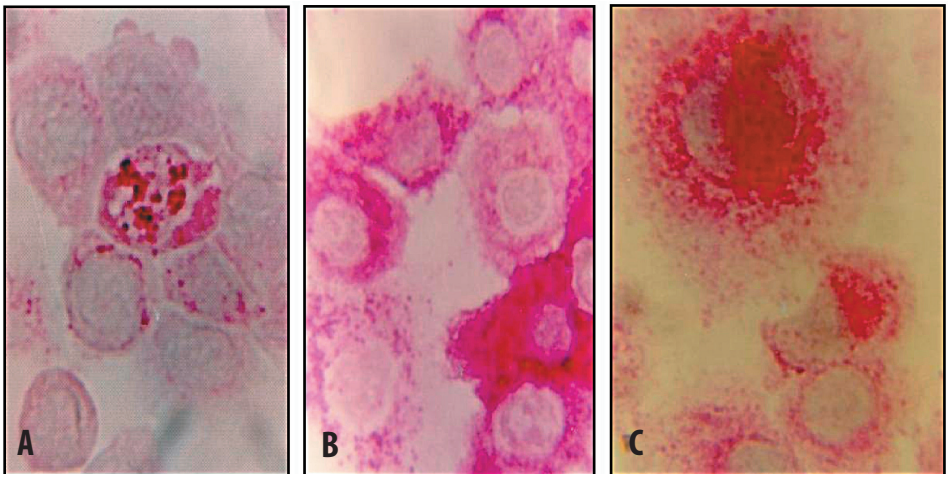

Fig. 2. Intracellular localization of HBc protein in BHK-21 cells. Cells were infected with recombinant SFV particles expressing different HBc genes. HBc protein was detected by immunostaining after reaction with monoclonal antibody 10c/6 (magnification × 108). A, the picture shows HBc protein expressed by HBc variant deleted from aminoacids 86 to 93 (described in Bruvere et al., 2004) in both nucleus and cytoplasm of the cells. B, HBc protein that is expressed from construct pSFV1/wt core is purely cytoplasmic. C, HBc protein that is expressed from construct pSFV1/HBVpg is found in both cytoplasm and nucleus of the cells.

with recombinant SFV viral particles (recSFV), which were generated by packaging the recombinant RNA replicons into the SFV capsid. In both cases the expression of HBc genes is subject to transcriptional regulation by the SFV subgenomic promoter. Synthesis of HBc protein was monitored by light microscopy with an immunocytochemical method after reaction of HBc antigen with a monoclonal antibody whose epitope comprises aminoacids 134 to 140. As the percentage of cells that stained positive increased during the first 24 h post infection and in most cases reached a maximum at this time, HBc synthesis was detected. For both constructs the numbers of cells that stained positive reached values of up to 80 % (but generally above 60 %). Cytoplasmic staining was strong in both cases. However, a striking difference regarding the presence of HBc protein in the nucleus was observed. No HBc protein was found in the nucleus when the HBc gene of the construct that encoded the HBc gene alone was expressed (Fig. 2B). A small amount of HBc protein was detected in the nucleus of BHK cells when the HBc gene was expressed from the construct that encoded the HBV pregenome (Fig. 1, Fig. 2C). The same expression pattern – cytoplasmic and nuclear staining – had been observed for internally deleted HBc proteins (Bruvere et al. 2004; Fig. 2A). We supposed that this staining pattern was explained by the stability of the core particles.

HBc protein contains a nuclear localization signal in the carboxy-terminus. In phosphorylated form core particles bind to the nuclear pore complex (Kann et al. 1999), probably by inducing a conformational change through which the otherwise hidden nuclear localization signal becomes exposed. Phosphorylation is thought to act as a maturation

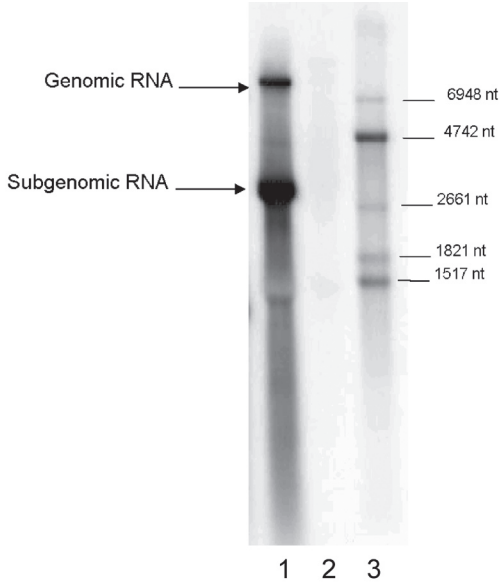

Fig. 3. Analysis of HBV transcripts. Total RNA was isolated from the cells lipofected with *in vitro* transcribed recombinant SFV/HBVpg RNA. The RNA was separated by agarose gel electrophoresis in denaturing conditions and blotted on a nylon membrane where specific RNA was visualized by a CCD camera after reaction with a DIG labeled probe directed against the HBV genome. Lane 1: isolation of RNA from BHK cells transfected with the HBV pregenome as described above, lane 2: negative control (uninfected cells), lane 3: RNA marker.

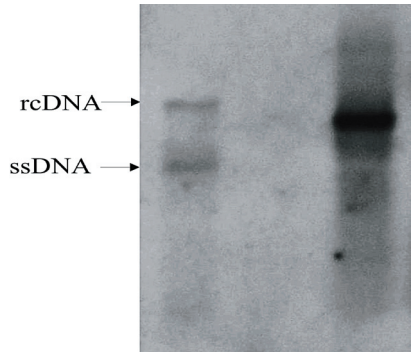

Fig. 4. Analysis of HBV replicative intermediates. BHK-21 cells were infected with recombinant pSFV1/HBVpg particles of the HBV pregenome. Total DNA was isolated from the cells, separated by agarose gel electrophoresis, and blotted on a nylon membrane where specific DNA was visualized after reaction with a DIG labeled probe directed against the HBV genome. DNA isolated from infected BHK cells shows two HBV specific bands, the upper band corresponds to relaxed circular DNA, the lower band is ssDNA. Lane 1: DNA isolated from cells infected with pSFV1/HBVpg, lane 2: negative control (DNA isolated from uninfected cells), lane 3: PCR fragment of HBV pregenome.

signal when RNA is degraded during reverse transcription of the HBV genome (Kann et al. 1997; Kann et al. 1999). Loss of nucleic acid binding renders the core particles less stable (Birnbaum, Nassal 1990). In the transgenic mouse model intact core particles do not pass the nuclear membrane (Guidotti et al. 1994) and disintegration of capsids is thought to be a prerequisite for HBc transport into the host cell's nucleus. This view has been challenged by recent research. It was found that the diameter of the nuclear pore is wider (Pante, Kann 2002) than originally thought (Dworetzki, Feldherr 1988), such that HBV capsids could pass it in intact form (Rabe et al. 2003). In any case, some kind of rearrangement of the capsids occurs as C-terminal sequences of HBc protein that contain the nuclear localization signal become exposed upon phosphorylation (Rabe et al. 2003).

We suppose that a replication cycle is initiated by the transfected pregenome and that HBc protein is imported concomitantly to the nucleus of BHK cells. Experimental evidence are two HBV specific DNA species that were detected at low frequency (Fig. 4) upon infection of BHK cells with viral particles expressing the HBV pregenome. It has been reported previously that the expression of the pregenome is enough to drive HBV replication in an alpha-viral system for duck HBV expression in Sindbis virus (Huang, Summers 1991). Also, a model of HBV replication in an alphaviral system has been proposed (Huang, Summers 1991). In the alphaviral system the transfected or infected (+)-RNA is transcribed *in vivo* into (-)-RNA from which (+)-genomic RNA and subgenomic RNA are transcribed. These RNA species were detected by Northern blot (Fig. 3). In pSFV1/HBVpg the alphaviral structural genes in the region of the subgenomic RNA are replaced by the HBV pregenome sequence. From this RNA the HBV proteins are translated. Upon translation of the HBV polymerase protein, reverse transcription of the HBV pregenome into (-)-DNA occurs followed by usually incomplete synthesis of (+)-DNA. The appearance of two DNA species probably marks these first steps of the replication cycle (Fig. 4). The larger DNA species, which migrates slower than a PCR fragment of the HBV genome, might correspond to double-stranded relaxed circular DNA whereas the smaller fragment may constitute single-stranded DNA. Although a full

replication cycle of the HBV pregenome in the SFV system cannot be proven, as it was not possible to detect covalently closed circular HBV DNA, which may be due to the fact that this is an inefficient process, we suppose that DNA is transferred to the nucleus. We assume that concomitantly HBc protein is imported to the host cells's nucleus either by disintegration of the capsids or in assembled form. As a consequence, wild type HBc protein is detected in the nucleus when expressed in the context of the HBV pregenome.

In contrast to the nuclear and cytoplasmic subcellular distribution of HBc protein in BHK cells expressing the HBV pregenome, only cytoplasmic location of HBc protein was detected in cells that were infected with recSFV expressing the wild type HBc gene. It has been suggested that empty capsids in the nucleus are formed from HBc protein, which is over-expressed and transported to the nucleus in unassembled form or as assembly intermediates, that is, in a form in which the nuclear localization signal is not hidden (Kann et al. 2007). In the SFV system however, no HBc protein is imported to the nucleus, probably as it quickly assembles to stable core particles. Contrary to this, internally deleted HBc protein had shown in previous research a staining pattern in which both nuclear and cytoplasmic location occur (Bruvere et al. 2004). As the deletions mapped in a region which is mostly α-helical (Wynne et al. 1999) and where mutations are hardly tolerated (Koschel et al. 1999), even small deletions lead to a deformation and partial unfolding of the protein. Internally deleted HBc protein is therefore unstable and quickly degraded by the proteasomal pathway (Braun et al. 2007). Due to the unfolding the nuclear localization signal becomes exposed and variant HBc protein is imported to the nucleus.

In summary, it seems that an at least partial unfolding of the HBc protein and the subsequent exposition of the nuclear localization signal is a precondition for nuclear import. It occurs during the replication of the genome. At least in the SFV system it does not occur when wild type HBc protein is over expressed, probably as it assembles and the nuclear localization signal is hidden.

Furthermore a replicating HBV pregenome in the SFV system may serve – after optimization – as a useful tool for the study of HBV biology.

Acknowledgements

The work was supported by a grant from the Bundesministerium für Bildung, Wissenschaft, Forschung und Technologie (Verbundvorhaben, project 01KI9861/0 and by the Humboldt-Universität zu Berlin, by the VZP-8 project of the Latvian State Scientific Programme and by the European Regional Development Fund (ERDF). The work was partially supported also by the European Social Fund (ESF). The authors thank Arija Ose, Irena Timofejeva, Natalija Gabrusheva, and Heike Lerch for excellent technical assistance.

References

Bichko V., Schodel F., Nassal M., Gren E., Berzinsh I., Borisova G., Miska S., Peterson D.L., Gren E., Pushko P., Will H. 1993. Epitopes recognized by antibodies to denatured core protein of hepatitis B virus. *Mol. Immun*ol. 30: 221–231.

Birnbaum F., Nassal M. 1990. Hepatitis B virus nucleocapsid assembly: primary structure requirements in the core protein. *J. Virol.* 64: 3319–3330.

Braun S., Zajakina A., Aleksejeva J., Sharipo A., Bruvere R., Ose V., Pumpens P., Garoff H., Meisel H., Kozlovska T. 2007. Proteasomal degradation of core protein variants from chronic hepatitis B patients. *J. Med. Virol*. 79: 1312–1321.

Bruvere R., Braun S., Zajakina A., Alekseeva E., Sharipo A., Meisel H., Pumpens P., Kozlovska T. 2004. Subcellular localisation of internally deleted HBV core proteins. *Acta Univ. Latv.* 676: 53–64.

Dworetzky S.I., Feldherr C.M. 1988. Translocation of RNA-coated gold particles through the nuclear pores of oocytes. *J. Cell Biol.* 106: 575–584.

Eckhardt S.G., Milich D.R., McLachlan A. 1991. Hepatitis B virus core antigen has two nuclear localization sequences in the arginine-rich carboxyl terminus. *J. Virol.* 65: 575–582.

Günther S., Baginski S., Kissel H., Reinke P., Krüger D.H., Will H., Meisel H. 1996. Accumulation and persistence of Hepatitis B Virus core gene deletion mutants in renal transplant patients are associated with end-stage liver disease. *Hepatology* 24: 751–758.

Günther S., Piwon N., Jung A., Iwanska A., Schmitz H., Will H. 2000. Enhanced replication contributes to enrichment of Hepatitis B virus with a deletion in the core gene. *Virology* 273: 286–299.

Guidotti L.G., Martinez V., Loh Y.T., Rogler C.E., Chisari F.V. 1994. Hepatitis B virus nucleocapsid particles do not cross the hepatocyte nuclear membrane in transgenic mice. *J. Virol.* 68: 5469–5475.

Huang M., Summers J. 1991. Infection initiated by the RNA pregenome of a DNA virus. *J. Virol.* 65: 5435–5439.

Kann M., Bischof A., Gerlich W.H. 1997. In vitro model for the nuclear transport of the hepadnavirus genome. *J. Virol.* 71: 1310–1316.

Kann M., Sodeik B., Vlachou A., Gerlich W.H., Helenius A. 1999. Phosphorylation-dependant binding of Hepatitis B virus core particles to the nuclear pore complex. *J. Cell Biol.* 145: 45–55.

Kann M., Schmitz A., Rabe B. 2007. Intracellular transport of hepatitis B virus. *World J. Gastroenterol.* 13: 39–47.

Koschel M., Thomssen R., Bruss V. 1999. Expensive mutagenesis of the Hepatitis B virus core gene and mapping of mutations that allow capsid formation. *J. Virol.* 73: 2153–2160.

Liao W., Ou J.H. 1995. Phosphorylation and nuclear localization of the Hepatitis B virus core protein: significance of serine in the three repeated SPRRR motifs. *J. Virol.* 69: 1025–1029.

Liljeström P., Garoff H. 1991. A new generation of animal cell expression vectors based on the Semliki Forest virus replicon. *Biotechnology*. 9: 1356–1361.

Melegari M., Wolf S.K., Schneider R.J. 2005. Hepatitis B virus replication is coordinated by core protein serine phosphorylation and HBx expression. *J. Virol.* 79: 9810–9820.

Pante N., Kann M. 2002. Nuclear Pore Complex is able to transport macromolecules with diameters of ~ 39 nm. *Mol. Biol. Cell* 13: 425–434.

Preikschat P., Guenther S., Reinhold S., Will H., Budde K., Neumayer H.H. et al. 2002. Complex HBV populations with mutations in core promoter, C gene, and pre-S region are associated with development of cirrhosis in long-term renal transplant recipients. *Hepatology* 35: 466-477.

Rabe B., Vlachou A., Pante N., Helenius A., Kann M. 2003. Nuclear import of hepatitis B virus capsids and release of the viral genome. *Proc. Natl. Acad. Sci. USA* 100: 9849–9854.

Seeger C., Mason W.S. 2002. Hepatitis B virus biology. *Microbiol. Mol. Biol. Rev*. 64: 51–68.

Wynne S.A., Crowther R.A., Leslie A.G.W. 1999. The crystal structure of the human Hepatitis B Virus capsid. *Mol. Cell* 3: 771–780.

Zajakina A., Kozlovska T., Bruvere R., Aleksejeva J., Pumpens P., Garoff H. 2004. Translation of hepatitis B virus (HBV) surface proteins from the HBV pregenome and precore RNAs in Semliki Forest virus-driven expression. *J. Gen. Virol*. 85: 3343–3351.

Semliki Meža vīrusa ekspresijas sistēmā ar diviem atšķirīgiem konstruktiem ekspresēta hepatīta B vīrusa serdes proteīna lokalizācija šūnā

Sabine Braun[1,2], Ruta Brūvere[3], Anna Zajakina[3]*, Jekaterina Aleksejeva[3], Tatjana Kozlovska[3]

[1]Institut für Virologie, Charité, Humboldt-Universität, Universitätsklinikum Charité, Schumannstraße 20/21, 10117 Berlin, Vācija
[2]Pašreizējā adrese: Klinikum Augsburg, Institut für Laboratoriums-medizin, Mikrobiologie und Umwelthygiene, Stenglinstraße 2, 86156 Augsburg, Vācija
[3]Proteīnu inženierijas nodaļa, Latvijas Biomedicīnas pētījumu and studiju centrs, Rātsupītes 1, Rīga LV-1067, Latvija

*Korespondējošais autors, E-pasts: anna@biomed.lu.lv

Kopsavilkums

Hepatīta B vīrusa (HBV) serdes proteīna lokalizāciju eikariotu šūnās pētīja ar imunocitoķīmijas metodi, izsekojot HBV serdes gēna (HBc) ekspresiju Semliki Meža vīrusa ekspresijas sistēmā ar divām atšķirīgām konstrukcijām. Izmantojot konstrukciju, kura kodēja HBV pregenomu, HBc proteīns bija lokalizēts citoplazmā un kodolā, kamēr, izmantojot konstrukciju, kura kodēja tikai pašu HBc gēnu, HBc proteīns bja atrodams tikai citoplazmā. Rakstā apspriesti šīs parādības iespējamie iemesli.

Acta Universitatis Latviensis, 2008, Vol. 745, Biology, pp. 17–23

Morphogenesis of wild orchid *Dactylorhiza fuchsii* in tissue culture

Gunta Jakobsone*

Tissue Culture Department, National Botanical Garden, Miera 1, Salaspils LV-2169 Latvia

*Corresponding author, E-mail: gunta.jakobsone@nbd.gov.lv

Abstract

Dactylorhiza fuchsii which is included in the Red Data Book of the Baltic Region and listed in Annex B of the EC Habitats Directive was chosen as a model to study the initial development stages of asymbiotic development in tissue culture. Half-mature seeds were removed from sterilized seed capsules and sown onto filter-paper bridges in culture tubes with initial liquid medium and kept in the dark at 23 °C. Germination started after two months of incubation. Protocorms formed were transplanted into fresh medium. Initiation of roots and tubers was observed after 3 to 6 months of germination. Plantlets with ~ 2 cm long shoots and well-developed roots were transferred into a light chamber. New plants of *D. fuchsii* with two leaves, tubers and roots appropriate for transplanting into soil were obtained in the next spring, e.g. about 8 to 9 months after the start of germination. The use of *in vitro* methods significantly reduced the relatively long period of time necessary for development of orchid plants in natural conditions.

Key words: asymbiotic development, *Dactylorhiza fuchsii,* morphogenesis, tissue culture.

Introduction

There are 33 species of wild terrestrial orchids growing in Latvia. All of these species are protected by the European Council Directive 92/43/EEC of May 21, 1992 *On the Conservation of Natural Habitats and of Wild Fauna and Flora* (Habitats Directive). In total 26 species of the family Orchidaceae are included in the Red Data Book of Latvia (2003). On them, one species is designated as extinct in the wild, five species as endangered, four species as vulnerable decreasing in number, seven species as rare, and nine species as commercially endangered. Both *in situ* and *ex situ* approaches are important for the protection of rare and endangered orchid species. Tissue culture collections are among the most important measures in *ex situ* conservation of terrestrial orchids (Jakobsone et al. 2007). Knowledge on physiological and morphological aspects of germination and development of particular orchid species is of critical importance for establishment of the collections.

Orchids have very small seeds completely lacking endosperm resembling spores of ferns. This makes it difficult to observe their further development after they are released from the seed capsule into the soil. Large seed production seems to be a common trait of plants that have a saprophytic-mycotrophic or parasitic seedling stage and therefore are extremely specific in requirements for the germination site (Rauh et al. 1975). Several

species of *Dactylorhiza* and *Orchis* can germinate in water and remain alive for some days or weeks without receiving any external nutrients (Rasmussen 1995). During the period after germination the seedlings can subsist on their own reserves while waiting for a compatible infection (Vermeulen 1947). However, the experiments of Knudson (1946) showed that asymbiotic germination of orchid seeds can be achieved using a medium with sugars as a source of reduced carbon and appropriate minerals.

The period of time necessary for development of individual plants before flowering of different terrestrial orchids is extremely long. On average period of a 12 years is necessary for development of *Cypripedium* species from seed germination until flowering (Curtis 1943; Kull 1999). The use of *in vitro* culture technique in orchid propagation allows to obtain flowering plants within 4 to 5 years of culture or even after 2 to 3 years (Stoutamire 1974; Rasmussen 1995).

Species of the genus *Dactylorhiza* Necker ex Nevski (Orchidaceae) are terrestrial orchids from the Northern Hemisphere. They grow on a wide range of relatively open habitats from dune slacks to alpine meadows (Pillon et al. 2006). *D. fuchsii* is found in both open woodland and a variety of grasslands (Cepurīte 2005). It is a relatively shade tolerant species (McKendrick 1996). *D. fuchsii* is included in Red Data Book of the Baltic Region and listed in the Annex B of the EC Habitats Directive. The aim of the present study was to follow the first development stages of *D. fuchsii* plants from germination until formation of new regenerant. The use of tissue culture methods allowed nondestructive monitoring of developmental processes of plantlets.

Materials and methods

Seed capsules for initialization of tissue culture of *Dactylorhiza fuchsii* (Druce) Soó were collected from naturally pollinated plants growing in the National Botanical Garden of Latvia, Salaspils in a semi-natural meadow. Seed capsules were surface sterilized by a rapid dip into 96 % ethanol with subsequent passing of the capsule through a flame. The capsules containing light brown incompletely developed seeds were used for experiments. Capsules were split with a sterilized scalpel and the seeds were sowed aseptically onto filter paper bridges in culture tubes (Ø 16 mm) and closed with foil. The liquid initial media were based on a modified formula of Knudson (1946) and ½ Murashige and Skoog (1962) medium with variation of different organic compounds without addition of growth regulators.

The obtained small protocorms were transplanted onto fresh new medium for further development. Subsequent transplantation procedures were performed according to growth rate and stage of development, usually after each 1 to 2 months. During the initial stages of development cultures were incubated in the dark at room temperature. Plantlets with ~ 2 cm long shoots and well-developed roots were transferred into a light chamber

Fig. 1. Morphogenesis of *Dactylorhiza fuchsii in vitro* in the dark at 23 °C. A, imbibed seeds; B, formation of protocorms with rhizoids (r); C - E, polarization and elongation of protocorms; F, sprouting (s); G, development of tuber at the basal part of the protocorm and shoot formation at the apical part; H - J, elongation of shoots and initiation of rooting (ro – root, tu – tuber); K, rooting; L, initiation of a new orchid plantlet (np) on the elongated tuber of the stock plant, branching of tuber (b); M, initiation of new orchid plantlet (np) on the tuber of the stock plant.

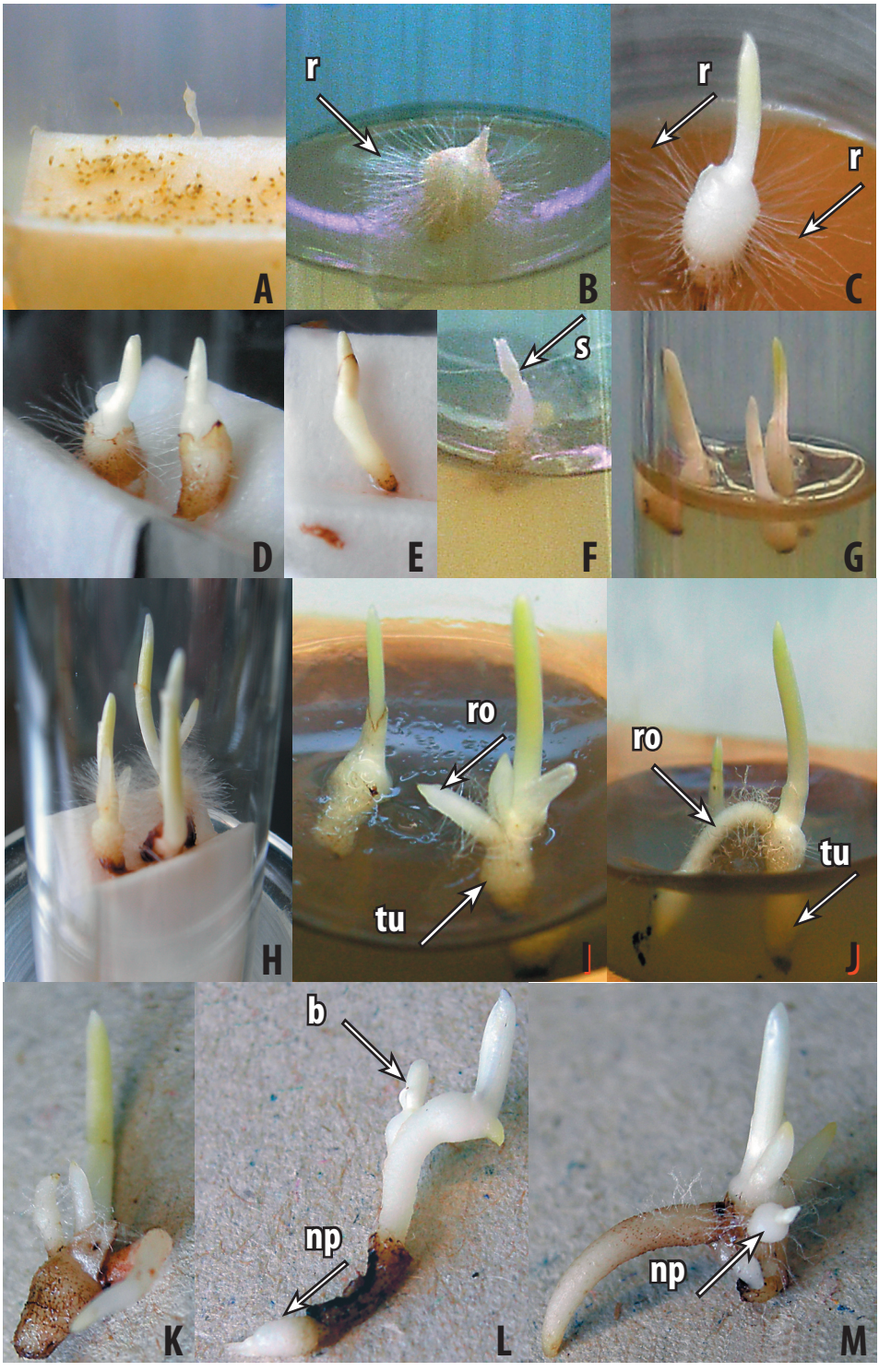
A
r
B
r
r
C
D
E
s
F
G
H
ro
tu
I
ro
tu
J
b
np
K
L
np
M

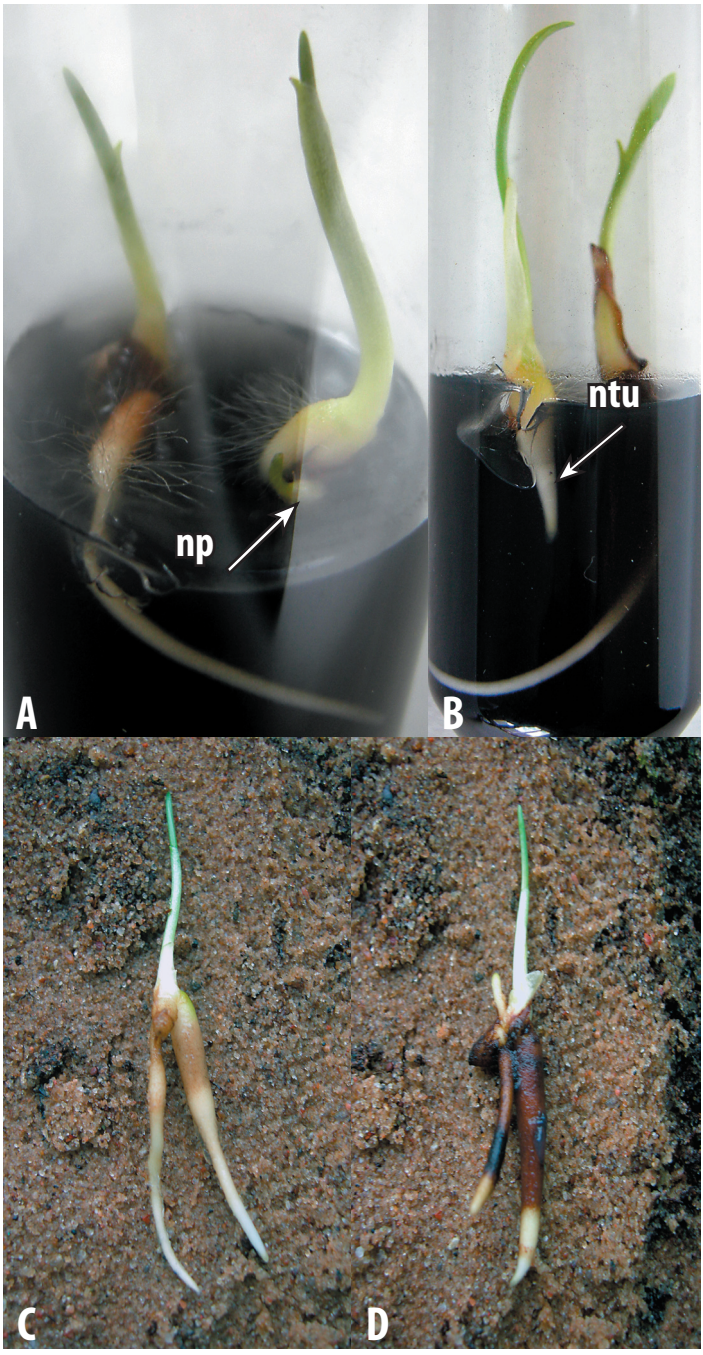

Fig. 2. Development of regenerants of *Dactylorhiza fuchsii* under light conditions. A, intensive growth of underground organs and initiation of secondary plantlets (np); B, unfolding of first leaves and start of development of true secondary tubers (ntu); C - D, obtained *in vitro* plants before transplanting in soil.

illuminated by white fluorescent lamps and a 16-h photoperiod. Photosynthetic photon flux density was 40 mmol m^{-2} s^{-1}. Temperature during incubation was 23 ± 2 °C. All stages of development were documented by photography.

Results and discussion

The development of most species of *Dactylorhiza* from germination to shoot and tuber formation is about four years (Rasmussen 1995). *D. fuchsii* belongs to a group of orchids with sympodial growth of attenuate root tubers (Tatarenko, Kondo 2003). In natural conditions a new shoot apex is formed in late autumn, remains in undifferentiated state for more than 18 months, and appears above ground during the 4th year after formation (Tatarenko, Kondo 2003). Thus, the estimated life span for underground shoots of *D. fuchsii* is more than 30 months, which is relatively long period. The present experiments confirmed that in conditions of tissue culture the whole development period of *D. fuchsii* from seed germination until formation of first leaves is about 8 months.

Seed germination started relatively slowly within 7 weeks of culture (Fig. 1 A). The seeds sown on August 19 started to germinate in October. The germination of ungerminated seeds continued for a prolonged period of time lasting more than 2.5 years. The first protocorms (about 1 mm in diameter) appeared in November. The presence of numerous rhizoids was evident (Fig. 1B). Rhizoid formation usually occurs in parallel with development of an apical bud. Polarization and subsequent elongation of protocorms started in December (Fig. 1 C - E).

Five initial stages during germination and protocorm development, universal for all terrestrial orchids, are described as follows (Dixon et al. 2003): ungerminated seed (stage 0); embryo (protocorm) ruptures testa (stage 1); protocorm appears to be larger than seed with production of rhizoids (stage 2); initial bud development on rapidly growing protocorm (stage 3); chlorophyllous leaf tissue or root initials produced (stage 4); protocorm enlargement with well developed leaf and initialization of dropper (stage 5). According to the other sources, six stages of orchid seedling development can be described (Kauth et al. 2006). Formation of leaves is related to stage 4, and is described morphologically as protocorm with developing leaves and rhizoids. In contrast to Dixon et al. (2003), in the present experiments with *D. fuchsii* the first well-developed leaf formed only on relatively highly-developed plantlets instead of protocorms (Fig. 2B). Polarization and elongation of protocorms was visible well before leaf formation (Fig. 1 E). The polarized protocorms further developed into sprouts and tubers (Fig. 1 F - G). In terrestrial orchids tubers represent dormancy survival structures that function as storage organs (Rasmussen 1995). Tubers are produced on a stalk often referred to as a dropper.

Initiation of rooting took place only after polarization and elongation of protocorm (Fig. 1 H) at the base of tubers (Fig. 1 I - K). Until this time the plantlets take up nutrient elements with the aid of rhizoids. *D. fuchsii* regenerants with only shoots and tubers did not initiate rooting in conditions of a light chamber. Consequently only the plantlets with relatively well-developed roots could be placed into the light chamber for further development. Initiation of tubers and roots were observed after 3 to 6 months from the start of germination.

Vegetative propagation was observed on *D. fuchsii* explants on medium without growth regulators in early stages of development by either of two mechanisms: as

elongation and branching of tubers (Fig. 1 L) or as direct formation of new plantlets in the form of protocorm-like bodies on the first developed tuber (Fig. 1 M). To our knowledge this is the first description of development of new orchid plantlets on tubers without a dormancy period for *Dactylorhiza* species, clearly showing intensification of development in conditions of tissue culture. In contrast, it was reported that tuberization of orchid seedlings occurs more rapidly and frequently *in situ* than under *in vitro* conditions (Debeljak et al. 2002).

Well developed plantlets of *D. fuchsii* were obtained by means of sterile culture in the next spring after sowing in August (Fig. 2 A and B). Unfolding of first leaves and start of development of true secondary tubers indicated the stage for transplanting of *D. fuchsii* plantlets to *ex vitro* conditions. The first germinated plants with two leaves, tubers and roots were appropriate for transplanting into soil after eight months (Fig. 2 C and D). Thus, the use of *in vitro* methods significantly reduced the relatively long period of time necessary for development of plants in natural conditions. Furthermore, application of *in vitro* methods gave a possibility to observe developmental stages and to record crucial morphogenic characteristics of orchids without destructive sampling.

Studies on *in vitro* propagation and subsequent *ex vitro* cultivation of rare and endangered terrestrial orchid species could be important also for species reintroduction programs. Recently asymbiotic propagation of the vulnerable Japanese orchid *Cephalanthera falcata* and successful introduction into natural habitat has been described (Yamato, Iwase 2007).

References

Cepurīte B. 2005. *Flora of Vascular Plants of Latvia. Vol. 7. Orchids (Orhidaceae).* Institute of Biology, Salaspils. 73 p. (in Latvian) /Latvijas vaskulāro augu flora. 7: Orhideju dzimta (Orchidaceae)/

Curtis J.T. 1943. Germination and seedling development in five species of *Cypripedium* L. *Am. J. Bot.* 30: 199–206.

Debeljak N., Regvar M., Dixon K.W., Sivasithamparam K. 2002. Induction of tuberisation *in vitro* with jasmonic acid and sucrose in an Australian terrestrial orchid, *Pterostylis sanguinea*. *Plant Growth Reg.* 36: 253–260.

Dixon K.W., Kell S.P., Barrett R.L., Cribb P.J. 2003. *Orchid Conservation*. Natural History Publications (Borneo), Kota Kinabalu.

Jakobsone G., Dapkūnienė S., Cepurīte B., Belogrudova I. 2007. The conservation possibilities of endangered orchid species of Latvia and Lithuania. *Monographs of Botanical Gardens "European botanic gardens together towards the implementation of plant conservation strategies"*, Warsaw/ Rogow, Poland, 1: 65–68.

Kauth P.J., Vendrame W.A., Kane M.E. 2006. *In vitro* seed culture and seedling development of *Calopogon tuberosus*. *Plant Cell Tissue Organ Cult.* 85: 91–102.

Knudson L. 1946. A new nutrient solution for orchid seed germination. *Amer. Orchid Soc. Bull.* 15: 214–217.

Kull T. 1999. *Cypripedium calceolus* L. *J. Ecol.* 87: 913–924.

McKendrick S.L. 1996. The effects of shade on seedlings of *Orchis morio* and *Dactylorhiza fuchsii* in chalk and clay soil. *New Phytol.* 134: 343–352.

Murashige T., Skoog F. 1962. A revised medium for rapid growth and bioassays with tobacco tissue cultures. *Physiol. Plant.* 15: 473–497.

Pillon Y., Fay M.F., Shipunov A.B., Chase M.W. 2006. Species diversity versus phylogenetic diversity: A practical study in the taxonomically difficult genus *Dactylorhiza* (Orchidaceae). *Biol. Conserv.* 129: 4–13.

Rasmussen H. 1995. *Terrestrial Orchids: from Seed to Mycotrophic Plant*. Cambridge University Press, Cambridge. 444 p.
Rasmussen H.N., Rasmussen F.N. 1991. Climatic and seasonal regulation of seed plant establishment of *Dactylorhiza majalis* inferred from symbiotic experiments *in vitro*. *Lindleyana* 6: 221–227.
Rauh W., Barthlott W., Ehler N. 1975. Morphologie und Funktion der Testa staubförmiger Flugsamen. *Botanische Jahrbücher* 96: 353–374.
Stoutamire W.P. 1974. Terrestrial orchid seedlings. In: Withner C.L. (ed) *The Orchids*. Scientific Studies. Wiley, New York, pp. 101–128.
Tatarenko I.V., Kondo K. 2003. Seasonal development of annual shoots in some terrestrial orchids from Russia and Japan. *Plant Species Biol.* 18: 43–55.
Yamato M., Iwase K. 2008. Introduction of asymbiotically propagated seedlings of *Cephalanthera falcata* (Orchidaceae) into natural habitat and investigation of colonized mycorrhizal fungi. *Ecol. Res.* 23: 329–337.

Savvaļas orhidejas *Dactylorhiza fuchsii* morfoģenēze audu kultūrā

Gunta Jakobsone*

Audu kultūru nodaļa, Nacionālais botāniskais dārzs, Miera 1, Salaspils LV-2169, Latvija
*Korespondējošais autors, E-pasts: gunta.jakobsone@nbd.gov.lv

Kopsavilkums

Dactylorhiza fuchsii, kura ir iekļauta Baltijas reģiona Sarkanajā grāmatā un minēta arī ES biotopu direktīvas B pielikumā, izmantoja par modeli, pētot asimbiotiskās attīstības sākuma stadijas audu kultūrā. Daļēji nobriedušas sēklas atdalīja no sterilizētas sēklu kapsulas, uzsēja uz filtrpapīra tiltiņiem kultivēšanas mēģenēs ar sākotnējo šķidro barotni un turēja tumsā 23 °C temperatūrā. Dīgšana sākās pēc divu mēnešu inkubācijas. Sakņu un gumu veidošanās bija novērojama 3 līdz 6 mēnešus no dīgšanas sākuma. Mikroaugus ar ~ 2 cm gariem dzinumiem un labi attīstītiem gumiem pārnesa tālākai audzēšanai gaismā. Jaunos *D. fuchsii* augus ar divām lapām, gumiem un saknēm, kuri bija piemēroti pārstādīšanai augsnē, ieguva nākamajā pavasarī, t.i., aptuveni 8 līdz 9 mēnešus pēc dīgšanas sākuma. *In vitro* metožu izmantošana ievērojami samazināja relatīvi ilgo laiku, kāds nepieciešams orhideju augu attīstībai dabiskos apstākļos.

Acta Universitatis Latviensis, 2008, Vol. 745, Biology, pp. 25–35

Medium pH affects regeneration capacity and oxidative enzyme activity of *Pinus sylvestris* in tissue culture

Una Andersone*, Gederts Ievinsh

Department of Plant Physiology, Faculty of Biology, University of Latvia, Kronvalda Bulv. 4, Rīga LV-1586, Latvia

*Corresponding author, E-mail: una.andersone@inbox.lv

Abstract

Medium pH that is one of the important factors of the physico-chemical environment during development of plant tissues in conditions of *in vitro* culture which is modified during preparation of media, but also changes with developing explants. The present experiments were performed to monitor the changes of medium pH and to determine the effect of medium pH on physiological characteristics of mature *Pinus sylvestris* L. tissue cultivated *in vitro*. The final changes of medium pH after addition of agar and autoclaving were towards alkalinity in the range of initial pH 3.0 to 5.5. Results of the experiments proved that in general cultivation of pine buds causes acidification of the medium. The degree of acidification of medium during cultivation depends on initial pH of medium, morphogenesis of explants and duration of cultivation period without transplantation. Lowered activity of oxidative enzymes in buds cultivated on more acidic medium and less necessity for acidification to reach the equilibrium in medium pH suggest that a low initial pH is more suitable for successful pine bud morphogenesis.

Key words: medium pH, morphogenesis, peroxidase, *Pinus sylvestris*, polyphenol oxidase, Scots pine, tissue culture.

Introduction

Medium pH is one of the important factors of physico-chemical environment during development of plant tissues in conditions of *in vitro* culture (Williams et al. 1990). The optimal pH of *in vitro* medium for different phases of morphogenesis (successful *in vitro* culture establishment, intensive shoot proliferation, induction of the rooting) for woody species varies (von Arnold, Eriksson 1982; Williams et al. 1985; Saborio et al. 1997; Ostrolucka et al. 2004).

Suboptimal pH levels can cause abnormalities in the development of explants e.a. reduction in growth of the hypocotyls, stem and roots, changes in leaf coloring (Gurel, Gulsen 1998; Laukkanen et al. 2000). Optimal pH of media *in vitro* can be different from that of soil *ex vitro* (Sen et al. 1994) and in *ex vitro* acclimatization in hydroponic culture (Ingestad 1979; Bozhkov, von Arnold 1998).

In tissue culture practice pH of medium is adjusted before autoclaving and changes of pH during autoclaving and cultivation of tissues are usually ignored. The changes during autoclaving depend upon the initial pH and characteristics of the gelling agent (Williams et al. 1990; Van Winkle, Pullman 2003). Contrary to common belief, the changes of medium

pH during cultivation are not a response to wounding. Although wounding stimulates the decrease in pH over the first few days, the effect is insignificant (Williams et al. 1990).

Plant tissues can maintain a relatively constant cytoplasmic pH across an external pH range of 4 to 9 (Caponetti et al. 1971). Plant cells can also modify the external pH – the explants raise or lower the pH, depending on which pH range they grow, until an equilibrium occurs (Mac AntSaoir, Damvoglou 1994). A localized change of pH takes place at the site of contact between the plant tissue and the medium in tissue culture as well as in soil (Constable 1963; Haussling et al. 1985).

For tissue culture of different *Pinus* species pH 5.5 to 6.0 is used (Durzan, Chalupa 1976; Sen et al. 1994; Saborio et al. 1997; Sul, Korban 2004; Tang et al. 2004). *Pinus sylvestris* L. usually is cultivated in media with pH 5.5 to 5.8 (Bornman, Jansson 1980; Hohtola 1988; Žel et al. 1988; Supriyanto, Rohr 1994; Laukkanen et al. 1997; Laukkanen at al. 1999; Lelu et al. 1999; Laukkanen et al. 2000). Conifers can also change the media pH during cultivation. Embryogenic cultures of Norway spruce, loblolly pine and Douglas-fir tend to decrease the pH of growth medium (Van Winkle, Pullman 2003), but suspension culture of *Pinus banksiana* slightly increases pH of the medium during cultivation (Durzan, Chalupa 1976).

The present experiments were performed to study changes of medium pH and the effect of medium pH on physiological characteristics of mature *Pinus sylvestris* tissue cultivated *in vitro*. Oxidative enzyme activities (peroxidase and polyphenol oxidase) were used as indicators of morphogenic potential (Andersone, Ievinsh 2005).

Materials and methods

Plant material

Plant material was collected from mature pine (*Pinus sylvestris* L.) trees in a seed orchard near Salaspils (Riga Region, Latvia). Buds were taken randomly from different trees from the lower part of the crown. Buds were surface sterilized with a half-diluted commercial bleach ACE (Procture and Gamble; containing 5 to 15 % sodium hypochlorite) for 20 min, rinsed for 10 min in sterile distilled water, sterilized again in 15 % hydrogen peroxide and rinsed three times for 10 min in sterile distilled water. The buds were peeled and dissected aseptically.

Culture conditions and media

Explants were cultivated in 40 × 100 mm glass tubes containing 20 mL agarized medium (for experiments with medium pH measurements after autoclaving) or in 20 × 200 mm glass test-tubes containing 10 ml agarized nutrient medium (for experiments with medium pH measurements before adding agar and autoclaving). Vessels were closed with cotton-wool plugs, and covered with polythene film fixed with a rubber band. Each vessel contained one explant. They were cultivated at temperature 20 ± 5 °C in natural light (if not indicated otherwise).

Explants were cultivated on Woody Plant Medium (Lloyd, McCown 1981) as modified by Andersone and Ievinsh (2002). 0.5 mM naphtyl acetic acid, 54 mM adenine, and 4.7mM kinetin were used as growth regulators. The medium was supplemented with 0.6 mM myo-inositol, 88.9 mM thiamine hydrochloride, 48.6 mM pyridoxine hydrochloride, 81.2 mM nicotinic acid and 131.4 mM sucrose. It contained 0.57 % of plant agar.

For experiments on the effect of tissues on medium pH, medium was adjusted to 5.8 before adding agar and autoclaving. For experiments of effect of medium pH on tissue development, pH was adjusted 3.0 to 7.0 with interval pH 0.5 before adding agar and autoclaving. The adjustment was performed either by 1N HCl or 1N KOH.

Measurement of pH

Measurements of pH were carried out with a pH meter pH 211, by immersion of the electrode HI 1131B (Hanna Instruments). For measurement of medium pH before autoclaving the electrode was stirred in the liquid medium before agar was added. For measurement of media after autoclaving the electrode was imbedded in it two days after autoclaving. To investigate medium pH changes after cultivation of mature tissue, pH was measured by placing the electrode into the hole from which the bud explant was removed.

Effect of media preparation

To determine changes of pH during media preparation the appropriate mineral salts and organic components of the medium were mixed and pH was adjusted (2.5 to 7.0 with 0.5 intervals). Agar was then added, dissolved in a half of the volume by heating, media were dispensed into cultivation vessels and autoclaved at 121 °C and 103 KPa for 20 min. The pH in each vessel was measured two days later.

Effect of in vitro *cultivated bud tissue on pH of the medium*

Buds were cultivated *in vitro* and placed on fresh medium (pH 5.8) weekly or after every 2, 3, 4 or 5 weeks. The third part of the explants were cultivated in a growth chamber with a 16 h photoperiod, where illumination was provided by fluorescent tubes OSRAM L 36/W77, the rest were cultivated near a window in laboratory under natural light with a brief period of direct sunlight or with a prolonged period of direct sunlight. Twenty sterile explants were taken for each variant. pH of the media was measured after autoclaving and after removal of bud explants weekly or after every 2, 3, 4 or 5 weeks. The changes of pH during cultivation were estimated for 6 to 8 weeks. The experiment was carried out for 10 months. The morphological condition of bud explants (development of brachyoblasts and needles, necroses) was recorded during cultivation and at the end of experiment.

Effect of medium on in vitro *cultivated bud tissue*

Buds were cultivated on media with different pH levels (pH 3.0 to 7.0 with intervals pH 0.5) adjusted before autoclaving.

To investigate the changes of medium pH during cultivation, buds were cultivated for two months, then transplanted on fresh medium with the same variant of pH and cultivated for 10 months. Media pH was measured after removal of cultured buds. To investigate the effect of different medium pH on bud morphogenesis, morphological characteristics (needle formation, amount of needles, length of needles, necroses) were recorded after 2, 4 and 8 months of cultivation.

To investigate the effect of different medium pH on activity of peroxidase and polyphenol oxidase, buds, cultivated in vitro for seven weeks, were frozen in liquid nitrogen and ground to fine powder with a mortar and pestle. The experiment was repeated twice. Enzymes were extracted with 25 mM HEPES/KOH buffer (pH 7.2) containing 1 mM

EDTA, 3 % (w/v) PVPP and 0.8 % (v/v) Triton X-100 for 15 min at 4 °C. The homogenate was centrifuged at 15 000 g for 20 min. The supernatant was used for assays.

Peroxidase activity was measured spectrophotometrically at 470 nm in reaction mixture containing 2 mL 50 mM sodium phosphate buffer (pH 7.0) with 10 mM guaiacol, 0.5 mL 0.03 M H_2O_2 and 0.01 mL enzymatic extract. The reaction mixture without H_2O_2 was used as a reference.

The activity of polyphenol oxidase was determined spectrophotometrically in a reaction mixture (3 ml) containing 20 mM sodium phosphate (pH 6.5) with 25 mM pyrocatechol and the enzymatic extract (0.01 mL). The change in absorbance was monitored at 410 nm.

Results

During medium preparation pH changed towards alkalinity. Strongly acidic (pH 2.5) or alkaline (6.0 to 7.0) media did not change significantly during autoclaving (Fig. 1). Results of both experiments proved that in general, cultivation of pine buds caused acidification of the medium (Fig. 1 to 4).

During bud cultivation on media with different initial pH the final pH was similar. Two- and 10-month long cultivation of buds on media with pH 3.5 to 7.0 resulted in almost the same acidity of medium for all variants of pH. After 2 months of cultivation the mean pH of medium was 5.26 ± 0.06, but in 10 months cultivation the mean medium pH declined to 4.18 ± 0.11 (Fig. 1). Buds, cultivated on medium with alkaline initial pH, acidified the medium more than buds cultivated on medium with initially acidic pH.

The rate of acidification depended on the duration of cultivation without transplantation. The maximal rate of acidification was observed during the first four weeks of cultivation,

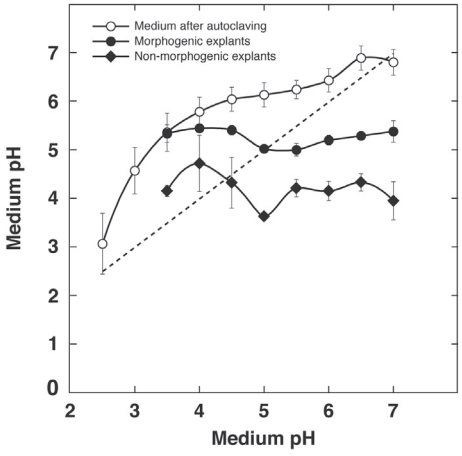

Fig. 1. Change of medium pH after autoclaving and with different types of pine bud explants during 10 months of cultivation without transplanting. Dashed line indicates no change in the pH values.

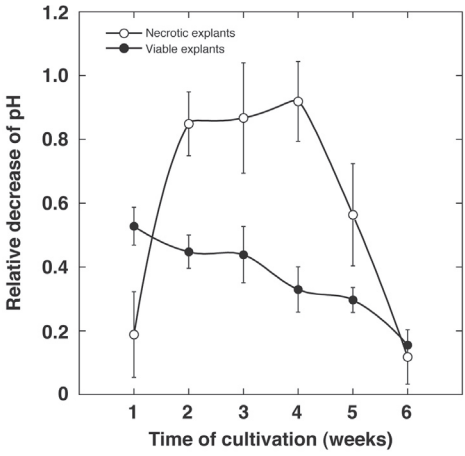

Fig. 2. Effect of time of cultivation and explant type on relative decrease of medium pH. Initial pH of the cultivation medium was 5.8 (6.25 after autoclaving). Explants were transplanted to the fresh medium with initial pH value every week.

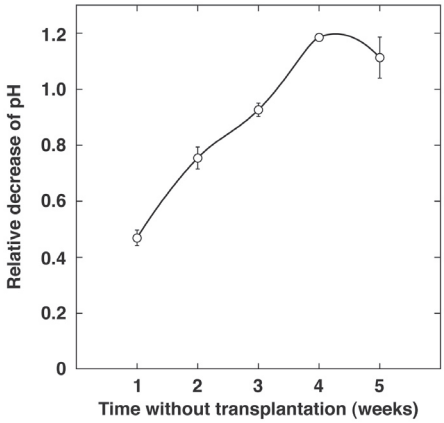

Fig. 3. Effect of time of cultivation before transplanting on relative decrease of medium pH. Initial pH of the cultivation medium was 5.8 (6.25 after autoclaving). Explants were transplanted on a fresh medium with initial pH after the indicated intervals of time and cultivated for 10 months.

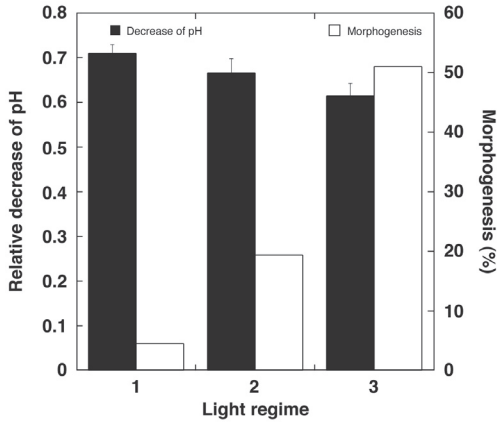

Fig. 4. Effect of illumination conditions on relative decrease of medium pH and percentage of morphogenesis in pine bud explants. Artificial light only (1), natural light with short periods of direct sunlight (2), natural light with long periods of direct sunlight (3). Initial pH of the cultivation medium was 5.8 (6.25 after autoclaving). Explants were cultivated for 10 months without transplanting.

then decreased, but slower acidification continued when explants were not transplanted for 10 months (Fig. 1, 3). In the first cultivation week acidification was from pH 6.25 to 5.76 (acidification rate 0.49), but in 10 months time from pH 6.25 to 4.18 (acidification rate 0.048 weekly).

The results of our experiments showed that the degree of acidification depended on the physiological condition of explants. To evaluate if morphogenesis affected the ability of pine buds to change medium pH buds were divided into groups according to different developmental events or lack of development. If constructive processes in buds dominated over destructive, medium acidification was less marked than for buds with dominating destructive processes. This relationship was characteristic for buds in the first experiment, transplanted every week (Fig. 2), for buds transplanted every 2, 3, 4 or 5 weeks (data not shown) or grown for 10 months without transplantation in the second experiment, when average medium pH with needle forming buds was 4.59 ± 0.15, but for buds without needles it was 3.91 ± 0.08.

The same relationship was characteristic also for buds, cultivated in different light intensities. Change of medium pH for different light intensities in the first experiment was lowest for explants cultivated in natural light with a prolonged period of direct sunlight (greater percentage of viable buds with enlarged brachioblasts and needle-forming buds), and highest for explants cultivated in artificial light that did not form needles and became necrotic sooner (Fig. 4).

The second experiment was performed to test if the initial pH of the medium affects pine tissue development. The morphological characteristics of buds (average percentage of needle forming buds, average amount of needle pairs on each needle forming bud, length of needles) varied (Fig. 5, 6A), but on the whole the results were not convincingly

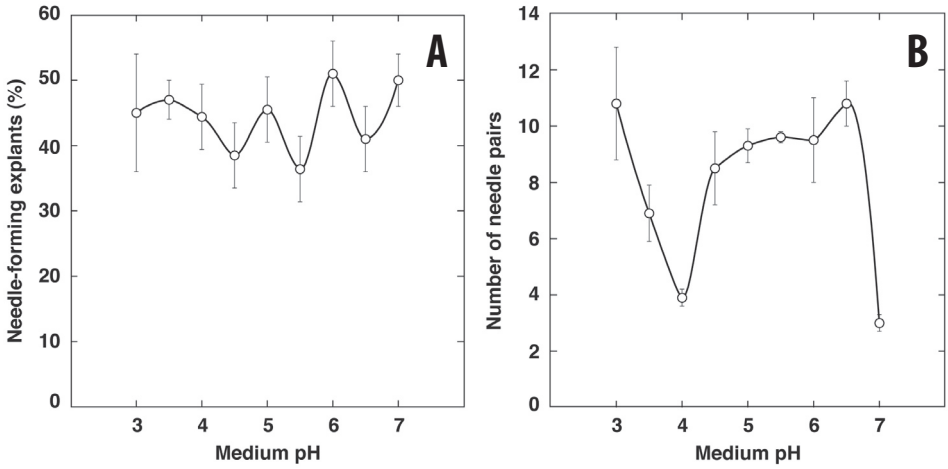

Fig. 5. Effect of initial medium pH on percentage of needle-forming explants (A) and number of needle pairs per needle-forming explant (B) within 10 months of cultivation. Explants were cultivated without transplanting.

affected by initial pH of medium.

The percentage of necrotic tissue in buds cultivated *in vitro* for four months (second experiment) was lowest on media with the most acidic and most alkaline initial pH (Fig. 6B).

The activity of peroxidase in buds cultivated *in vitro* for 7 weeks on media with different pH was significantly lower for buds cultivated on pH 3.0, increased for higher pH values up to 5.0, but lowered again and stopped decreasing at pH 6.5 (Fig. 7A). The activity of polyphenol oxidase in the same buds was also lowest for pH 3.0 and increased up to pH 6.5 (Fig. 7B).

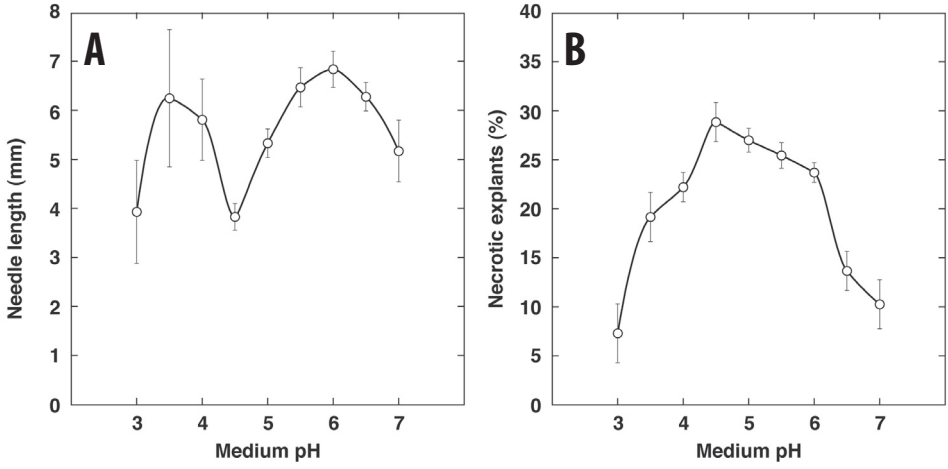

Fig. 6. Effect of initial medium pH on percentage of needle length (A) and percentage of necrotic pine bud explants (B) within 10 months of cultivation. Explants were cultivated without transplanting.

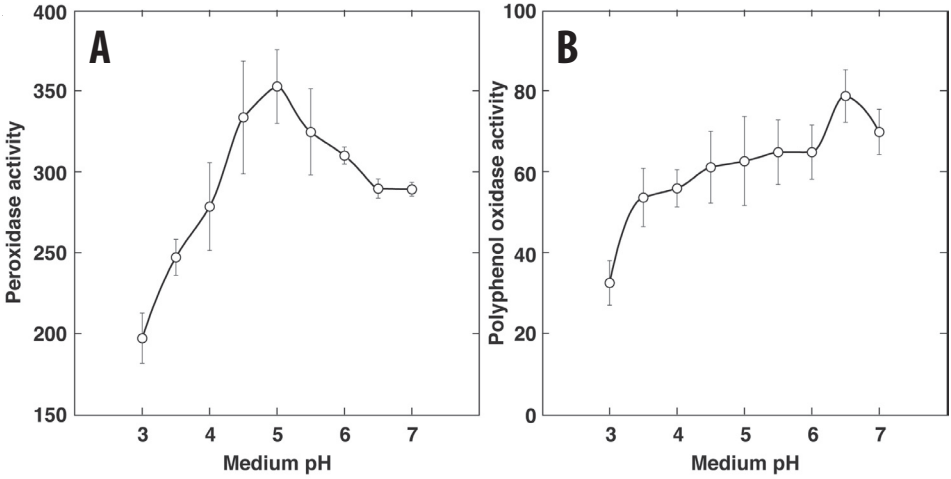

Fig. 7. Effect of initial medium pH on peroxidase (A) and polyphenol oxidase (B) activity in pine bud explants after 7 weeks of cultivation. Explants were cultivated without transplanting.

Discussion

Changes of medium pH should be taken in to the account when using plant tissue culture both for practical purposes as well as for research. Changes of pH can occur from preparation of medium until *ex vitro* transplantation and are affected both by interactions between chemical constituents as well as plant tissues and medium constituents.

Adjustment of medium pH is usually performed before adding agar, but the agar itself and subsequent autoclaving change medium pH. The addition of agar to the nutrient solution raised the pH when initial pH was below 5.5, but autoclaving decreased pH, except when pH was lower than 4.0 (Williams at al. 1990). In our investigation we recorded only the final medium pH after addition of agar and autoclaving which were towards alkalinity (Fig. 1). Differences in pH may arise from different types of agar, other medium components or medium preparation features.

Medium pH changed during cultivation of tissues usually towards acidity. The degree of acidification of the medium during cultivation is influenced by several factors, including the source of nitrogen, physiological status of cultivated tissues, duration of cultivation, frequency of transplanting etc.

The source of nitrogen in the medium and its utilization by cells can play an important role in determining the shift in the pH value of the medium (Sathyanarayana, Blake 1994). Plant growth *in vitro* can occur regardless of initial pH as the medium contains both N forms (Mac AntSaoir 1994). Nitrogen uptake as nitrate is higher at an acidic pH and shifts the medium pH towards alkalinity, while ammonium utilization rate increases with increasing pH and shifts the medium pH towards acidity (Gamborg, Shyluk 1970; Martin, Rose 1976; Wetherell, Dougall 1976; Dougall, Verma 1978). In *Pinus sylvestris* callus cultures the medium became acidic when it contained NH_4NO_3 (from pH 5.7 to 4.3), but the pH of the medium containing KNO_3 remained close to the initial value (from pH 5.7 to 5.4; Laukkanen et al. 1997). Seedlings of a number of forest tree species, including *Pinus sylvestris* grow better when nitrogen is supplied as ammonium or as ammonium

plus nitrate, and when ammonium is preferred as the nitrogen source, the rhizosphere will be acidified by induced H^+ extrusion (Arnold 1992). In our second experiment where medium contained ammonium and nitrate pine bud explants changed the medium pH to a constant value for the whole range of initial pH of medium (Fig. 1).

The degree of acidification in our experiments depended on the morphogenesis of explants. Needle formation on buds was associated with less acidified medium. From the results of the experiment on light intensity and changes of medium pH we can also conclude that pH change was less for natural illumination conditions, which stimulated morphogenesis, and promoted enlarged brachyoblast development and needle formation (Fig. 4). The degree of acidification of medium during cultivation depended also on the duration of cultivation period before transplantation. The observed change of medium pH for different cultivation periods before transplantation shows that it is not necessary to transplant pine buds to fresh medium more often than every two months or even less frequently.

The initial pH of medium also affects the degree of acidification during cultivation. If the initial pH is more alkaline, explants consume more energy to acidify the medium than explants cultivated on medium with initially acidic pH. Moreover production of acidic compounds by the mycobacterium living in pine buds may also cause acidification of the growth medium (Laukkanen et al. 2000).

Medium pH was changing due to release of some compounds from the plant or as a result of uptake of specific ions from the medium. Tissue secretes phytosiderophores, organic acids and proteins, which may react with metal ions present and change chemical dissociation kinetics, in turn altering their bioavailability (Friborg et al. 1978; Egertsdotter et al. 1993; Zhang 1993; Van Winkle, Pullman 2003). It is possible that buds becoming necrotic secrete into the medium compounds different from those of needle forming buds, which may result in different effects on medium pH.

Although the difference in initial pH may have a significant effect on the culture system even though the pH difference is eliminated after some time of cultivation (Williams et al 1990), the obtained morphological data in our experiment do not show any simple trend of relationship between initial pH of medium and development of explants (Fig. 5, 6). In the acidic part of medium pH range the morphological development occurred during longer cultivation periods and the morphological parameters were better and buds less necrotic. For *Pinus sylvestris* callus cultures a lower pH in the presence of ammonium in culture medium correlated with better growth (Laukkanen et al. 1997). However, differences between pH variants may be caused also by biological diversity of the material used for experiments.

In our study peroxidase and polyphenol oxidase activity was lowest in the acidic end of medium pH range (Fig. 7). A low peroxidase and polyphenol oxidase activity correlated with increased morphogenic potential of mature *Pinus sylvestris* buds *in vitro* (Andersone, Ievinsh 2002; Andersone, Ievinsh 2005). Buds cultivated on initially more acidic medium need less acidification to reach equilibrium. These results may confirm the morphological results of the experiment with different initial pH of medium, e.g. that mature *Pinus sylvestris* buds *in vitro* need acidic initial medium pH (pH 3.0 to 3.5 before adding agar and autoclaving). The presence of ammonium in culture medium might have an effect on polyphenol oxidase and peroxidase by decreasing the pH and altering the water potential of the cells. However, increased browning in the presence of only nitrate

may result in significantly higher pH, because at higher pH levels phenolics will oxidize to form quinones, which will bind irreversibly to proteins in a non-enzymatic fashion (Laukkanen et al. 1997).

In conclusion the degree of acidification of medium during cultivation of mature *Pinus sylvestris* buds depends not only on the source of nitrogen, products of mycobacteria living in pine buds as described previously, but also on initial pH of medium, morphogenesis of explants and duration of cultivation period without transplantation. Lowered activity of oxidative enzymes in buds cultivated on more acidic medium, and that needed less acidification to reach equilibrium, suggests that low initial pH is more suitable for successful pine bud morphogenesis.

Acknowledgements

The present study was supported by Latvian Council of Science and the European Social Fund.

References

Andersone U., Ievinsh G. 2002. Changes of morphogenic competence in mature *Pinus sylvestris* L. buds *in vitro*. *Ann. Bot.* 90: 293–298.

Andersone U., Ievinsh G. 2005. *In vitro* regeneration of mature *Pinus sylvestris* buds stored at freezing temperatures. *Biol. Plant.* 49: 281–284.

Arnold G. 1992. Soil acidification as caused by the nitrogen uptake pattern of Scots pine (*Pinus sylvestris*). *Plant Soil* 142: 41–51.

Bornman C.H., Jansson E. 1980. Organogenesis in cultured *Pinus sylvestris* tissue. *Z. Pflanzenphysiol.* 96: 1–6.

Bozhkov P.V., von Arnold S. 1998. Polyethylene glycol promotes maturation but inhibits further development of *Picea abies* somatic embryos. *Physiol. Plant.* 104: 211–224.

Caponetti J.D., Hall G.C., Farmer R.E. 1971. *In vitro* growth of black cherry callus: effects of medium, environment and clone. *Bot. Gaz.* 132: 313–318.

Constable F. 1963. Untersuchugen über extracellulare Hydrolyse von Kohlenhydraten. *Planta* 59: 330–337.

Dougall D.K., Verma D.C. 1978. Growth and embryo formation in wild carrot suspension cultures with ammonium ion as a sole nitrogen source. *In Vitro* 14: 180–182.

Durzan D.J., Chalupa V. 1976. Growth and metabolism of cells and tissue of jack pine (*Pinus banksiana*). 3. Growth of cells in liquid suspension cultures in light and darkness. *Can. J. Bot.* 54: 456–467.

Egertsdotter U., Mo L.H., von Arnold S. 1993. Extracellular proteins in embryogenic suspension cultures of Norway spruce (*Picea abies*). *Physiol. Plant.* 88: 315–321.

Fridborg G., Pedersen M., Landstrom L.E., Eriksson T. 1978. The effect of activated charcoal on tissue cultures: adsorbtion of metabolites inhibiting morphogenesis. *Physiol. Plant.* 43: 104–106.

Gamborg O.L., Shyluk J.P. 1970. The culture of plant cells with ammonium salts as the sole nitrogen source. *Plant Physiol.* 45: 598–600.

Gürel S., Gülsen Y. 1998. The effects of different sucrose, agar and pH levels on in vitro shoot production of almond *Amygdalus communis* L.). *Turk. J. Bot.* 22: 363–373.

Haussling M., Leisen E., Marschner H., Römheld V. 1985. An improved method for non-destructive measurements of the root-soil interface (rhizosphere). *J. Plant Physiol.* 117: 371–375.

Hohtola A. 1988. Seasonal changes in explant viability and contamination of tissue cultures from mature Scots pine. *Plant Cell Tissue Organ Cult.* 15: 211–222.

Ingestad T. 1979. Mineral nutrient requirements of *Pinus sylvestris* and *Picea abies* seedlings. *Physiol. Plant.* 45: 373–380.

Laukkanen H., Julkunen-Tiitto R., Hohtola A. 1997. Effect of different nitrogen nutrients on the viability, protein synthesis and tannin production of Scots pine callus. *Physiol. Plant.* 100: 982–988.

Laukkanen H., Häggman H., Kontunen-Soppela S., Hohtola A. 1999. Tissue browning of *in vitro* cultures of Scots pine: Role of peroxidase and polyphenol oxidase. *Physiol. Plant.* 106: 337–343.

Laukkanen H., Soini H., Kontunen-Soppela S., Hohtola A., Viljanen M. 2000. A mycobacterium isolated from tissue cultures of mature *Pinus sylvestris* interferes with growth of Scots pine seedlings. *Tree Physiol.* 20: 915–920.

Lelu M.A., Bastien C., Drugeault A., Gouez M.L., Klimaszewska K. 1999. Somatic embryogenesis and plantlet development in *Pinus sylvestris* and *Pinus pinaster* on medium with and without growth regulators. *Physiol. Plant.* 105: 719–728.

Lloyd G., McCown B. 1981. Commercially-feasible micropropagation of Mountain laurel, *Kalmia latifolia*, by use of shoot tip culture. *Int. Plant Propag. Soc. Proc.* 30: 421–427.

Mac AntSaoir S., Damvoglou V. 1994. The effect of carbohydrate source and pH on *in vitro* growth of *Vitis vinifera* cultivars Black Hamburg and Alvarino. In: Lumsden P.J., Nicholas J.R., Davies W.J. (eds) *Physiology, Growth and Development of Plants in Culture*. Kluwer Academic Publishers, Dordrecht, pp. 94–97.

Martin S.M., Rose D. 1976. Growth of plant cells (*Ipomoea*) suspension cultures at controlled pH levels. *Can. J. Bot.* 54: 1264–1270.

Ostrolucká M.G., Libiaková G., Ondrušková E., Gajdošová A. 2004. *In vitro* propagation of *Vaccinium* species. *Acta Univ. Latv.* 670: 7–15.

Saborio F., Dvorak W.S., Donahue J.K., Thorpe T.A. 1997. *In vitro* regeneration of plantlets from mature embryos of *Pinus ayacahuite*. *Tree Physiol.* 17: 787–796.

Sathyanarayana B.N., Blake J. 1994. The effect of nitrogen sources and initial pH of the media with or without buffer on *in vitro* rooting of jackfruit (*Artocarpus heterophyllus* Lam.). In: Lumsden P.J., Nicholas J.R., Davies W.J. (eds) *Physiology, Growth and Development of Plants in Culture*. Kluwer Academic Publishers, Dordrecht, pp. 77–82.

Sen S., Magallanes Cedeno M.E., Kamps R.H. 1994. *In vitro* micropropagation of Afgan pine. *Can. J. For. Res.* 24: 1248–1252.

Sul W., Korban S.S. 2004. Effects of salt formulations, carbon sources, cytokinins, and auxin on shoot organogenesis from cotyledons of *Pinus pinea* L. *Plant Growth Reg.* 43: 197–205.

Supriyanto, Rohr R. 1994. *In vitro* regeneration of plantlets of Scots pine (*Pinus sylvestris*) with mycorrhizal roots from subcultured callus initiated from needle adventitious buds. *Can. J. Bot.* 72: 1144–1150.

Tang W., Harris L.C., Outhavong V., Newton R.J. 2004. The effect of different plant growth regulators on adventitious shoot formation from Virginia pine (*Pinus virginiana*) zygotic embryo explants. *Plant Cell Tissue Organ Cult.* 78: 237–240.

Van Winkle S.C., Pullman G.S. 2003. The combined impact of pH and activated carbon on the elemental composition of a liquid conifer embryogenic tissue initiation medium. *Plant Cell Rep.* 22: 303–311.

Von Arnold S., Eriksson T. 1982. *In vitro* studies of adventitious shoot formation in *Pinus contorta*. *Can J. Bot.* 59: 870–874.

Wetherell D.F., Dougall D.K. 1976. Sources of nitrogen on growth and embryogenesis in cultured wild carrot tissue. *Physiol. Plant.* 37: 97–103.

Williams R.R., Taji A.M., Bohon J.A. 1985. Specifity and interaction among auxins light and pH in rooting Australian woody species *in vitro*. *HortScience* 20: 1052–1053.

Williams R.R., Taji A.M., Winney K.A. 1990. The effecy of *Ptilotus* plant tissue on pH of *in vitro* media. *Plant Cell Tissue Organ Cult.* 22: 153-158.

Zel J., Gogala N., Camloh M. 1988. Micropropagation of *Pinus sylvestris*. *Plant Cell Tissue Organ Cult.* 14: 169–175.

Zhang F.S. 1993. Mobilisation of iron and manganese by plant-borne and synthetic metal chelators. *Plant Soil* 155/156: 111–114.

Barotnes pH ietekmē reģenerācijas spējas un oksidatīvo fermentu aktivitāti *Pinus sylvestris* audu kultūrā

Una Andersone*, Ģederts Ieviņš

Augu fizioloģijas katedra, Latvijas Universitātes Bioloģijas fakultāte, Kronvalda bulv. 4, Rīga LV-1586, Latvija
*Korespondējošais autors, E-pasts: una.andersone@inbox.lv

Kopsavilkums

Barotnes pH ir viens no svarīgākajiem fizikālķīmiskās vides faktoriem augu audu attīstības laikā *in vitro* kultūras apstākļos. To ietekmē barotnes sagatavošana un tas mainās arī līdz ar eksplantu attīstību. Dotos ekesperimentus veica, lai novērotu barotnes pH izmaiņas un noteiktu barotnes pH ietekmi uz *in vitro* kultivētu nobriedušu *Pinus sylvestris* L. audu fizioloģiskajām īpašībām. Pēc agara pievienošanas un autoklavēšanas barotnes ar sākuma pH no 3.0 līdz 5.5 kļuva sārmainākas. Pētījumu rezultāti apstiprināja, ka priežu pumpuru kultivēšana izraisa barotnes paskābināšanos. Barotnes paskābināšanās pakāpe bija atkarīga no sākotnējā barotnes pH, eksplantu morfoģenēzes un kultivēšanas ilguma bez pārstādīšanas. Pazemināta oksidatīvo fermentu aktivitāte pumpuros uz skābākas barotnes un īsāks šādu kultūru pH stabilizācijai nepieciešamais laika periods liecina, ka veiksmīgai priežu pumpuru morfoģenēzei nepieciešams zemāks sākotnējais barotnes pH.

Acta Universitatis Latviensis, 2008, Vol. 745, Biology, pp. 37–41

The embryogenesis and development of newly obtained interspecific lily hybrids *in vitro*

Gunta Jakobsone[1]*, Guntis Grants[2]

[1]Tissue Culture Department, National Botanical Garden, Miera 1, Salaspils LV-2169, Latvia
[2]Lilium Balticum, Latvia

*Corresponding author, E-mail: gunta.jakobsone@nbd.gov.lv

Abstract

Interspecific hybridization is the most important source for variation in ornamental breeding. Tissue culture methods are used to overcome fertilization barriers in these hybrids. The aim of the present study was to establish a microcultivation system for explanted zygotic embryos of lilies from interspecific crossings of Asiatic, Oriental, Trumpet hybrids and *Lilium longiflorum* in different combinations and their backcross derivatives based on the embryo rescue method. Five combinations of lily crosses in 2002, and 11 of 16 combinations in 2004 gave positive results, although with different percent of germination and embryo survival.

Key words: embryogenesis, lily hybrids, *in vitro*.

Introduction

The breeding strategies of ornamental plants e.a. lilies include a wide range of *in vitro* methods. Three most important groups of modern commercial lilies are the Asiatic hybrids (A), originating from interspecific crosses within the *Sinomartagon* section, the Oriental hybrids (O), obtained from crosses within the *Archelirion* section, and the *Longiflorum* group (L; Van Creij et al. 1993). Pedigree analysis shows that the majority of lily cultivars from the group LA (*Lilium longiflorum* Thunb. × Asiatic hybrid) were derived after back crossing of alloploid hybrids producing non-reduced 2*n* gametes on diploid Asiatic cultivars (Proscevičus 2004). In the genus *Lilium*, interspecific hybridization has been conducted to produce novel hybrids that can combine resistance of Orientals against *Botrytis*, virus resistance of Asiatics, and *Fusarium* resistance of Trumpets, with attractive flowers and good cultivation qualities (Chi 2002).

The Asiatic lilies are most resistant in open areas in wet and cool maritime climates but the flowers have average ornamental value and have no fragrance. Most ornamental lilies with enjoyable delicate fragrance are from the Oriental group. However, they are completely unadapted for the above-mentioned climate. Therefore, it is necessary to perform interspecific crossings between different groups of lilies, which do not produce fertile seeds in natural conditions or do not produce seeds at all. Because of pre- and post-fertilization barriers, successful interspecific crosses have not been reported for *Lilium* using an Asiatic hybrid as a mother plant in crossings with Oriental or *Lilium longiflorum* as a pollen source (Chi 2000). To overcome pre-fertilization barriers, the cut-style method,

the grafted style method and the placenta pollination method have been tested (Van Tuyl et al. 1991; Janson et al. 1993; Willemse et al. 1995). Embryo rescue, ovary-slicing, and ovule culture have been used to overcome post-fertilization barriers (Van Tuyl et al. 1991; Okazaki et al. 1992; Chi 2002; Ikeda et al. 2003).

The purpose of the present study was to establish a microcultivation system for explanted zygotic embryos of lilies from interspecific crossings of Asiatic, Oriental, Trumpet hybrids (T) and *Lilium longiflorum* in different combinations and their backcross derivatives based on the embryo rescue method.

Materials and methods

The *in situ* hybridization method was used for this study. Five combinations used in 2002 were: (I) *Lilium longiflorum* × Asiatic hybrid, *3n*) × Asiatic hybrid, 4*n* (LAA); (II to V) Oriental hybrids × Trumpet hybrids (OT). In 2004, four crossing combinations were used: OT × OT – (three crossings); OT × T (Trumpet) – (nine crossings); TA (Trumpet hybrids × Asiatic hybrids) × A – (two crossings); and TA × T- (two crossings). Seed buds were isolated from capsules which were sterilized by briefly dipping them in 96 % ethanol and passing them through the flame. Seed coats were removed aseptically, and embryos with endosperm were placed on filter paper bridges in test tubes (19 mm diameter) with liquid initial medium for 4 days (Fig. 1A). Then, embryos were removed from browned endosperm (Fig. 1B, C) and placed on a new medium for further development (Fig.1 D). Both media were made after an original protocol designed by the Tissue Culture Department of the National Botanical Garden (Jakobsone, unpublished data).

All cultures were maintained in a growth chamber in continuous darkness at 23 to 25 °C until the formation of a first leaf. From this stage all the plant material was cultivated as bulblets on agar-solidified modified Murashige and Skoog (1962) medium supplemented with 0.08 mg L^{-1} α-naphthalene acetic acid. Plantlets were placed in an illuminated chamber with white fluorescent lamps at 23 to 25 °C. Further transplantations were carried out depending on the stage of development. Regenerants with well developed bulbs were transplanted *ex vitro* on soil for further regrowth and selection.

Results and discussion

Interspecific hybridization is the most important source for variation in ornamental breeding. It is indispensable to combine diverse gene pools allowing to add a new characteristics into the current cultivars. Interspecific hybrids have an enormous potential to extend not only their qualitative but also quantitative traits such as the type of flower, plant phenotypes, other single dominant traits from parent species related to environmental adaptation etc. While natural hybrids can exist between species with overlapping flowering times, pre- and post-fertilization barriers hinder the frequency of these hybrids (Van Tuyl et al. 2003). Establishment of a microcultivation system for the rescue of zygotic embryos is necessary to overcome post-fertilization barriers. In our experiments, 60 to 80 days after pollination was too long, and did not allow to prevent embryo abortion occurring at very early developmental stages. Van Tuyl et al. (1991) noted that embryos at 8th day after pollination were successfully rescued by ovary slice culture in an interspecific cross of *L. longiflorum*.

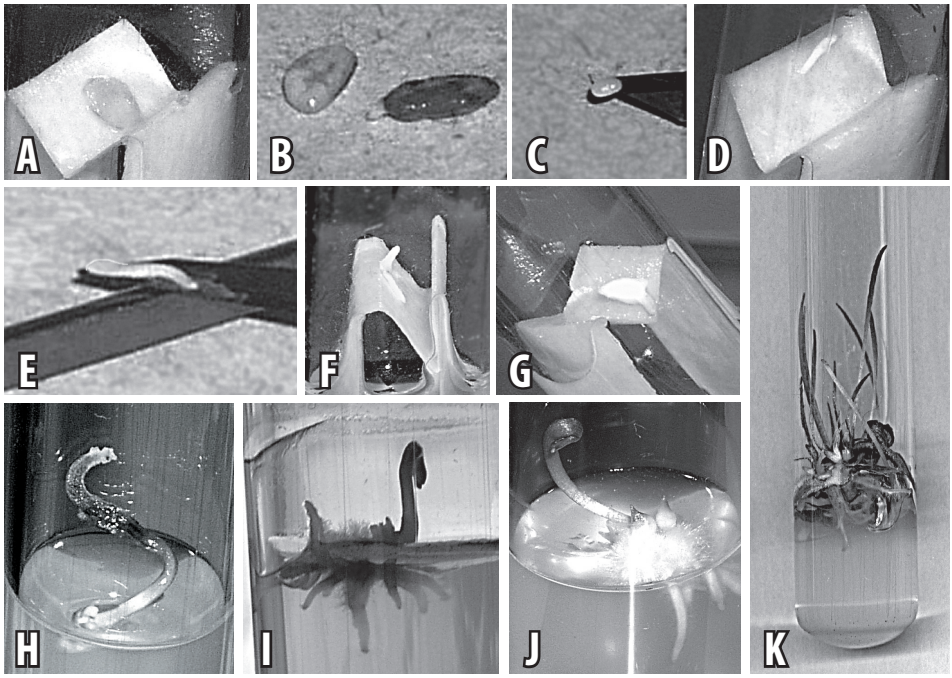

Fig. 1. Embryo- and morphogenesis of interspecific lily hybrids *in vitro*. A, hybrid seed-bud without seed-coat transplanted *in vitro*. B, 4 days after transplantation. C, zygotic embryo, after a globular stage. D, elongated embryo. E, transplantation of embryo, torpedo stage. F, polarization of embryo. G, formation of cotyledon. H, development of the shoot. I, rooting phase. J, formation of bulblets. K, normally developed microplant of lily *in vitro*.

Five combinations of lily crosses in 2002, and 11 out of 16 combinations in 2004 gave positive results although with different percent germination and embryo survival. In general the method used in the present study was more successful than the cutting of seed vessels into slices, as described in the literature (Chi 2002).

In our experiments, a torpedo stage (Fig. 1E) started in a short time after isolation of embryos, approximately in a week. The embryogenesis stage *in vitro* ended with formation of a bipolar structure – embryo –prepared to form a completely new plant body (Preťová, Olbert 2006). As shown in Fig. 1F, the polarization started immediately after the torpedo stage.

The polarization stage ended with formation of cotyledon (Fig. 1G) further developing into first shoot (Fig. 1H) which appeared after about 2.5 to 3 months. After that explants could be cultivated in the light. Rooting (Fig. 1I) and bulb formation (Fig. 1J) took place only in light conditions. The proliferation and normal *in vitro* cultivation of lilies (Fig. 1K) was achieved after five-six months. Transplanting to soil was performed in August, 10 months after the initiation of sterile culture.

The OA lily hybrids (Oriental hybrids × Asiatic hybrids) are of practical interest in horticulture as well as of basic scientific importance. Distantly related species have been used in crop improvement where the traditional approach was to produce an alloploid from

F_1 hybrid through somatic chromosome doubling. Such allopolyploids are appropriately called "permanent hybrids" because the parental characteristics almost never segregate in their progenies (Barba-Gonzalez et al. 2005).

The condition of embryos cultured *in vitro* and subsequent quality of bulblets was very variable within one crossing, and clones from one seed showed different developmental quality as well. The first flowering of hybrids obtained *in vitro* was noticed in 2006 and will be a source of further selection outdoors. The method used suggested as a very important wide-range possibility in the breeding process. We conclude that this approach can be successful in selecting the most quality clones in *in vitro* cultivation. We must assess whether these differences are observed in the field, including the proliferation rate.

References

Barba-Gonzalez R., Lim K.-B., Ramanna M.S., Visser R.G.F., Van Tuyl J.M. 2005. Occurrence of 2*n* gametes in the F_1 hybrids of Oriental × Asiatic lilies (*Lilium*): Relevance to intergenomic recombination and backcrossing. *Euphytica* 143: 67–73.

Chi H.S. 2000. Interspecific crosses of lily by *in vitro* pollinated ovules. *Bot. Bull. Acad. Sin.* 41: 143–149.

Chi H.S. 2002. The efficiencies of various embryo rescue methods in interspecific crosses of *Lilium*. *Bot. Bull. Acad. Sin.* 43: 139–146.

Ikeda N., Niimi Y., Han D.-S. 2003. Production of seedlings from ovules excised at the zygote stage in *Lilium* spp. *Plant Cell Tissue Organ Cult.* 73: 159–166.

Janson J., Reinders M.C., Van Tuyl J.M., Keijzer C.J. 1993. Pollen tube growth in *Lilium longiflorum* following different pollination techniques and flower manipulations. *Acta Bot. Neerl.* 42: 461–472.

Murashige T., Skoog F. 1962. A revised medium for rapid growth and bioassays with tobacco tissue cultures. *Physiol. Plant*. 15: 473–497.

Okazaki K., Umada Y., Urashima O., Kawada J., Kunishige M., Murakami K. 1992. Interspecific hybrids of *Lilium longiflorum* and *L.* × *formolongi* with *L. rubellum* and *L. japonicum* through embryo culture. *J. Jap. Soc. Hort. Sci.* 60: 997–1002.

Preťová A., Olbert B. 2006. Some aspects of embryo development *in vitro*. *Acta Hort.* 725: 83–88.

Proscevičius J. 2004. Fertility of lilies from group LA (*Longiflorum* – Asiatic hybrids). In: *Horticulture and Vegetable Growing.* Scientific Works of the Lithuanian Institute of Horticulture and Lithuanian University of Agriculture. 23: 232–241.

Van Creij M.G.M., Van Raamsdonk L.W.D., Van Tuyl J.M. 1993. Wide interspecific hybridization of Lilium: Preliminary results of the application of pollination and embryo-rescue methods. *North American Lily Society Yearbook* 46: 29–37.

Van Tuyl J.M., Van Diën M.P., Van Creij M.G.M., Van Kleinwee T.C.M., Franken J., Bino R.J. 1991. Application of *in vitro* pollination, ovary culture, ovule culture and embryo rescue for overcoming incongruity barriers in interspecific *Lilium* crosses. *Plant Sci*. 74: 115–126.

Van Tuyl J.M., Lim K.-B. 2003. Interspecific hybridization and polyploidisation as tools in ornamental plant breeding. *Acta Hort.* 612: 13–22.

Jauniegūtu starpsugu liliju hibrīdu embrioģenēze un attīstība *in vitro*

Gunta Jakobsone[1]*, Guntis Grants[2]

[1]Audu kultūru nodaļa, Nacionālais botāniskais dārzs, Miera 1, Salaspils LV-2169, Latvija
[2]*Lilium Balticum*, Latvija
*Korespondējošais autors, E-pasts: gunta.jakobsone@nbd.gov.lv

Kopsavilkums

Starpsugu hibridizācija ir vissvarīgākais izmaiņu avots dekoratīvo augu selekcijā. Audu kultūru metodes izmanto, lai pārvarētu apaugļošanās barjeras šiem hibrīdiem. Pētījuma mērķis bija izveidot mikrokultivēšanas sistēmu zigotisko embriju eksplantiem no starpsugu krustojumiem starp Āzijas, orientālo un trompešliliju grupu lilijām un atgriezenisko krustojumu derivātiem pamatojoties uz embriju izglābšanas metodi. Piecas liliju krustojumu kombinācijas 2002. gadā un 11 no 16 kombinācijām 2004. gadā deva pozitīvus rezultātus, lai gan ar atšķirīgu dīgšanas un embriju izdzīvošanas procentu.

Acta Universitatis Latviensis, 2008, Vol. 745, Biology, pp. 43–52

Late summer and autumn swarming of bats at Sikspārņu caves in Gauja National Park

Jurģis Šuba[1]*, Viesturs Vintulis[2], Gunārs Pētersons[3]

[1]Department of Zoology and Animal Ecology, Faculty of Biology, University of Latvia, Kronvalda Bulv. 4, Rīga, LV-1010, Latvia
[2]Museum of Zoology, University of Latvia, Kronvalda Bulv. 4, Rīga, LV-1010, Latvia
[3]Faculty of Veterinary Medicine, Latvian University of Agriculture, K. Helmaņa 8, Jelgava, LV-3004, Latvia

*Corresponding author, E-mail: jurgiss@imap.cc

Abstract

Late summer and autumn swarming of bats at underground hibernacula has so far been poorly investigated in the north-eastern part of Europe. This study was conducted at Sikspārņu caves in Gauja National Park in 2005 to 2007 with the main aim to determine the species composition of swarming bats and the swarming phenology for different species. Mist-nettings of swarming bats were performed once per fortnight from the end of June until the beginning of November. Altogether 3,448 bats of seven species were caught of which *Myotis daubentonii* and *M. brandtii* were the most numerous. For all species adult males predominated initially, but numbers of adult females and subadult individuals increased as the season progressed. The capture-mark-recapture method revealed an individual-specific trend of visitations by adult males of *M. daubentonii* in subsequent swarming seasons. Migration between different swarming and hibernation sites located at 5- to 21-km distances were also recorded.

Key words: autumn swarming, bats, Gauja National Park, *Myotis brandtii*, *Myotis daubentonii*.

Introduction

At the end of summer and in autumn bats gather at underground sites in great numbers and perform a peculiar flying behaviour, which involves circling inside or outside the hibernaculum, chasing each other and emitting various social calls (Fenton 1969; Thomas et al. 1979; Kretzschmar, Heinz 1995). This behaviour was first reported from North America in the 1960s and was termed autumn 'swarming' (Davis 1964). The most popular hypotheses regarding this behaviour are: (i) assessing hibernacula, (ii) show the location of hibernacula to offspring (Fenton 1969) and (iii) mating activities, hence facilitating the gene flow and preventing inbreeding (Kerth et al. 2003; Veith et al. 2004; Rivers et al. 2005). In the Baltics this phenomenon has been reported previously (Liiva, Masing 1987; V. Vintulis, unpublished data), but so far it has remained without further examination.

Sikspārņu (Bat) caves were discovered in the 1980s and a colony of about 150 hibernating *Myotis dasycneme* was found at this site (Busha 1986). Since then census of hibernating bats at these caves has been conducted every year.

The main aim of this study was to describe changes in the species composition, sex

and age structure of the bats during the autumn swarming period (further referred to as swarming season) to obtain basic knowledge about this phenomenon. Capture-mark-recapture method was used to check for possible migration between swarming sites and hibernacula and to analyze visitation tendencies for recaptured individuals within the same season and in consecutive seasons.

Materials and methods

The Sikspārņu caves are located in Gauja National Park near the town of Cēsis (57° 19', 25° 21'). Altogether six dolomite caves and holes have been discovered in this area. The largest of them – Lielā Sikspārņu cave (ca. 60 m in length) – was chosen as a study site for this research (Fig. 1). Seven bat species are known to hibernate in these caves regularly: *Myotis daubentonii* (Kuhl), *M. dasycneme* (Boie), *M. brandtii* (Eversmann, 1845), *M. mystacinus* (Kuhl), *M. nattereri* (Kuhl), *Eptesicus nilssonii* (Keyserling & Blasius) and *Plecotus auritus* (Linnaeus).

The study was conducted in 2005 to 2007. Swarming bats were mist-netted from the end of June until the beginning of November. During this period bat nettings (n = 6 in 2005, n = 7 in 2006, n = 8 in 2007) were performed only once per fortnight (usually twice per month) to minimize disturbance. Weather conditions varied during the netting events. We avoided only nights with strong wind and heavy rain, when nettings were not performed. The main entrance of the cave was covered by a mist-net for the entire night (Kunz, Kurta 1988), and two nearby entrances were closed by polythene, branches, and leaves. Captured bats were identified to species, sexed, aged and banded with numbered wing bands. We used aluminum bird rings, which were specially adapted for the bats (for *M. dasycneme* the ring diameter was 4.5 mm, but for other species – 3.0 mm). There were two classes of age (adults and subadults) used for age estimation according to degree of ossification and form of the metacarpal-phalageal joints (Anthony 1988). The bats were released after banding at the site of capture. Bat nettings using the same approach were additionally performed at two sandstone caves in the Gauja National Park at 8- and 21-km

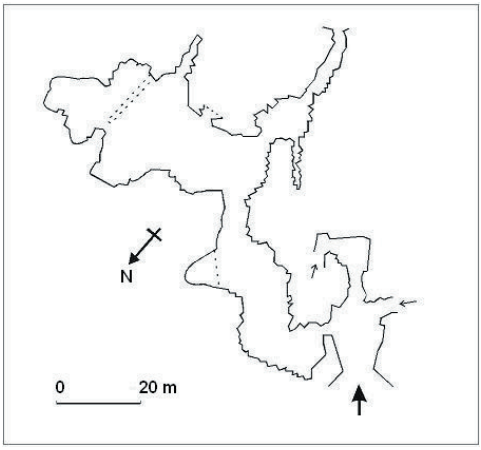

Fig. 1. Schematic plan of the Lielā Sikspārņu cave adapted from Eniņš (2004) (the main entrance and two other entrances covered in netting events are showen by arrows).

distances from the study site.

To compare species composition of bats in swarming and hibernation seasons at the Sikspārņu caves data from the annual hibernating bat census were used. In 2005 to 2007 census was conducted once every year in December or January. Hibernating bats were identified to species, except *M. brandtii* and *M. mystacinus*, which were pooled in one group '*M. brandtii*/*mystacinus*' (the accurate determination of these sibling species is impossible without disturbing their torpor). There are many deep and immense crevices in these caves, hence the actual number of hibernating bats might be considerably larger than recorded. Since 1992 all the important hibernacula in Gauja National Park as well as in other parts of Latvia have been surveyed every winter (V. Vintulis, unpublished data), and in the framework of this survey, search was made for bats with wing bands to check for possible migration between sites.

During most of the study period the presence of a roaming cat was noticed at the study site. This cat had adapted itself to catch and kill bats in the narrowest paths of the cave. The corpses and remains of the bats as well as the wing bands found were collected in every netting event. Dead recoveries were taken into account only in tests where the exact time of recapture was not required.

To compare the species composition between swarming and hibernation seasons Pearson's chi-squared goodness-of-fit test was used. This test was also performed in sex and age structure analysis and to compare the number of recoveries within one swarming season and consecutive swarming seasons, respectively. Spearman's rank correlation analysis was used to test the relationship of visitation timing in consecutive swarming seasons for individual bats if the sample size was greater than 15.

Results

During the swarming seasons altogether 3,448 individual bats of seven species were caught. The same species were found both in swarming and hibernation seasons, but their proportions differed between seasons (Table 1). In comparison with the swarming

Table 1. Number of bats found during hibernation seasons and caught during swarming seasons at the Lielā Sikspārņu cave in 2005 to 2007 (recaptures are not included)

Species	Hibernation seasons	Swarming seasons
M. daubentonii	23 (12.4 %)	1601 (46.4 %)
M. dasycneme	43 (23.1 %)	387 (11.2 %)
M. brandtii	–	973 (28.2 %)
M. mystacinus	–	141 (4.1 %)
M. brandtii/*mystacinus*	76 (40.9 %)	–
M. nattereri	5 (2.7 %)	289 (8.4 %)
Myotis sp.	12 (6.5 %)	–
E. nilssonii	3 (1.6 %)	36 (1.0 %)
P. auritus	15 (8.1 %)	21 (0.6 %)
Not identified	9 (4.8 %)	–
Total	186 (100 %)	3448 (100 %)

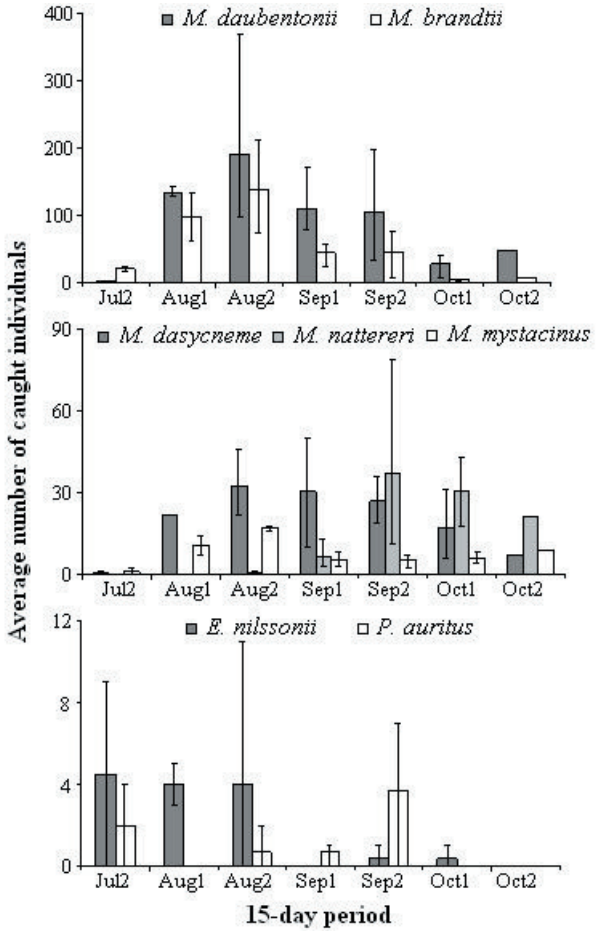

Fig. 2. Seasonal changes in mean, minimum and maximum number of caught bats during swarming seasons at the Lielā Sikspārņu cave in 2005 to 2007.

seasons, in the hibernation seasons *M. dasycneme* ($\chi^2 = 25.77$, d.f. = 2, $p < 0.001$) and *M. brandtii/mystacinus* ($\chi^2 = 6.15$, d.f. = 2, $p < 0.05$) were observed significantly more than expected, while *M. daubentonii* were found significantly less often than expected ($\chi^2 = 48.91$, d.f. = 2, $p < 0.001$).

For most species the greatest swarming activity was observed at the end of August and in September. Temporal distribution of swarming activity differed among species (Fig. 2). For *M. brandtii* and *M. mystacinus* the greatest swarming activity was observed at the end of August. *M. daubentonii* reached its peak activity at the end of August and in September. For *M. dasycneme* a clear maximum was not observed; the swarming activity for this species was high at the end of August and in September. *M. nattereri* was the last species to begin swarming with peak activity at the end of September and beginning of October. The greatest activity of *E. nilssonii* was observed at the end of July and in August, reaching its peak at the end of August. Later this species rarely visited the study site. The majority of *P.*

Table 2. Number of all autumn swarming captures at the Lielā Sikspārņu cave in 2005 to 2007 (recaptures are not included). The male dominance between adults and subadults tested by Pearson's chi-squared goodness-of-fit test (* – $p < 0.05$, ** – $p < 0.01$, *** – $p < 0.001$)

Sex and age group	*M. daubentonii*	*M. dasycneme*	*M. brandtii*	*M. mystacinus*	*M. nattereri*	*E. nilssonii*	*P. auritus*
Ad. males	654 (40.8 %)***	152 (39.3 %)***	357 (36.7 %)***	62 (44.0 %)*	142 (49.1%)**	14 (38.9 %)	12 (57.1 %)
Ad. females	379 (23.7 %)	86 (22.2 %)	202 (20.8 %)	37 (26.2 %)	93 (32.2%)	7 (19.4 %)	6 (28.6 %)
Total ad.	1027 (64.5 %)	238 (61.5 %)	559 (57.5 %)	99 (70.2 %)	235 81.3%)	21 (58.3 %)	18 (85.7 %)
Subad. males	330 (20.6 %)***	94 (24.3 %)***	216 (22.2 %)	21 (14.9 %)	23 (8.0%)	6 (16.7 %)	2 (9.5 %)
Subad. females	229 (14.3 %)	49 (12.7 %)	183 (18.8 %)	21 (14.9 %)	25 (8.7%)	7 (19.4 %)	1 (4.8 %)
Total subad.	559 (34.9 %)	143 (37.0 %)	399 (41.0 %)	42 (29.8 %)	48 (16.6%)	13 (36.1 %)	3 (14.3 %)
Indet. males	4 (0.2 %)	4 (1.0 %)	7 (0.7 %)	0	3 (1.0%)	0	0
Indet. females	3 (0.2 %)	2 (0.5 %)	8 (0.8 %)	0	1 (0.3%)	0	0
Indet. sex	2 (0.1 %)	0	0	0	2 (0.7%)	2 (5.6 %)	0
Total indet.	9 (0.6 %)	6 (1.6 %)	15 (1.5 %)	0	6 (2.1%)	2 (5.6 %)	0

Table 3. Number of recaptures in different years during swarming seasons at the Lieā Sikspārņu cave in 2005 to 2007 (dead recoveries included)

Year of banding	Year(s) of recapture	*M. daubentonii*	*M. dasycneme*	*M. brandtii*	*M. mytacinus*	*M. nattereri*	Total
2005	2005	8 (8.3 %)	4 (10.5 %)	4 (12.9 %)	0	2 (16.7 %)	18 (10.1 %)
2005	2006	26 (27.1 %)	15 (39.5 %)	14 (45.2 %)	1 (50 %)	2 (16.7 %)	58 (32.4 %)
2005	2006, 2007	1 (1.0 %)	1 (2.6 %)	0	0	1 (8.3 %)	3 (1.7 %)
2005	2007	7 (7.3 %)	4 (10.5 %)	2 (6.5 %)	0	7 (58.3 %)	20 (11.2 %)
2006	2006	13 (13.5 %)	2 (5.3 %)	3 (9.7 %)	1 (50 %)	0	19 (10.6 %)
2006	2007	31 (32.3 %)	8 (21.1 %)	6 (19.4 %)	0	0	45 (25.1 %)
2007	2007	10 (10.4 %)	4 (10.5 %)	2 (6.5 %)	0	0	16 (8.9 %)
Total		96 (100 %)	38 (100 %)	31 (100 %)	2 (100 %)	12 (100 %)	179 (100 %)

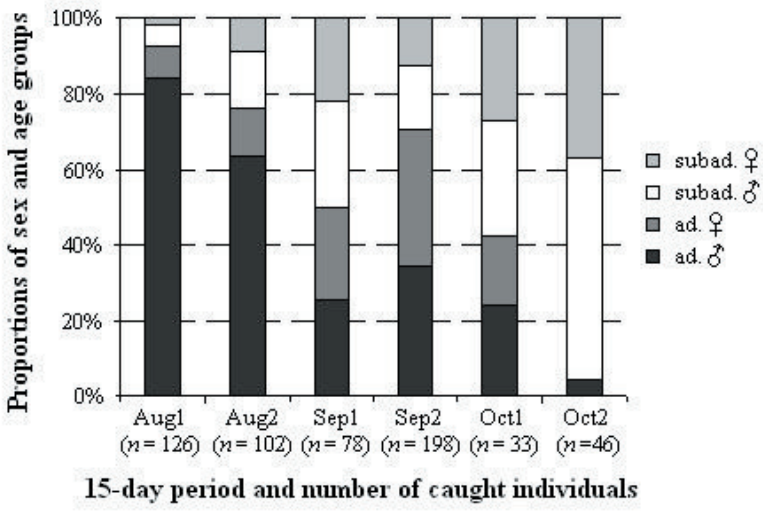

Fig. 3. Dynamics of particular sex and age groups of *M. daubentonii* netted at the Lielā Sikspārņu Cave in 2007 (recaptures are included).

auritus individuals were caught at the end of July and at the end of September.

The sex and age structure of caught individuals is shown on Table 2. Among adults significantly more males than females were observed for all *Myotis* species, but this difference was not significant for *E. nilssonii* ($\chi^2 = 2.38$, d.f. = 1, p = 0.12) and *P. auritus* ($\chi^2 = 2.06$, d.f. = 1, p = 0.15). The difference in numbers of subadult males and subadult females was not significant except for *M. daubentonii* ($\chi^2 = 18.25$, d.f. = 1, $p < 0.001$) and *M. dasycneme* ($\chi^2 = 14.17$, d.f. = 1, $p < 0.001$) – in these cases subadult males predominated. Temporal changes in sex and age structure during the swarming season, however, were common for all species. At the beginning of swarming the dominant group was formed by adult males, but the proportion of the adult females and subadult individuals increased as the season progressed (Fig. 3).

In this study 3,285 individual bats were banded. Only *Myotis* species were recaptured (Table 3). The total number of recaptured individuals, including dead recoveries, was 177 (5.4 %). There were significantly more cases where bats were recaptured in consecutive swarming seasons rather than in the same season ($\chi^2 = 31.35$, d.f. = 3, $p < 0.001$, the sample size for *M. mystacinus* was too small to include in this test). Spearman's rank correlation analysis revealed a significant relationship of visitation timing in consecutive swarming seasons for *M. daubentonii* adult males ($r = 0.97$, d.f. = 27, $p < 0.001$). For other species and sex-age groups this test was not performed due to small sample sizes.

Three bats were recaptured outside the banding sites (Fig. 4). One swarming *M. nattereri* subadult male was first caught and banded at an artificial sandstone cave ca. 21 km southwest of the study site, but later in the same year recaptured at the study site. At the same sandstone cave a lactating *M. mystacinus* female was recaptured, which was banded at the Lielā Sikspārņu cave in the previous year. Another *M. nattereri* adult male banded at the study site was found hibernating in a sandstone cave ca. 5 km northeast of the study site.

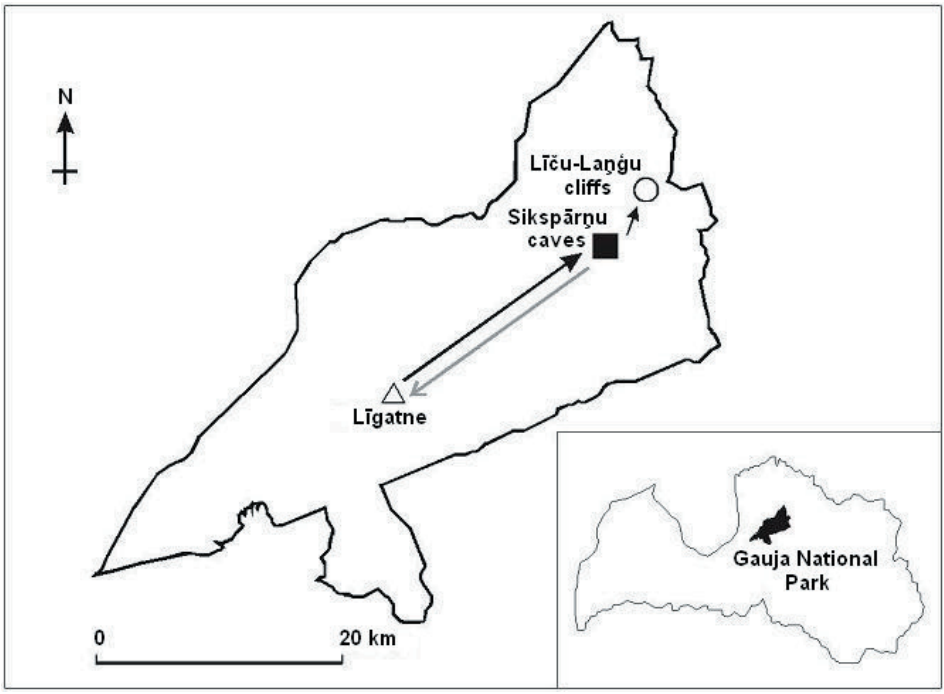

Fig. 4. Discovered bat movements among the Lielā Sikspārņu cave and other swarming (△) and hibernation (○) sites. Movements of *M. nattereri* are showed by black arrows, but the gray arrow represents *M. mystacinus* (see details in the text).

Discussion

In this study swarming behaviour was recorded for seven bat species, which all usually hibernate in underground sites. This supports the general opinion that autumn swarming behaviour is characteristic to those bat species using underground sites for hibernation (Fenton 1969; Kretzschmar, Heinz 1995; Parsons et al. 2003a). Therefore, swarming can be distinguished from another behaviour of bats at the end of summer called 'invasions' (Sachteleben 1991), which usually involves subadult and inexperienced individuals of *Pipistrellus* species, which accidentally enter buildings.

The differences in the species composition of the bats during the swarming and hibernation seasons can be explained by different habitat selection of species regarding hibernation in deep and large crevices (Furmankiewicz, Górniak 2002). For example, *M. dasycneme* are more likely to hibernate in bigger crevices than smaller species. Hence the proportions of this species observed in hibernation seasons may appear greater than they really are.

In this study the greatest swarming activity for most species was observed at the end of August and in September. Other studies performed in Czech Republic (Berková, Zukal 2006), Denmark (Degn et al. 1995), Germany (Harrje 1994), Great Britain (Parsons et al. 2003b; Rivers et al. 2006) and Poland (Furmankiewicz, Górniak 2002) suggest that the autumn swarming phenology in Latvia does not differ much from other parts of Europe.

The temporal distribution of swarming activity was species-specific. For example, *M. brandtii* and *M. mystacinus* had their activity peak in August, *M. daubentonii* – at the end of August and in September, and *M. nattereri* at the end of September and in October. It is known that these species leave their hibernacula in spring in the opposite order (Degn 1987; Parsons et al. 2003a). Parsons et al. (2003a) associate these observations with the foraging strategies of these species. *M. nattereri* is a gleaning species, which is able to capture prey from surfaces. Therefore, this species might be active for a longer period in the year than *M. daubentonii* and *M. brandtii*, which are specialized in catching flying insects. Moreover, *M. brandtii* and *M. mystacinus* are considerably smaller in size than other *Myotis* species. Hence their early swarming and start of hibernation could be related to thermoregulation as they have a large body surface-to-volume ratio (Ransome 1990).

In previous studies the visits of *E. nilssonii* at underground sites during the swarming seasons were considered occasional (Furmankiewicz, Górniak 2002; Karlsson et al. 2002). This study and other research in Latvia (J. Šuba, unpublished data) confirm that the swarming behaviour is characteristic of this species. For *Myotis* species it is known that their swarming activity overlaps with the start of hibernation (Fenton 1969; Harrje 1994; Trappmann 2005). In contrast, *E. nilssonii* actively swarm in August and up to the beginning of November they visit underground sites rarely.

Overall the proportions of different sex and age groups among the caught individuals tended to be species-specific, yet the temporal changes of the sex and age structure were common for all species. At the beginning of the swarming season the study site was mostly visited by adult males, but at the end of the season subadult individuals of both sexes predominated. Fenton (1969) suggests that swarming behavior could be related to the information transfer from adults to subadults, indicating the location of the hibernacula. Adult males may emerge earlier than females due to their idleness during the summer while females are rearing their offspring (Parsons et al. 2003a).

There were significantly more cases when bats were recaptured in consecutive swarming seasons than in the same season. An exhausting behaviour like swarming would considerably inhibit the fat deposition for the winter if performed continuously. Therefore, bats are expected to visit the swarming sites only once or a few times per season. The analysis of recaptured *M. daubentonii* adult males in consecutive swarming seasons shows that these bats tended to visit the swarming site at the same time every year. Similar results have been obtained in other studies (e.g. Fenton 1969; Parsons et al. 2003a).

The maximum distance of the diurnal roosts or hibernacula to swarming sites can be from 20 up to 60 km (Parsons, Jones 2003, Rivers et al. 2006). Capture-mark-recapture and radio-tracking studies indicate that bats from different summer roosts visit a common swarming site, which may also function as a hibernaculum, though migrations to other hibernacula have also been recorded (Fenton 1969; Parsons et al. 2003a; Parsons, Jones 2003; Rivers et al. 2006). There are two opinions about the swarming sites per se. There is evidence that bats show a great fidelity to a particular swarming site and do not visit other swarming sites (Parsons et al. 2003a; Parsons, Jones 2003), however, migration between different swarming sites have been recorded (Rivers et al. 2006). Bat migration found in this study indicate that two distant caves may serve as swarming sites for the same individuals.

Acknowledgements

This study was partly funded by Latvian Environmental Protection Fund and target program „Izglītībai, zinātnei, kultūrai" (for education, science and culture) of Latvian Educational Fund. We are grateful to all the fieldwork participants, especially to Ilze Čakare, Ineta Kalniņa, Normunds Kukārs, Saiva Lisovska, Ainis Platais, Urzula Nora Urbāne and Digna Vietniece, and Nancy Schnore for the linguistic corrections of the manuscript. The research was permitted by Gauja National Park Administration.

References

Anthony E.L.P. 1988. Age determination in bats. In: Kunz T. H. (ed.) *Ecological and Behavioral Methods for the Study of Bats.* Smithsonian Institute Press, Washington DC: 47–58.

Berková H., Zukal J. 2006. Flight activity of bats at the entrance of a natural cave. *Acta Chiropterol.* 8: 187–195.

Busha I.K. 1986. Hibernating colony of pond bats (*Myotis dasycneme* Boie) in Latvia. In: *Animal conservation, Ecology and Ethology.* University of Latvia, Rīga, pp. 45–52. (in Russian)

Davis W.H. 1964. Fall swarming of bats at Kentucky caves. *Bull. Nat. Speleol. Soc.* 26: 82–83.

Degn H.J. 1987. Bat counts in Mønsted limestone cave during the year. *Myotis* 25: 85–90.

Degn H.J., Andersen B.B., Baagøe H. 1995. Automatic registration of bat activity through the year at Mønsted Limestone Mine, Denmark. *Z. Säugetierkd*. 60: 129–135.

Eniņš G. 2004. *Caves in Latvia*. Zvaigzne ABC, Riga. 76 p. (in Latvian) /Alas Latvijā/

Fenton M. B. 1969. Summer activity of *Myotis lucifugus* (Chiroptera: Vespertilionidae) at hibernacula in Ontario and Quebec. *Can. J. Zool.* 47: 597–602.

Furmankiewicz J., Górniak J. 2002. Seasonal changes in number and diversity of bat species (Chiroptera) in Stolec mine (SW Poland). P*rzyroda Sudetów Zachodnich* S2: 49–70.

Harrje C. 1994. Etho-ökologische Untersuchung der ganzjahrigen Aktivität von Wasserfledermäusen (*Myotis daubentoni* Kuhl, 1819) am Winterquartier. *Mitt. natf. Ges. Schafthausen* 39: 15–52.

Karlsson B.-L., Eklöf J., Rydell J. 2002. No lunar phobia in swarming insectivorous bats (family Vespertilionidae). *J. Zool.* 256: 473–477.

Kerth G., Kiefer A., Trappmann C., Weishaar M. 2003. High gene diversity at swarming sites suggest hot spots for gene flow in the endangered Bechstein's bat. *Cons. Genet.* 4: 491–499.

Kretzschmar F., Heinz B. 1995. Social behaviour of a large population of *Pipistrellus pipistrellus* (Schreber, 1774) (Chiroptera: Vespertilionidae) and some other bat species in the mining-system of a limestone quarry near Heidelberg (South West Germany). *Myotis* 32/33: 221–229.

Kunz T.H., Kurta A. 1988. Capture methods and holding devices. In: Kunz T. H. (ed) *Ecological and Behavioral Methods for the Study of Bats*. Smithsonian Institute Press, Washington DC: 1–29.

Liiva E., Masing M. 1987. Ecological observations in hibernation shelters. *Tartu Riikliku Ülikooli toimetised* 769(XV): 41–55. (in Russian)

Parsons K.N., Jones G. 2003. Distribution and habitat use by *Myotis daubentonii* and *Myotis nattereri* during the swarming season: implications for conservation. *Anim. Conserv.* 6: 283–290.

Parsons K.N., Jones G., Davidson-Watts I., Greenaway F. 2003a. Swarming of bats at underground sites in Britain – implications for conservation. *Biol. Conserv.* 111: 63–70.

Parsons K.N., Jones G., Greenaway F. 2003b. Swarming activity of temperate zone microchiropteran bats: effects of season, time of night and weather conditions. *J. Zool.* 261: 257–264.

Ransome R. 1990. *The Natural History of Hibernating Bats*. Christopher Helm, London. 235 p.

Rivers N.M., Butlin R.K., Altringham J.D. 2005. Genetic population structure of Natterer's bats explained by mating at swarming sites and philopatry. *Mol. Ecol.* 14: 4299–4312.

Rivers N.M., Butlin R.K., Altringham J.D. 2006. Autumn swarming behaviour of Natterer's bats in the UK: Population size, catchment area and dispersal. *Biol. Conserv.* 127: 215–226.

Sachteleben J. 1991. Zum "Invasions" verhalten der Zwergfledermaus (*Pipistrellus pipistrellus*).

Nyctalus 4: 51–66.
Thomas D.W., Fenton M.B., Barclay R.M.R. 1979. Social behaviour of the little brown bat, *Myotis lucifugus*. 1. Mating behavior. *Behav. Ecol. Sociobiol*. 6: 129–136.
Trappmann C. 2005. *Die Fransenfledermaus in der Westfälischen Bucht*. Laurenti Verlag, Bielefeld. 120 S.
Veith M., Beer N., Kiefer A., Johannsen J., Seitz A. 2004. The role of swarming sites for maintaining

Sikspārņu vēlās vasaras un rudens spietošana Gaujas nacionālā parka Sikspārņu alās

Jurģis Šuba[1]*, Viesturs Vintulis[2], Gunārs Pētersons[3]

[1]Zooloģijas un dzīvnieku ekoloģijas katedra, Latvijas Universitātes Bioloģijas fakultāte, Kronvalda bulv. 4, Rīga LV-1586, Latvija
[2]Latvijas Universitātes Zooloģijas muzejs, Kronvalda bulv. 4, Rīga LV-1586, Latvija
[3]Latvijas Lauksaimniecības universitātes Veterinārmedicīnas fakultāte, K. Helmaņa 8, Jelgava LV-3004, Latvija
*Korespondējošais autors, E-pasts: jurgiss@imap.cc

Kopsavilkums

Rakstā aplūkota Eiropas ziemeļaustrumu daļā maz pētīta tēma – sikspārņu „spietošana" pie ziemošanas mītnēm vasaras beigās un rudenī. Pētījums veikts Sikspārņu alās (Gaujas nacionālajā parkā) no 2005. līdz 2007. gadam, un tā galvenais mērķis bija noskaidrot spietojošo sikspārņu sugu sastāvu un to spietošanas fenoloģiju. No jūnija beigām līdz novembra sākumam reizi divās nedēļās veikta spietojošo sikspārņu ķeršana un gredzenošana. Pavisam pētījuma periodā noķerti 3448 sikspārņi no septiņām sugām. Visām sugām spietošanas sezonas sākumā dominēja pieaugušie tēviņi, bet sezonas laikā ievērojami palielinājās pieaugušo mātīšu un nepieaugušo īpatņu īpatsvars. Pieaugušajiem ūdeņu naktssikspārņa tēviņiem konstatēta individuāla spietošanas laika izvēles tendence dažādās spietošanas sezonās. Konstatētas arī atsevišķu īpatņu pārvietošanās starp dažādām spietošanas un ziemošanas mītnēm piecu līdz divdesmit viena kilometra attālumā.

Acta Universitatis Latviensis, 2008, Vol. 745, Biology, pp. 53–61

Territorial and temporal distribution of Whooper Swan *Cygnus cygnus* marked with neck collars in Latvia in 2003 - 2005

Dmitrijs Boiko*

Natural History Museum of Latvia, Krišjāņa Barona 4, Rīga LV-1050, Latvia
Institute of Biology, University of Latvia, Miera 3, Salaspils LV-2169, Latvia

*Corresponding author, E-mail: dmitrijs.boiko@gmail.com

Abstract

In total 149 Whooper Swans *Cygnus cygnus* were marked with neck collars in Latvia from 2003 to 2005: 113 cygnets, 29 moulting non-breeders and seven breeding birds. Blue plastic neck collars with white inscription were used for marking. This article includes all data the author has received from 14 August 2003 till 31 December 2006. A total of 1329 resightings were received. Birds arrive in wintering places during November and December. The majority of these sites are located in the eastern part of Germany along the banks of River Elbe and Oder and in Poland near Oder River. Some birds were observed in Denmark, in The Netherlands and in the western part of Germany. The airline distance from ringing to wintering sites was 623 - 1189 km. In June birds ringed in previous year as cygnets were observed in Latvia and Estonia, during autumn migration – in Finland and Estonia. All these sightings show that Latvian young birds use locations far to the North from Latvia for moulting.

Key words: cygnets, migration, moulting, neck collar, Whooper Swan.

Introduction

In the middle of the 20th century Whooper Swan (*Cygnus cygnus* L.) bred only in North Russia and Scandinavia. In the 1970s it started to expand breeding range to the south. The breeding population of Whooper Swan in Europe is increasing. Now it has started to breed, for example, in Ukraine (M. Gavrilyuk, personal communication) and Hungary (Kovács 2005).

The first nesting Whooper Swan in Latvia was found in 1973 (Baumanis 1975). In the beginning of the 1980s 10 to 20 breeding pairs were counted (Priednieks et al. 1989), in 2000 to 2004 – 150 pairs (Boiko 2005). The number of breeding pairs in Latvia increased very rapidly, and in 2007 reached about 200 pairs.

Intensive ringing programmes for the Whooper Swan are implemented in Finland, Iceland and Sweden. Birds from Finland migrate along the Baltic Sea western coast and fly through Sweden to wintering places in Denmark, Germany, Belgium, England and The Netherlands (Laubek et al. 1998). The author began a Whooper Swan ringing programme in Latvia in 2003 because nothing was known about migration, wintering grounds and moulting locations. Since that time much material has been accumulated. The goal of the

present study is to summarize all the accumulated ringing data dealing with territorial and temporal distribution of the Latvian Whooper Swan population.

Materials and methods

Ringing of Whooper Swans

The author started a ringing programme for Whooper Swans in Latvia in summer 2003. The number of ringed birds is shown in Table 1. The umbers of ringed birds in different districts of Latvia are shown in Table 2. The most important ringing sites of moulting non-breeders are Skrunda fish ponds (56°42'N, 21°59'E), for cygnets Renda fish ponds (57°04'N, 22°17'E) and Rimzāti fish ponds (56°58'N, 22°10'E).

For ringing blue plastic neck collars with white inscription were used: 1C00 - 1C99, 2C01 - 2C49. Neck collars are 83 mm in height, plastic thickness – 3 mm, inner diameter – 57 mm and weight – 71 g. Number and letter height is 77 mm and width 33 mm. It is possible to read the numbers from a distance 50 to 300 m using a 20 - 60 × telescope. Each bird was also ringed with a metal leg ring.

Cygnets were caught at age of 8 - 11 weeks for ringing. At this age they are large enough to implace a neck collar, but they are still flightless. They reach this age in Latvia during the end of July to beginning of August. Moulting birds were ringed from early July till late August. Breeding birds moult on breeding grounds and therefore it was possible to captive them.

In Latvia Whooper Swans stay mainly in ponds and fish ponds with a depth of 0.3 to 2 m (D. Boiko, unpublished data). For captive we used a plastic boat. The catching team consisted of 2 to 12 persons: one on the boat, others wading tried to find and catch cygnets by hand or with a "swan hook" (3 m long bamboo handle with hooked wire on the end which helps to grab the swans neck) in vegetation.

In deeper places (more than 1 m) we used motorboats. Very often cygnets dove and then emerged 10 - 50 m from the boat.

In breeding places bordering with wood cygnets often run into shrubs while catching, making capture difficult. In breeding places with high and dense vegetation cygnets remain still.

In Skrunda fish ponds we used motorboats and a "swan hook" for catching. During moulting the bird is flightless. It was very hard to catch adult swans because often they dove. Some birds were caught only after some 40 minutes effort. During this time other moulting birds ran far into the woods.

Table 1. Number of ringed Whooper Swans *Cygnus cygnus* with neck collars in Latvia

Year	Cygnets	Moulting breeding birds	Moulting non-breders	Total
2003			2	2
2004	33	3	7	43
2005	80	4	20	104
Total	113	7	29	149

Table 2. Number of ringed Whooper Swans *Cygnus cygnus* in different districts of Latvia in 2003 - 2005 (C - cygnets, M - moulting non-breeders plus moulting breeders)

District	2003		2004		2005		Total	
	C	M	C	M	C	M	C	M
Kuldiga	–	2	14	8	44	21	58	31
Liepaja	–	–	18	2	22	2	40	4
Saldus	–	–	1	–	10	1	11	1
Talsi	–	–	–	–	3	–	3	–
Valmiera	–	–	–	–	1	–	1	–
Total	–	2	33	10	80	24	113	36

Data collecting and processing

The author entered the information about the swan ringing project with blue neck rings into the web: www.lob.lv, www.cr-ebirding.be where bird watchers can obtain the author`s address and e-mail. They were asked to give information about the neck collar inscription, location, state, country, coordinates, habitat and flock size. After receiving of data author checked the coordinates, and the observer was provided with all available information about the bird observed.

All information about ringing and all resightings were entered in Microsoft Access database. Distance between ringing and recovering place was calculating using the Google Earth programme. Maps were produced using the ArcMap9.1.

This article includes all data obtained from 14 August 2003 till 31 December 2006. A total of 149 birds during summers 2003 - 2005 were ringed, and 1329 resighting reports were received. The resighting data was divided into four periods: spring – from March 1 till May 31; summer – from June 1 till August 31; autumn – from September 1 till November 31; winter – from December 1 till February 28 or 29.

Results and discussion

Migrations and wintering places

The number of ringed cygnets in different districts of Latvia is shown in Table 2. Cygnets were mostly ringed in the western part of Latvia where about 85 % of Latvian Whooper Swan population is breeding (D. Boiko, unpublished data).

In September and October cygnets and their parents left breeding places and arrived in wintering locations after 1 to 2 months (Fig. 1). The birds from Finland breeding grounds also spend about 1 to 2 months travelling to wintering grounds (Laubek et al. 1998).

During November and December birds arrive in wintering places. The majority of these are located in eastern Germany along the banks of River Elbe and Oder (Fig. 1, 3). Some birds were observed in Poland close to the German border near River Oder. Only a few birds were observed in western Germany. During the second winter of study one bird was found in Denmark (Jutland) and two in The Netherlands. The distance from ringing place to wintering places was 623 to 1189 km. Gardarsson (1991) studied the Iceland breeding population from which birds fly 800 to 1200 km from breeding grounds to wintering places. Whooper Swans from Finland fly 700 to 2100 km to wintering places

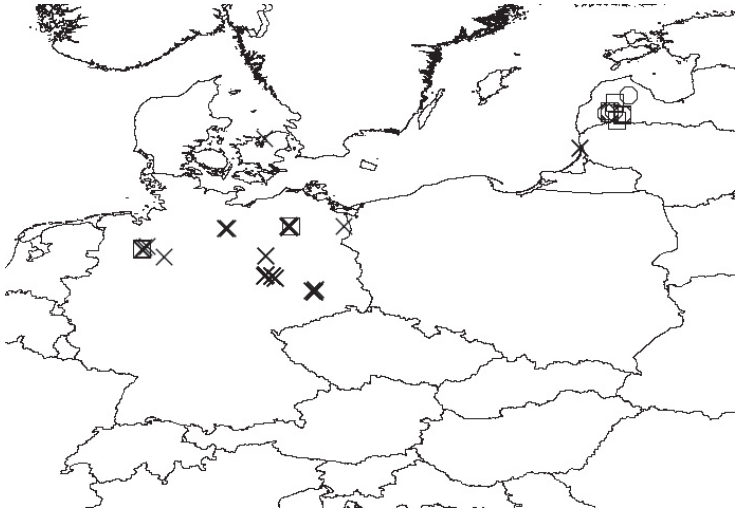

Fig. 1. Recoveries of Whooper Swan *Cygnus cygnus* ringed in Latvia as cygnets and observed during their first autumn (O - September, □ - October, × – November).

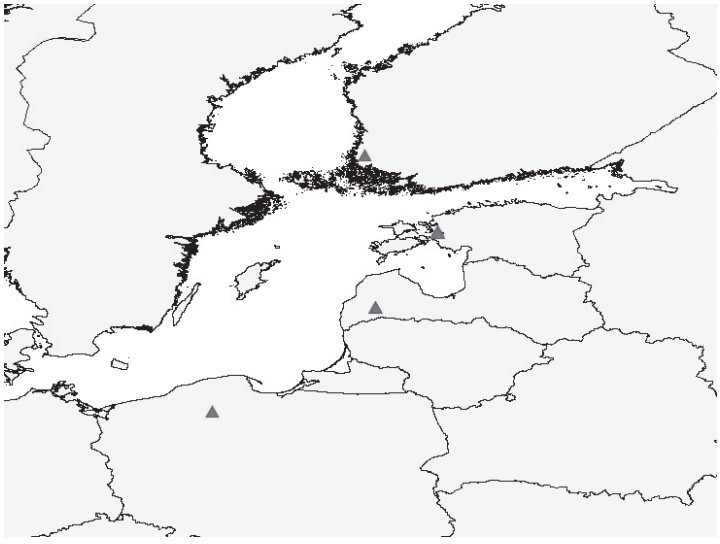

Fig. 2. Summer (June) recoveries of Whooper Swan *Cygnus cygnus* ringed in Latvia as cygnets, and recovered during the second calendar year.

(Laubek et al. 1998) located in Sweden, Denmark, Germany, The Netherlands and Great Britain. Our study shows that Latvian Whooper Swans possibly migrate along the eastern coast of the Baltic Sea. From Finland Whooper Swans migrate along the western coast of the Baltic Sea (through Sweden) (Laubek et al. 1998). Until 31 October 2006 we have no reports from Finland Whooper Swans with a neck collar seen in Latvia.

In March some of our birds started to migrate in the East and North-East direction but others still remained in wintering places.

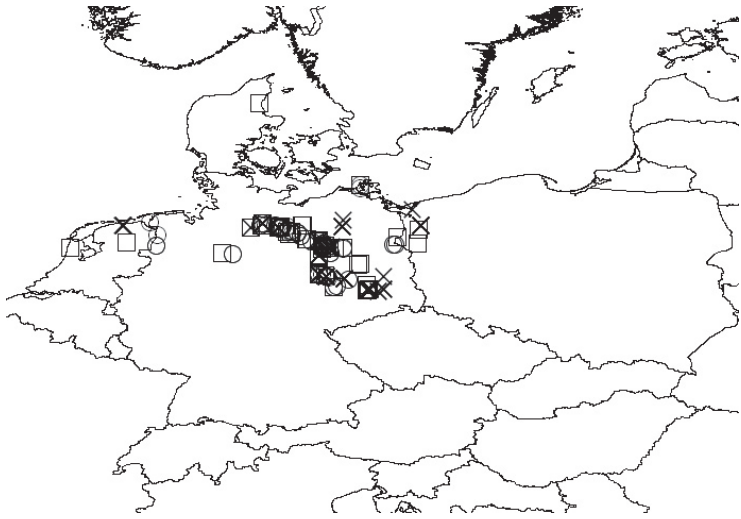

Fig. 3. Winter recoveries of Whooper Swan *Cygnus cygnus* ringed as cygnets in Latvia (× - December, □ - January, O - February).

Ten birds in April were observed in Poland in Wartha Mouth National Park or near this location. Seven birds in April were observed still in wintering sites in Germany but eight of young birds were observed already in Latvia 0 to 117 km from their hatching sites.

In May twelve young birds were observed near their hatching sites (0 to 38 km). Four of them were observed there already in April.

Moulting non-breeders were ringed mostly in Kuldiga district in Skrunda fish ponds. In total 28 birds were ringed in Skrunda fish ponds: two in 2003, seven in 2004, and 19 in 2005. The majority of birds were ringed in August.

The number of moulting non-breeders in Skrunda fish ponds was 60 - 70 birds in 2003 - 2005. In autumn (September and October) 53 % of ringed non-breeders were observed in the ringing location. After draining of fish ponds (early and middle October) birds left area. At the end of September and early October 167 % of ringed non-breeders were observed outside Skrunda fish ponds in Saldus district in the Sātiņi fish ponds (distance 24 km).

At the end of October and November the first birds arrive in wintering sites in Germany near Elbe and Oder River banks. We have just one observation in December and two observations of two birds in January from the western part of Poland at the Milicz fish ponds.

During spring migration (March) birds fly to the East and North-East. Six birds were observed in the Wartha Mouth National Parki in Poland where they have not been observed in winter.

In April we received records of two birds: the first from Milicz fish ponds where a Whooper Swan with neck collar 1C01 was observed each spring in April and May (distance 664 km. South-West direction), the second are from Konicpol fish ponds (distance 674 km. South-West direction). We have no other observations of birds ringed as moulting birds and observing during migration in April.

Table 3. Whooper Swans *Cygnus cygnus* ringed as cygnets in Latvia and observed in Finland during migration in the 2nd and 3rd autumn

Neck collar	Ringing date	Observation date	Distance from ringing place (km)
1C23	26 July 2004	24 October 2006	668
1C74	29 July 2005	4 October 2006	569
1C81	29 July 2005	3 October 2006	699
1C98	30 July 2005	2 October 2006	716
1C98	30 July 2005	3 October 2006	716
1C98	30 July 2005	8 October 2006	716
1C99	30 July 2005	2 October 2006	716
1C99	30 July 2005	3 October 2006	716
1C99	30 July 2005	8 October 2006	716
2C18	1 August 2005	18 October 2006	655
2C18	1 August 2005	4 October 2006	662
2C18	1 August 2005	5 October 2006	662

Distribution of non-breeders during summer

In June 2006 we have records of ten birds ringed in summer 2005 as cygnets in Latvia. One bird was observed in Poland in 2 June 2006, 416 km South-West from the hatching site. In Latvia we observed seven birds (all in Skrunda fish ponds). Four of them were ringed in the previous summer in the same location. Others were observed 15 to 17 km from hatching sites. Six of them were observed in the Skrunda fish ponds in 5 June 2006 and in 13 June 2006 five of them observed 250 km North-East in Estonia in Matsalu Bay. In the same location in Estonia in June 2006 three more Whoopers were recorded (ringed in summer 2005 in Latvia as cygnets). For two of them these were first observations. In 2 June 2005 one bird (ringed in Latvia in 2004 as a cygnet) was observed 465 km from the ringing place in South Finland (Fig. 2).

During autumn migration six birds were observed in Finland. Ringing and recovery dates as well as distance from ringing place to observation site in Finland (all these observations are of birds in the 2nd and 3rd autumn) are shown in Table 3.

The autumn observations from Finland, Latvia and Estonia in June show that our young birds after first and second wintering fly far away from hatching locations to the North. A bird with neck collar 1C23 in 24 October 2006 was observed in Finland and on the next day, in Western Estonia at a distance of 455 km. Until now this is the longest distance covered in one day.

The number of sight records of cygnets ringed in Latvia in 2004 - 2005 and seen after one year (September 1 till August 31) is very high – 79 % of all ringed cygnets, compared to 47 % in Finland (Ohtonen 1996) and 62 % in Iceland (Gardarsson 1991). This suggests that our Whooper Swan cygnets have a comparatively low mortality, which may be because they have enough time after hatching to remain in the breeding location and to grow up – about two months. In Finland cygnets fledge in September and they have only few weeks to start migration (Haapanen 1991).

Ohtonen (1996) found that two birds ringed as cygnets in Finland were recorded in

the NE direction from the ringing site: one ringed in 3 October 1989 was found dead in 23 June 1991 in Finland 338 km North-East of the ringing site; the second ringed in 13 September 1987 was found dead in 16 June 1990 590 km North-East from the ringing site in Murmansk region in Russia. Both of these recoveries and our observations show that birds in their second summer fly in the North and North-East direction from their ringing locations. Possibly this migration direction is genetically determined, as North regions are their historical homeland. Haapanen (1991) considers north regions to be superior for moulting, but for breeding there is too short a time even if the habitats are suitable.

Up till now we have no recoveries in July and August (this is the time when birds moult) from Latvian Whooper Swans ringed as cygnets neither from abroad nor in the well known Whooper Swan moulting ground in Latvia – in the Skrunda fish ponds.

In May two birds ringed as moulting non-breeders were observed in the ringing site in Skrunda fish ponds and one in Satini fish ponds. In June this number increased to nine birds and decreased in July (time when birds moult) to two birds.

There was a resighting from Finland in 21 July 2006 when a pair of birds was observed and one of the partners had a neck collar with code 1C66. This bird was ringed in 22 July 2005 as a two-year-old male, and was observed also in Latvia in 14 May 2006 in the Satini fish ponds. Probably this bird occupied a breeding territory. The distance between ringing and recovery locations is 620 km. Whooper Swans start breeding at the age of three or four years (Cramp et al. 1994). This means that before breeding Whooper Swans occupy potential breeding territory and protect it to breed during the next years.

A bird with neck collar 1C01 ringed in 09 August 2003 as three-year-old non-breeder (moulting) female in Skrunda fish ponds was observed each year in the Milicz fish ponds in Poland: in 2004 from 10 April to 30 May, in 2005 on 4 June and from 30 October to 20 November, in 2006 from 31 July to 19 November. In summers 2004 and 2005 this bird moulted also in the Skrunda fish ponds and was observed there till early October. Perhaps in 2006 it bred unsuccessfully in the Milicz fish ponds or nearby (observed pair without cygnets), which might explain why in summer 2006 it was observed in Poland but not in Latvia. There are about 20 to 50 moulting Whooper Swans in Milicz fish ponds each summer (Wieloch, personal communication). This may be a bird from the Polish Whooper Swan population, which each year moults in Latvia when we ringed it in summer 2003.

In summer 2005 in the Skrundas fish ponds a Whooper Swan with yellow neck collar and code 3R03 moulted. This bird was ringed in the central part of Poland in 20 August 2004 as a cygnet (649 km from ringing site). Later after moulting this bird was observed in Poland in the Milicz fish ponds. Unfortunately, we subsequently not observed this bird in Latvia. This is the first observation in Latvia of a Whooper Swan ringed in Poland. Perhaps, some of the moulting birds in Skrunda fish ponds are from the Poland Whooper Swan population. This means that other cygnets fly great distances for moulting to Finland or Russia, but some birds, for example from Poland, to Latvia. More studies are needed for clarification.

Brazil (1983) calculated that in the first ten months after ringing of moulting birds in Iceland he obtained recoveries from 48 % birds. In Latvia during the first year after ringing we achieved 86 % of all ringed moulting non-breeders. It is possible that 24 years ago in Iceland the recording intensity was less intense or that the optics were insufficient for observations.

Conclusions

The majority of Whooper Swans ringed in Latvia (cygnets and moulting non-breeders) winter in Eastern Germany along the Rivers Elbe and Oder banks or near them. A few birds have been observed also in Western Germany, Poland, Denmark and The Netherlands. They arrive to wintering sites using the southern coast of the Baltic Sea.

Some observations during migration in Estonia and Finland provide evidence that part of our Whooper Swans moult in Finland and perhaps in Russia.

Acknowledgements

The study was supported by the Environmental Protection Fund of Latvia, Natural History Museum of Latvia, and the European Social Fund to the University of Daugavpils 2004/0003/VPD1/ESF/PIAA/04/NP/3.2.3.1/0001/0003/0065. Much thanks is given to my scientific adviser, prof. Jānis Vīksne. Artūrs Laubergs, Jānis Bisters, Aigars Lamberts, Linda Madžule, Matīss Žagars, Oskars Keišs, Iļja Boiko, Juris Lipsbergs, Ruslans Matrozis, Maria Wieloch, Trinus Haitjema, Pelle Andersen-Harild, Radoslaw Wlodarczyk, Axel Degen and many others are acknowledged for assistance in the field and useful discussions about the study. Many thanks go to numerous observers who sent me the recovery data.

References

Baumanis J. 1975. Nesting of Whooper Swan (*Cygnus cygnus* L.) in Latvia. *Zooloģijas Muzeja Raksti* 12: 79–81. (in Latvian) /Ziemeļu gulbja (*Cygnus cygnu*s L.) ligzdošana Latvijā/

Boiko D. 2005. Whooper Swan *Cygnus cygnus* breeding in Latvia in 2004. Materials of the 3rd International Conference "*Research and Conservation of Biological Diversity in Baltic Region*", Daugavpils, April 20-22, 2005, Daugavpils University, p. 43.

Brazil M. 1983. Preliminary results from a study of Whooper Swan movements using neck-collars. *J. Coll. Dairying* 10: 79–90.

Cramp S. (ed). 1994. *Handbook of the Birds of Europe the Middle East and North Africa*. Vol. 1. Oxford University Press, Oxford. 385–391 p.

Gardarsson A. 1991. Movements of Whooper swans neckbanded in Iceland. *Proceedings of the Third IWRB International Swan Symposium, Oxford, 1989.* S1: 189–194.

Haapanen A. 1991. Whooper Swan *Cygnus cygnus* population dynamics in Finland. *Proceedings of the Third IWRB International Swan Symposium, Oxford, 1989*. Wildfowl S1: 137–141.

Kovács S.Á. 2005 Whooper swan as a breeding bird again in Hungary. *Madártávlat* XII/4: 10. (in Hungarian)

Laubek B, Knudsen HL, Ohtonen A. 1998. Migration and winter range of Whooper Swans *Cygnus cygnus* breeding in different regions of Finland. In Laubek B. (ed) *The Northwest European Whooper Swan (*Cygnus cygnus*) population: ecological and management aspects of an expanding waterfowl population*. PhD thesis, University of Aarhus, Denmark.

Ohtonen A. 1996. Resightings of the Whooper Swan (*Cygnus cygnus*) marked with neck-collars on their breeding grounds in Finland. *Gibier Faune Sauvage, Game and Wildl.* 13: 13–47.

Priednieks J., Strazds M., Strazds A., Petriņš A. 1989. *An Atlas of Latvian Nesting Birds 1980 - 1984*. Rīga, Zinātne. Pp. 95–96. (in Latvian) /Latvijas ligzdojošo putnu atlants 1980.-1984./

Ar kakla gredzeniem 2003. - 2005. gadā Latvijā iezīmēto ziemeļu gulbju *Cygnus cygnus* izplatība telpā un laikā

Dmitrijs Boiko*

Latvijas Dabas muzejs, Krišjāņa Barona 4, Rīga LV-1050, Latvija
Latvijas Universitātes Bioloģijas institūts, Miera 3, Salaspils LV-2169, Latvija
*Korespondējošais autors, E-pasts: dmitrijs.boiko@gmail.com

Kopsavilkums

No 2003. līdz 2005. gadam Latvijā ar kakla gredzeniem iezīmēja 149 ziemeļu gulbjus *Cygnus cygnus*. No tiem, 113 mazuļus, 29 neligzdojošos pieaugušos gulbjus spalvu maiņas laikā un septiņus pieaugušos gulbjus ligzdošanas laikā. Iezīmēšanai izmantoja zilas krāsas kakla gredzenus ar baltas krāsas ciparu un burtu kodu. Šai rakstā apkopota informācija, ko autors ir saņēmis laika posmā no 2003. gada 14. augusta līdz 2006. gada 31. decembrim Kopumā saņemti dati par 1329 kakla gredzenu nolasījumiem. Latvijas ziemeļu gulbji ierodas ziemošanas vietās novembrī un decembrī. Lielākā daļa no šīm ziemošanas vietām atrodas Vācijā gar Elbas and Odras upes krastiem, kā arī Polijā netālu no Odras upes. Dažus putnus novēroja arī Dānijā, Holandē un Vācijas rietumu daļā. Attālums starp gredzenošanas un ziemošanas vietām bija 623 - 1189 km. Jūnijā putni, kas bija gredzenoti iepriekšējā gadā kā mazuļi Latvijā, ir novēroti Igaunijā un, rudens migrācijas laikā, Somijā. Visi šie novērojumi liecina par to, ka mūsu ziemeļu gulbji maina spalvas tālu uz ziemeļiem no Latvijas. Nepieciešami tālāki pētījumi, lai atrastu tam pierādījumus.

Acta Universitatis Latviensis, 2008, Vol. 745, Biology, pp. 63–74

Influence of inorganic nutrients and dissolved organic matter on the growth of cyanobacteria *Microcystis aeruginosa* isolated from the Gulf of Riga

Santa Purvina[1]*, Christian Béchemin[2], Maija Balode[1], Daniel Grzebyk[2], Serge Y. Maestrini[2]

[1]Latvian Institute of Aquatic Ecology, Daugavgrīvas 8, LV-1048, Riga, Latvia
[2]Centre de Recherche en Ecologie Marine et Aquaculture de L'Houmeau (CNRS-IFREMER), B.P. 5, F-17137 L'Houmeau, France

*Corresponding author, E-mail: santa.purvina@lhei.lv

Abstract

The influence of nutrient additions in N-limiting, P-limiting and in DIN:DIP-balanced conditions with and without dissolved organic matter (DOM) of land origin was studied on the growth and toxin content of *Microcystis aeruginosa* isolated from the Gulf of Riga. The dissolved inorganic nitrogen (DIN) and dissolved inorganic phosphorus (DIP) supply in balanced ratio of DIN : DIP = 16 is the main determinative factor for *M. aeruginosa* development, promoting increases in cell biomass, chlorophyll *a* content and particulate organic matter. In medium enriched only by DOM, *M. aeruginosa* used 31 % of the available dissolved organic nitrogen and 53 % of the dissolved organic phosphorus. The experiment conditions did not invoke increment of toxicity. The experiments showed that the development of *M. aeruginosa* is promoted by the raised load of inorganic nutrients and dissolved organic matter to the brackish ecosystems of the Baltic Sea.

Key words: cyanobacteria, dissolved organic matter, *Microcystis aeruginosa*, nutrient limitation, the Gulf of Riga.

Introduction

Nutrients, light and temperature are the most important factors for the development of marine phytoplankton. Human activities contribute to increased nutrient discharge to aquatic ecosystems from agriculture, municipal and industrial waste waters world wide. These anthropogenic nutrient sources have led to increased nutrient fluxes also in the Baltic Sea invoking eutrophication processes, followed by reduced water transparency, increased phytoplankton primary production, changes of planktonic species composition etc. (HELCOM 2007). Significant impact on nutrient input is favored also in terms of climate change. For the Baltic Sea ecosystems important changes are in the timing of the seasonal events: water discharge increment in winter in association with the reduction of spring runoff and shortening of the ice and snow cover period. Estimates indicate that river runoff may increase by up to 15 % averaged over the Baltic Sea catchment region, enlarging the export of dissolved organic matter to the brackish ecosystems (HELCOM 2007). Significant dependence of the river discharge on climate change has been also

found in Latvia (Kļaviņš, Rodionovs 2007).

Two bottom-up mechanisms have been invoked as major contributors in the increase of toxic algal blooms in last decades. From one side, human activities significantly increase the input of algal nitrogenous and phosphorus nutrients to estuarine and coastal waters, while the silicon concentration has remained constant or has even decreased in river loads to brackish estuaries (Rahm et al. 1996). It is assumed that in such conditions the proliferation of organisms having little or no requirement for silicon, such as flagellates and cyanobacteria, is favored (Humborg et al. 2000). On the other side coastal waters close to estuaries receive large quantities of dissolved organic matter (DOM), which may favor the growth of auxotrophic/photo-heterotrophic species versus that of autotrophic species (Paerl 1988).

Cyanobacteria have been responsible for the most harmful phytoplankton events in the Baltic Sea. Over the entire Gulf of Riga the potentially toxic cyanobacteria *Aphanizomenon flos-aquae*, *Nodularia spumigena*, *Snowella lacustris* and *Anabaena lemmermannii* can develop, whereas in the coastal areas common species are *Anabaena spiroides*, *Anabaena flos-aquae* and *Microcystis aeruginosa* (Balode, Purina 1996). The potentially toxic cyanobacteria *Microcystis aeruginosa* is mostly known to develop in freshwater, but it is also frequently observed in marine coastal waters (Kononen, Sellner 1995). Additionally, high concentration of *M. aeruginosa* biomass is transported to estuarine areas via rivers. In the coastal areas of the Gulf of Riga maximum development of *M. aeruginosa* continues from late June till September., the development usually occurs sporadically, but often are initiated blooms in the coastal zones (Balode, Purina 1996; Seppälä, Balode 1999). *M. aeruginosa* abundance is related with high nutrient concentrations (Rantajärvi et al. 1998). Studies on this species have intensified in the last decades mainly due to the discovery of potent hepatotoxic heptapeptides, called microcystins, shown to be deleterious to wild and domestic animals and also humans.

In natural water-bodies *M. aeruginosa* is found as several toxic and non-toxic genotypes. Whether a genotype can produce microcystins depends on the presence of intact genes from the microcystin synthetase gene complex (Kurmayer et.al. 2002). A seasonal succession of different *Microcystis* genotypes might often be a key mechanism determining microcystin concentrations in *Microcystis*-dominated lakes (Kardinaal et.al. 2007a) and other water-bodies. In nature several mechanisms might be involved in seasonal succession of toxic and non-toxic *Microcystis* strains: selective feeding by bivalves (Dionisio-Pires, Van Donk 2002) and zooplankton (Lürling 2003), *Microcystis* strains may differ in their buoyancy (Dunton, Walsby 2005) and competitive ability for light (Kardinaal et al. 2007b). The changes in nutrient concentrations and ratios in the environment affect not only phytoplankton community structure, but also algal physiology. Thus N-rich PSP toxins are synthesized during excess N and P-limitation but not during N-limitation (Granéli et al. 1998).

The estimated microcystin concentrations of *M. aeruginosa* isolated from the Gulf of Riga are low and range between 0.8 to 4.5 ng mg^{-1} dry mass. The potentially toxic cyanobacteria *Nodularia spumigena* also can produce hepatotoxic toxin nodularin in high concentrations. However the observed toxicity of *Nodularia spumigena* in the Gulf of Riga is lower (nodularin 0.030 - 0.123 mg L^{-1}) than in the Open Baltic Sea (0.03 - 1.35 ng mg^{-1}); the toxin content of the Gulf of Riga *Nodularia spumigena* filaments is about 12 times higher than those from the open Baltic (Balode, unpublished data).

The aim of the present study was to test the effect of dissolved organic matter and raised inorganic nitrogen and phosphorus concentrations in different DIN : DIP ratios on the growth and toxicity of potentially toxic cyanobacteria *M. aeruginosa*, isolated from the coastal area of the Gulf of Riga, the Baltic Sea.

Materials and methods

The clone culture of *Microcystis aeruginosa* Kützing (MAGR-2) was isolated from the Gulf of Riga, Baltic Sea. The stock culture was grown in F medium of Guillard and Ryther (1962), the N : P ratio was adjusted to the Redfield value – 16 (1934). Iron was added in the form of Fe-EDTA.

The *M. aeruginosa* mother culture was obtained after centrifugation in sterile conic flasks. Supernatant containing the growth media was removed and cells were re-suspended in nutrient-free sterile seawater and left for 24 h in the culture room. Then, centrifugation and re-suspension were repeated, resulting in partly nutrient-depleted *M. aeruginosa* cells in a mother suspension free from dissolved nutrients. The culture was inoculated to experimental 5 L bottles, providing an initial concentration of *M. aeruginosa* 18.7×10^6 cells per liter. The cultures were grown at 18 ± 1 °C, with a 16 h / 8 h light/dark period at 53 μmol m^{-2} s^{-1} irradiance from cool white fluorescent lamps.

The growth of *M. aeruginosa* was tested in natural seawater (control), in phosphorus limitation condition (DIN : DIP = 100), in nutrient balanced (DIN : DIP = 16), as well as in nitrogen limitation (DIN : DIP = 3) conditions. All experimental treatments were incubated in three replicates. To test the effect of dissolved organic matter (DOM) a parallel set of treatments was established with DOM addition, also in three replicates. For the experimental phosphorus limitation, balanced N and P and nitrogen limitation treatments, pre-autoclaved sterile nutrient solutions of $NaNO_3$ and/or KH_2PO_4 and 0.22 μm filtered DOM were aseptically added (Table 1). Cultures were grown in filter-sterilized (0.22 μm) seawater (4 L) in 5-L polycarbonate pre-autoclaved bottles. Enrichments of Fe-EDTA, metals and vitamins were added. Nutrient additions were made gradually from Day 0 to Day 6. Pure seawater and seawater with DOM addition was used as a control in triplicate.

M. aeruginosa growth was monitored daily by *in vivo* fluorescence with a 10 AU Turner Fluorometer (Brand et al. 1981). Estimation of cell number and nutrient concentration was performed on Day 7 (one day after the end of the nutrient addition), Day 9 (end of exponential growth phase), Day 12 and Day 15 (stationary phase). Cell counting was performed until Day 24.

M. aeruginosa cell samples (5 mL; Neubaeur cell) were fixed with acid Lugol's solution and counted under a microscope. Chlorophyll *a* was determined spectrophotometrically after filtration through glass microfibre filters (Whatman GF/F), and extraction with pure methanol, at 4 °C, for 1 h in the dark (Jespersen, Christofersen 1987).

Inorganic nutrient concentrations were measured with a Skalar autoanalyzer, following standard procedures for seawater (Valderrama 1995).

Samples for particulate organic carbon (POC) and particulate organic nitrogen (PON) analysis were collected on precombusted glass microfibre filters Whatman GF/F, then decarbonated (HCl fumes, overnight), and analyzed using a CHN analyzer, model 1500 from Carlo Erba. Samples for particulate organic phosphorus (POP) were collected as for

Table 1. Concentration of dissolved organic matter (DOM), dissolved inorganic nitrogen (DIN) and dissolved inorganic phosphorus (DIP) added to control (Control + DOM), nutrient balanced (DIN : DIP = 16; (DIN : DIP = 16) + DOM)), phosphorus limited (DIN : DIP = 100; (DIN : DIP = 100) + DOM) and nitrogen limited treatments (DIN : DIP = 3; (DIN : DIP = 3) + DOM), dissolved organic nitrogen – DON; dissolved organic phosphorus – DOP; nitrate – NO_3; phosphate – PO_4.

Treatment	Nutrient	Concentration (µM)
Control	-	-
+ DOM	DON	23.1
	DOP	0.18
DIN : DIP = 100	NO_3	66.4
	PO_4	0.66
(DIN : DIP = 100) + DOM	NO_3	66.4
	PO_4	0.66
	DON	23.1
	DOP	0.18
DIN : DIP = 16	NO_3	66.4
	PO_4	4.16
(DIN : DIP = 16) + DOM	NO_3	66.4
	PO_4	4.16
	DON	23.1
	DOP	0.18
DIN : DIP = 3	NO_3	12.5
	PO_4	4.16
(DIN : DIP = 3) + DOM	NO_3	12.8
	PO_4	4.16
	DON	23.1
	DOP	0.18

POC and PON. POP concentration was obtained as the PO_4 concentration after persulfate digestion at 120 °C (Pujo-Pay, Raimbault 1994).

DOM extract was obtained in May, June and July 1999 from the River Pärnu water, which flows into the Gulf of Riga. Extraction was made using a tangential flow ultra filter (Benner et al. 1997). Firstly, river water was filtered through 1.2 µm and 0.2 µm Opticap filter units (Millipore); then, DOM was concentrated with a tangential device, the Prep/scaleTM TFF 6 ft2 cartridge (Millipore). The fraction of U = 10^3 - 10^6 Daltons [Da] [abridged >1000] was obtained and used. Total dissolved nitrogen and phosphorus concentrations were determined after persulfate digestion at 120 °C (Pujo-Pay, Raimbault 1994); DON was calculated as the difference between total nitrogen concentration and DIN (NO_3 + NO_2 + NH_4), and DOP concentration was obtained as difference between total phosphorus and PO_4. The obtained concentrations of DON and DOP in concentrates of DOM were 639 µM and 5.14 µM, respectively (DON : DOP = 124). The DOM extract contained 49 µM NO_3 and 3.37 µM PO_4.

The microcystin content was estimated by protein phosphatase 1A inhibition assay (Ward et al. 1997).

Statistical analysis of variance (ANOVA) was used to test the significance of differences in *M. aeruginosa* growth, biomass increase and nutrient dynamics between experimental conditions

Results

The growth of *M. aeruginosa* started without any lag phase in the control and the + DOM conditions. The cell concentration increased until Day 6 in the control, and until Day 14 in the + DOM condition (Fig. 1). With inorganic and organic nutrient additions, cyanobacteria growth occurred according to the typical pattern for a batch cultures: a 1 to 2 day lag phase followed by an exponential-growth phase lasting from Day 3 until Day 10 or Day 11. During the last five days of the experiment the cell concentration decreased. Differences in cell concentration due to the addition of DOM were visible mostly during the stationary phase.

Chlorophyll *a* concentrations started to increase exponentially from Day 1. Maximal chlorophyll *a* concentrations in the control and the + DOM condition were observed already on Day 5, in other conditions with inorganic and organic nutrient additions at Days 6 - 8 (Fig. 2).

As nutrient additions ended on Day 6, the cultures evolved as batch cultures after that time. Nutrient supplies decreased continuously until the end of culturing. In some cases nutrients were taken up rapidly. This occurred for nitrates (NO_3) in the DIN : DIP-balanced conditions ($p < 0.05$), where NO_3 concentration already reached <1 μM on Day 9 and

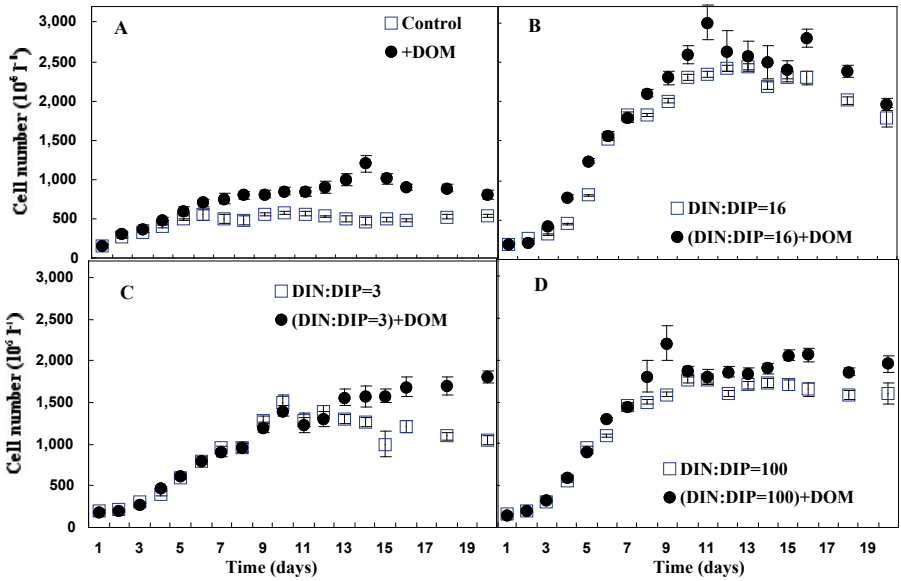

Fig. 1. Cell number of *Microcystis aeruginosa* versus time (days) in the treatment without inorganic nutrient enrichments (A), treatment with nutrient enrichments in balanced ratio (B), N – limited (C) and P – limited treatment (dissolved inorganic nitrogen – DIN; dissolved inorganic phosphorus – DIP; dissolved organic matter – DOM), vertical bars indicates standard deviation between triplicate.

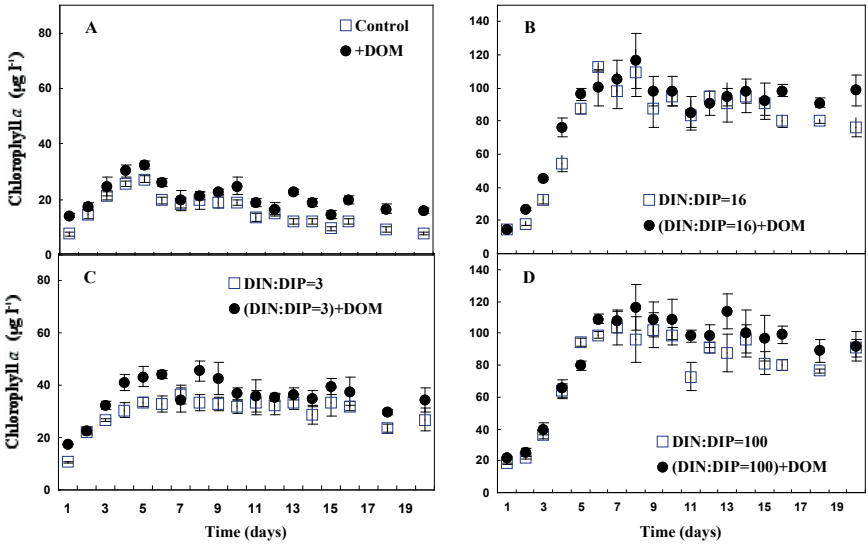

Fig. 2. Chlorophyll *a* concentration of *Microcystis aeruginosa* versus time (days) in the treatment without inorganic nutrient enrichments (A), treatment with nutrient enrichments in balanced ratio (B), N – limited (C) and P – limited treatment (dissolved inorganic nitrogen – DIN; dissolved inorganic phosphorus – DIP; dissolved organic matter – DOM), vertical bars indicates standard deviation between triplicate.

decreased near to detection limit at the end of sampling on Day 15. In contrast, phosphate (PO_4) concentration decreased slightly in the same condition and large amounts of PO_4 were left unused in the cultures on Day 15. In all treatments, NO_3 and PO_4 concentrations were lowest on Day 15.

In all nutrient-enriched cultures cell number together with particulate organic carbon (POC), particulate organic nitrogen (PON) and particulate organic phosphorus (POP) concentrations continued to increase after the last nutrient addition on Day 6, indicating uptake of N and P and biomass production. For all replicates particulate organic carbon, nitrogen and phosphorus concentration on Days 12 and 15 reached the maximum values. Thus, values recorded on Day 15 were used to determine yields and to estimate the relative cellular contents of carbon, nitrogen and phosphorus.

Nitrogen : phosphorus balanced treatment (DIN : DIP = 16 and DIN : DIP = 16) + DOM)

The highest *M. aeruginosa* numbers and chlorophyll *a* concentrations were observed in the DIN : DIP balanced treatment. Nitrate and phosphate addition in balanced ratio yielded the highest POC, PON and POP increment, while addition of dissolved organic matter had little effect. The biomass increases sustained by DOM were only 7 % for POC, 8 % for PON and 9 % for POP (Table 2).

Phosphorus limited treatment (DIN : DIP = 100 and (DIN : DIP = 100) + DOM)

The second highest cyanobacteria cell and chlorophyll *a* concentrations were obtained under P-limitation. Biomass increases obtained by nitrate and phosphate additions

were lower as in the balanced treatment. *M. aeruginosa* growth in phosphorus-limiting conditions did not benefit so much from the addition of DOM; the corresponding value for POC was 14 %; for PON 13 % and 10 % for POP.

Nitrogen-limiting treatment (DIN : DIP = 3 and (DIN : DIP = 3) + DOM)

Cell number, chlorophyll *a* concentration, POC and PON concentrations were significantly lower ($p < 0.05$) under N limitation than in nitrogen: phosphorus balanced and phosphorus limited conditions (Fig. 1, 2, Table 2). Cells that were nitrogen-limited seemed to benefit from the addition of DOM; POP concentration in the (DIN : DIP = 3) + DOM treatment represented an increase of 20 % compared to the DIN : DIP = 3 treatment ($p < 0.05$).

Unenriched seawater with and without DOM (Control and + DOM)

The *M. aeruginosa* counts in the control and + DOM treatment were lower than in all inorganic nutrient addition treatments ($p < 0.05$, Fig. 1, 2, Table 2). However the addition of DOM to the unenriched seawater (control) significantly ($p < 0.01$) increased cyanobacteria *M. aeruginosa* cell number (Fig. 1) and chlorophyll *a* concentration (increase coefficient: 1.8 ± 0.3, $n = 24$) in comparison to the control. The increase of cell number was followed by a significant increase of PON and POP concentrations in the +DOM treatment compared to the unenriched control (Table 2). The highest increase by 53 % ($p < 0.05$) occurred for POP concentration, compared to 31 % ($p < 0.05$) for PON concentration. We infer that *M. aeruginosa* acquired nitrogen and phosphorus from DOM in conditions where inorganic nutrients were not added, and that DOP of land origin is to some extent a substitute for PO_4 in P-depleted condition.

Table 2. Mean particulate organic carbon (POC) concentrations, particulate organic nitrogen (PON), particulate organic phosphorus (POP) and PON : POP ratios of Microcystis aeruginosa recorded on Day 15 in nutrient balanced and nutrient limited experimental treatments (dissolved inorganic nitrogen – DIN; dissolved inorganic phosphorus – DIP; dissolved organic matter – DOM). Number after (±) indicates standard deviation between three replicates. Numbers within parentheses show relative increase of POC, PON and POP concentrations sustained by the addition of dissolved organic matter, in percents.

Treatment	POC (µM)	PON (µM)	POP (µM)	PON : POP
Control	250 ± 23	12.1 ± 2.5	0.53 ± 0.23	22.8 ± 8.3
+ DOM	340 ± 37 (26 %)	17.5 ± 1.4 (31 %)	1.12 ± 0.09 (53 %)	15.6 ± 1.7
DIN : DIP = 100	700 ± 32	54.9 ± 1.5	1.28 ± 0.02	42.8 ± 1.0
(DIN : DIP = 100) + DOM	820 ± 21 (14 %)	62.8 ± 1.5 (13 %)	1.43 ± 0.03 (10 %)	43.9 ± 1.3
DIN : DIP = 16	790 ± 39	61.2 ± 0.2	3.04 ± 0.11	20.1 ± 0.9
(DIN : DIP = 16) + DOM	850 ± 38 (7 %)	66.9 ± 1.5 (8 %)	3.33 ± 0.17 (9 %)	20.2 ± 1.4
DIN : DIP = 3	450 ± 19	23.7 ± 2.6	3.02 ± 0.09	7.8 ± 0.8
(DIN : DIP = 3) + DOM	610 ± 12 (26 %)	26.8 ± 0.9 (12 %)	3.79 ± 0.25 (20 %)	7.1 ± 0.7

Discussion

M. aeruginosa reached the highest cell and chlorophyll *a* concentrations in the nitrogen and phosphorus balanced treatment (DIN : DIP = 16 and (DIN : DIP = 16) + DOM). Since the time when Redfield (1934) observed that NO_3-N and PO_4-P are taken up by phytoplankton at a constant atomic ratio of 16 : 1 and Fleming (1940) pointed out that this value is also that of the elemental composition of phytoplankton, it has been commonly accepted that values >16 would reflect P-limited and values < 16 would reflect N-limited cell contents. PON : POP values recorded in our two DIN : DIP balanced conditions were somewhat higher (approximately 20) than the expected Redfield's value – 16. It has been reported that chemical contents of cells vary between species. For example Sakshaug and Holm-Hansen (1977) concluded that the point of change for P-deficiency in cells differs between species, for example, for *Skeletonema costatum* PON : POP = 23. We assume that cells of *M. aeruginosa* in DIN : DIP = 16 conditions were neither N- nor P-limited. The DIN and DIP supply in balanced ratio (16) is the main determinative factor for development of *Microcystis aeruginosa,* promoting high cell biomass and chlorophyll *a* content. The addition of DOM did not affect the cell N : P ratio in the presence of NO_3 and PO_4 additions.

In the phosphorus limited treatments (DIN : DIP = 100 and (DIN : DIP = 100) + DOM) the *M. aeruginosa* count was lower than in the DIN : DIP balanced treatment. As the PON : POP ratios of the cells grown in the phosphorus-limiting treatments were 42.8 ± 1.0 and 43.9 ± 1.3 (Table 2) we infer that the cells in both treatments were clearly phosphorus-limited. The DOM addition raised *M. aeruginosa* biomass and cell POP and PON content, while the PON : POP ratio became more P limited, showing that DOP could not compensate the P-deficiency. Similarly Panosso and Gràneli (2000) showed that DIP-limited *Nodularia spumigena* was unable to use DOM as a source of phosphorus.

M. aeruginosa cells grown in the nitrogen-limiting treatment (DIN : DIP = 3 and (DIN : DIP = 3) + DOM) clearly showed nitrogen-limitation, as cell PON : POP was 7.8 ± 0.8 and 7.1 ± 0.7. Hillebrand and Sommer (1999) considered that a N : P < 13 in microalgae indicates nitrogen limitation. In contrast, Panosso and Gràneli (2000) observed than DON can provide cyanobacteria cells with nitrogen and increase the yield of *Nodularia spumigena* under conditions of N deficiency. These differing results might have originated from different protocols – extremely severe N and P limitation (DIN : DIP 0.02 and 643) and high amount of DOM added, while in our experiment DOM was added at in-situ like concentrations.

The addition of DOM to unenriched seawater promoted a significant decrease of cell PON : POP ratio by 32 %, changing from a P-limited (PON : POP = 22.8) to a N : P-balanced (PON : POP = 15.6) content (Table 2). As in this treatment the DON : DOP ratio in the medium was 9.2, we infer that cells took up proportionally more organic phosphorus than nitrogen. This idea is supported by the literature, as it is known that several cyanobacteria can acquire phosphorus from organic compounds, and *M. aeruginosa* has large capacity for organic phosphorus mineralization Giraudet et al. (1997). Therefore, we conclude that in the treatment where inorganic phosphorus was not added, *M. aeruginosa* mostly took up dissolved organic phosphorus from river DOM.

The utilization of dissolved organic matter (DOM) in aquatic ecosystems was long thought to be the purview of heterotrophic microorganisms, till Paerl (1991) asked a

fundamental question: how can relatively high numbers of actively growing picoplankton survive and periodically flourish in dissolved inorganic nitrogen-depleted waters? He was the first who showed the light-stimulated incorporation of amino acids by cyanobacteria *Synechococcus* species. Other studies have shown that algal biomass and alkaline phosphatase activity are significantly higher in the presence of riverine humic substances than in nitrate-enriched controls (Carlsson et al. 1993). DOM contributes to a biomass increase of cyanobacteria (Ponosso, Granéli 2000) and iron bound in DOM ensures the iron demands (Stolte et al. 2006). According to Maestrini et al. (1999) the DOM from Daugava River promoted *M. aeruginosa* yield to 38 % of that sustained by optimal nitrate concentration.

Our experiments show that the growth of *M. aeruginosa* was promoted by DOM, but since our cyanobacteria cultures were not bacteria-free, we do not infer that *M. aeruginosa* directly obtained all used N and P from DOM. Bacteria associated with *M. aeruginosa* are involved in ammonification and nitrification (Purvina, unpublished data), but still the mechanisms of DOM and particularly DOP uptake are not unequivocal. DOM enhances cyanobacteria biomass production via algal mixotrophy together with bacterial degradation and photochemical modification of marine humic substances. Altogether, the best growth of *M. aeruginosa* isolated from the Gulf of Riga was achieved by nitrate and phosphate additions in the DIN : DIP balanced (16) treatment. The addition of DOM to the control and the different DIN + DIP conditions increased cell number and raised cellular POC, PON and POP concentrations. In inorganic nutrient depleted conditions, *M. aeruginosa* can acquire nitrogen and phosphorus from riverine dissolved organic matter.

Acknowledgements

This study was supported by the European Community Project «DOMTOX» (MAS3-CT97-0149) and ESF. Especial thanks is given to M. Pfeifere (LHEI, Dep. of Experimental Hydrobiology) for *M. aeruginosa* culture isolation and to C. Ward (Department of Biological Sciences, University of Dundee) for microcystin analyses.

References

Balode M., Purina I. 1996. Harmful phytoplankton in the Gulf of Riga (the Baltic Sea). In: Yasumoto T., Oshima Y., Fukuyo Y. (eds) *Harmful and Toxic Algal Blooms.* Intergovernmental Oceanographic Commission of UNESCO, pp. 69–72.

Benner R., Biddanda B., Black B., McCarthy M. 1997. Abundance, size distribution, and stable carbon and nitrogen isotopic compositions of marine organic matter isolated by tangential-flow ultrafiltration. *Mar. Chem.* 57: 243–263.

Brand L.E., Guillard R.R.L., Murphy L.S. 1981. A method for the rapid and precise determination of acclimated phytoplankton reproduction rates. *J. Plankton. Res.* 3: 193–201.

Carlsson P., Segatto Z.A., Granéli E. 1993. Nitrogen bound to humic matter of terrestrial origin – a nitrogen pool for coastal phytoplankton? *Mar. Ecol. Progr. Ser.* 97: 105–116.

Dionisio-Pires L.M., Van Donk E. 2002. Comparing grazing by *Dreissena polymorpha* on phytoplankton in the presence of toxic and non-toxic cyanobacteria. *Freshwater Biol.* 47: 1855–1865.

Dunton P.G., Walsby A.E. 2005. The diameter and critical colapse pressure in gas vesicles of *Microcystis* are correlated with GvpCs of different length. *FEMS Microbiol. Ecol.* 247: 37–43.

Fleming R.H. 1940. The composition of plankton and units for reporting populations and production. *Proceedings of the 6th Pacific Scientific Congress*, California, 1939, pp. 535–540.

Giraudet H., Berthon J.L., Buisson B. 1997. A comparison of the daily alkaline phosphatase activity of a cyanobacterium (*Microcystis aeruginosa*) and a diatom (*Synedra capitata*). *C. R. Acad. Sci. III* 320: 451–458.

Granéli E., Johansson N., Panosso, R. 1998. Cellular toxin contents in relation to nutrient conditions for different groups of phycotoxins. In: Reguera B., Blanco J., Fernandez M.L., Wyatt T. (eds) *Harmful Algae*. Xunta de Galicia and Intergovern. Oceanographic Commission of UNESCO, pp. 321–324

Guillard R.R.L., Ryther J.H. 1962. Studies on marine planktonic diatoms I. *Cyclotella nana* Hustedt and *Detonula confervacea* (Cleve) Gran. *Can. J. Microbiol.* 8: 229–239.

HELCOM 2007. *Climate Change in the Baltic Sea Area*. HELCOM Thematic Assessment Report on Climate Change in the Baltic Sea Area. Helsinki Commission. 49 p.

Hillebrand H., Sommer U. 1999. The nutrient stoichiometry of benthic microalgal growth: Redfield proportions are optimal. *Limnol. Oceanogr.* 44: 440–446.

Humborg C., Conley D.J., Rahm L., Wulff F., Cociasu A., Ittekkot V. 2000. Silicon retention in river basins: Far-reaching effects on biogeochemistry and aquatic food webs in coastal marine environments. *Ambio* 29: 45–50.

Jespersen A.M., Christofersen K., 1987. Measuremnets of chlorophyll-a from phytoplankton using ethanol as extraction solvent. *Arch. Hydrobiol.* 109: 445–454.

Juhel G., Davenport J., O'Halloran J., Culloty S., Ramsay R., James K., Furey A., Allis O. 2006. Pseudodiarrhoea in zebra mussels *Dreissena polymorpha* (Pallas) exposed to microcystins. *J. Exp. Biol.* 209: 810–816.

Kardinaal W.E.A., Janse I., Agterveld M.K., Meima M., Snoek J., Mur L.R., Huisman J., Zwart G., Visser P.M. 2007a. Microcystis genotype succession in relation to microcystin concentrations in freshwater lakles. *Aquat. Microb. Ecol.* 48: 1–12.

Kardinaal W.E.A., Tonk L., Janse I., Hol S., Slot P., Huisman J., Visser P.M. 2007b. Competition for light between toxic and non-toxic strains of the harmful cyanobacterium *Microcystis*. *Appl. Environ. Microbiol.* 73: 2939–2946.

Kļaviņš M., Rodionovs V. 2007. Long-term changes of river discharge regime in Latvia. In: Kļaviņš M. (ed) *Climate Change in Latvia*. University of Latvia, Riga, pp. 21–36.

Kononen K., Sellner K.G. 1995. Toxic cyanobacteria blooms in marine, estuarine and coastal ecosystems. In: Lassus P., Arzul G., Erard-Le Denn E., Gentien P., Marcaillou-Le Baut C. (eds) *Harmful Marine Algal Blooms*, 6th International Conference on Toxic Marine Phytoplankton, Nantes, France. Lavoisier, Paris, pp. 858–860.

Kurmayer R., Dittmann E., Fastner J., Chorus I. 2002. Diversity of microcystin genes within a population of the toxic cyanobacterium *Microcystis* spp., in Lake Wannsee (Berlin, Germany). *Microbial Ecol.* 43: 107–118.

Lürling M. 2003. Daphnia growth on microcystin-producing and microcystin-free *Microcystis aeruginosa* in different mixtures with the green alga *Scenedesmus obliguus*. *Limnol. Oceanogr.* 48: 2214–2220.

Maestrini S.Y, Balode M., Béchemin C., Purina I. 1999. Nitrogenous organic substances as potential nitrogen sources, for summer phytoplankton in the Gulf of Riga, eastern Baltic Sea. *Plankton Biol. Ecol.* 46: 8–17.

Paerl H.W. 1988. Nuisance phytoplankton blooms in coastal, estuarine, and inland waters. *Limnol. Oceanogr.* 33: 823–847.

Paerl H.W. 1991. Ecophysiological and trophic implication of light-stimulated amino acid utilization in marine picoplankton. *Appl. Environ. Microbiol.* 57: 473–479.

Panosso R., Granéli E. 2000. Effects of dissolved organic matter on the growth of *Nodularia spumigena* (Cyanophyceae) cultivated under N or P deficiency. *Mar. Biol.* 136: 331–336.

Pujo-Pay M., Raimbault P. 1994. Improvement of the wet-oxidation procedure for simultaneous determination of particulate organic nitrogen and phosphorus collected on filters. *Mar. Ecol. Progr. Ser.* 105: 203–207.

Rahm L., Conley D., Sandén P., Wulff F., Stalnacke P. 1996. Time series analysis of nutrient inputs to the Baltic Sea and changing DSi:DIN ratios. *Mar. Ecol. Progr. Ser.* 130: 221–228.

Rantajärvi E., Gran V., Hällfors S., Olsonen R. 1997. Effects of environmental factors on the phytoplankton community in the Gulf of Finland – unattended high frequency measurements and multivariate analyses. *Hydrobiologia* 363: 1–3.

Redfield A.C. 1934. On the proportions of organic derivatives in sea water and their relation to the composition of plankton. In: Daniel R.J. (ed) *James Johnstone Memorial Volume*, The University Press, Liverpool, pp. 176-192.

Sakshaug E., Holm-Hansen O. 1977. Chemical composition of Skeletonema costatum (Grev.) Cleve and *Pavlova* (*Monochrysis*) *lutheri* (Droop) Green as a function of nitrate-, phosphate-, and iron-limited growth. *J. Exp. Mar. Biol. Ecol.* 29: 1–34.

Seppälä J., Balode M., 1999 Spatial distribution of phytoplankton in the Gulf of Riga during spring and summer stages. *J. Marine Syst.* 23: 51–67

Stolte W., Balode M., Carlsson P., Grzebyk D., Janson S., Lips I., Panosso R., Ward C.J., Granéli E. 2007. Stimulation of nitrogen-fixing cyanobacteria in a Baltic Sea plankton community by land-derived organic matter or iron addition. *Mar. Ecol. Progr. Ser.* 327: 71–82.

Valderrama J.C., 1995. Methods of nutrient analysis. In: Hallegraeff G.M., Anderson D.M., Cembella A.D. (eds) *Manual on Harmful Marine Microalgae*, IOC Manuals and Guides N° 33. UNESCO, Paris, pp. 251–282.

Ward C.J., Beattie K.A., Lee E.Y.C., Codd G.A. 1997. Colorimetric protein phosphatase inhibition assay of laboratory strains and natural blooms of cyanobacteria: comparison with high-prformance liquid chromatographic analysis for microcystins. *Microbial Ecol.* 153: 465–473.

Yentsch C.S., Menzel D.W. 1963. A method for the determination of phytoplankton and pheophytin by fluorescence. *Deep-Sea Res.* 10: 221–231.

Neorganisko barības vielu un izšķīdušās organiskās vielas ietekme uz Rīgas līča cianobaktērijas *Microcyctis aeruginosa* augšanu

Santa Purviņa[1]*, Christian Bechemin[2], Maija Balode[1], Daniel Grzebyk[2], Serge Y. Maestrini[2]

[1]Latvijas Hidroekeoloģijas institūts, Daugavgrīvas 8, Rīga LV-1048, Latvija
[2]Centre de Recherche en Ecologie Marine et Aquaculture de L'Houmeau (CNRS-IFREMER), B.P. 5, F-17137 L'Houmeau, Francija

*Korespondējošais autors, E-pasts: santa.purvina@lhei.lv

Kopsavilkums

Pētīja barības vielu ietekmi N-limitējošos, P-limitējošos un DIN : DIP līdzsvarotos apstākļos, ar un bez sauszemes izcelsmes izšķīdušās organiskās vielas (DOM) klātbūtnes, uz cianobaktērijas *Microcystis aeruginosa*, kas izolēta no Rīgas līča, augšanu un toksīna saturu. Izšķīdušā neorganiskā slāpekļa (DIN) un izšķīdušā neorganiskā fosfora (DIP) pievienošana līdzsvarotā attiecībā DIN : DIP = 16 ir galvenais *M. aeruginosa* attīstību noteicošais faktors, kas veicina šūnu biomasas, hlorofila *a* un daļiņveida organiskās vielas pieaugumu. Vidē, kas bija bagātināta tikai ar DOM, *M. aeruginosa* izmantoja 31 % no pieejamā izšķīdušā organiskā slāpekļa un 53 % no izšķīdušā organiskā fosfora. Eksperimenta apstākļi neveicināja cianobaktērijas toksiskuma palielināšanos. Eksperiments parādīja, ka *M. aeruginosa* attīstību veicina paaugstināta neorganisko barības vielu un izšķīdušās organiskās vielas ieplūde iesāļajās Baltijas jūras piekrastes ekosistēmās.

Acta Universitatis Latviensis, 2008, Vol. 745, Biology, pp. 75–85

High-level expression and purification of bacteriophage GA virus-like particles from yeast *Saccharomyces cerevisiae* and *Pichia pastoris*

Jānis Freivalds, Jānis Rūmnieks, Velta Ose, Regīna Renhofa, Andris Kazāks*

Latvian Biomedical Research and Study Centre, Ratsupites 1, Riga LV-1067, Latvia

*Corresponding author, E-mail: andris@biomed.lu.lv

Abstract

The recombinant virus-like particles (VLPs) generated by heterologous expression of RNA bacteriophage coat protein genes have been proposed as promising carriers of foreign epitopes and nucleic acids for development of novel vaccines and gene therapy tools. Here, we investigated the possibility to produce bacteriophage GA coat protein-derived VLPs in yeast *Saccharomyces cerevisiae* and *Pichia pastoris*. To optimize growth conditions, three expression systems have been explored: GAL1 and GAL10 promoter-directed expression in *S. cerevisiae* as well as AOX1 promoter-directed expression in *P. pastoris*. Synthesis of GA coat protein and formation of VLPs was observed in all three cases. GA VLPs were purified by a single size-exclusion chromatography step till 80 to 90 % of homogeneity. The final amount of purified VLPs varied between 0.6 to 2.0 mg per 1 g of cells for *S. cerevisiae*, while expression in *P. pastoris* resulted in VLP yield of up to 3 mg from the same amount of cells. The recombinant VLPs obtained may be further used for exposition of foreign epitopes on their surface via chemical coupling and/or packaging of immunostimulatory DNA sequences internally.

Key words: bacteriophage GA, coat protein, expression, virus-like particles, yeast.

Introduction

The RNA bacteriophages (phages) are small viruses with a simple organization. Their T = 3 icosahedral shell is composed of 180 copies of the coat protein (CP) and one copy of the maturation protein that encapsidates approximately 3,500-nucleotide-long genomic RNA. These phages were first isolated from *Escherichia coli* (Loeb, Zinder 1961), but later were also found in *Caulobacter* (Schmidt 1966), *Pseudomonas* (Bradley 1966) and *Acinetobacter* (Coffi 1995). To date, the coliphages have been classified into four groups based on their serological and physicochemical properties. Groups I and II with MS2 and GA phages as the type species are quite similar and are collectively called group A. Phages Qβ and SP, members of groups III and IV, respectively, together form group B (Furuse 1987).

The molecular biology of the RNA phages has been extensively studied (van Duin 1999; Weber 1999). In addition, high-resolution X-ray structures of several RNA phages have been determined (Valegård et al. 1990; Liljas et al. 1994; Golmohammadi et al. 1996; Tars et al. 1997; Tars et al. 2000). These data together with the observation that phage CPs alone in

absence of the viral nucleic acid are able to form non-infectious virus-like particles (VLPs) in *E. coli* (Kozlovska et al. 1993; Pushko et al. 1993) have made icosahedral phage shells attractive as objects for gene and protein engineering manipulations. Thus, recombinant VLPs formed by CPs of group-I RNA phages fr and MS2 have been successfully used for presentation of foreign protein sequences on their surface via genetic fusion (Mastico et al. 1993; Heal et al. 1999; Voronkova et al. 2002). However, steric factors limit the length of peptides that can be added to the CP while still preserving its ability to self-assemble into VLPs. Alternatively, the desired peptides can be chemically coupled to surface-exposed lysine residues (Jegerlehner et al. 2002).

Recently, we and others have demonstrated the potential of yeast cells as a host for producing properly folded phage MS2 and Qβ CP-derived VLPs (Legendre, Fastrez 2005; Freivalds et al. 2006). Here, we continue our investigations to show the formation of group-II RNA phage GA VLPs in two different yeasts to therefore extend a way for further development of a yeast-derived phage VLP technology.

Materials and methods

Strains and plasmid constructions

The GA CP-encoding gene was amplified with desired oligonucleotide primers by polymerase chain reaction (PCR) from *Escherichia coli* expression plasmid pGA-355-24 (I. Cielēns, personal communication). The CP sequence encoded by this plasmid differs from that deposited in GenBank (Acc. No. X03869; Inokuchi et al. 1986) at positions 59 and 79 and is identical to that published by Tars et al. (1997). Construction details are summarized in Table 1. For expression in *S. cerevisiae* strain YPH499, the appropriate PCR fragment was digested with *Bam*HI/*Hind*III and cloned in pESC-URA vector, resulting in a pESC-GA plasmid. For expression in the *S. cerevisiae* strain AH22, the PCR fragment was digested with *Xba*I/*Bgl*II and cloned in pFX-Qβ, resulting in a pFX-GA plasmid. The *P. pastoris* expression plasmid pPIC-GA was generated by cloning of the respective PCR fragment into pPIC3.5K vector using *Bam*HI and *Sna*BI restriction sites. PCR and cloning procedures were carried out using standard molecular biology protocols (Sambrook et al. 1989).

Yeast transformation and expression conditions

S. cerevisiae strains AH22 and YPH499 were transformed with pFX-GA and pESC-GA, respectively, using standard lithium acetate/polyethylene glycol procedure as decribed by Gietz et al. (1992). The YPH499/pESC-GA transformants were selected on uracil-free agarized synthetic dextrose (SD) minimal medium according to manufacturer's protocol. For expression, individual transformants were cultivated in liquid synthetic galactose (SG) medium for up to 72 h, until OD_{590} reached 6 - 7.

Transformed AH22/pFX-GA clones were selected on agarized rich YEP medium containing 2 % glucose (YEPD medium) supplemented with 10 mM formaldehyde. Individual transformants were then incubated in liquid YEPD medium supplemented with 5 mM formaldehyde for 20 to 24 h until optical density OD_{590} reached 6 - 8. For induction, the cells were collected by low-speed centrifugation and resuspended in YEP medium with 3 % galactose (YEPG medium), and cultivation was continued for another 20 - 24 h, with final OD_{590} 10 - 14.

Electroporation of *P. pastoris* with the *Ecl*136II-linearized pPIC-GA plasmid and selection of clones containing multiple integrations of expression cassette into yeast chromosome were performed as described by Freivalds et al. (2006). GA CP gene expression in *P. pastoris* was achieved according to recommendations of the manufacturer. Briefly, selected clones were incubated in BMGY medium for 20 to 24 h until OD_{590} reached 4 - 6; then the cells were collected by low-speed centrifugation and resuspended in BMMY induction medium and cultivated for 72 h. All cultivations were performed in 500 mL flasks with 100 mL of expression media at 30 °C on a rotary shaker either at 200 rpm (*S. cerevisiae*) or at 250 rpm (*P. pastoris*). The cells were collected by low-speed centrifugation, washed with distilled water and stored at –20 °C until use.

Purification of GA VLPs

For purification of GA VLPs, 1 g of yeast cells was resuspended in 4 mL of lysis buffer (20 mM Tris-HCl, 5 mM EDTA, 0.65 M NaCl, 1 mM PMSF, pH 7.8). To disrupt the cells, suspension was applied to the French press (three strokes, 20 000 psi). The unsoluble cell debris was separated by centrifugation (1 h, 15 500 g) and discarded. Soluble supernatant proteins were concentrated by addition of solid ammonium sulfate to 60 % of saturation and incubation overnight at 4 °C. After centrifugation 20 min at 8000 g, the proteins were solubilized into 1 mL of lysis buffer without PMSF and loaded onto a Sepharose CL4B gelfiltration column (V = 90 mL, h = 110 cm), with the buffer flow rate approximately 1.0 mL h^{-1}, and 1.5 mL fractions were collected. All of the purification steps were performed at 4 °C.

Protein content in cell and protein samples was analyzed in denaturating polyacrylamide gels (PAAG), with 4 % stacking and 15 % separating gel, according to standard protocols. To visualize protein bands, the gels were stained with Coomassie Brilliant Blue (CBB). Ouchterlony's double radial immunodiffusion with cell lysates was performed using rabbit polyclonal anti-GA antibodies. VLP electrophoresis in 1 % native agarose gels was performed in TAE buffer (pH 8.4) for about 1 h at a constant 90 mA current. VLPs were concentrated

Table 1. Description of vectors and strains used for expression of phage GA CP gene in yeast *S. cerevisiae* and *P. pastoris*. Cloning sites in forward (Fw) and reverse (Rv) primers are underlined. Start and termination codons of the GA CP gene are shown in bold

Strain/genotype	Vector	Primers (5' _ 3')	Construct
S. cerevisiae YPH499	pESC-URA (Stratagene)	Fw: CAGGATCC**ATG**GCAACTTTACGCAGTTTCGT	pESC-GA
MATa ura3-52 lys2-801_amber		Rv: TGAAGC**TTA**CGCGTAGAAGCCACTCTG	
ade2-101_ochre trp1-_63 his3-_200 leu2-_1			
S. cerevisiae AH22	pFX-Qβ (Samuel et al. 2002;	Fw: TTTCTAGAACA**ATG**GCAACTTTACGCAGTTTCG	pFX-GA
MATa leu2 his4	Freivalds et al. 2006)	Rv: TTAGATC**TTA**CGCGTAGAAGCCACTCTG	
P. pastoris GS115	pPIC3.5K (Invitrogen)	Fw: TTGGATCCACC**ATG**GCAACTTTACGCAG	pPIC-GA
his4		Rv: TTTACGTA**TTA**CGCGTAGAAGCCACTC	

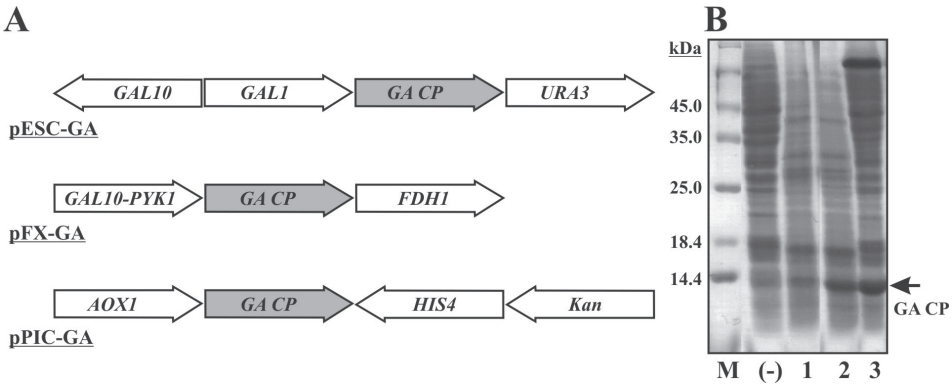

Fig. 1. Expression of the GA CP gene in yeast. A, schematic presentation of the vectors used. The relative direction of genes and promoters is indicated by arrows. *URA3*, *HIS4*, and *FDH1* encode for genes used as primary markers for selection of yeast transformants, while the Kan gene allows secondary screening of *P. pastoris* for high-copy integrants. B, CBB-stained PAAG demonstrating the total synthesis level of GA CP. M, protein molecular weight marker, (-), non-transformed *P. pastoris* cells as a negative control. Lanes 1, 2 and 3 represent cell lysates from strains YPH499, AH22, and GS115, respectively. Accumulation of GA CP is indicated by an arrow.

by dialysis against storage buffer (50 % glycerol, 10 mM Tris-HCl, 2.5 mM EDTA, 325 mM NaCl, pH 7.8) for at least 24 h. Protein concentration measurements were made according to Bradford (1976).

For electron microscopy, samples were adsorbed on carbon-formvar coated grids and stained with 2 % phosphotungstic acid (pH 6.8); the grids were examined with a JEM 100C electron microscope (JEOL Ltd., Tokyo, Japan) at an accelerating voltage 80 kV.

Results

Design of constructs and expression

In order to establish optimal conditions for generation of GA VLPs in yeast, we aimed to compare three well-described expression systems by cloning of phage GA CP gene in three different vectors. The resulting expression units are schematically presented in Fig. 1A. In the first approach, the pESC-URA vector was selected as a template for cloning and *GAL1* promoter-directed expression. This vector was previously used for generation of phage MS2 VLPs (Legendre, Fastrez 2005). In a second approach, we focused on the pFX-derived plasmid, which represents an already established VLP producing system exploiting hybrid *GAL10-PYK1* promoter. In addition, this vector encodes for the *FDH1* gene of *Candida maltosa*, conferring resistance to formaldehyde (Sasnauskas et al. 1992), which is very convenient for quick selection of transformants on rich media. In a third approach, the strong *AOX1* promoter-directed expression provided by the *P. pastoris* expression vector pPIC3.5K was undertaken.

All three constructs pESC-GA, pFX-GA, and pPIC-GA were transformed in their corresponding yeast host (YPH499, AH22, and GS115, respectively). While both *S. cerevisiae* vectors exist in the cells as episomes, pPIC3.5K does not contain a yeast replication origin and needs to be integrated into the host genome via homologous recombination. Due to

Table 2. Summary of generation of phage GA VLPs in yeast. Replication in at least two independent experiments

Strain/plasmid	Amount of cells after cultivation (g L^{-1})	Immunologic anti-GA titers	GA VLPs (mg from 1 g of cells)
YPH499/pESC-GA	15 - 20	1:4 - 1:8	0.6 - 0.8
AH22/pFX-GA	40 - 50	1:16	1.5 - 2
GS115/pPIC-GA	40 - 50	1:32	2.5 - 3

the presence of *Kan* gene in the expression unit, we have selected clones with multiple expression units integrated in the yeast chromosome, which accordingly exhibited increased resistance to Geneticin in *P. pastoris*.

The selected clones were cultivated in appropriate conditions ensuring maximal expression level in each particular case. Optical densities of yeast cells notably varied between strains due to the content of cultivation media, resulting in different amounts of cells obtained at the end of cultivation (Table 2). Total synthesis of GA CP was monitored by CBB-stained PAAG (Fig. 1B) showing well-detectable accumulation of ~13.6 kDa protein in strains AH22 and GS115, while in strain YPH499 the production was significantly lower. Nevertheless, presence of the specific product in the latter case was verified by Western blot with GA-specific antibodies (data not shown). Therefore synthesis of GA CP was confirmed in all three cases and we proceeded to analyze solubility and self-assembly of the target protein.

Purification and characterization of GA VLPs

As the first step of purification, the cells were disrupted by French press and the soluble protein fraction was analyzed by Ouchterlony double radial immunodiffusion with anti-GA antibodies. The obtained titres (Table 2) correlated well with the absolute GA CP amounts (Fig. 1B), suggesting that the majority of the target protein was in the soluble protein fraction and also providing indirect evidence of the presence of VLPs in cell lysates, since unassembled CP usually accumulates as unsoluble aggregates in cells (our unpublished observations).

For further purification, a concentrated mixture of soluble proteins was subjected to size-exclusion chromatography on Sepharose CL4B beads. As expected, the majority of the target protein was eluted between 36 to 42 ml, which corresponds to the calculated volume where VLPs may appear. The respective part of the elution profile is presented in Fig. 2A. Importantly, the larger part of contaminants was removed during the chromatography, indicating the effectiveness of the particular method.

To verify the presence of VLPs, the same fractions were also subjected to native agarose gel electrophoresis (Fig. 2B). The gel was stained with ethidium bromide demonstrating a strong nucleic acid signal that was correlated with the amount of GA CP (Fig. 2A). Taken together, these data strongly suggest formation of VLP nucleoprotein complexes migrating towards anode in native agarose gel. In part, this might be explained by presence of a large amount of negatively charged nucleic acid non-specifically packed inside the VLPs.

Based on the information presented above, the peak VLP-containing fractions were pooled and concentrated. Overall amounts of the obtained VLPs are presented in Table 2. These data correlated well with both the total synthesis level of GA CP (Fig. 1B) and

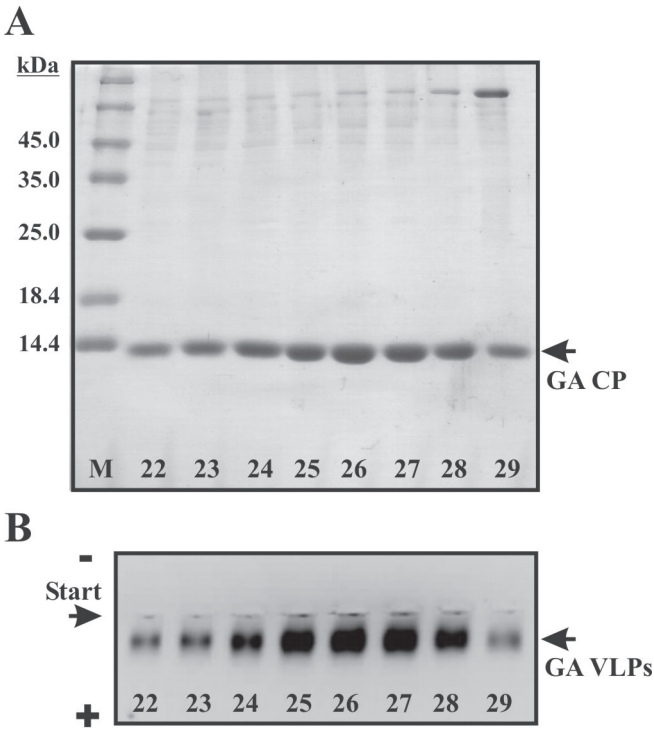

Fig. 2. Purification and detection of recombinant GA VLPs. A, CBB-stained PAAG that demonstrates protein content in *P. pastoris*-derived peak column fractions. The numbers below correspond to appropriate fractions. Both S. cerevisiae strains gave similar profiles but with accordingly lower protein amount (data not shown). M, protein molecular weight marker. The same samples were analyzed in ethidium bromide stained native agarose gel (B). Target proteins are marked by arrows. Anode and cathode are designated as "+" and "-", respectively.

immunological anti-GA titers obtained in supernatant (Table 2). Visually, the overall purity of the VLP samples in PAAG can be estimated as 80 to 90 %, which is rather high after only a single purification step (Fig. 3A). Not surprisingly, the highest purity was associated with the highest expression level, obtained for *P. pastoris*. Finally, the samples were subjected to electron microscopy, which confirmed the formation of icosahedral phage GA-like particles in all three cases (Fig. 3B).

Taken together, an efficient GA VLP generation system was established in both yeast *S. cerevisiae* and *P. pastoris*. The highest yield of VLPs was found in the case of *P. pastoris*. Such recombinant wild-type GA VLPs may be further used for exposition of foreign peptides on their surface via chemical coupling and/or packaging of immunostimulatory DNA sequences internally.

Discussion

Highly immunogenic VLPs generated by heterologous expression of viral structural genes have become a powerful tool for vaccine development. In addition to being effective

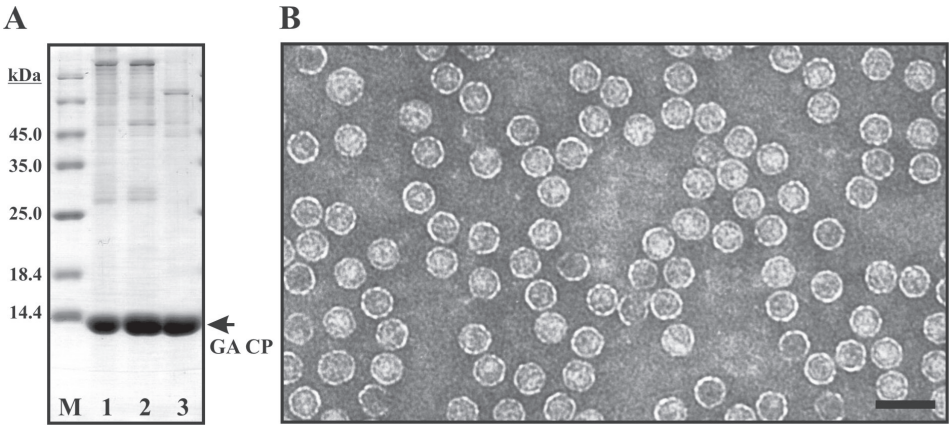

Fig. 3. Characterization of purified GA VLPs. A, CBB-stained PAAG of the final product after size-exclusion chromatography. M, protein molecular weight marker. Lanes 1, 2 and 3 demonstrate the purity of VLPs obtained from strains YPH499, AH22, and GS115, respectively. B, direct evidence of VLP formation by electron microscopy. Only VLPs purified from yeast *P. pastoris* are presented. Scale bar: 50 nm.

vaccines against the corresponding virus from which they were derived, VLPs can also be used to present foreign epitopes to the immune system. This approach might be combined with the packaging of selected genes and drugs inside VLPs (for recent review articles see Georgens et al. 2005; Xu et al. 2006; Jennings, Bachmann 2008).

Icosahedral capsids of the simple RNA phages have attracted attention of scientists as promising carriers of foreign epitopes and nucleic acids. A special interest has been devoted to group III phage Qβ VLPs. Bacterially expressed Qβ VLPs have been explored for chemical coupling of desired peptides to surface-exposed lysine residues. To increase their immunogenicity, such chimeric VLPs can be further engineered by loading them with short synthetic DNA sequences (Storni et al. 2004; Schwarz et al. 2005). Several Qβ phage-derived therapeutic vaccine candidates have already entered phase I to III clinical trials (Kündig et al. 2006; Maurer, Bachmann 2007; Tissot et al. 2008).

However, for vaccine development, *E. coli*-derived VLPs need to be purified from contamination of bacterial endotoxins, which is costly and time-consuming. Alternatively, VLPs could be produced in "endotoxin-free" organisms, such as yeast, which has been regarded as generally safe for human use. Up to now, a large number of structural genes from mammalian viruses have been expressed in yeast resulting in formation of VLPs (Valenzuela et al. 1982; Kniskern et al. 1986; Sasnauskas et al. 1999; Samuel et al. 2002; Slibinskas et al. 2004; Juozapaitis et al. 2007). The yeast expression system has been used successfully to produce licensed prophylactic vaccines against human hepatitis B virus (McAleer et al. 1984) and human papillomavirus (Bryan 2007).

An important drawback of repetitive vaccination with chimeric VLPs might be their limited effectiveness due to the presence of neutralizing antibodies against capsid protein induced after the first application (Da Silva et al. 2001). Therefore, technologies to generate a broad spectrum of carrier VLPs need to be developed. It should be also noted that humans normally do not possess pre-existing antibodies to RNA phages and the immune response will therefore not be impaired. Taking into account these considerations, we extended our

investigations to optimize generation of phage GA-derived VLPs in yeast. The phage GA CP gene was therefore cloned and expressed in three different vectors.

Despite the rather small production of GA CP observed under GAL1 promoter in pESC-URA, this vector contains another GAL10 promoter located in the opposite orientation. This might be advantageous for co-expression of two genes for protein-protein or protein-nucleic acid interaction studies in *S. cerevisiae*. Significantly higher expression of target protein was observed in case of pFX-GA. This is in line with previous data about pFX-directed high-level expression and VLP formation of polyomavirus VP1 and mumps virus nucleoprotein in *S. cerevisiae* (Sasnauskas et al. 1999; Samuel et al. 2002). Finally, methylotrophic yeast, *P. pastoris*, was superior in production of GA CP and yield of recombinant VLPs, therefore confirming its selection as a host microorganism for high-level expression of recombinant genes for both basic laboratory research and industrial manufacture (for a review see Macauley-Patrick et al. 2005).

Recently, we demonstrated the assembly of phage Qb VLPs in *S. cerevisiae* and *P. pastoris* using pFX- and pPIC3.5K-derived expression vectors, respectively (Freivalds et al. 2006). The results obtained were quite similar to those described in this article in that selection of *P. pastoris* clones with multiple expression units integrated in the yeast chromosome resulted in increased expression and outcome of recombinant VLPs while those with single insertion demonstrated rather low synthesis of the target protein. However, not always more integration events leads to higher production, as shown for synthesis of the measles virus nucleoprotein (Slibinskas et al. 2004). Thus, wide screening and selection of individual *P. pastoris* clones is needed for obtaining maximum production in each particular case.

Acknowledgements

This work was supported by the National Research Program 07-VP2.6 from the Latvian Council of Sciences and by a European Social Fund. The *S. cerevisiae* strain AH22 and expression plasmid pFX7 was a kind gift from Dr. K. Sasnauskas (Institute of Biotechnology, Vilnius, Lithuania). We thank Dr. I. Cielēns and Dr. D. Skrastiņa for providing plasmid pGA-355-24 and anti-GA antibodies, respectively.

References

Bradford M. 1976. A rapid and sensitive method for the quantitation of microgram quantities of protein utilizing the principle of protein-dye binding. *Anal. Biochem.* 72: 248–254.

Bradley D.E. 1966. The structure and infective process of a *Pseudomonas aeruginosa* bacteriophage containing ribonucleic acid. *J. Gen. Microbiol.* 45: 83–96.

Bryan J.T. 2007. Developing an HPV vaccine to prevent cervical cancer and genital warts. *Vaccine* 25: 3001–3006.

Coffi H. 1995. *Lysotypie des Acinetobacter.* Thèse de Maîtrise dès Sciences, Laval University, Québec, Canada.

Da Silva D.M., Pastrana D.V., Schiller J.T., Kast W.M. 2001. Effect of preexisting neutralizing antibodies on the anti-tumor immune response induced by chimeric human papillomavirus virus-like particle vaccines. *Virology* 290: 350–360.

Freivalds J., Dislers A., Ose V., Skrastina D., Cielens I., Pumpens P., Sasnauskas K., Kazaks A. 2006. Assembly of bacteriophage Qβ virus-like particles in yeast *Saccharomyces cerevisiae* and *Pichia pastoris*. *J. Biotechnol.* 123: 297–303.

Furuse K. 1987. Distribution of the coliphages in the environment: general considerations. In: Goya S.M, Gerba C.P., Bitton G. (eds) *Phage Ecology*. Wiley Interscience, New York, pp. 87–124.

Georgens C., Weyermann J., Zimmer A. 2005. Recombinant virus like particles as drug delivery system. *Curr. Pharm. Biotechnol*. 6: 49–55.

Gietz D., St Jean A., Woods R.A., Schiestl R.H. 1992. Improved method for high efficiency transformation of intact yeast cells. *Nucleic Acids Res.* 20: 1425.

Golmohammadi R., Fridborg K., Bundule M., Valegård K., Liljas L. 1996. The crystal structure of bacteriophage Qβ at 3.5 Å resolution. *Structure* 4: 543–554.

Heal K.G., Hill H.R., Stockley P.G., Hollingdale M.R., Taylor-Robinson A.W. 1999. Expression and immunogenicity of a liver stage malaria epitope presented as a foreign peptide on the surface of RNA-free MS2 bacteriophage capsids. *Vaccine* 18: 251–258.

Inokuchi Y., Takahashi R., Hirose T., Inayama S., Jacobson A.B., Hirashima A. 1986. The complete nucleotide sequence of the group II RNA coliphage GA. *J. Biochem*. 99: 1169–1180.

Jegerlehner A., Tissot A., Lechner F., Sebbel P., Erdmann I., Kündig T., Bächi T., Storni T., Jennings G., Pumpens P., Renner W.A., Bachmann M.F. 2002. A molecular assembly system that renders antigens of choice highly repetitive for induction of protective B cell responses. *Vaccine* 20: 3104–3112.

Jennings G.T., Bachmann M.F. 2008. The coming of age of virus-like particle vaccines. *Biol. Chem*. 389: 521–536.

Juozapaitis M., Serva A., Kucinskaite I., Zvirbliene A., Slibinskas R., Staniulis J., Sasnauskas K., Shiell B.J., Bowden T.R., Michalski W.P. 2007. Generation of menangle virus nucleocapsid-like particles in yeast *Saccharomyces cerevisiae*. *J. Biotechnol.* 130: 441–447.

Kniskern P.J., Hagopian A., Montgomery D.L., Burke P., Dunn N.R., Hofmann K.J., Miller W.J., Ellis R.W. 1986. Unusually high-level expression of a foreign gene (hepatitis B virus core antigen) in *Saccharomyces cerevisiae*. *Gene* 46: 135–141.

Kozlovska T.M., Cielens I., Dreilina D., Dislers A., Baumanis V., Ose, V., Pumpens, P. 1993. Recombinant RNA phage Qβ capsid particles synthesized and self-assembled in *Escherichia coli*. *Gene* 137: 133–137.

Kündig T.M., Senti G., Schnetzler G., Wolf C., Prinz Vavricka B.M., Fulurija A., Hennecke F., Sladko K., Jennings G.T., Bachmann M.F. 2006. Der p 1 peptide on virus-like particles is safe and highly immunogenic in healthy adults. *J. Allergy Clin. Immunol.* 117: 1470–1476.

Legendre D., Fastrez J. 2005. Production in *Saccharomyces cerevisiae* of MS2 virus-like particles packaging functional heterologous mRNAs. *J. Biotechnol.* 117: 183–194.

Liljas L., Fridborg K., Valegård K., Bundule M., Pumpens P. 1994. Crystal structure of bacteriophage fr capsids at 3.5 Å resolution. *J. Mol. Biol.* 244: 279–290.

Loeb T., Zinder N.D. 1961. A bacteriophage containing RNA. *Proc. Natl. Acad. Sci. USA* 47: 282–289.

Macauley-Patrick S., Fazenda M.L., McNeil B., Harvey L.M. 2005. Heterologous protein production using the *Pichia pastoris* expression system. *Yeast* 22: 249–270.

Mastico R.A., Talbot S.J., Stockley P.G. 1993. Multiple presentation of foreign peptides on the surface of an RNA-free spherical bacteriophage capsid. *J. Gen. Virol.* 74: 541–548.

Maurer P., Bachmann M.F. 2007. Vaccination against nicotine: an emerging therapy for tobacco dependence. *Expert Opin. Investig. Drugs* 16: 1775–1783.

McAleer W.J., Buynak E.B., Maigetter R.Z., Wampler D.E., Miller W.J., Hilleman M.R. 1984. Human hepatitis B vaccine from recombinant yeast. *Nature* 307: 178–180.

Pushko P., Kozlovskaya T., Sominskaya I., Brede A., Stankevica E., Ose V., Pumpens P., Grens, E. 1993. Analysis of RNA phage fr coat protein assembly by insertion, deletion and substitution mutagenesis. *Protein Eng.* 6: 883–891.

Sambrook J., Fritsch E.F., Maniatis T. 1989. *Molecular Cloning: a Laboratory Manual*. Cold Spring Harbor, N.Y.

Samuel D., Sasnauskas K., Jin L., Beard S., Zvirbliene A., Gedvilaite A., Cohen B. 2002. High level

expression of recombinant mumps nucleoprotein in *Saccharomyces cerevisiae* and its evaluation in mumps IgM serology. *J. Med. Virol.* 66: 123–130.

Sasnauskas K., Buzaite O., Vogel F., Jandrig B., Razanskas R., Staniulis J., Scherneck S., Krüger D.H., Ulrich R. 1999. Yeast cells allow the high-level expression and formation of polyomavirus - virus like particles. *Biol. Chem.* 380: 381–386.

Schmidt J.M. 1966. Observations on the adsorption of Caulobacter bacteriophages containing ribonucleic acid. *J. Gen. Microbiol.* 45: 347–53.

Schwarz K., Meijerink E., Speiser D.E., Tissot A.C., Cielens I., Renhof R., Dishlers A., Pumpens P., Bachmann, M.F. 2005. Efficient homologous prime-boost strategies for T cell vaccination based on virus-like particles. *Eur. J. Immunol.* 35: 816–821.

Slibinskas R., Samuel D., Gedvilaite A., Staniulis J., Sasnauskas K. 2004. Synthesis of the measles virus nucleoprotein in yeast *Pichia pastoris* and *Saccharomyces cerevisiae*. *J. Biotechnol.* 107: 115–124.

Storni T., Ruedl C., Schwarz K., Schwendener R.A., Renner W.A., Bachmann M.F. 2004. Nonmethylated CG motifs packaged into virus-like particles induce protective cytotoxic T cell responses in the absence of systemic side effects. *J. Immunol.* 172: 1777–1785.

Tars K., Bundule M., Fridborg K., Liljas L. 1997. The crystal structure of bacteriophage GA and a comparison of bacteriophages belonging to the major groups of *Escherichia coli* leviviruses. *J. Mol. Biol.* 271: 759–773.

Tars K., Fridborg K., Bundule M., Liljas L. 2000. The three-dimensional structure of bacteriophage PP7 from *Pseudomonas aeruginosa* at 3.7–A resolution. *Virology* 272: 331–337.

Tissot A.C., Maurer P., Nussberger J., Sabat R., Pfister T., Ignatenko S., Volk H.D., Stocker H., Müller P., Jennings G.T., Wagner F., Bachmann M.F. 2008. Effect of immunisation against angiotensin II with CYT006-AngQβ on ambulatory blood pressure: a double-blind, randomised, placebo-controlled phase IIa study. *Lancet* 371: 821–827.

Valegård K., Liljas L., Fridborg K., Unge T. 1990. The three-dimensional structure of the bacterial virus MS2. *Nature* 345: 36–41.

Valenzuela P., Medina A., Rutter W.J., Ammerer G., Hall B.D. 1982. Synthesis and assembly of hepatitis B virus surface antigen particles in yeast. *Nature* 298: 347–350.

van Duin J. 1999. Single-stranded RNA phages. In: Webster R.G., Granoff A. (eds) *Encyclopedia of Virology,* Academic Press, London, pp. 1663–1668.

Voronkova T., Grosch A., Kazaks A., Ose V., Skrastina D., Sasnauskas K., Jandrig B., Arnold W., Scherneck S., Pumpens P., Ulrich R. 2002. The highly flexible and immunodominant C-terminal region of hamster polyomavirus VP1 exposed on chimeric bacteriophage fr capsids induced a strong VP1-specific antibody response in mice. *Viral Immunol.* 15: 627–643.

Weber, H. 1999. Qb replicase. In: Creighton T.E. (ed) *Encyclopedia of Molecular Biology*. John Wiley, New York, pp. 2085–2087.

Xu Y.F., Zhang Y.Q., Xu X.M., Song G.X. 2006. Papillomavirus virus-like particles as vehicles for the delivery of epitopes or genes. *Arch. Virol.* 151: 2133–2148.

Efektīva bakteriofāga GA vīrusveidīgo daļiņu iegūšana no raugiem *Saccharomyces cerevisiae* un *Pichia pastoris*

Jānis Freivalds, Jānis Rūmnieks, Velta Ose, Regīna Renhofa, Andris Kazāks*

Latvijas Biomedicīnas pētījumu un studiju centrs, Rātsupītes 1, Rīga LV-1067, Latvija

*Korespondējošais autors, E-pasts: andris@biomed.lu.lv

Kopsavilkums

RNS bakteriofāgu apvalka proteīnu veidotās rekombinantās vīrusveidīgās daļiņas (virus-like particles; VLPs) uzskata par daudzsološu peptīdu un nukleīnskābju transportformu jauna tipa vakcīnu un gēnu terapijas līdzekļu konstruēšanai. Šajā darbā mēs pētījām iespēju iegūt bakteriofāga GA VLPs raugos *Saccharomyces cerevisiae* un *Pichia pastoris*. Kultivēšanas apstākļu optimizācijai salīdzināja GAL1 un GAL10 promoteru kontrolētu ekspresiju *S. cerevisiae*, kā arī AOX1 promotera kontrolētu ekspresiju *P. pastoris*. Visos trīs gadījumos konstatēja GA apvalka proteīna sintēzi un VLP veidošanos. Pēc viena hromatogrāfijas cikla gēlfiltrācijas kolonnā frakcionētās GA VLPs sasniedza 80 līdz 90 % tīrību. Kopumā attīrīto VLP iznākums bija 0.6 līdz 2.0 mg no 1 g *S. cerevisiae* šūnu, bet *P. pastoris* gadījumā tas sasniedza pat 3 mg no identiska šūnu daudzuma. Iegūtās rekombinantās VLPs potenciāli varētu izmantot ķīmiski piesaistītu peptīdu eksponēšanai uz virsmas, kā arī imunostimulatoru DNS sekvenču pakošanai daļiņu iekšienē.

Acta Universitatis Latviensis, 2008, Vol. 745, Biology, pp. 87–101

Cloning and characterization of barley homologues of the *Arabidopsis LSD1* gene: putative regulators of hypersensitive response

Anete Keiša[1], Krista Kānberga[1], Upinder Gill[2], Andris Kleinhofs[2], Nils Rostoks[1]*

[1]Faculty of Biology, University of Latvia, Kronvalda Bulv. 4, Riga LV-1586, Latvia
[2]Department of Crop and Soil Sciences, Washington State University, Pullman, WA, 99164, USA

*Corresponding author, E-mail: nils.rostoks@lu.lv

Abstract

Plant hypersensitive response (HR) is a highly controlled reaction to prevent spread of biotroph pathogens. Understanding the mechanisms of HR could potentially allow development of crop plant varieties with improved resistance to pathogens. HR and its molecular control mechanisms have been extensively studied in model organisms, such as *Arabidopsis thaliana*, allowing to identify numerous necrotic or lesion-mimic mutants that constitutively express the HR even in absence of pathogen. *Arabidopsis LSD1* gene encodes a zinc finger protein characterized as a central regulator of HR. Here we identified three genes homologous to the *LSD1* in barley and compared them to *LSD1* homologues in other grass species. Barley gene *CBC04043* appeared to be more similar to the *Arabidopsis LOL1* gene, however, the two other genes originating from gene duplication after the monocot - dicot divergence represented candidate genes for the *LSD1* orthologue. As the sequence analysis alone did not allow identification of the *LSD1* orthologue in barley, expression of the three genes was studied in barley necrotic mutants *nec1* and *nec3*.

Key words: *Arabidopsis LSD1* gene, barley, gene expression, lesion-mimic mutant, necrotic mutant, phylogeny.

Introduction

Incompatible plant-pathogen interactions cause series of stress response reactions involving ion fluxes, accumulation of reactive oxygen species and altered production of the endogenous signal molecules (Heath 2000). Biotic stress often triggers hypersensitive response (HR) – cell death in tissues directly surrounding infection site. HR is a highly controlled physiological process requiring specific initiation, propagation and restriction mechanisms directed by crosstalk of plant signalling pathways (Shirasu, Schulze-Lefert 2000; Lam et al. 2001). Alterations in HR have been shown to affect plant defense mechanisms by increasing disease resistance or rendering plants more susceptible to pathogen infection (Govrin, Levin 2000; Vleeshouwers et al. 2000; Kombrink, Schmelzer 2001). Despite the involvement of HR in plant defense mechanisms, knowledge concerning the genetic basis of HR is still scarce. Characterization of genetic disorders causing the lesion-mimic phenotype (constitutively expressed HR) or preventing pathogen-induced

cell death (inability to initiate HR) is a common approach to uncover the genetics behind the HR (Glazebrook 2001; Lorrain et al. 2003). Mutant plants exhibiting impaired HR are categorized into two groups depending on a stage of HR altered (Lorrain et al. 2003). Lesion-mimic mutants (LMM) belonging to the class of initiation mutants display spontaneous induction of HR. In contrast, LMM showing normal initiation of HR, but incapable of restricting propagation of programmed cell death belong to the propagation class of mutants. In order to obtain more thorough insight into the molecular mechanisms involved in HR, studies examining both types of LMM would be required.

One of the best characterized propagation LMM is *lsd1* (*lesion simulating disease 1*), which cannot restrict lesion propagation initiated in response to superoxide (Jabs et al. 1996). *LSD1* has been proposed to be a negative regulator of plant cell death involved in regulation of copper zinc superoxide dismutase expression (Kliebenstein et al. 1999; Epple et al. 2003). The role of LSD1 in reactive oxygen species (ROS) homeostasis regulation has also been confirmed by the fact that *LSD1* acts in acclimation to excess excitation energy operating through repression of *PAD4* and *EDS1*-dependent stomatal closure (Mateo et al. 2004). More recently, LSD1 has been implicated in control of lysigenous aerenchyma formation in *A. thaliana* roots in response to hypoxia (Muhlenbock et al. 2007). LSD1 function in regulation of ROS homeostasis has been shown to depend on antagonistic interaction with LOL1, a closely related protein also belonging to the class of LSD1-type Zn-finger domain-containing proteins (Epple et al. 2003). Although the precise mechanism by which LSD1 and LOL1 interaction affects PCD is not known, in *A. thaliana* LSD1 is considered to operate as a cellular hub ensuring retention of the pro-apoptotic transcription factor AtbZIP10 in the cytoplasm (Kaminaka et al. 2006). Functional involvement of *LSD1* in regulation of plant cell death and its central role in HR propagation control renders the gene interesting for HR studies. Apart from *A. thaliana*, *LSD1* has also been cloned from *Oryza sativa*, where it is proposed to be involved also in callus differentiation (Wang et al. 2005), and from *Brassica oleracea*, where AtLSD1 homologues have been shown to function during senescence-related PCD (Coupe et al. 2004). In this study we describe *A. thaliana LSD1* homologues in barley and characterize the phylogenetic relationships between *LSD1* gene homologues in different grass (*Poaceae*) species. Possible interactions between the identified genes and previously characterized HR related genes were studied by analyzing gene expression using real time quantitative PCR in barley initiation LMMs *nec1* and *nec3*.

Materials and methods

Identification and sequence analysis of barley homologues of Arabidopsis *gene* LSD1

The *Arabidopsis thaliana* LSD1 amino acid sequence AAC49660 was used as a query in TBLASTN search against the barley Expressed Sequence Tags (ESTs) at the NCBI GenBank database and against the barley EST unigene database HarvEST assemblies 21 and 35 (http://harvest.ucr.edu). Coding sequences of two barley homologues of the *A. thaliana LSD1, ABC10220* and *ABC06454*, were identified by sequencing cv. *Morex* cDNA clones HvCEa0008p08 and HvSMEb0007a07. The coding sequence of the third homologue, *CBC04043*, was predicted from the unigene sequence. Intron-exon structure of the barley genes was predicted by comparing the cDNA and unigene sequences with the respective genomic clones. cDNA and genomic sequences of the barley homologues of

the *Arabidopsis LSD1* gene have been deposited in the GenBank under accession numbers EU545232 and EU545233 for *ABC10220* gDNA and cDNA sequences respectively, EU 545231 and EU545234 for *ABC06454* gDNA and cDNA sequences respectively, EU545230 for gDNA sequence of *CBC04043*.

Phylogenetic analysis of LSD1 *homologues in* Poaceae

Coding sequences were predicted using NCBI ORF Finder (http://www.ncbi.nlm.nih.gov/gorf/gorf.html). Predicted amino acid sequences of barley *LSD1* homologues were used in TBLASTN query of the NCBI EST-others database (search parameters: score > 100, E value < 0.00005) to identify homologous sequences in other *Poaceae* species. EST sequences showing the highest homology were translated using NCBI ORF Finder and aligned using ClustalX 1.81 (Thompson et al. 1997). The amino acid sequence alignment was manually edited and gene phylogeny was reconstructed with Maximum Likelihood method using the proml programme from the PHYLIP3.66 package (Felsenstein 1989). Bootstrap confidence levels were calculated from 100 iterations using the seqboot programme from the PHYLIP package. The phylogenetic tree was visualized using TreeView (Page 1996).

Plant material, cultivation and DNA extraction

Plants for DNA extraction and *LSD1* expression analysis were grown in a growth room at 22 °C under long-day (16 h day/ 8 h night) low light (ca. 130 μmol m^{-2} s^{-1}) conditions. DNA was extracted from fresh leaf tissue as described by Edwards et al. 1991.

The barley necrotic mutant *nec1* (GSHO 1284) containing mutation in the *Cyclic Nucleotide Gated Ion Channel 4* (*CNGC4*) gene (Rostoks et al. 2006) and necrotic mutant *nec3* (GSHO 2065) were used for the barley *LSD1* expression analysis. GSHO 1284 is described as a natural mutant in cv. *Parkland* (Fedak et al. 1972), while GSHO 2065 is a backcross of the *nec3.d* allele into a Bowman genetic background (Lundqvist et al. 1997).

RNA extraction

For RNA extractions 5 cm long segments of the first leaf from 2-week-old plants of necrotic mutants *nec1* and *nec3* and their parents, Parkland and Bowman, were snap-frozen in liquid nitrogen immediately after harvesting. Total RNA was extracted from frozen leaf tissues using a RNeasy Plant Mini Kit (QIAGEN, Hilden, Germany) following manufacturer's instructions. Each RNA sample was extracted from a pool of five plants and three biological replicates of each barley line (15 plants in total) were used for expression analysis of the barley *LSD1* homologues in necrotic mutants and their respective parents. Integrity of the extracted RNA was monitored using non-denaturing agarose gel electrophoresis. One to two μg of the extracted RNA was treated with DNaseI (Fermentas, Vilnius, Lithuania) following manufacturer's instructions and afterwards purified using a QIAGEN RNeasy Plant Mini Kit. The quantity of purified total RNA was monitored using a spectrophotometer Ultrospec 3100 pro (Amersham Biosciences, Little Chalfont, UK).

PCR, RT-PCR and quantitative real-time PCR

Gene-specific primers (Table 1) were designed by Primer3 software (Rozen, Skaletsky 2000). PCR reactions were carried out in a 20 μL of total volume containing 50 - 100 ng genomic DNA, 0.5 μM primers, 1.8 mM $MgCl_2$, 0.2 mM dNTPs and 1 u Hot Start or TrueStart *Taq* DNA polymerase (Fermentas, Vilnius, Lithuania) used with manufacturer-

Table 1. Oligonucleotide primers for PCR, sequencing and quantitative real time PCR. *, primers used for quantitative real time PCR

Primer	Sequence 5'-3'	Primer	Sequence 5'-3'
ABC10220_L01	cgagggatttctcgtctgct	ABC06454_R03_b	caagattgactgtactgcaacatgagc
ABC10220_L02	cgtctgctcggttcctctcg	ABC06454_R04	gtgtacatcagcaaagttcggcaac
ABC10220_L03	atgcgtcggctgtcgaactt	ABC06454_R05	gtgcatgctttccttggtg
ABC10220_L04	ctctggtctcccccgtttgt	ABC06454_R06	ataagctgagccatttccactg
ABC10220_L05	caacgtcgtagtcggggtta	ABC06454_R07	ttgttaatccttcggaagtctgtgc
ABC10220_L07*	ccatacggagcatcttctgtcaagt	ABC06454_R08	atatcacgtgccactaaggtcttgc
ABC10220_R01	ccgcgctttgggtttttgtt	CBC04043_L01	cattccaactcatgttgttattctgag
ABC10220_R02	cacacttgacagaagatgctccgta	CBC04043_L02	gtccgcctcttcctctgaac
ABC10220_R03_b	gtgctggtctggcaaggttga	CBC04043_L03	gacgagcaggatttcatgtagag
ABC10220_R04	gggcccctctggggtagag	CBC04043_L04	agtctcgtccgcagcaac
ABC10220_R05	gacagctactccctccgttcc	CBC04043_L05	ctcaaagccaacttgtctgctc
ABC10220_R07*	gtggtaaccccgactacgacgtt	CBC04043_L06*	gagatggcgcagctagtttg
ABC06454_L01	gacccaggagccctctgtca	CBC04043_L07	aatcaggttgcgcatgtaaact
ABC06454_L02	tggttgccgaactttgctga	CBC04043_L08	atcatcgggtgcagagcag
ABC06454_L03_b	aaacgccatgtcacctgcac	CBC04043_R01	tgcccggttcagaggaagag
ABC06454_L04	catgtgccgagccatcacc	CBC04043_R02	gaagtcgaggggatgagaacagat
ABC06454_L05	ctgtacattcacagctgaatagtgg	CBC04043_R03	cgtgaagggcgcaggag
ABC06454_L06	tggtcagcaacgtcgtagtc	CBC04043_R04	ggaacagcggtcacggtact
ABC06454_L07	cagtggaaatggctcagctt	CBC04043_R05	cttccattgccaggttgacagt
ABC06454_L08	gtgtgattcatagttcgatgccatt	CBC04043_R06*	actgatgtcacgaaactgcagac
ABC06454_L09*	aatatagcccacgtgaattgtggtc	CBC04043_R07	ctatacatgtgcactcaaagcattc
ABC06454_R01	tcaggcagcaaccaatcacc	CBC04043_R08	caacgaagggagaaatggagag
ABC06454_R02*	cgtcgacagtcatagggttctcaa	CBC04043_R09	ggttcatgtatctgtctgacccagt

supplied buffers. PCR was carried out on an Eppendorf Mastercycler (Eppendorf, Hamburg, Germany) as follows: initial denaturing step for 5 min at 95 °C, 7 cycles of touch down of 30 s at 95 °C, 30 s at 65 - 58 °C, 3 min at 72 °C, followed by 25 cycles of 30 s at 95 °C, 30 s at 58 °C, 3 min at 72 °C and final extension of 5 min at 72 °C.

cDNA was synthesized with oligo (dT)18 primer in a total volume of 15 µL containing 0.5 µg of total RNA using a RevertAid H Minus First Strand cDNA synthesis kit (Fermentas, Vilnius, Lithuania).

For real-time PCR aliquots of cDNA were amplified on an ABI Prism 7300 instrument (Applied Biosystems, Foster City, CA, USA) using a QuantiTect SYBR Green PCR kit (QIAGEN, Hilden, Germany) in a total volume of 25 µL containing 2 µL of cDNA and 0.3 µM primers. Primers used for real-time PCR are listed in Table 1. Reaction was carried out as follows: initial denaturing step for 15 min at 95 °C followed by 35 cycles of 15 s at 94 °C, 30 s at 60 °C and 30 s at 72 °C (data acquisition step). Standard curves for the quantification of the transcript levels were calculated from serial dilutions of appropriate cDNA fragments amplified from cv *Morex*. Transcript levels of *LSD1* homologues were expressed as a percentage of *HvGAPDH* transcript amount in the same sample. Combined

Table 2. CAPS markers for linkage mapping of barley homologues of the *LSD1* gene

Gene	PCR Primers	Restriction enzyme	Restriction fragment size (bp)	
			OwbD	OwbR
ABC10220	ABC10220_L02 /ABC10220_R03b	NdeI	2350	2150
				200
ABC06454	ABC06454_L02 /ABC06454_R02	TaqI	720	620
			300	300
			230	230
				100
CBC04043	CBC04043_L04 /CBC04043_R05	SspI	1070	700
				370

values of two technical replicates of the three biological replicates (n = 6) were used to calculate the average values and standard deviations. Analysis of variance (ANOVA) of transcript abundance between the mutant and the corresponding parent was conducted using Microsoft Excel (Redmond, WA, USA).

Sequencing

LSD1 barley homologues were sequenced from cvs. *Morex* and *Steptoe*. PCR products were purified using DNA Extraction Kit (Fermentas, Vilnius, Lithuania) or treated with exonuclease I and shrimp alkaline phosphatase (Fermentas, Vilnius, Lithuania) prior to sequencing. *LSD1* barley homologues were sequenced by subcloning PCR products into vector pTZ57R/T (Fermentas, Vilnius, Lithuania) or directly by primer walking. Sequencing reactions were carried out using BigDye Terminator Cycle Sequencing Kit (Applied Biosystems, Foster City, CA, USA) in 10-µL total volume containing 10 - 50 ng of purified PCR product, 1 µM primer, 1 µL BigDye and manufacturer-supplied buffer. Base calling and sequence assembly were done with Staden package (Staden 1996).

Linkage mapping

The Oregon Wolf Barley Dominant × Oregon Wolf Barley Recessive population (Costa et al. 2001) consisting of 94 doubled haploid lines was used for linkage mapping of the three barley *LSD1* homologues. Cleaved Amplified Polymorphic Sequences (CAPS) markers differentiating the parents of the mapping population were developed for each gene based on single nucleotide polymorphisms detected by sequencing (Table 2).

Results

Identification of barley homologues of Arabidopsis thaliana *gene* LSD1

TBLASTN query of the NCBI GenBank barley EST database and HarvEST EST unigene database with *Arabidopsis thaliana* LSD1 amino acid sequence AAC49660 identified three groups of barley ESTs represented by two HarvEST assembly 21 unigenes, *ABC10220*, *ABC06454*, and one HarvEST assembly 35 unigene, *CBC04043*. Sequences of the two cv. *Morex* cDNA clones, HvCEa0008p08 and HvSMEb0007a07, which matched unigenes

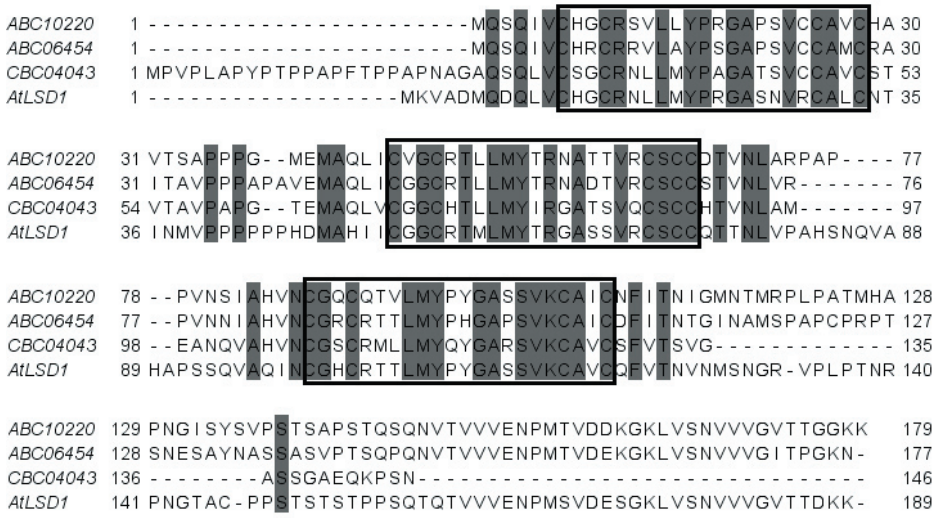

Fig. 1. Multiple sequence alignment of deduced amino acid sequences of *Arabidopsis thaliana LSD1* and the identified barley homologues. Zn-finger domains are denoted by black frame. aa acids identical in all four sequences are indicated by colored background.

ABC10220 and *ABC06454*, as well as the unigene sequence *CBC04043* were used to predict the encoded amino acid sequences. The three barley homologues showed approximately equal amino acid identity (ABC10220 – 54 %, ABC06454 – 55 %, CBC04043 – 57 %) with the *Arabidopsis* LSD1 (Fig. 1), however, the CBC04043 was more similar (86 % amino acid identity) to *Arabidopsis* LOL1.

Genetic mapping of barley LSD1 *homologues*

The Oregon Wolfe Barley Dominant by Recessive doubled haploid mapping population (Costa et al. 2001) was used for linkage mapping of barley homologues of the *LSD1* gene. Segregation data of the three CAPS markers (Table 2) was used for linkage mapping in Map Manager QTX software (Manly et al. 2001) relative to restriction fragment length polymorphism and simple sequence repeat markers (Costa et al. 2001). The *CBC04043* gene was mapped to chromosome 5(1H) between JS10C (bin09) and Bmac0113A (bin11) markers, *ABC10220* was mapped to chromosome 7(5H) between ABG395 (bin04) and NRG045A (bin05) and *ABC06454* was located on chromosome 7(5H) between BE456118C (bin11) and Tef3 (bin11 - 12).

Structure of barley LSD1 *homologues*

Pairwise alignment of cDNA and gDNA sequences identified the exon–intron structure of barley *LSD1* homologues (Fig. 2). Genes *ABC10220* and *ABC06454* showed highly conserved exon-intron organization, each comprising six exons of conserved size and sequence. Similarly to *Arabidopsis LSD1*, barley genes encode three putative Zn finger domains (pfam 06943) detected by conserved domain search of the Pfam 22.0 database (Finn et al. 2006). The position of Zn-finger domains is highly conserved in ABC10220

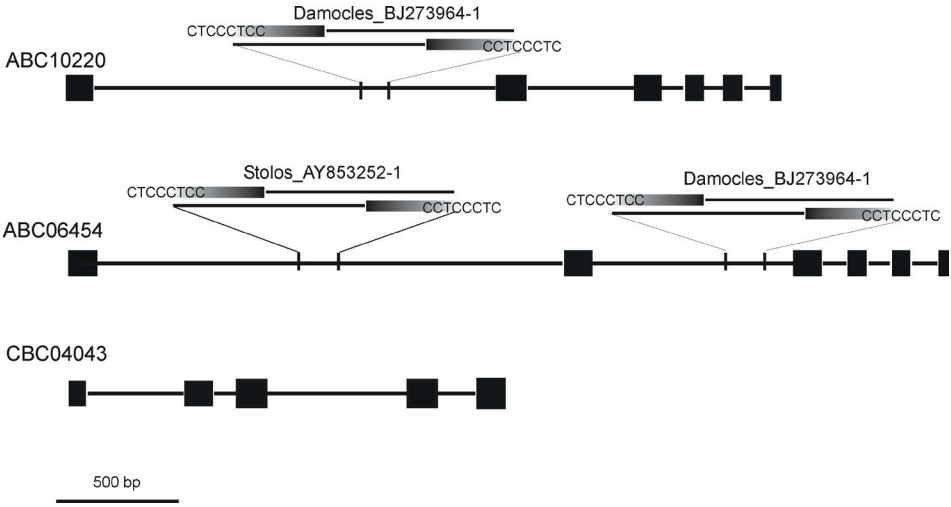

Fig. 2. Gene structure of LSD1 barley homologues with exons shown as black boxes. Stowaway MITE insertions are shown above the gene structure.

Table 3. List of LSD1 gene homologues from *Poaceae* species used for phylogenetic analyses

Barley *LSD1* homologue	Species (designation in phylogenetic tree, Fig. 3)	GenBank accessions
ABC10220	*Triticum aestivum* (2)	BJ268629
	Brachypodium distachyon (2)	DV489172
	Oryza sativa (2)	CF316414
	Zea mays (2)	DY39886
	Saccharum officinarum (2)	CA122488
	Sorghum bicolour (2)	CX609698
ABC06454	*Triticum aestivum* (1)	CJ689628
	Brachypodium distachyon (1)	DV487362
	Oryza sativa (1)	CT848680
	Zea mays (1)	EC872597
	Saccharum officinarum (1)	CA215734
	Sorghum bicolour (1)	CF486644
CBC04043	*Triticum aestivum* (3)	CJ603752
	Brachypodium distachyon (3)	DV477202
	Oryza sativa (3)	CI036551
	Zea mays (3)	DV505906
	Saccharum officinarum (3)	CA088897
	Sorghum bicolour (3)	BG241556
	Secale cereale (1)	BE705617
	Triticum monococcum (1)	BG607068

and ABC06454, in which the first three exons each contain a single Zn-finger domain. In addition, C-termini of ABC10220 and ABC06454 contained highly conserved Val rich regions.

Homology-based annotation of genomic sequences indicated presence of repetitive sequences within gene structure. BLASTN search against the TREP *Triticeae* Repeat database (http://wheat.pw.usda.gov) showed that the 1st intron of *ABC10220* and 1st and 2nd intron of *ABC06454* contained sequences sharing high homology with several Stowaway MITEs (miniature inverted repeat transposable elements) (Fig. 2).

Exon-intron organization and position of the conserved domains of *CBC04043* differed from that deduced for *ABC10220* and *ABC06454*. According to the pairwise alignment of cDNA and gDNA, the coding sequence of *CBC04043* consisted of five exons with Zn-finger domains positioned in the 2nd, 3rd and 4th exons.

Comparison of Arabidopsis LSD1 *with homologues in barley and other* Poaceae *species*

TBLASTN search with deduced amino acid sequences of barley LSD1 homologues was performed to identify homologues sequences in other *Poaceae* species (Table 3). Amino acid sequence alignment was used to reconstruct phylogenetic relationships among the barley *LSD1* homologues and related genes in other *Poaceae* species. Identified sequences clustered into three distinct groups, each including a single barley gene (Fig. 3). The cluster represented by the barley CBC04043 sequence showed a high degree of sequence conservation.

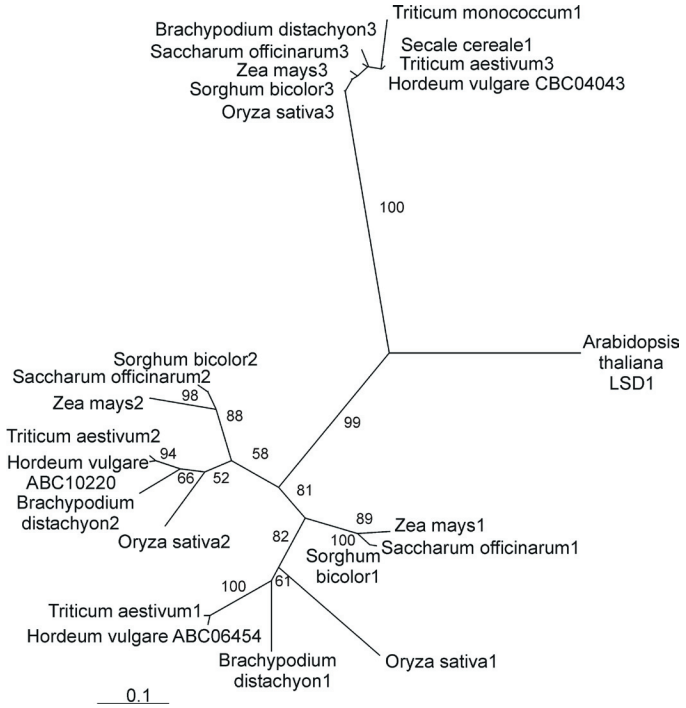

Fig. 3. Phylogenetic relationships among the barley *LSD1* homologues and related genes in other *Poaceae* species reconstructed with Maximum Likelihood method. Bootstrap confidence levels (calculated from 100 iterations) higher than 50% are shown.

Table 4. List of LSD1-like genes from *Arabidopsis thaliana*, *Oryza sativa* and *Hordeum vulgare* used for phylogenetic analysis in Fig. 4. a – designation consistent with TAIR (The Arabidopsis Information Resource) information; b – designation consistent with (Liu, Xue 2007); c – designation corresponds to HarvEST Assembly 21 unigene represented by a EST sequence

Designation in phylogenetic tree	*Arabidopsis* gene or GenBank accession
AtLOL1a	At1g32540
AtLOL2a	At4g216210
AtLOL3a	At1g02170
AtLSD1a	At4g20380
OsLOL1b	AK061509
OsLOL2b	AK111837
OsLOL3b	AK111569
OsLOL4b	AK120454
OsLOL5b	AK065375
OsLSD1b	AY525368
Hv14621c	CV063671
Hv15713c	BE421616
Hv2281c	AV933097

In order to better estimate the relationships of the three barley genes with rice and Arabidopsis LSD1 genes, more distant LSD1-like genes were identified in barley, rice and Arabidopsis using TBLASTN search. Three additional barley ESTs comprising LSD1-like Zn-finger domains were identified (Table 4) and used to reconstruct the phylogeny of barley, Arabidopsis and rice LSD1-like genes (Fig. 4).

Expression of barley LSD1 *homologues in lesion-mimic mutants* nec1 *and* nec3

Arabidopsis LSD1 is a negative regulator of cell death (Dietrich et al 1997). *lsd1* mutants are hypersensitive to cell death signals and unable to control the extent of cell death (propagation type of LMM). Expression of barley homologues of the *AtLSD1* was studied in initiation LMM *nec1* and *nec3* in comparison to parental varieties (Fig. 5).

A two-fold decrease ($p = 0.0003$) in transcript abundance of *CBC04043* was observed in *nec1* mutant, while in *nec3 CBC04043* expression showed a slight, but statistically significant ($p = 0.015$) increase. Although no remarkable difference in transcript abundance of *ABC10220* was detected between the LMMs and the respective parents, gene was slightly repressed in *nec1* ($p = 0.003$). Observed differences in expression of *ABC06454* were not statistically significant (Fig. 5).

Discussion

Three barley homologues of *A. thaliana LSD1* were identified based on sequence homology searches. All three genes encoded three Zn-finger-LSD1 domains and showed a very similar level of amino acid homology with the AtLSD1. Two of the barley homologues, *ABC10220* and *ABC06454*, showed highly conserved exon sizes and organization, as well as almost identical arrangement of the Zn-finger-LSD1 domains. The third homologue,

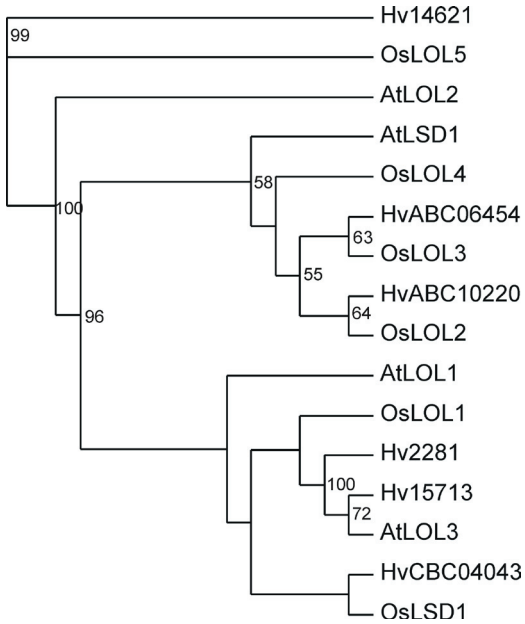

Fig. 4. Phylogenetic relationships among known *LSD1*-like genes and barley genes comprising LSD1-like Zn-finger domains. Phylogenetic tree was reconstructed with Maximum Likelihood method. Bootstrap confidence levels (calculated from 100 iterations) higher than 50 are shown. Barley genes are designated according to the corresponding HarvEST assembly 21 unigene number.

CBC04043, had substantially different exon-intron organization and distribution of the Zn-finger domains. The structural distinctiveness of the *CBC04043* and considerable similarity of *ABC10220* and *ABC06454* implied the putative divergence of the *CBC04043* from the common ancestor before the separation event of *ABC10220* and *ABC06454*.

Phylogenetic analysis of the barley *LSD1* gene homologues from other *Poaceae* species partitioned sequences into three clusters, each comprising homologues from all analyzed grass species including barley (Fig. 3). The two groups including barley genes *ABC06454* and *ABC10220* each included wheat, rice, sorghum and sugarcane genes, thus the apparent gene duplication must have happened after the monocot - dicot split, but before the divergence of Pooideae (barley, brachypodium and wheat), Panicoideae (maize, sorghum and sugarcane) and Ehrhartoideae (rice) (Kellogg 2001). The ancient origin and functional divergence of the *LSD1*-like gene family has also previously been described in rice (Liu, Xue 2007).

Monocots and dicots diverged about 140 - 150 million years ago (Chaw et al. 2004). Since then, *A. thaliana* has undergone whole genome duplication (Arabidopsis Genome Initiative 2000). Similar genome duplication has occurred in rice (Yu et al. 2005). There is emerging evidence confirming similar genome duplications in a lineage leading to barley (Stein et al. 2007). Following duplication, one of the copies can continue to perform the old function, while the selective pressure is now lifted from the second copy which can accumulate mutations and can become a pseudogene or acquire a novel function. Thus gene and genome duplications may complicate identification of functional orthologues in

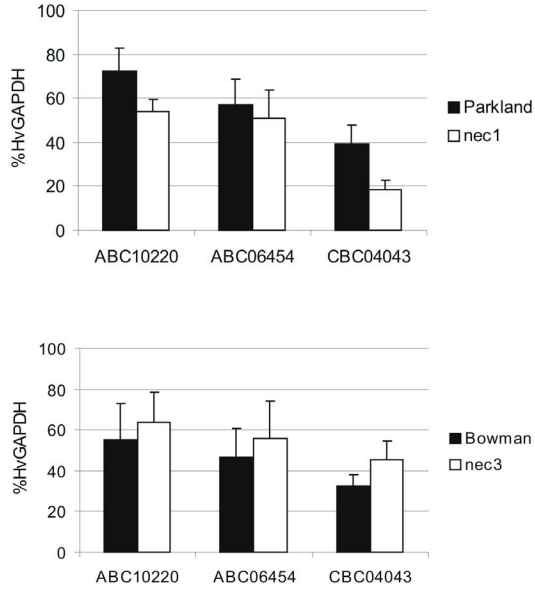

Fig. 5. Expression of barley homologues of *Arabidopsis LSD1* gene in barley necrotic mutants *nec1* and *nec3*. Gene expression levels are expressed as percent of HvGAPDH expression. Error bars represent standard deviations.

distant taxonomic groups based on sequence homology alone.

The phylogenetic analysis of more distant *LSD1*-like gene homologues from different monocots provide deeper insight into the putative origin and divergence time of the three barley homologues (Fig. 4). Analogy of rice and barley *LSD1*-like gene phylogeny suggests putative functional characteristics of studied barley homologues. According to the phylogenetic analysis, OsLOL2 and OsLOL3 are the closest rice homologues of ABC10220 and ABC06454 respectively, whereas the closest *A. thaliana* homologue of these genes was AtLSD1. Similar discrepancies between *A. thaliana* and rice homology with barley were also observed in the case of CBC04043, which clustered with OsLSD1, whereas the closest *A. thaliana* homologue is AtLOL1 (Fig. 4). Clustering of CBC04043 with AtLOL1 indicated that CBC04043 may be the functional homologue of LOL1 in barley. LOL1 is highly conserved throughout monocots, as well as dicots, and has been predicted to function as a positive regulator of plant cell death, probably taking part in developmental processes (Epple et al. 2003). Discrepancies in clustering of barley homologues with *A. thaliana* or rice *LSD1*-like genes prevented from an unambiguous designation of the ABC10220 and ABC06454 to a certain functional group of *LSD1*-like genes. ABC10220 and ABC06454 clustered with AtLSD1 but not with OsLSD1. As reported by Epple et al. (2003) and Wang et al. (2005), the rice gene AY525368 was designated as *OsLSD1* based on its functional characterization despite the fact that it showed higher sequence homology to the *AtLOL1* than to *AtLSD1*. Discrepancies in barley *LSD1*-like gene homology with rice and *Arabidopsis* could be caused by differences in stress regulation requirements of these species. It has been reported that AtLSD1 is involved in lysogenic aerenchyma

formation in roots of *A. thaliana* in response to hypoxia (Muhlenbock et al. 2007). Since growth habits of rice might be associated with higher stress of hypoxia compared to *A. thaliana* or barley, putative functional divergence of *LSD1*-like genes in these species could be anticipated. Considering different environmental pressure imposed on different species, it might be difficult to assign a correct functional annotation to the *LSD1*-like genes involved in plant stress response regulation based only on sequence homology and phylogenetic analysis. Therefore, in order to identify the functional homologue of *AtLSD1* in barley, further experiments were needed.

The expression analysis of the identified LSD1 homologues in barley initiation LMMs *nec1* and *nec3* showed that the *CBC04043* expression was significantly decreased in the *nec1* genetic background and slightly increased in the *nec3* background. In the case of *AtLOL1*, reduction of transcript abundance to 25 - 60 % of the wild type level was enough to increase susceptibility to virulent pathogen and alter HR elicitor treatment response (Epple et al. 2003). Therefore, a two-fold decrease in transcript abundance of *CBC04043* (putative *HvLOL1*) in nec1 could serve as indication for a functional link between *LOL1* and *NEC1* in barley. Because the expression of *CBC04043* was suppressed in *nec1* in spite of spontaneous HR, lesion formation in *nec1* may depend on other pro-apoptotic genes functioning in an alternative pathway. Of the other two barley genes, *ABC10220* and *ABC06454*, representing candidates for barley *LSD1* gene, only the *ABC10220* showed statistically significant reduction of expression in the *nec1* mutant, while its expression was not affected in the *nec3* genetic background. The finding that *LSD1*-like gene expression can be affected in the *nec1* mutant with a deficient *NEC1* gene served to suggest involvement of cyclic nucleotide regulated ion channels in a *LSD1*-related HR pathway. Intuitively it would have been expected that expression of pro-apoptotic genes like *LOL1* will be increased in necrotic mutants and that different patterns of expression of the *LSD1* homologues will be observed due to the antagonistic nature of *LOL1* and *LSD1*. Contrary to the initial hypothesis, the expression of all three barley *LSD1* homologues in *nec1* was slightly suppressed.

In conclusion we have identified three barley *LSD1* homologues. Based on the phylogenetic analysis one of the identified genes, *CBC04043*, can be designated as barley *LOL1*. Sequence analysis indicate that *ABC10220* and *ABC06454* genes represent the best candidates for homologues of the *LSD1* gene, however, further gene expression analyses may be required to identify the functional homologue of *LSD1*.

Acknowledgements

This study is supported by a grant ZP-59 from the University of Latvia to Dr. Rostoks and USDA NRI grant 2004-35301-14635 to Dr. Kleinhofs. Seed of the barley necrotic mutants and their parents was obtained from USDA National Plant Genetic Resource Collection, Aberdeen, ID, USA.

References

Arabidopsis Genome Initiative. 2000. Analysis of the genome sequence of the flowering plant *Arabidopsis thaliana*. *Nature* 408: 796–815.

Chaw S.M., Chang C.C., Chen H.L., Li W.H. 2004. Dating the monocot-dicot divergence and the origin of core eudicots using whole chloroplast genomes. *J. Mol. Evol.* 58: 424–441.

Costa J.M., Corey A., Hayes P.M., Jobet C., Kleinhofs A., Kopisch Obusch A., Kramer S.F., Kudrna

D., Li M., Riera Lizarazu O., Sato K., Szucs P., Toojinda T., Vales M.I., Wolfe R.I. 2001. Molecular mapping of the Oregon Wolfe Barleys: a phenotypically polymorphic doubled-haploid population. *Theor. Appl. Genet.* 103: 415–424.

Coupe S.A., Watson L.M., Ryan D.J., Pinkney T.T., Eason E.J. 2004. Molecular analysis of programmed cell death during senescence in *Arabidopsis thaliana* and *Brassica oleracea*: cloning broccoli *LSD1*, Bax inhibitor and serine palmitoyltransferase homologues. *J. Exp. Bot.* 55: 59–68.

Dietrich R.A., Richberg M.H., Schmidt R., Dean C., Dangl J.L. 1997. A novel zinc finger protein is encoded by the *Arabidopsis LSD1* gene and functions as a negative regulator of plant cell death. *Cell* 88: 685–694.

Edwards K., Johnstone C., Thompson C. 1991. A simple and rapid method for the preparation of plant genomic DNA for PCR analysis. *Nucleic Acids Res.* 19: 1349.

Epple P., Mack A.A., Morris V.R.F., Dangl J.L. 2003. Antagonistic control of oxidative stress-induced cell death in Arabidopsis by two related, plant-specific zinc finger proteins. *Proc. Natl. Acad. Sci. USA* 100: 6831-6836.

Fedak G., Tsuchiya T., Helgason S.B. 1972. Use of monotelotrisomics for linkage mapping in barley. *Can. J. Gen. Cytol.* 14: 949–957.

Felsenstein J. 1989. PHYLIP - Phylogeny Inference Package (Version 3.2). *Cladistics* 5: 164–166.

Finn R.D., Mistry J., Schuster-Bockler B., Griffiths-Jones S., Hollich V., Lassmann T., Moxon S., Marshall M., Khanna A., Durbin R., Eddy S.R., Sonnhammer E.L.L., Bateman A. 2006. Pfam: clans, web tools and services. *Nucleic Acids Res.* 34: D247–D251.

Glazebrook J. 2001. Genes controlling expression of defense responses in Arabidopsis – 2001 status. *Curr. Opin. Plant Biol.* 4: 301–308.

Govrin E. M., Levin A. 2000. The hypersensitive response facilitates plant infection by the necrotrophic pathogen *Botrytis cinerea*. *Curr. Biol.* 10: 751–757.

Heath M. C. 2000. Hypersensitive response-related death. *Plant Mol. Biol.* 44: 321–334.

Jabs T., Dietrich R.A., Dangl J.L. 1996. Initiation of runaway cell death in an *Arabidopsis* mutant by extracellular superoxide. *Science* 273: 1853–1586.

Kaminaka H., Näke C., Epple P., Dittgen J., Schütze K., Chaban C., Holt B. F., Merkle T., Schäfer E., Harter K., Dangl J. L. 2006. bZIP10-LSD1 antagonism modulates basal defense and cell death in *Arabidopsis* following infection. *EMBO J.* 25: 4400–4411.

Kellogg E.A. 2001. Evolutionary history of the grasses. *Plant Physiol.* 125: 1198–1205.

Kliebenstein D. J., Dietrich R. A., Martin A. C., Last R.L., Dangl J.L. 1999. *LSD1* regulates salicylic acid induction of copper zinc superoxide dismutase in *Arabidopsis thaliana*. *Mol. Plant-Microbe Interact.* 12: 1022–1026.

Kombrink E., Schmelzer E. 2001. The hypersensitive response and its role in local and systemic disease resistance. *Eur. J. Plant Pathol.* 107: 69–78.

Lam E., Kato N., Lawton M. 2001. Programmed cell death, mitochondria and the plant hypersensitive response. Nature, 411: 848-853.

Liu Q., Xue Q. 2007. Molecular phylogeny, evolution, and functional divergence of the *LSD1*-like gene family: inference from the rice genome . *J. Mol. Evol.* 64: 354–363.

Lorrain S., Vaillea F., Balague C., Roby D. 2003. Lesion mimic mutants: keys for deciphering cell death and defense pathways in plants? *Trends Plant Sci.* 8: 263-271.

Lundqvist U., Franckowiak J., Konishi T. 1997. New and revised descriptions of barley genes. *Barley Genetics Newsletter* 26: 22.

Manly K.F., Cudmore R.H., Meer J.M. 2001. Map Manager QTX, cross-platform software for genetic mapping. *Mamm. Genome* 12: 930–932.

Mateo A., Muhlenbock P., Rustérucci C., Chang C.C.C., Miszalski Z., Karpinska B., Parker J.E., Mullineaux P.M., Karpinski S. 2004. *LESION SIMULATING DISEASE 1* is required for acclimation to conditions that promote excess excitation energy. *Plant Physiol.* 136: 2818–2830.

Muhlenbock P., Plaszczyca M., Plaszczyca M., Mellerowicz E., Karpinski S. 2007. Lysigenous aerenchyma formation in *Arabidopsis* is controlled by *LESION SIMULATING DISEASE1*. *Plant*

Cell 19: 3819–3830.

Page R.D. 1996. TreeView: an application to display phylogenetic trees on personal computers. *Comput. Appl. Biosci.* 12: 357–358.

Rozen S., Skaletsky H. J. 2000 Primer3 on the WWW for general users and for biologist programmers. In: Krawetz S., Misener S. (eds) B*ioinformatics Methods and Protocols: Methods in Molecular Biology*. Humana Press, Totowa, NJ, pp. 365–386

Shirasu K., Schulze-Lefert P. 2000. Regulators of cell death in disease resistance. Plant Mol Biol, 44: 371-385.

Staden R. 1996. The Staden sequence analysis package. *Mol. Biotechnol.* 5: 233–241.

Stein N., Prasad M., Scholz U., Thiel T., Zhang H., Wolf M., Kota R., Varshney R., Perovic D., Grosse I., Graner A. 2007. A 1,000-loci transcript map of the barley genome: new anchoring points for integrative grass genomics. *Theor. Appl. Genet.* 114: 823–839.

Thompson J.D., Gibson T.J., Plewniak F., Jeanmougin F., Higgins D.G. 1997. The CLUSTAL_X windows interface: flexible strategies for multiple sequence alignment aided by quality analysis tools. *Nucleic Acids Res.* 25: 4876–4882.

Vleeshouwers V. G. A. A., van Doojieweert W., Govers F., Kamoun S., Colon L. T. 2000. The hypersensitive response is associated with host and nonhost resistance to P*hytophthora infestans*. *Planta* 210: 853–864.

Wang L., Pei Z., Tian Y., He C. 2005. OsLSD1, a rice zinc finger protein, regulates programmed cell death and callus differentiation. *Mol. Plant-Microbe Interact.* 18: 375–384.

Yu J., Wang J., Lin W., Li S., Li H., Zhou J., Ni P., Dong W., Hu S., Zeng C., Zhang J., Zhang Y., Li R., Xu Z., Li S., Li X., Zheng H., Cong L., Lin L., Yin J., Geng J., Li G., Shi J., Liu J., Lv H., Li J., Wang J., Deng Y., Ran L., Shi X., Wang X., Wu Q., Li C., Ren X., Wang J., Wang X., Li D., Liu D., Zhang X., Ji Z., Zhao W., Sun Y., Zhang Z., Bao J., Han Y., Dong L., Ji J., Chen P., Wu S., Liu J., Xiao Y., Bu D., Tan J., Yang L., Ye C., Zhang J., Xu J., Zhou Y., Yu Y., Zhang B., Zhuang S., Wei H., Liu B., Lei M., Yu H., Li Y., Xu H., Wei S., He X., Fang L., Zhang Z., Zhang Y., Huang X., Su Z., Tong W., Li J., Tong Z., Li S., Ye J., Wang L., Fang L., Lei T., Chen C., Chen H., Xu Z., Li H., Huang H., Zhang,F., Xu H., Li N., Zhao C., Li S., Dong L., Huang Y., Li L., Xi Y., Qi Q., Li W., Zhang B., Hu W., Zhang Y., Tian,X., Jiao Y., Liang X., Jin J., Gao L., Zheng W., Hao B., Liu S., Wang W., Yuan L., Cao M., McDermott J., Samudrala R., Wang J., Wong G.K., Yang H. 2005. The genomes of *Oryza sativa*: a history of duplications. *PLoS Biol.* 3: e38.

Ar hipersensitīvo atbildi saistītā *Arabidopsis LSD1* gēna homologu identifikācija un raksturošana miežu genomā

Anete Keiša[1], Krista Kānberga[1], Upinder Gill[2], Andris Kleinhofs[2], Nils Rostoks[1]*

[1]Latvijas Universitātes Bioloģijas fakultāte, Kronvalda bulv. 4, Rīga LV-1586, Latvija
[2]Department of Crop and Soil Sciences, Washington State University, Pullman, WA, 99164, ASV
*Korespondējošais autors, E-pasts: nils.rostoks@lu.lv

Kopsavilkums

Augu hipersensitīvā atbilde (HA) ir kontrolēta atbildes reakcija uz stresu, kura fenotipiski izpaužas kā lokalizēta šūnu bojāeja tiešā infekcijas vietas tuvumā. Lai gan HA ir cieši saistīta ar augu slimību izturību, izpratne par HA molekulārās norises mehānismiem ir nepilnīga. HA molekulāro mehānismu izpēte ir nozīmīga gan augu programmētās šūnu bojāejas izpētei, gan praktiskai jaunu slimībizturīgu lauksaimniecības augu šķirņu radīšanai. Līdzšinējie HA pētījumi lielākoties veikti modeļorganismos, pētot nekrotiskos mutantus ar traucētu HA norisi. Lai nodrošinātu praktisko pielietojamību, būtu nepieciešama iegūto zināšanu pārnese uz lauksaimnieciski nozīmīgiem augiem. Šajā pētījumā esam identificējuši un raksturojuši HA iesaistītā *Arabidopsis thaliana* gēna *LSD1* homologus miežos, kā arī raksturojuši identificēto gēnu ekspresiju miežu nekrotiskajos mutantos *nec1* un *nec3*.

Acta Universitatis Latviensis, 2008, Vol. 745, Biology, pp. 103–114

Ecology of epixylic bryophytes in Eurosiberian alder swamps of Latvia

Linda Madžule*, Guntis Brūmelis

Department of Botany and Ecology, Faculty of Biology, University of Latvia, Kronvalda Bulv. 4, Rīga LV-1586, Latvia

*Corresponding author, E-mail: linda.madzule@gmail.com

Abstract

Fallen dead wood is an important structural element in Eurosiberian alder swamp forests that supports diversity of epixylic bryophyte species. The aim of the present study was to assess the bryophyte diversity on logs in relation to abiotic and biotic factors. Four Eurosiberian alder swamp forests stands were studied in three territories of Latvia – Moricsala Nature Reserve, Zvarde Mezi Nature Park and Slitere National Park. In total 102 logs were described. Overall 59 bryophyte species were recorded. The main factor affecting the richness of bryophyte species was decay stage. Composition of bryophyte species gradually changed during succession. Logs that were in the mid decay stage supported the largest number of bryophyte species. The visible perimeter of logs did not affect composition and number of bryophyte species. Differences in bryophyte species composition were found between deciduous and coniferous logs. Some differences in flora of epixylic bryophyte species were recognized between the studied territories.

Key words: decay stage, epixylic bryophytes, Eurosiberian alder swamps, indicator species analysis, logs.

Introduction

Natural Eurosiberian alder swamp forests are wet, fireproof, adapted to water level fluctuations, characterized by mosaic ground vegetation and hummocks (Priedītis 1999; Lārmanis et al. 2000). Decayed logs in different decay stages are an important feature of alder swamp forests (Priedītits 1999; Lārmanis et al. 2000), as they represent a structural element increasing biological diversity (Suško 1998).

The quantity of decayed wood depends on the forest gap creation rate, the decomposition rates of different tree species, and environmental conditions. Dead wood has been removed from forests due to the past forest management in Northern Europe, which has led to a decline in bryophyte species diversity (Andersson, Hytteborn 1991; Bambe 2008). Many bryophyte species depend on decayed wood, and they are often rare as their populations are small, unstable and their dispersal is limited (Ödor, Standovár 2001; Baldwin, Bradfield 2007). The diversity of epixylic bryophyte species is also closely connected with the quantity of logs in the studied territory (Ödor, Standovár 2001; Ödor, Standovár 2002; Pyle, Brown 2002; Ödor et al. 2006), which are often short-term and a patchy substrate for epixylic bryophytes (Bambe 2008).

Bryophytes are one of the first plants that colonize newly formed decay logs and bryophyte composition depends on decay stage and chemical processes in wood (Zielonka, Piatek 2004), tree species (Āboliņa 1968), diameter of decayed log (Bērmanis, Spuņģis 2002), local area (Lindström 2003), moisture content and age of decayed log, presence of bark on log and type of fungus destroying the log (Ödor, Standovár 2001; Ek et al. 2002; Lindström 2003). Humidity is especially important for liverworts, as they are sensitive to microclimatic changes (Hallingbäck, Holmåsen 2000). A large proportion of liverworts grow on decayed logs (Vellak, Paal 1999), and many have a narrow ecological range (Suško 1998).

The aim of the present study was to investigate the distribution of epixylic bryoflora in relation to abiotic factors on decayed wood in Eurosiberian alder swamp forests in different locations of Latvia. We examined the importance of log tree species, decay stage and log visible perimeter for the epixylic bryophytes.

Materials and methods

Study area

The study areas were located in four territories in Latvia – one swamp forest in Moricsala and Zvarde and two in Sliteres Zilo kalnu nogaze (Fig. 1). Moricsalas Island is located in the south - west part of Latvia in Moricsala Nature Reserve, where the climate is relatively moderate.

Zvardes swamp is located in the south-west part of Latvia, in the Zvardes Mezi Nature Park. European alder swamp forests are the most valuable feature of ecological diversity in Zvardes Mezi Nature Park (Celmiņš 2005). Sliteres Zilo Kalnu Nogaze is located in the Slitere National Park. This area contains a wide diversity of natural ecosystems due to

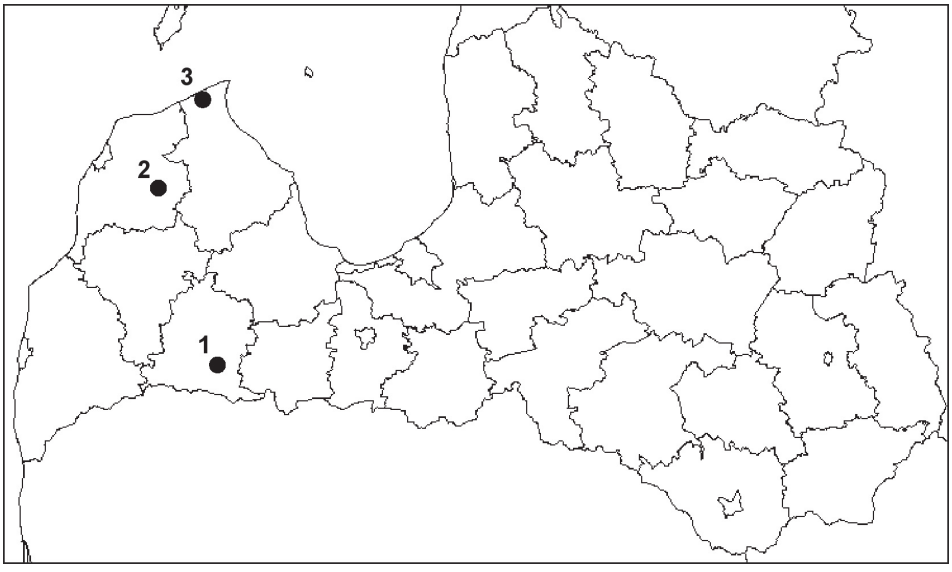

Fig. 1. Map of the Latvia showing the study areas (•). 1, "Zvārdes meži" Nature Park; 2, Moricsala Nature Reserve; 3, "Slīteres Zilo kalnu nogāze", Slitere National Park.

unique geological, geomorphologic, hydrological and climatic conditions (Sāmīte 2007).

Average temperature in January is –4.8 °C and average temperature in July is +16.7 °C. Precipitation in western Latvia is from 650 to 700 mm (Temņikova 1975).

Data sampling

The field work was conducted in Zvarde in October 2005, where 11 decayed logs were described. Investigations in Moricsala were carried out in July 2007. A total of 30 decayed logs were described in Eurosiberian alder swamp forest and 10 in other wet sites in Moricsala. The swamps in Sliteres Zilo Kalnu Nogaze (Z1 and Z2) at the base of the ancient Baltic Sea coast were investigated in July, August and October 2006; in total 51 decayed logs were surveyed. Decayed logs were chosen randomly in each territory.

On each decayed log randomly a maximum of three 1-m-long plots were established. The number of plots was selected depend on the length of the decayed log. Features described were decay stage, length, visible perimeter and species of tree. Logs with visible perimeter less than 0.1 m and length less than 1.5 m were not sampled. All bryophyte species were described in each plot and their projective cover was estimated using the Braun–Blanquet scale (Pakalne, Znotiņa 1992).

Bryophyte species that could not be identified in the field were collected for identification in the laboratory. Species nomenclature follows (Smith 1996; Hallingbäck, Holmåsen 2000; Āboliņa 2002; Ignatovs, Ignatova 2003; Ignatovs, Ignatova 2004; Smith 2004).

Determination of decay stage as a five-part scale followed Pyle and Brown (1998): (1) wood cannot be penetrated with thumbnail, wood is sound, bark is intact, smaller to medium branches are present; (2) thumbnail penetrates in the bark till three centimeters, bark may or may not be attached, wood is sound, bark is decay; (3) thumbnail penetrates till seven centimeters, bark may or may not be attached, wood is somewhat rotten, the biggest trunks and only larger stubs are present; (4) thumbnail penetrates readily, bark is lightly attached, sloughing off or detached, wood texture is soft, decayed log may assume oval shape; (5) all wood texture is squashy and powdered, bark is detached or absent, can be decayed in pieces, wood is indistinguishable from ground.

Each log was assigned one decay stage. If different parts of log were in several decay stages, the predominant stage was chosen.

Study area

Bryophyte community structure and gradients were analyzed with CCA (Canonical Correspondence analysis) and Indicator Species Analysis using the PC-ORD program package (1999 Version 4.17.). CCA species ordination was used to identify major factors that affected variability of composition of bryophyte species. Significant indicator bryophyte species were determined for each decay stage.

The relations of bryophyte species richness with visible perimeter and decay stage were determined by Spearman's correlation.

The term "signal species" is considered here as including special habitat species, indicator species, and species of microreserve as well as specially protected bryophyte species in the woodland key habitat inventory. Special habitat species are species with a narrow ecological range that need very specific conditions. Indicator species are species with high requirements for a specific environment (Ek et al. 2002).

Results

Bryophyte flora

In total 59 bryophyte species from 29 families were recorded, of which 42 were mosses and 17 liverworts. The most common bryophytes were *Hypnum cupressiforme*, *Brachythecium rutabulum*, *Lophocolea heterophylla*, *Dicranum scoparium*, *Plagiomnium cuspidatum* and *Chiloschyphus pallescens*. In total 13 bryophyte species were found only in one site on one log (Table 1).

In the studied territories one habitat specialist species, *Anastrophyllum hellerianum*, was found in the Zilo Kalnu Nogazes Swamp (Z2). Five bryophyte species were indicator species – *Homalia trichomanoides*, *Jungermannia leiantha*, *Metzgeria furcata*, *Neckera complanata* and *Trichocolea tomentella*.

Comparison between bryophyte species and decay stages of logs

In total 102 decayed logs were described in all territories, representing five tree species (Table 2). Tree species was not determined for 27 decayed logs that were mostly in the fourth and fifth decay stage.

Logs in decay stages 1 and 5 were found in all studied territories, but their number was low. Logs in all decay stages (1, 2, 3, 4, 5) were represented only in the Zilo Kalnu Nogazes Swamp Z1 and Moricsala Island.

Table 1. Occurrence of bryophyte species in studied territories. Number of decayed logs where species were found is shown

Bryophyte species	Zilo kalnu nogaze (Z1)	Zilo kalnu nogaze (Z2)	Zvarde	Moricsala
Amblystegium serpens	-	-	-	1
Anastrophyllum hellerianum	-	7	-	-
Aulacomnium androgynum	-	-	1	-
Blepharostoma trichophyllum	-	-	3	1
Brachythecium rutabulum	28	5	8	29
Brachythecium salebrosum	-	4	-	-
Calliergon cordifolium	2	-	5	1
Calliergonella cuspidata	2	1	4	20
Chiloscyphus pallescens	10	1	4	15
Cirriphyllum piliferum	-	4	-	1
Climacium dendroides	-	2	-	12
Dicranum majus	-	1	-	-
Dicranum montanum	-	4	3	-
Dicranum scoparium	4	16	9	16
Eurhynchium angustirete	-	4	-	-
Eurhynchium hians	1	-	-	-
Eurhynchium striatum	-	1	-	-
Frullania dilatata	-	-	-	1

(continued)

Bryophyte species	Zilo kalnu nogaze (Z1)	Zilo kalnu nogaze (Z2)	Zvarde	Moricsala
Herzogiella seligeri	-	12	1	1
Homalia trichomanoides	3	-	-	1
Homalothecium sericeum	-	-	-	3
Hylocomium splendens	3	3	3	2
Hypnum cupressiforme	19	14	9	30
Jungermannia leiantha	-	-	6	-
Lepidozia reptans	-	4	6	2
Leskea polycarpa	-	-	-	1
Leucodon sciuroides	1	1	-	2
Lophocolea heterophylla	20	6	7	14
Lophozia sp.	2	1	-	3
Metzgeria furcata	1	-	-	3
Mnium hornum	1	5	1	10
Neckera complanata	-	3	-	-
Nowellia curvifolia	3	6	3	-
Plagiochila asplenioides	-	2	-	-
Plagiochila porelloides	-	-	1	-
Plagiomnium affine	9	4	3	6
Plagiomnium cuspidatum	10	3	1	17
Plagiomnium ellipticum	-	-	-	9
Plagiomnium medium	-	1	-	-
Plagiomnium undulatum	10	8	4	1
Plagiothecium laetum	-	-	-	2
Platygyrium repens	-	-	-	2
Pleurozium schreberi	3	11	-	2
Polytrichum commune	-	-	2	-
Polytrichum juniperinum	-	-	-	4
Ptilidium pulcherrimum	3	-	3	1
Pylaisia polyantha	-	-	1	-
Radula complanata	7	1	1	3
Rhizomnium punctatum	2	8	4	-
Rhodobryum roseum	1	2	1	-
Rhytidiadelphus triquetrus	4	10	5	1
Riccardia multifida	1	-	-	-
Riccardia palmata	1	15	1	7
Sanionia uncinata	7	5	2	5
Sphagnum girgensohnii	-	1	-	-
Tetraphis pellucida	-	1	3	-
Thuidium tamariscinum	-	10	3	1
Trichocolea tomentella	-	1	-	-
Ulota crispa	9	-	1	3

Table 2. Parameters of studied decaying logs of different tree species

Tree species	Number	Visible perimeter (m)	Length (m)	Decaying stage
Alnus glutinosa	50	0.1 - 0.98	1.5 - 25	1, 2, 3, 4
Betula sp.	14	0.03 - 1.12	2 - 20	2, 3, 4
Picea abies	6	0.15 - 0.8	5 - 19	2, 3, 4
Alnus incana	4	0.34 - 1.26	5 - 10	1, 2, 3
Quercus robur	1	1.11	18	2
Not identified	27	0.15 – 0.85	2 - 20	2, 3, 4, 5

A significant relation between number of bryophyte species and decay stage was not found. The highest bryophyte species richness (mean 7 species per log) was found on logs in decay stages 3 and 4 (Fig. 2).

A total of 14 bryophyte species were significant ($p > 0.05$) indicators of decay stages (Table 3). Nine epiphytic bryophyte species were specific to the first decay stage. In this stage decayed logs still had hard attached bark. Two epixylic bryophyte species were characteristic to the decay stage 4 – *Nowellia curvifolia* and *Riccardia palmata*. In the decay stage 4 bark was not attached and structure of decayed wood was soft. Four indicator species characterized the decay stage 5, of which the two most common were *Calliergonella cuspidata* and *Plagiomnium cuspidatum* (Table 3).

The first axis of the CCA bryophyte species ordination was explained as decay stage (Fig. 3). Logs in the initial decay stage were associated with epiphytic bryophyte species – *Frullania dilatata*, *Metzgeria furcata* and *Radula complanata*. In mid decay stages (mid Axis I) typical bryophyte species were *Lophocolea heterophylla*, *Chiloscyphus pallescens* and *Jungermania leiantha*. In the late decay stages ground bryophytes such as *Climacium dendroides*, *Rhodobryum roseum* and *Dicranum majus* appeared (Fig. 3).

Distribution on tree species

The CCA bryophyte species ordination showed that a unique composition of bryophyte species was found on *Alnus glutinosa* and *Picea abies* logs (Fig. 3). The most common bryophyte species on spruce were *Anastrophyllum hellerianum* and *Pleurozium schreberi* and the highest species richness was also found on these logs (Fig. 3, 4). *Hypnum*

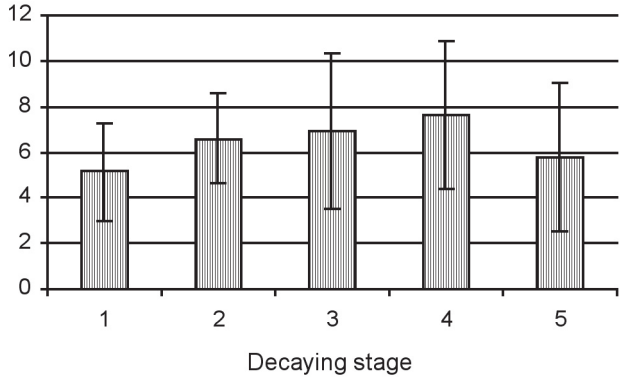

Fig. 2. Average number of bryophyte species per one log in various decay stages.

Table 3. Indicator species of bryophytes in different decay stages. Only significant ($p < 0.05$) indicator species are shown. Bryophyte species are arranged by decay stage. Bryophyte species with larger observed indicator values are more characteristic of the respective decaying stage

Bryophyte species	Decay stage	Observed Indicator Value	P
Hypnum cupressiforme	1	25.6	0.0010
Radula complanata	1	28.3	0.0010
Ulota crispa	1	24.5	0.0010
Homalia trichomanoides	1	7.7	0.0070
Ptilidium pulcherrimum	1	11.0	0.0070
Metzgeria furcata	1	23.1	0.0010
Leucodon sciuroides	1	14.1	0.0010
Homalothecium sericeum	1	20.2	0.0010
Nowellia curvifolia	4	7.9	0.0430
Riccardia palmata	4	10.1	0.0440
Plagiomnium cuspidatum	5	19.5	0.0010
Plagiomnium affine	5	9.8	0.0400
Calliergonella cuspidata	5	27.8	0.0010
Cirriphyllum piliferum	5	5.3	0.0450

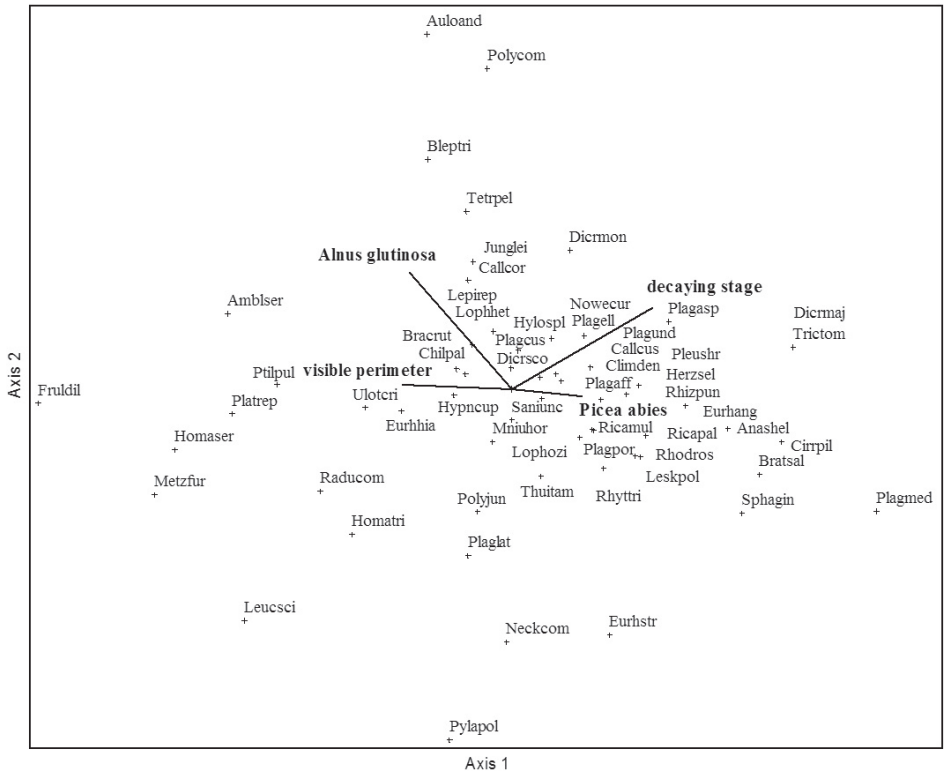

Fig. 3. CCA bryophyte species ordination. Only significant ($p < 0.05$) effects are shown. A longer vector indicates greater correlation.

cupressiforme and *Brachythecium rutabulum* were the most common species on alders (Fig. 3). However, the epixylic bryophyte species were not restricted to any tree species.

In the CCA species ordination visible perimeter was an important factor (p = 0.05) (Fig. 3), but a significant correlation between visible perimeter and species richness was not found.

Distribution in territories

The largest number of bryophyte species was found in the Zilo Kalnu Nogazes Swamp Z2 and the largest mean number of bryophyte species per log was in Zvardes Swamp (Fig. 5). The highest number of signal species was in Zilo Kalnu Nogazes Swamp Z1 and Z2 (Fig. 5). *Dicranum scoparium* was one of the most common bryophyte species in Zilo Kalnu Nogazes Swamp Z2 and in the Zvardes swamp. *Calliergonella cuspidata* was common in Moricsala and *Riccardia palmata* was a widespread species in Zilo Kalnu Nogazes Swamp Z2.

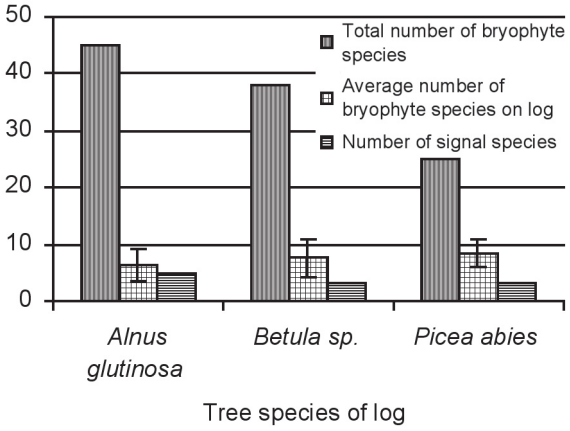

Fig. 4. Occurrence of bryophyte species richness on tree species.

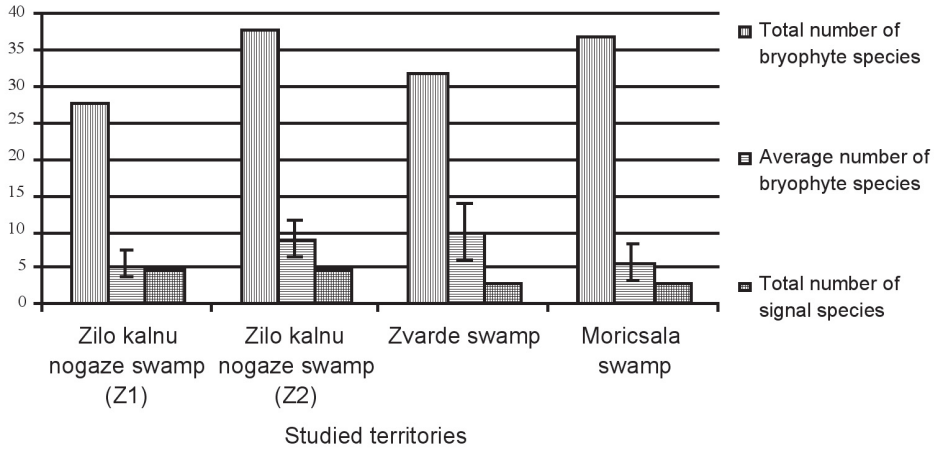

Fig. 5. Bryophyte species richness in relation to territory.

Discussion

In the present study *Hypnum cupressiforme* was found on logs in all decay stages. This, the most common species, has a wide ecological valence and can grow on different substrata (Āboliņa 1968).

Several authors have described decayed logs rich with liverworts (Āboliņa 1968; Vellak, Paal 1999). However in the present study this bryophyte species group represented slightly less than half of all bryophytes and richness was low. A possible explanation may be:

(1) *Picea abies* decayed logs in the studied swamps were not frequent, conifers support rich liverwort diversity (Hallingbäck, Holmåsen 2000; Ódor, Standovár 2002);

(2) liverwort species richness is affected by bark of the decayed log. Epixylic bryophytes grow and develop best when bark has fallen off (Crites, Dale 1998) but in our investigation bark was still attached also in the fourth decay stage.

The decay stage was the main factor affecting bryophyte species composition on decayed logs in Eurosiberian alder swamp forests. The epiphytes growing on living bark are already present on logs in the initial decay stage and remain for a long time until decay stage 4. In the next successional stage epixylic bryophyte species establish in the decay process as bark is lost. Epixylic bryophyte species reach their maximum in decay stage 4. This explains the high number of bryophyte species in the mid decay stages. However epixylic bryophytes are poor competitors and can soon disappear (Andersson, Hytteborn 1991). The decay process continues and ground bryophytes begin to dominate till the wood is not recognizable. Several authors have described this type of succession of bryophyte species on logs (Āboliņa 1979; Crites, Dale 1997; Rambo, Muir 1998; Lindström 2003).

Significant indicator species were not found in decay stages 2 and 3. The composition of bryophyte species also changed little in the decay stages 2 and 3, probably due to intact tree bark.

One problem with our chose field method was that if parts a decayed log were in different decay stages, only the main decay stage was recorded. This has been noted also in other work (Lindström 2003), but distinguishing different parts of logs for establishment of separate sampling plots is problematic.

A relation between decay stage and number of bryophyte species was not found, possibly because logs in I and V decay stage were less frequent. The low amount of logs in decay stage 5 may be related to past forestry management (Stokland 2001) or possibly they were simply missed in the studied territories.

Among the studied factors tree species of log showed an effect on bryophyte species composition and richness. Decay speed depends on tree species of log. Most deciduous trees decay faster than conifers, which do not provide a lasting microenvironment to bryophytes. Deciduous logs are most variable and unstable for bryophyte species (Stokland 2001). Logs of *Picea abies* were observed to be richer with bryophyte species compare with deciduous logs, which is consistent with other studies in Latvia (Bambe 2002; Bambe 2008). The average number of bryophyte species on spruce was nine species, on alder – seven species.

Several authors (Ódor, Standovár 2001; Bērmanis, Spuņģis 2002; Ek et al. 2002; Ódor et al. 2006) have described a relationship between diameter of logs and number of bryophyte species. While it also might be expected that large logs support more space for species, this was not found in our study and in Bambe (2002). In our study no significant correlation

between the number of bryophyte species and the visible perimeter was found. Possible explanations may be: (1) biased sampling (few numbers of sampled decayed logs in some perimeter classes); (2) in previous studies, the forest microclimate differed from the studied Eurosiberian alder swamp forest.

The mean number of bryophyte species was not large in Moricsala compared with other studied territories, but there were examined a relative high number of decayed logs. This may be related with the moisture regime. Swamps mostly receive moisture from groundwater (Bušs 1981), but the moisture regime in Moricsala depends on fluctuations of the lake level (Laiviņa, Laiviņš 1980). This might mean greater fluctuation of water level. In summer dry conditions may prevent colonization by many epixylic bryophyte species.

Calliergonella cuspidata was an indicator species in Moricsala of the fifth decay stage. Considering that the largest number of decay logs in decay stage 5 was found in this territory, uneven stratified design likely has caused problem in interpretation, i.e. is this species an indicator of the specific conditions at Moricsala or a typical indicator of the more decayed classes? This problem can be avoided only greatly increasing the number of sampled territories.

Acknowledgements

We are grateful to Ligita Liepiņa for assisting in field work and to help collect data. Thanks Anna Mežaka for bryophyte species identification, Vija Znotiņa for advice on statistics and data interpretation.

References

Āboliņa A.A. 1968. *Mosses in Latvian SSR*. Zinātne, Rīga, 329 p. (in Russian)

Āboliņa A. 1979. Bryophytes and their substrata. In: *Dabas un vēstures kalendārs 1980. gadam*. Zinātne, Rīga, pp. 168–173. (in Latvian) /Sūnas un to substrāts/

Āboliņa A. 2001. List of bryophytes of Latvia. *Latvijas Veģetācija* 3: 47–87. (in Latvian) /Latvijas sūnu saraksts/

Andersson I.L., Hytteborn H. 1991. Bryophytes and decay wood – a comparison between managed and natural forest. *Holarctic Ecol.* 14: 121–130.

Baldwin L.K., Bradfield G.E. 2007. Bryophyte responses to fragmentation in temperate coastal rainforests: A functional group approach. *Biol. Conserv.* 136: 408–422.

Bambe B. 2002. Epixylic and epiphytic bryophyte societies on tree tranks and decayed wood in banks of small rivers. In: *Latvijas Universitātes 58. zinātniskā konference. Zemes un Vides zinātņu sekcijas. Refeātu tēzes.* University of Latvia, Rīga, pp. 14–18. (in Latvian) /Epiksilās un epifītiskās augu sabiedrības uz koku stumbriem un trupošiem kokiem mazo upju krastos/

Bambe B. 2008. Factors influencing distribution of bryophytes on dead coniferous wood. *LLU Raksti* 20: 93–102.

Bērmanis R., Spuņģis V. 2002. *Dead Wood*. Valsts meža dienests, Jelgava. 6 p. (in Latvian) /Atmirusi koksne/

Bušs K. 1981. *Ecology and Typology of Forest*. Zinātne, Rīga. 64 p. (in Latvian) /Meža ekoloģija un tipoloģija/

Celmiņš A. 2005. *Nature Park "Zvārdes meži" Plan of Nature Protection*. Rīga. 65 p. (in Latvian) / Dabas parka "Zvārdes meži" dabas aizsardzības plāns/

Crites S., Dale R. T. 1998. Diversity and abundance of bryophytes, lichens, and fungi in relation to woody substrate and successional stage in aspen mixewood boreal forests. *Can. J. Bot.* 76: 641–651.

Ek T., Suško U., Auziņš R. 2002. *Inventory of Woodland Key Habitats. Methods.* Valsts mežu dienests, Rīga. 76 p. (in Latvian) /Mežaudžu atslēgas biotopu inventarizācija. Metodika/

Hallingbäck T., Holmåsen I. 2000. *Bryophytes Fieldhandbook*. Interpublishing, Stockholm. 287 p. (in Finnish)

Ignatov M.G., Ignatova E.A. 2003. *Bryophytes flora in European Russia Part 1. Sphagnaceae – Hedwigiaceae.* Scientific Press KMK, Moscow. 608 p. (in Russian)

Ignatov M.G., Ignatova E.A. 2004. *Bryophytes flora in European Russia Part 2. Fontinalaceae – Amblystegiaceae*. Scientific Press KMK, Moscow. 960 p. (in Russian)

Laiviņa S., Laiviņš M. 1980. *Moricsala Reserve.* Zinātne, Rīga. 71 p. (in Latvian) /Moricsalas rezervāts/

Lārmanis V., Priedītis N., Rudzīte M. 2000. *Reference Book of Woodland Key Habitats*. Valsts meža dienests, Rīga. 127 p. (in Latvian) /Mežaudžu atslēgas biotopu rokasgrāmata/

Lindström K. 2003. *Wood-living Bryophyte Species Diversity and Distribution – Differencies between Small-stream and Upland Spruce Forests.* Umeå University, Umeå. 19 p.

Ódor P. Heilmann-Clausen J., Christenen M., Aude E., Dort K.W., Piltaver A., Siller I., Veerkamp M.T., Walleyn R., Standovár T., Hees A.F.M., Kosec J., Matočec N., Kraigher H., Grebenc T. 2006. Diversity of dead wood inhabiting fungi and bryophytes in semi-natural beech forests in Europe. *Biol. Conserv.* 131: 58–71.

Ódor P., Standovár T. 2001. Richness of bryophyte vegetation in near-natural and managed beech stands: the effects of management-induced differencies in dead wood. *Ecol. Bull*. 49: 219–229.

Ódor P., Standovár T. 2002. Substrate specificity and community structure of bryophyte vegetation in a near-natural montane beech forest. *Commun. Ecol.* 3: 39–49.

Pakalne M., Znotiņa V. 1992. *Vegetation Classification: Braun-Blanquet Method.* Latvijas Universitāte, Rīga. 32 p. (in Latvian) /Veģetācijas klasifikācija. Brauna–Blankē metode/

Priedītis N. 1999. Forest of Latvia: Nature and Diversity. WWF, Rīga. 209 p.

Pyle C., Brown M. M. 2002. The effects of microsite (logs versus ground surface) on the presence of forest floor biota in a second-growth hardwood forest. In: *Proceedings of the Symposium on the Ecology and Management of Dead Wood in Western Forests*. Pacific Southwest Research Station, pp. 393–403.

Pyle C., Brown M. M. 1998. A rapid system of decay classification for hardwood logs of the eastern deciduous forest floor. *J. Torrey Bot. Soc.* 125: 237–245.

Rambo T. R., Muri P. S. 1998. Bryophyte species associations with coarse woody debris and stand ages in Oregon. *Bryologist* 101: 366–376.

Sāmīte D. 2007. *Nature Protection Plan of Slitere National Park*. Slīteres nacionālā parka administrācija, Dundaga. 85 p. (in Latvian) /Slīteres Nacionālā parka dabas aizsardzības plāns/

Smith A.J.E. 1996. *The Liverworts of Britain & Ireland.* Cambridge University Press, Cambridge. 362 p.

Smith A.J.E. 2004. *The Moss Flora of Britain and Ireland* (2nd ed.). Cambridge University Press, Cambridge. 1012 p.

Stokland J.N. 2001. The coarse woody debris profile: an archive of recent forest history and an important biodiversity indicator. *Ecol. Bull.* 49: 71–83.

Suško U. 1998. *Natural forests of Latvia. Investigations About Structures of Biological Diversity, Depended Species and Forest History.* WWF, Rīga. 186 p. (in Latvian) /Latvijas dabiskie meži. Pētījums par bioloģiskās daudzveidības strukūrām, atkarīgajām suām un meža vēsturi/

Temņikova N. 1975. Climate. In: Pūriņš V. (ed) *Geography of Latvian SSR*. Zinātne, Rīga, pp. 45–54. (in Latvian) /Klimats. Latvijas PSR ģeogrāfija/

Vellak K., Paal J. 1999. Diversity of bryophyte vegetation in some fores types in Estonia: a comparison of old unmanaged and managed forests. *Biodiversity Conserv.* 8: 1595–1620.

Zielonka T., Piatek G. 2004. The herb and dwarf shrubs colonization of decay logs in subalpine forest in the Polish Tatra Mountains. *Plant Ecol*. 172: 63–72.

Epiksīlo sūnu ekoloģija Eirosibīrijas melnalkšņu dumbrājos Latvijā

Linda Madžule*, Guntis Brūmelis

Botānikas un ekoloģijas katedra, Latvijas Universitātes Bioloģijas fakultāte, Kronvalda bulv. 4, Rīga LV-1586, Latvija
*Korespondējošais autors, E-pasts: linda.madzule@gmail.com

Kopsavilkums

Atmirusi koksne ir nozīmīgs struktūrelements Eirosibīrijas melnalkšņu staignāju mežos, kas nodrošina epiksīlo sūnu sugu daudzveidību. Pētījuma mērķis bija noskaidrot sūnaugu daudzveidību uz kritalām un abiotiskos, biotiskos faktorus, kas ietekmē sūnu floru. Lai to veiktu, apskatīti četri Eirosibīrijas melnalkšņu dumbrāji trīs Latvijas teritorijās – Moricsalā, Zvārdes mežu dabas parkā un Slīteres Nacionālajā parkā. Pētījumā kopumā aprakstītas 102 kritalas, uz kurām konstatētas 59 sūnu sugas. Par galveno faktoru, kas ietekmē sūnu sugu bagātību uz kritalām, noteikta sadalīšanās pakāpe. Notiekot kritalas trūdēšanas procesam, sūnu sugu sastāvs pamazām nomainās. Vislielākais sūnu sugu skaits vērojams kritalām, kas ir vidēji sadalījušās. Kritalas redzamais apkārtmērs būtiski neietekmēja sūnu sugu sastāvu un skaitu uz kritalām. Sūnu sugu sastāvs atšķīrās starp lapu kokiem un skujkokiem, kā arī nelielas atšķirības epiksīlo sūnu florā konstatētas katrā apskatītajā teritorijā.

Acta Universitatis Latviensis, 2008, Vol. 745, Biology, pp. 115–130

Expression of hepatitis C virus structural genes controlled by alphaviral recombinant replicons

Ekaterina Alekseeva*, Irina Sominskaya, Ruta Bruvere, Velta Ose, Anna Zajakina, Tatyana Kozlovska

Department of Protein Engineering, Latvian Biomedical Research and Study Centre, Ratsupites 1, Riga LV-1067, Latvia

*Corresponding author, E-mail: kate@biomed.lu.lv

Abstract

Since no highly efficient treatment for the hepatitis caused by hepatitis C virus (HCV) is available yet, the development of an anti-HCV vaccine candidate remains a goal of high priority. In our study, two different alphaviral expression systems were applied for expression of HCV structural protein genes in cell culture. For this purpose, the HCV genome fragment encoding the core-E1-E2-p7 polyprotein, and HCV core and E2 genes, separately, were cloned in Semliki Forest virus (pSFV1) and Sindbis virus (pCytTS) expression vectors. Efficient synthesis of structural HCV proteins in a BHK-21 cell line was demonstrated. HCV polyprotein precursor was authentically post-translationally processed. Identification of HCV proteins was confirmed by immunoprecipitation, immunocytochemical analysis, and by Western blotting with corresponding anti-HCV antibodies.

Key words: alphavirus, expression, Hepatitis C virus, Semliki Forest virus, Sindbis virus.

Introduction

Viral hepatitis C, caused by hepatitis C virus (HCV), is a major public health concern worldwide since more than 3 % of the world population is infected with this virus. Worst of all, up to 4 million persons are becoming newly infected each year. Approximately 80% of infected patients develop chronic hepatitis, among which 20 % to 30 % progress to liver cirrhosis and end-stage liver disease. Current therapy relies on the use of pegylated interferon and ribavirin, but outcomes are unsatisfactory, since only 42 % of patients infected with HCV genotype 1 prevalent in Latvia respond positively to treatment. Therefore, despite many obstacles, there is a compelling need to develop an effective anti-HCV vaccine. Unfortunately, the traditional approach to use whole-organism vaccines containing inactivated whole or live attenuated viruses cannot be adapted for HCV, because no cell culture system is available to propagate HCV so far. Our research develops the newer types of anti-HCV vaccine candidates, based on the general concept that one or several genes of the viral pathogen (HCV in this study) are incorporated into the genome of a viral carrier (in our case, alphavirus) for amplification and expression of the putative immunogens.

HCV virion carries RNA genome of 9.5 kb. The genome consists of a highly conserved 5' noncoding region (Baumert et al. 1998) followed by a long open reading frame of 9,030

to 9,099 nucleotides that is translated into a single polyprotein of 3,010 to 3,030 amino acids (Krekulova 2006). The polyprotein is co- and post-translationally processed by cellular and viral proteases to yield ten mature protein products (core, E1, E2, p7, NS2, NS3, NS4A, NS4B, NS5A, and NS5B). The HCV genome encodes three structural proteins: a core protein (core) and two envelope glycoproteins (E1 and E2) (Penin et al. 2004). These proteins are released from the N-terminal region of the polyprotein by signal peptidase cleavage (Dubuisson 2002). In addition, processing at the C-terminal region of the core protein by a signal peptidase leads to generation of a mature core protein (McLauchlan 2002).

Non-mature HCV core protein (aa 1-191) appears to be conserved among several HCV strains isolated in different regions worldwide (for review see Krekulova 2006). HCV core is not only involved in the formation of the HCV virion, but also has a number of regulatory functions: it effects host cell gene expression and modulates apoptosis. The C-terminal domain of HCV core is essential for virus secretion (Suzuki at al. 2007). HCV envelope glycoproteins E1 (aa 192-383) and E2 (aa 384-746) are believed to be type 1 of transmembrane proteins, with N-terminal ectodomains and C-terminal hydrophobic anchors and together are expected to form the viral envelope. HCV E1 protein displays two main glycosylated forms with molecular weights of 33 kDa and 35 kDa (30 kDa and 35 kDa in Baumert et al. 1998). HCV E2 is a 70-kDa glycoprotein, which demonstrates large variation among HCV genotypes. N-terminal 27 residues of E2 (aa 384-410) show an especially high degree of variation, also within genotypes. This portion of the E2 sequence is known as a hypervariable region 1 (HVR1). The HVR1 is likely to be involved in virus infection, since virus-neutralizing antisera to HVR1 have been reported in vitro and in vivo models, although other studies showed that HCV with the deleted HVR1 remains infectious (Keck et al. 2004). Mature E1 and E2 proteins assemble into a non-covalent heterodimer, although the exact nature of this interaction is still poorly understood (Patel et al. 1999).

Therefore, structural HCV proteins seem to be perspective as a source of the immunological antigens for the development of anti-HCV vaccine, especially when combination of two or more proteins with different immunological properties in one genetic construction is possible.

Viral vectors with the property to self-replicate in transfected cells are a favourable approach to be used as candidate vehicles in the development of the genetic vaccines. Alphaviral vectors with their ability of efficient cytoplasmic replication established themselves rapidly as tools for basic research and biotechnology. Semliki Forest virus (SFV) (Liljestrom, Garoff 1991) and Sindbis virus (SINV) (Boorsma et al. 2000) are the most commonly used alphaviral expression vectors. Since all alphaviruses have very similar biology, the major structural elements of these expression vectors are identical. The vectors are generated in such a way that the heterologous gene insert should be placed, replacing the viral structural genes, under the subgenomic 26S promoter. In general, the vectors have a non-structural coding region, which is required for the production of the alphaviral replicase complex (nsP1-4), 26S subgenomic promoter, and a polylinker with several unique restriction sites for foreign gene insertion. An SP6 promoter is introduced upstream of the recombinant alphaviral replicon for RNA transcription *in vitro*. Recombinant replicons are packed into viral envelopes, which are provided with co-transfected defective "helper" RNAs *in trans* (Smerdou et al. 1999). In the first generation

of alphaviral expression vectors, the high-level expression of a foreign gene is coupled with a shutdown of the host protein translation followed by cell death within 12 to 24 h after infection. The cytotoxicity of these alphaviral vectors is caused by p53 independent apoptosis (Glasgow et al. 1998), which is induced by the alphaviral non-structural region. This is a major drawback for many applications, and the first generation of RNA-based vectors is used only for transient gene expression. HCV structural proteins (genotype 1a) have also been expressed by using recombinant SFV replicon in mammalian cells; this system has been shown to allow the visualization of HCV budding events *in situ*, but budding is abortive or slow (Blanchard et al. 2002; Hourioux at al. 2007).

In this work we applied SFV and Sindbis virus-based expression systems for the efficient expression of the structural HCV genes (core, E1 and E2) in cell culture, to assess the applicability of recombinant alphaviruses as anti-HCV vaccine prototypes.

Materials and methods

Constructs carrying HCV genes

Constructs used in this work are presented in Fig. 1. The HCV isolate 274933RU (GeneBank accession no. AF176573) genome (Mokhonov at al. 2002) was used for amplification of target genes with corresponding primers. These HCV cDNA fragments were inserted after SP6 promoter to construct a plasmid pSFV1/HCVpolyP, which contained core, E1, E2, and p7 genes, as well as the pSFV1/HCVcore gene and pSFV1/HCVE2p7 gene separately. Recombinant plasmids were multiplied, linearized at the 3′ end of the HCV cDNA by *Bcu*I (*Spe*I) restriction endonuclease. The linearized DNAs were then purified and used as templates for in vitro transcription.

Primers used for HCV core-E1-E2-p7 genes amplification to create pSFV1/HCVpolyP recombinant plasmid were: 5′-GTG AGA TCT GCA CCA TGA GCA CGA ATC CTA AAC-3′ and 5′-CTC TAG ATC TTT AGG CGT ATG CTC GTG GTG GTA G-3′. After amplification, the PCR fragment was cut out with *Bgl*II restriction endonuclease and ligated into pSFV1 vector, which was cleaved with *Bam*HI restriction endonuclease and dephosphorylated with bacterial alkaline phosphatase (Fermentas).

Primers for HCV core gene amplification to create pSFV1/HCVcore recombinant plasmid were: 5′-GTG AGA TCT GCA CCA TGA GCA CGA ATC CTA AAC-3′ and 5′-GAT CGT TAA CTA AGC GGA AGC TGG AAT GG-3′. After amplification, the PCR fragment was cut out with *Bgl*II and *Hpa*I restriction endonucleases and ligated into pSFV1 vector, which was cleaved with *Sma*I and then with *Bam*HI restriction endonucleases.

In order to construct recombinant pSFV1/HCVE2p7, a DNA fragment carrying E2 and p7 genes was cut out with *Sal*I and *Hpa*I restriction endonucleases from plasmid pGMV-E2p7.9.3 (obtained from Maria Isaguliants, Ivanovsky Institute, Moscow). The DNA fragment was treated with Klenow fragment (Fermentas) to blunt the DNA end after SalI digestion and ligated into pSFV1 vector, which was cleaved with *Sma*I restriction endonuclease.

In order to construct the recombinant plasmid pCyt/HCVpolyP containing core, E1, E2, and p7 protein genes, the pCytTS vector was cleaved with *Xba*I and *Xho*I restriction endonucleases. The HCV genome fragment was amplified with primers 5′-GCA TCT CTA GAC GTA GAC CGT GCA CCA TGA GCA CG-3′ and 5′-GCA TCC TCG AGT TAG GCG TAT GCT CGT GGT GGT AGT G-3′, cut out with *Xba*I and *Xho*I restriction

endonucleases and ligated into pCytTS vector.

The recombinant plasmid pSFV1/EGFP carrying Enhanced green fluorescence protein (EGFP) gene was used as a control for infection of BHK-21 cells. In order to generate this plasmid, the DNA fragment carrying the EGFP gene was cut out from pEGFP-C1 plasmid (Clontech) with *Nhe*I and *Hpa*I restriction endonucleases and treated with T4 DNA polymerase (Fermentas) to blunt the DNA end after *Nhe*I digestion. The DNA fragment was ligated into pSFV1 vector, which was cleaved with *Sma*I restriction endonuclease.

Cell culture

Baby hamster kidney (BHK-21) cells (ATCC) were grown in BHK medium (Gibco-BRL) containing 5 % fetal calf serum, 10 % tryptose phosphate broth, 20 mM HEPES and 2 mM glutamine. Cells were incubated in a 5 % CO_2 atmosphere at 37 °C.

Generation of recombinant viruses and cell infection

For *in vivo* packaging of recombinant RNA into SFV particles, *in vitro*-transcribed RNA was electroporated into BHK-21cells together with SFV "helper" RNA under the above-mentioned conditions. After 24 to 48 h, SFV particles were collected from the culture medium and frozen rapidly to be stored as a virus stock. Titres of stocks were determined by infecting cells with serial dilutions of the stocks followed by indirect immunocytochemistry assay. The achieved titres were from 1×10^7 to 5×10^7 viral particles per ml. Infection of BHK-21 cells was carried out in serum-free medium with the appropriate dilution of the virus stocks, which enabled 100 % infection of the cells.

Metabolic labelling

Metabolic labelling of transfected cells and immunoprecipitation of proteins from cells lysates were performed as described previously (Kozlovska et al. 2004).

RNA transcription and transfection

RNA transcripts were produced *in vitro* from 3 mg of SpeI-linearized recombinant plasmids in reactions containing 7mG(5′)ppp(5′G) (New England Biolabs) using SP6 RNA polymerase (Fermentas). RNA (3 to 5 mg) was transfected into BHK-21 cells by electroporation at 850 V, 25 mF, pulsed twice using Bio-Rad Gene Pulser apparatus without the pulse controller unit. Electroporated cells were diluted in 15 mL of complete BHK medium, transferred into tissue culture plates, and incubated at 37 °C (5 % CO_2).

DNA transfection and selection of puromycin-resistant cell populations

Slightly sub-confluent monolayers (60 to 70 %) of BHK-21 cells in 35-mm tissue culture plates were used for DNA transfection. DNA was transfected by using ExGene (Fermentas) according to the manufacturer's recommendations. After transfection, cells were incubated 18 to 48 h at 37 °C. For termoinduction of target gene expression, transfected cells were incubated at 29 °C. For selection of puromycin-resistant cell populations, cells were passaged after 18 to 24 h, media was changed then at 24 h to standard growth media containing 5 μg mL^{-1} of puromycin (Sigma). Thereafter, cells were maintained in media with puromycin and were passaged or frozen as standard BHK-21 cells.

Cell lysis and anti-HCV antibodies

Cell monolayers were lysed in buffer containing 50 mM Tris-HCl, pH 7.6, 150 mM NaCl, 2 mM EDTA, 1 % Nonidet P-40 (NP-40), 1 μg mL^{-1} PMSF. After 10 min on ice, cell nuclei were removed by centrifugation. Supernatants were analysed by immunoprecipitation or by Western blotting.

For analysis of total cell lysates on PAGE, Laemmli buffer was used for lysis of cells.

The polyclonal rabbit anti-core and anti-E2 antibodies were obtained from Maria Isaguliants (Ivanovsky Institute, Moscow) and used as described earlier (Sominskaya et al. 2005).

Western blot analysis of HCV proteins

The protein samples prepared from pSFV1/HCVpolyP- or pSFV1/HCVcore-infected and pCyt/HCVpolyP- or pCyt/HCVcore-transfected BHK-21 cells were separated by SDS-PAGE (15 %). The Prestained Protein Molecular Weight Markers (Fermentas) were used as molecular mass markers. After electrophoresis, proteins were electrotransferred to Hybond-P membranes (Amersham Pharmacia Biotech) with a blotting apparatus. After transfer, membranes were incubated with blocking buffer (5 % non-fat dry milk in PBS). Anti-HCV core polyclonal rabbit antibodies or anti-HCV E2 polyclonal rabbit antibodies diluted 1 : 1000 in blocking buffer containing 2.5 % of non-fat dry milk and 0.05 % Tween 20 were used as primary antibodies. Membranes were subsequently treated with horseradish peroxidase-conjugated anti-rabbit Ig (Amersham Pharmacia Biotech) at 1 : 3000 dilution for 60 min at room temperature. Protein binding was detected with the ECL Plus system (Amersham Pharmacia Biotech).

Indirect immunofluorescence microscopy

BHK-21 cells cultured on glass slides (Nagle Nunc International) were infected with pSFV1/HCVpolyP or pSFV1/HCVcore recombinant viruses and fixed after designated cultivating periods. The fixed cells were first incubated with antibody dilution buffer (1 % bovine serum albumin, 2.5 mM EDTA, phosphate-buffered saline, pH 7.4) for 10 min at room temperature. Then, cells were incubated for 60 min at room temperature with anti-HCV core or anti-E2 polyclonal antibodies as primary antibodies at 1 : 1000 dilution. After incubation, cells were washed three times with PBS. Anti-rabbit TRITC-labelled antibodies were used as secondary antibodies at 1 : 100 dilution. Cells were mounted then with PermaFluor aqueous mounting medium (Immunon, Pittsburgh, USA) and analyzed under a Leica DM 6000 fluorescence microscope (Leica Camera AG, Solms, Germany). DAPI was used for visualization of nucleus.

Purification of HCV-like particles

At 48 h postinfection or postelectroporation, cells were lysed in 50 mM Tris-Cl, pH 7.6, 150 mM NaCl, 2 mM EDTA, 1 % Nonidet P40 buffer with 10 μg mL^{-1} of PMSF. Lysate was subjected to low-speed centrifugation (15 min at 4 °C and 15000 g) to remove cell debris. Supernatant was layered over a 20 % (w/v) sucrose cushion in TNE buffer (50 mM Tris/HCl, pH 7.4, 100 mM NaCl, 0.5 mM EDTA) and centrifuged at 30000 rpm, rotor TLS-55 (TL-100 centrifuge, Beckman) for 18 h at 4 °C. Pellet containing HCV-like particles was resuspended in TNE buffer and analyzed by Western blotting and electron microscopy.

Results

Generation of recombinant plasmids carrying HCV genes

In order to test the ability of the SFV expression system for translation of HCV genes, we generated constructs expressing poly P (core-E1-E2-p7), HCV core and E2p7 genes (Fig. 1). DNA copies of poly P (core-E1-E2-p7), HCV core, and E2p7 genes were amplified and cloned in the pSFV1 expression vector under the control of the SFV subgenomic 26S promoter. Resulting plasmids pSFV1/HCVpolyP, pSFV1/HCV core, and pSFV1/HCV E2p7 were used as templates for *in vitro* transcription of the recombinant SFV region by SP6 RNA polymerase. Subgenomic RNAs carrying in our case different HCV sequences (depending on the construct) served as templates for translation of HCV genes.

Recombinant SFV particles were produced for each construct by simultaneous electroporation of cells with the subgenomic RNA of the appropriate constructs and helper SFV RNA. BHK-21 cells, which were used in these experiments, are not natural host cells for HCV. However, they are optimal for infection with and production of recombinant SFV particles, allowing the highest yields of recombinant proteins.

HCV polyP fragment encoding structural proteins and protein p7 was cloned also in the pCytTS vector. The pCytTS is an expression vector based on Sindbis virus. The recombinant plasmid specified as pCyt/HCV polyP was used for transfection of BHK-21 cells to express HCV proteins using another alphavirus besides SFV (Fig. 1). HCV sequences in all DNA constructs were verified by direct nucleotide sequencing.

Expression of HCV genes in BHK-21 cells

BHK-21 cells were transfected with recombinant RNA or, alternatively, infected with recombinant SFV viral particles. At 24 h postinfection, cells were metabolically labelled with ^{35}S-methionine for 1 h and lysed with NP-40 containing lysis buffer. The lysates were analyzed for the presence of HCV proteins. The analysis of cells lysate in SDS-PAGE is demonstrated in Fig. 2. HCV proteins were observed in cell lysate without concentration of lysates. The pattern of proteins showed a band about 70 kDa corresponding to E2 protein, 33 and 35 kDa bands corresponding to major glycosylated forms of the E1 and bands corresponding to the HCV core (Fig. 2, lane 3). The heaviest form of the HCV core was not detected in all experiments, probably because the level of protein production was not equivalent in different cases and minor forms of the HCV core protein remained undetectable. The molecular mass of proteins expressed from a construct that encoded the HCV core gene alone was identical to the molecular mass of the HCV core protein expressed from the construct, which encoded HCV structural proteins (Fig. 2, Fig. 3A). Expression of the HCV core gene was more efficient in the case of infection than in the case of electroporation (data not shown), perhaps due to strong reduction of the growth rate of electroporated cells and damage of many cells.

Expression of HCV genes was analysed in BHK-21 cells also after transfection by pCyt/HCVpolyP plasmid. Cells were lysed at 72 h after thermoinduction in lysis buffer containing NP-40 or in Laemmli buffer. Efficiency of expression of the HCV genes and immunological specificity of the corresponding proteins were demonstrated by Western blotting. Two species of HCV core protein with molecular mass 21 kDa and 23 kDa were identified in the total cell lysate. Bands, which were observed under major p23 and p21 forms of HCV core protein, corresponded to HCV core form 16 kDa (Fig. 3B).

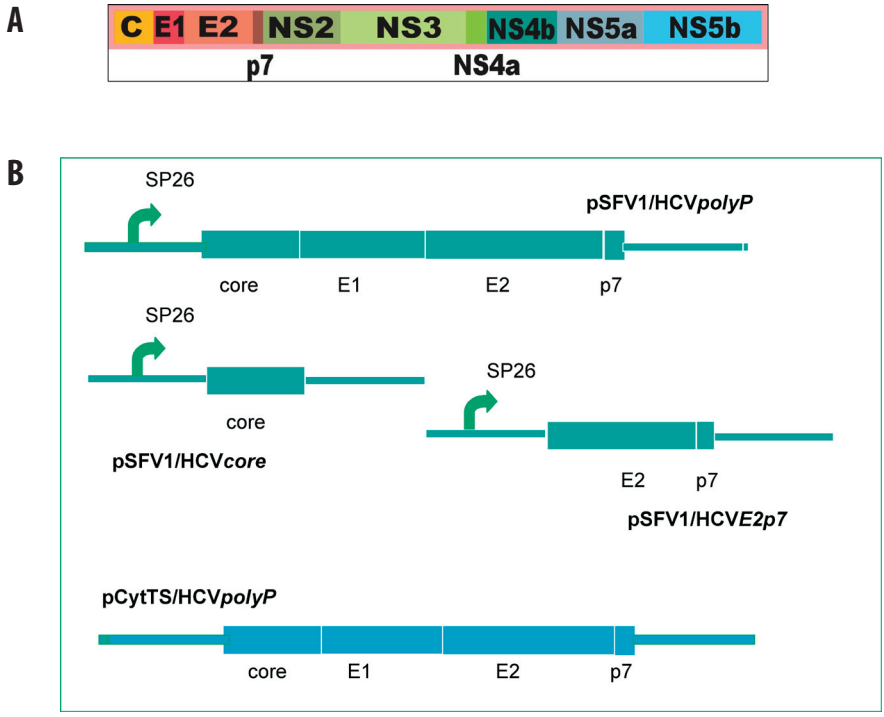

Fig. 1. Schematic diagram of recombinant constructs for analysis of HCV protein translation. A, HCV proteins: core, E1, E2 – structural proteins, NS2, NS3, NS4A, NS4B, NS5A, NS5B -nonstructural proteins, p7 – small protein with unclear functions. B, HCV proteins genes used in this study for recombinant plasmids construction.

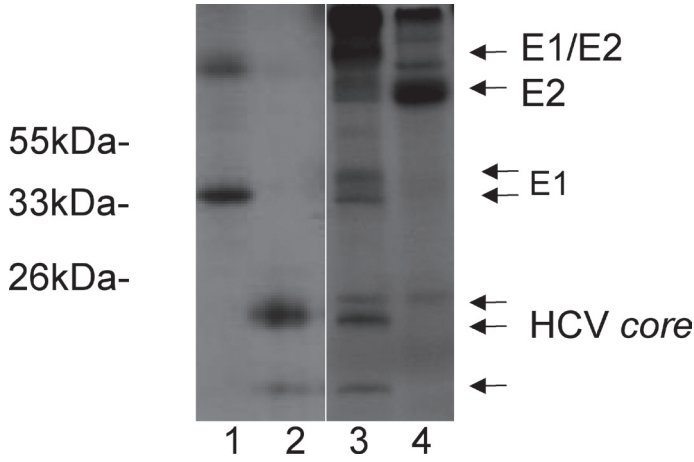

Fig. 2. HCV structural proteins genes expression in BHK-21 cells after infection by recombinant viruses. Lane1. BHK-21 cells lysate (NP-40 contained buffer) after infection by SFV1/EGFP as control; lane 2. BHK-21 cells lysate (NP-40 contained buffer) after infection by SFV1/HCVcore; lane 3. BHK-21 cells lysate (NP-40 contained buffer) after infection by SFV1/HCVpolyP; lane 4. BHK-21 cells lysate (NP-40 contained buffer) after infection by rSFV1/HCV E2p7. The Prestained Protein Molecular Weight Markers (Fermentas) were used as molecular mass markers.

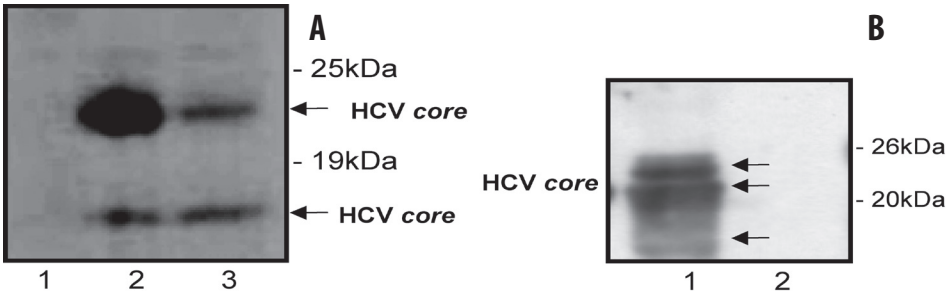

Fig. 3. HCV core protein gene expression in BHK-21 cells: Western-blot with polyclonal anti-HCV core antibody from rabbit. A, HCV core protein gene expression in BHK-21 cells after infection by recombinant viruses rSFV1/HCVpolyP and rSFV1/HCVcore. Lane 1: BHK-21 cell lysate (NP-40 contained buffer) after infection by SFV1/EGFP as control. Lane 2: BHK-21 cell lysate (NP-40 contained buffer) after infection by SFV1/HCVcore. Lane 3: BHK-21 cell lysate (NP-40 contained buffer) after infection by rSFV1/HCVpolyP. B, HCV core gene expression in BHK-21 cells after plasmid pCyt/HCVpolyP transfection by commertial kit (Fermentas). Western-blot with polyclonal anti-HCV core antibody from rabbit. Lane 1: BHK-21 cell total lysate (Laemmli buffer) after transfection by pCyt/HCVpolyP. Lane 2: negative control – noninfected BHK-21 cell lysate (Laemmli buffer). The Prestained Protein Molecular Weight Markers (Fermentas) were used as molecular mass markers.

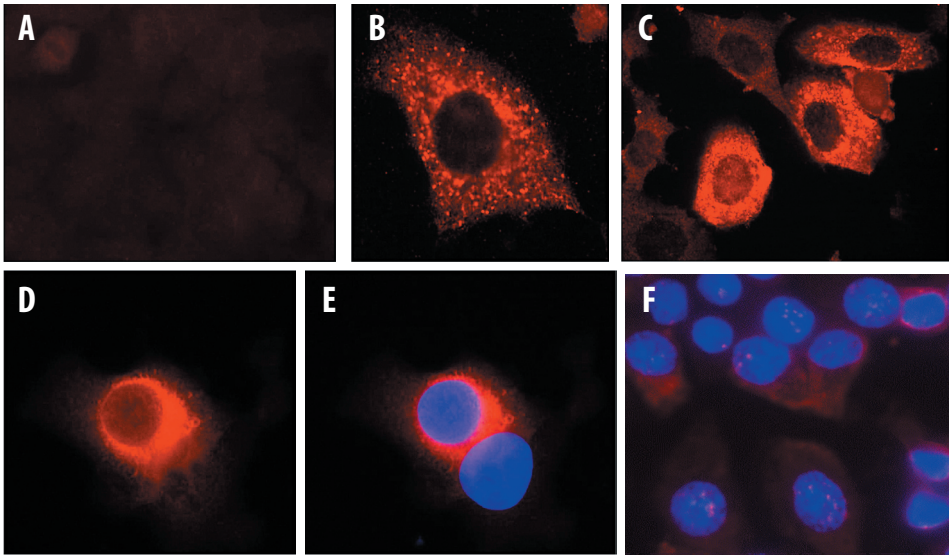

Fig. 5. Immunocytochemical detection of HCV core protein gene expression. BHK-21 cells were infected were with recombinant virus SFV1/HCVcore. Infected cells were stained with rabbit anti-HCV core antibodies (1:1000) and secondary anti-rabbit TRITC-antibodies (1:100). A, noninfected BHK-21 cells stained with rabbit anti-HCV core antibodies (1:1000) and secondary anti-rabbit TRITC-antibodies (1:100). Core protein distribution at 4 h (B), 8 h (C), 16 h (D) post infection. Nucleus visualization with DAPI 16 h (E) and 24 h (F) post infection.

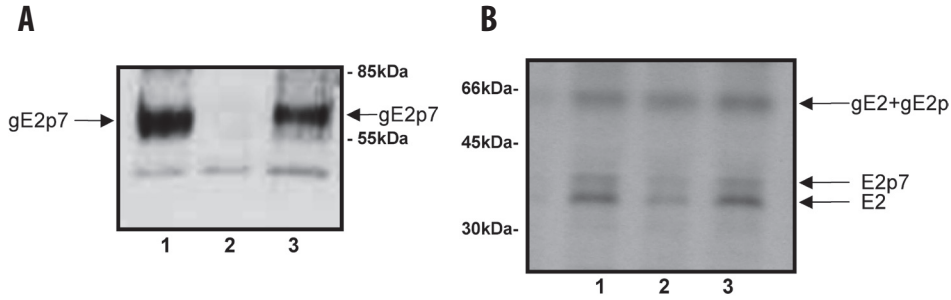

Fig. 4. HCV E2 protein gene expression in BHK-21 cells after infection by recombinant viruses SFV1/HCVpolyP and SFV1/HCVE2p7. A, Western-blot with polyclonal anti-HCV E2 antibody from rabbit. Lane1. BHK-21 cell total lysate (Laemmli buffer) after infection by SFV1/HCVpolyP. Lane 2: negative control – noninfected BHK-21 cell lysate (Laemmli buffer). Lane 3: BHK-21 cell total lysate (Laemmli buffer) after infection by SFV1/HCV E2p7. B, Immunoprecipitation of E2 and E2p7 proteins from cells lysates after infection by recombinant viruses SFV1/HCVpolyP and SFV1/HCVE2p7. Lane 1, 2, 3: immunoprecipitation with different polyclonal rabbit anti-E2 antibodies. The Prestained Protein Molecular Weight Markers (Fermentas) were used as molecular mass markers.

Efficient expression of HCV E2 protein gene from pCyt/HCVpolyP, pSFV1/HCVpolyP, and pSFV1/HCVE2p7 plasmids was also demonstrated. Specificity of the E2 protein was confirmed by Western blotting, imunoprecipitation, and imunocytochemical analysis with corresponding anti-E2 antibodies. Fig. 4 shows an analysis of BHK-21 cells lysates after infection by recombinant SFV1/HCVE2p7 and SFV1/HCVpolyP viruses. In our study, both protein patterns after infection with recombinant viruses were similar and E2 protein existed in a glycosylated form of about 70 kDa (Fig. 4A). Different E2 proteins forms represented by glycosylated E2 (about 70kDa), ngE2p7 (41 kDa), and ngE2 (36 kDa) were concentrated from cells lysates after infection with recombinant SFV1/HCV E2p7 virus using imunoprecipitation with corresponding anti-E2 antibody (Fig. 4B). Localization of the HCV E2 protein in the cytoplasm of infected cells was oserved using immunocytochemical analysis (data not shown).

Localization of HCV core protein in the cells

Localization of the HCV core protein was monitored by immunocytochemical analysis using binding of polyclonal rabbit antibody to HCV antigens. The percentage of cells stained positive increased during the first 24 h post infection, in most cases reaching a maximum in 24 h. For all constructs, the number of cells stained positive reached a value of up to 80 %. HCV core protein was localized mainly in the cytoplasm, but its localization was different at different times post infection. At 4 h and 8 h after infection of cells with recombinant viruses, HCV core protein was found in cytoplasm only. At 16 h after infection, HCV core protein concentrated in the perinuclear region. Only 24 h after infection, about 15 % of the HCV core protein was found in the nucleus (Fig. 5). However, correlation of each HCV core protein form with its localization was not established. At 4 h postinfection, a p21 form was detectable only in cell lysate. At 8 h postinfection, the p21 form and the same amount of a p23 form were detected in cell lysate. The smallest form of the HCV core protein of p16 kDa was detected at 24 h postinfection only (Fig. 6).

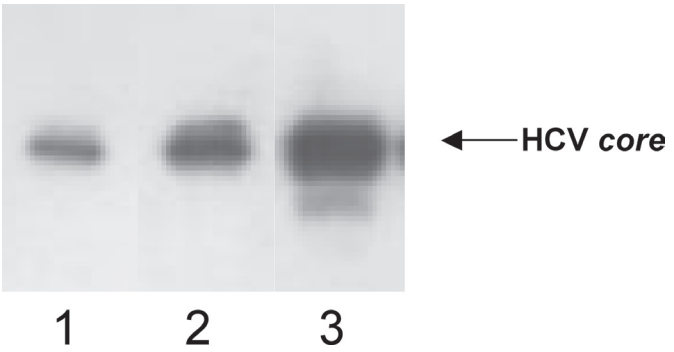

Fig. 6. HCV core protein gene expression in BHK-21 cells after infection by recombinant virus SFV1/HCV core at different times postinfection: different forms of HCV core proteins detection by Western-blot with polyclonal anti-HCV core antibody from rabbit. Lane 1: HCV core protein p21 form in BHK-21 cell total lysate (Laemmli buffer) at 4 h post infection. Lane 2: HCV core protein p21 form and some amount of p23 form in BHK-21 cells total lysate (Laemmli buffer) at 8 h post infection. Lane 3: HCV core protein p21 form, p23 form and p16 in BHK-21 cells total lysate (Laemmli buffer) at 24 h post infection. The Prestained Protein Molecular Weight Markers (Fermentas) were used as molecular mass markers.

Assembly of HCV structural proteins

To assess the ability of HCV structural proteins to be associated into virus-like particles, clarified cell lysates after infection with recombinant viruses pSFV1/HCVpolyP or pSFV1/HCVcore (or electroporation by the corresponding RNAs) were subjected to centrifugation through a sucrose cushion. The pellets were dissolved in TNE buffer and analyzed by Western blotting for two HCV structural proteins: core and E2. Both proteins were found in pellets (data not shown). Viral HCV particles were visualized by electron microscopy. First, HCV core particles of 35 to 37 nm in diameter were detected after infection with SFV1/HCVpolyP recombinant virus or SFV1/HCVcore (Fig. 7A, B). HCV-like particles with a diameter of 60 nm formed by HCV structural proteins were observed in the cells infected with SFV1/HCVpolyP recombinant virus (or electroporated with the corresponding RNAs), but the number of such particles in cell lysates was low (Fig. 7C).

Discussion

The absence of a suitable cellular model for HCV propagation has led to the use of various heterologous expression systems. Among others, the baculovirus insect cell system has proved useful for production and maturation of HCV structural (Baumert et al. 1998) and non-structural proteins (Overton et al. 1995). In addition, this system was a valuable tool for the (i) production of large amounts of antigens for immunological studies (Chiba et al. 1991) and (ii) investigation of viral protein interactions and assembly. Using recombinant baculovirus, Baumert et al. (1998) showed formation of pseudoviral particles. Pseudotyped and recombinant viruses carrying HCV envelope proteins were developed on the basis of Vesicular Stomatitis virus (VSV) vectors. Recombinant VSV expressed incorporated HCV genes, the products of which became fully processed and assembled into HCV-like particles (Ezelle et al. 2002). Moreover, recombinant VSV carrying unmodified HCV E1 and E2 proteins was able to infect Huh7 cells (Tani et al. 2007).

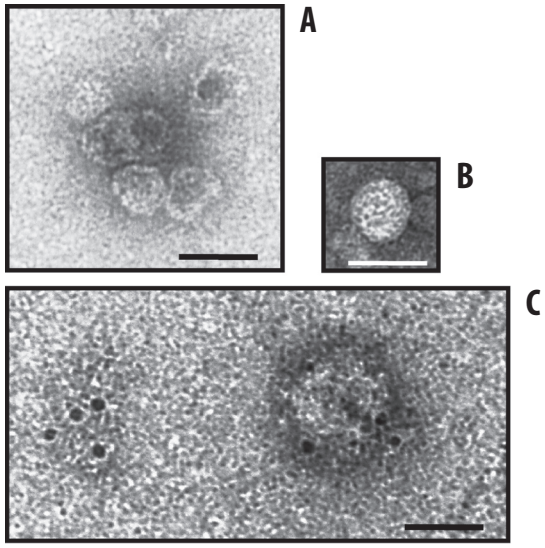

Fig. 7. Electron microscopy of purified HCV-like particles. A, HCV core particles in the NP-40 containing lysate of SFV1/HCVcore-transfected cells. B, HCV core particle. C, mmunogold labeling of HCV-like particles with anti-E2 polyclonal antibodies. The bar represents 50 nm.

Recently, a mammalian cell culture for a JFH1 strain of the 2a genotype (HCVcc) isolated from a fulminant HCV patient was developed for HCV replication *in vitro* (Zhong et al. 2005). However, a robust cell culture system for HCV of the 1a and 1b genotypes, the most prevalent genotypes in the world, has not yet been successfully developed, except for the cell culture producing H77 or H77-S strains of HCV, genotype 1a (Yi et al. 2006) and the replicons derived from Con1, a strain of HCV, genotype 1b (Lohmann et al. 1999).

The recombinant SFV replicon was used for production of HCV, genotype 1a, structural proteins in mammalian cells (Blanchard et al. 2002; Hourioux et al. 2007). Interestingly, the expression level of the HCV E1 and E2 proteins seems to be higher in the mammalian SFV expression system than that in the baculovirus expression system in insect cells. However, budding of the HCV-like particles in the SFV system seems to be abortive. Nevertheless, more information about translation and processing of HCV proteins, virus replication and maturation, molecular interactions between HCV virions and hosts are required to clarify details of HCV pathogenesis and persistence. In principle, each step of the HCV life cycle is a target for antiviral intervention.

We are developing a non-replicating recombinant SFV with a genome encoding unmodified HCV core, E2, and polyproteins, and not SFV envelope proteins, in cultivated cell lines. Expression of HCV, genotype 1b, structural genes provides novel information about translation and posttranslational processing of HCV structural proteins in cell cultures, as well as about their self-assembly. All structural HCV proteins appear in lysates after infection of BHK-21 cells with recombinant viruses. The pattern of HCV proteins after infection with SFV1/HCVpolyP virus presented several bands: a band of about 70 kDa corresponding to E2 protein, 33 and 35 kDa bands corresponding to major glycosylated forms of the E1, and bands of 23 kDa, 21 kDa, and 26 kDa corresponding to different forms of the HCV core (Fig. 2, lane 3). The heaviest form and smallest form of the HCV core are

not detectable; only the major form of the HCV core with the molecular mass of 21 kDa is observed. HCV core protein products are identical after infection with recombinant SFV1/HCVcore and SFV1/HCVpolyP viruses. However, expression of HCV core protein by SFV1/HCVcore virus is more efficient (Fig. 3A). The observations on production and posttranslational processing of HCV core proteins obtained in our study are in a good correlation with the literature. HCV core proteins, reviewed by Krekulova et al. (2006), were established as 21 kDa (191 aa), 19 kDa (173 aa), and 16 kDa. According to more recent observations, the molecular mass of two forms generated by posttranslational splicing at sites near aa residue 191 and near aa residue 173 are 23 kDa and 21 kDa (Vauloup-Fellous et al. 2006). The smallest form of HCV core protein is generated by translation from the alternative reading frame (Xu et al. 2001). The 21 kDa and 23 kDa proteins are bound to membranes of ER, while the 16 kDa form is localized preferentially in the perinuclear space (Lo et al. 1995). However, information about localization of the HCV core proteins in the cells is controversial. Krekulova et al. (2006) notes that a small portion of 19 kDa (21 kDa in other studies) protein was translocated into nucleus. Matured HCV core protein was found in nucleus by Yasui et al. (1998). However, Rouille et al. (2006) did not find HCV core protein in the nucleus. In our study, localization of the HCV core protein monitored by an immunocytochemical method leads to conclusion that the HCV core protein appears mainly in cytoplasm, but it is present also in nucleus (Fig. 5). During early stages of cell infection with recombinant viruses, HCV core protein is detectable in cytoplasm only. In 16 h after infection, HCV core protein moves to the perinuclear region and is detectable in nucleus only after 24 h after infection (Fig. 5).

Based on the observation of the variable location of the HCV core protein forms, one can estimate multiple roles of HCV core protein in the HCV replication cycle and in the course of HCV infection. Earlier publications assumed that the p21 form of the HCV core protein provides a regulatory function in nucleus and affects expression of the host cell genome (Ray at al. 1996). Later papers showed that the ratio of specific HCV core protein variants, as well as their location within the host cell, is important for cell transformation (Chang et al. 1998).

The HCV envelope glycoprotein E2 binds to CD81 receptor on human cells. Therefore, it is a prime candidate for inclusion in HCV vaccines. Expression of the HCV E2 protein gene in BHK-21 cells is shown in Fig. 4. The E2 protein exists in a glycosylated form of about 70 kDa in BHK-21 cell lysates, after infection with recombinant SFV1/HCVpolyP or SFV1/HCVE2p7 viruses (Fig. 4A).

It is known that HCV core, envelope glycoproteins E1 and E2, and p7 are cleaved from the polyprotein by host signal peptidases. The precursor product E2-p7 was described by Lin et al. (1994). This protein is relatively stable and it is cleaved slowly to produce the E2 protein. It seems that cleavage at sites of E2p7/NS2 and E2/p7 is not necessarily co-translational, in contrast to the C/E1 and E1/E2 cleavages. Forms of the HCV E2 proteins observed in this study in cells infected with recombinant SFV1/HCV E2p7 after imunoprecipitation with corresponding anti-E2 antibody consist of glycosylated E2 (about 70kDa), ngE2p7 (41 kDa), and ngE2 (36 kDa) (Fig. 4B). Therefore, correct processing of HCV E2 protein is possible also in the SFV based expression system. Moreover, a surrogate SFV model system for expression of HCV structural genes exhibits high efficiency in BHK-21 cells.

A SFV replicon carrying HCV NS3/4A protein genes was used to enhance

immunogenicity of NS3/4A by mRNA amplification (Frelin et al. 2004). However, in Brinster´s (Brinster et al. 2002) study replicating SFV DNA vaccines and rSFVs expressing HCV core or E2 antigens were compared with classical CMV-driven plasmids (pCMV) in single or bimodal vaccine protocols. Comparison of different injection modes did not show any increased efficacy of the SFV-core and SFV-E2 plasmids or rSFVs compared with the CMV-driven vectors (Vidalin et al. 2000). Despite the contradictory data, combination of "genetic vaccines" (DNA, RNA, or viral particles, carrying target proteins gene) and corresponding proteins for prime-boost immunization in order to enhance immunoresponce remains very promising. These results indicate that the recombinant SFV carrying HCV structural proteins genes developed in this study can be used to study HCV proteins with respect to not only the biological functions in the virus life cycle, but also for development of HCV vaccines.

SFV-based expression systems have a serious disadvantage: overproduction of viral proteins stimulates a strong cytotoxic effect on host cells. The pCytTS expression vector, which is based on Sindbis virus, was created specially for routine production of difficult or toxic proteins (Boorsma et al. 2000). In our study, however, Sindbis-driven expression of HCV genes is not more efficient than the initial SFV-driven expression system, which allows to obtain sufficient amount of target proteins in the shortest time.

Immunocytochemical data, imunoprecipitation from cell lysates, and Western blot analysis with appropriate anti-core and anti-E2 polyclonal antibodies show that recombinant alphaviruses can provide high levels of authentically posttranslationally processed HCV core and E2 proteins. As known from literature (Baumert et al. 1998, Blanchard et al., 2002), cooperative production of structural HCV proteins results in self-assembly of the structural proteins into HCV-like particles. Production of HCV-like particles using a recombinant baculovirus in insect cells has already been reported. These particles, 40 to 60 nm in diameter, are polymorphic in appearance. In some electron micrographs (Blanchard et al. 2002; Vauloup-Fellous et al.,2006), HCV core-like particles of 30-40 nm in diameter are surrounded by ER-derived envelope, yielding a particle with a total diameter of 50-60 nm. Some authors explain the morphological heterogeneity of HCV-like particles by incorporation of partially uncleaved structural polypeptides into the envelope of such particles (Khromykh et al. 1998). The functional importance of RNA-protein interactions for assembly of HCV-like particles in heterologous system was reported by Girard et al. (2004). We detected homogeneous HCV core-like particles of 35-37 nm in diameter by electron microscopy (Fig. 7A, B), despite the fact that some of them may be damaged during preparation and concentration. Moreover, HCV-like particles with the diameter of 60 nm are observed randomly (Fig. 7C). This fact confirms once again the ability of correct processing of the HCV proteins in alphaviral expression systems.

As previously reported, formation of HCV-like particles is hampered by inefficient retention of HCV envelope proteins in the aggregated form on the ER (Deleersnyder et al. 1997). Moreover, formation of native HCV glycoprotein complexes is a limiting step in particle morphogenesis, this process varying efficiency from one HCV genotype to another (Girarg et al. 2004). The difficulties encountered in observing complete particles may be related to their high intrinsic instability or to their high sensitivity to the purification process. As known, it is currently not possible to obtain a sufficient amount of HCV particles for biological and physiochemical studies due to low viral load in the sera of hepatitis C patients and the low yield of HCV particles in cell cultures. Thus, HCV-like

particles obtained in the SFV expression system may serve, after optimization, as a useful tool for development of tissue culture model of HCV infection, for a better understanding of the mechanism of HCV assembly, and for the study of HCV morphogenesis. Moreover, the HCV proteins in HCV-like particles presumably are presented in a native, virion-like conformation and may therefore be superior in eliciting protective humoral and cellular immune responses. Since HCV-like particles synthesized in cells cultures are derived from partial viral genomes, without nonstructural genes required for viral replication, they are noninfectious and therefore represent excellent candidates for an HCV vaccine.

Acknowledgements

The work was supported by the VZP-8 project of the Latvian State Scientific Programme, by ERAF grants VPD1/ERAF/CFLA/05/APK/2.5.1/000021 and VPD1/ERAF/CFLA/05/APK/2.5.1/000018 and by the European Social Fund (ESF). The work was partially supported also by New Visby project. The authors thank Arija Ose, Irena Timofejeva, Natalija Gabrusheva for excellent technical assistance and Anton Mozgalevsky for plazmid pSFV1/HCV E2p7 construction. The authors are grateful to Prof. Pauls Pumpens for critical reading of the article.

References

Baumert T.F., Ito S., Wong D.T., Liang T.J. 1998. Hepatitis C virus structural proteins assemble into virus like particles in insect cells. *J. Virol.* 72: 3827–3836.

Blanchard E., Brand D., Trassard S., Goudeau A., Roingeard P. 2002. Hepatitis C virus-like particle morphogenesis. *J. Virol.* 76: 4073–4079.

Boorsma M., Nieba L., Koller D., Bachmann M.F., Bailey J.E., Renner W.A. 2000. A temperature-regulated replicon-based DNA expression system. *Nature Biotechnol.* 18: 429–432.

Brinster C., Chen M., Boucreux D., Paranhos-Baccala G., Liljeström P., Lemmonier F., Inchauspé G. 2002. Hepatitis C virus non-structural protein 3-specific cellular immune responses following single or combined immunization with DNA or recombinant Semliki Forest virus particles. *J. Gen. Virol.* 83: 369–381.

Dubuisson J., Penin F., Moradpour D. 2002. Interaction of hepatitis C virus proteins with host cell membranes and lipids. *Trends Cell. Biol.* 12: 517–523.

Ezelle H., Markovic D., Barber G. 2002. Generation of hepatitis C virus-like particles by use of a recombinant vesicular stomatitis virus vector. *J. Virol.* 76: 12325-12334.

Frelin L., Ahlén G., M Alheim, O Weiland, C Barnfield, P Liljeström, M Sällberg. 2004. Codon optimization and mRNA amplification effectively enhances the immunogenicity of the hepatitis C virus nonstructural 3/4A gene. *Gene Therapy* 11: 522–533.

Chang J., Yang S.H., Cho Y.G., Hwang S.B., Hahn Y.S., Sung Y.C. 1998. Hepatitis C virus core from two different genotypes has an oncogenic potential but is not sufficient for transforming primary rat embryo fibroblasts in cooperation with the H-ras oncogene. *J. Virol.* 72: 3060–3065.

Chiba J., Ohba H., Matsuura Y., Watanabe Y., Katayama T., Kikuchi S., Saito I., Miyamura T. 1991. Serodiagnosis of hepatitis C virus (HCV) infection with an HCV core protein molecularly expressed by a recombinant baculovirus. *Proc. Natl. Acad. Sci. USA* 88: 4641–4645.

Girard C., Ravallec M., Mariller M., Bossy J.P., Cahour A., López-Ferber M., Devauchelle G., Inchauspé G., Duonor-Cérutti M. 2004. Effect of the 5' non-translated region on self-assembly of hepatitis C virus genotype 1a structural proteins produced in insect cells. *J. Gen. Virol.* 85: 3659–3670.

Glasgow G.M., McGee M.M., Tarbatt C.J., Mooney D.A., Sheahan B.J., Atkins G.J. 1998. The Semliki Forest virus vector induces p53-independent apoptosis. *J. Gen. Virol.* 79: 2405–2410.

Hourioux C., Ait-Goughoulte M., Patient R., Fouquenet D., Arcanger-Doudet F., Brand D., Martin

A., Roingeard P. 2007. Core protein domains involved in hepatitis C virus-like particle assembly and budding at the endoplasmic reticulum membrane. *Cell Microbiol*. 9: 1014–1027.

Keck Z., Op De Beeck A., Hadlock K.G., Xia J., Li T., Dubuisson J., Foung S.K.H. 2004. Hepatitis C virus E2 has three immunogenic domains containing conformational epitopes with distinct properties and biological functions. *J. Virol.* 78: 9224–9232.

Khromykh A.A., Varnavski A.N., Westaway E.G. 1998. Encapsidation of the flavivirus kunjin replicon RNA by using a complementation system providing Kunjin virus structural proteins in trans. *J Virol.* 72: 5967–5977.

Kozlovska T., Zajakina A., Ose V., Bruvere R., Aleksejeva J., Pumpens P., Garoff H. 2004. Synthesis of all hepatitis B structural proteins in the Semliki Forest virus expression system. *Acta Univ. Latvi* 676: 53–64.

Krekulova L., Lehak V., Riley L.W. 2006. Structure and functions of hepatitis C virus proteins: 15 years after. Review. *Folia Microbiol*. 51: 665–680.

Liljeström P., Garoff H. 1991. A new generation of animal cell expression vectors based on the Semliki Forest virus replicon. *Biotechnology* 9: 1356–1361.

Lin C., Lindenbach B.D., Pragai B.M., McCourt D.W., Rice C.M. 1994. Processing in the hepatitis C virus E2-NS2 region: identification of p7 and two distinct E2-specific products with different C termini. *J. Virol.* 68: 5063–5073.

Lo S.-Y., Masiarz F., Hwang S.B., Lai M.M.C., Ou J.-H. 1995. Differential subcellular localization of hepatitis C virus core gene products. *Virology* 213: 455–461.

Lohmann V., Korner F., Koch J., Herian U., Theilmann L., Bartenschlager R. 1999. Replication of subgenomic hepatitis C virus RNAs in a hepatoma cell line. *Science* 285: 110–113.

McLauchlan J., Lemberg M.K., Hope R.G., Martoglio B. 2002. Intramembrane proteolysis promotes trafficking of hepatitis C virus core protein to lipid droplets. *EMBO J.* 21: 3980–3988.

Mokhonov V.V., Novikov D.V., Samokhvalov E.I., Shatalov A.G., Selivanov N.A., Prilipov A.G., Lvov D.K. 2002. Genome analysis of hepatitis C virus strain 274933RU isolated in Russian Federation. *Vopr. Virusol.* 47: 9–12.

Overton H., McMillan D., Gillespie F., Mills J. 1995. Recombinant baculovirus-expressed NS3 proteinase of hepatitis C virus shows activity in cell-based and *in vitro* assays. *J. Gen. Virol.* 76: 3009–3019.

Patel J., Patel A.H., McLauchlan J. 1999. Covalent interactions are not required to permit or stabilize the non-covalent association of hepatitis C virus glycoproteins E1 and E2. *J. Gen. Virol.* 80: 1681–1690.

Penin F., Dubuisson J., Rey F.A., Moradpour D., Pawlotsky J.M. 2004. Structural biology of hepatitis C virus. *Hepatology* 39: 5–19.

Ray R.B., Meyer K., Ray R. 1996. Suppression of apoptotic cell death by hepatitis C virus core protein. *Virology* 226: 176–182.

Smerdou C., Liljeström P. 1999. Two-helper RNA system for production of recombinant Semliki forest virus particles. *J. Virol.* 73: 1092–1098.

Sominskaya I., Alekseeva E., Skrastina D., Mokhonov V., Starodubova E., Jansons J., Levi M., Prilipov A., Kozlovska T., Smirnov V., Pumpens P., Isaguliants M.G. 2006. Signal sequences modulate the immunogenic performance of human hepatitis C virus E2 gene. *Mol. Immunol.* 43: 1941–1952.

Suzuki T., Ishii K., Aizaki H., Wakita T. 2007. Hepatitis C viral life cycle. Review. *Adv. Drug Deliv. Rev.* 59: 1200–1212.

Tani H., Komoda Y., Matsuo E., Suzuki K., Hamamoto I., Yamashita T., Moriishi K., Fujiyama K., Kanto T., Hayashi N., Owsianka A., Patel A. H.,. Whitt M. A, Matsuura Y. 2007. Replication-competent recombinant vesicular stomatitis virus encoding hepatitis C virus envelope proteins. *J. Virol.* 81: 8601–8612.

Vauloup-Fellous C., Pene V., Garaud-Aunis J., Harper F., Bardin S., Suire Y., Pichard E., Schmitt A., Sogni P., Pierron., Briand P., Rosenberg A. 2006. Signal peptide peptidase-catalyzed cleavage of hepatitis C virus core protein is dispensable for virus budding but destabilizes the viral capsid. *J.*

Biol. Chem. 281: 27679–27692.
Vidalin O., Fournillier A., Renard N., Chen M., Depla E., Boucreux D., Brinster C., Baumert T., Nakano I., Fukuda Y., Liljeström P., Trépo C., Inchauspé G. 2000. Use of conventional or replicating nucleic acid-based vaccines and recombinant semliki forest virus-derived particles for the induction of immune responses against hepatitis C virus core and E2 antigens. *Virology* 276:259-270.
Xu Z., Choi J., Yen T.S.B., Lu W., Strohecker A., Govindarajan S., Chien D., Selby M.J., Ou J. 2001. Synthesis of a novel hepatitis C virus protein by ribosomal frameshif. *EMBO J.* 20: 3840–3848.
Yaisui K., Wakita T., Tsukiyama-Kohara K., Funahashi S., Ichikawa M., Kajita T., Moradpour D., Wands J., Kohara M. 1998. The native form and maturation process of hepatitis C virus core protein. *J. Virol.* 72: 6048–6055.
Yi M., Villanueva R.A., Thomas D.L., Wakita T., Lemon S.M. 2006. Production of infectious genotype 1a hepatitis C virus (Hutchinson strain) in cultured human hepatoma cells. *Proc. Natl. Acad. Sci. USA* 103:2310-2315.
Zhong J., Gastaminza P., Cheng G., Kapadia S., Kato T., Burton D.R., Wieland S.F., Uprichard S.L., Wakita T., Chisari F.V. 2005. Robust hepatitis C virus infection *in vitro*. *Proc. Natl. Acad. Sci. USA* 102: 9294–9299.

Hepatīta C vīrusa strukturālo gēnu ekspresija alfavirālo rekombinanto replikonu kontrolē

Jekaterina Aleksejeva*, Irina Sominska, Ruta Brūvere, Velta Ose, Anna Zajakina, Tatjana Kozlovska

Proteīnu inženierijas nodaļa, Latvijas Biomedicīnas pētījumu and studiju centrs, Rātsupītes 1, Rīga LV-1067, Latvia
*Korespondējošais autors, E-pasts: kate@biomed.lu.lv

Kopsavilkums

Tā kā pašlaik vēl nav pieejami efektīvi hepatīta C vīrusa (HCV) izraisītā hepatīta ārstēšanas paņēmieni, anti-HCV vakcīnas kandidāta izstrādāšana ir mērķis ar augstu prioritāti. Mūsu pētījumos izmantotas divas dažādas alfavirālās ekspresijas sistēmas HCV strukturālo proteīnu gēnu ekspresijai šūnu kultūrā. Šī mērķa sasniegšanai HCV genoma fragmentu, kas kodē serdes-E1-E2-p7 poliproteīnu, kā arī HCV serdes un E2 gēnus atsevišķi klonēja Semliki meža vīrusa (pSFV1) un Sindbis vīrusa (pCytTS) ekspresijas vektoros. Parādīta efektīga HCV strukturālo proteīnu sintēze BHK-21 līnijas šūnās. HCV poliproteīna priekštecis bija autentiski procesēts pēctranslācijas laikā. HCV proteīnus identificēja ar imunoprecipitāciju, imunocitoķīmisko analīzi, kā arī ar *Western blotting* analīzi ar atbilstošajām anti-HCV antivielām.

Acta Universitatis Latviensis, 2008, Vol. 745, Biology, pp. 131–144

Effect of burial by sand on Scots pine (*Pinus sylvestris* L.) radial growth on seacoast wooded dunes at Cape Kolka, Latvia

Roberts Matisons*, Guntis Brūmelis

Department of Botany and Ecology, Faculty of Biology, University of Latvia, Kronvalda Bulv. 4, Riga LV-1586, Latvia

*Corresponding author, E-mail: robism@inbox.lv

Abstract

Scots pine is a widely distributed species in Latvia, stress tolerant and able to grow in poor habitats. It is the dominating species of seacoast wooded dunes. Dunes in the Cape Kolka area are characterized with moving sand, resulting in stem burial of pines growing close to the beach. Main burial events are thought to occur during major storms, particularly as in 1967 - 1969. The aim of the study was to evaluate the effect of burial and climatic factors on radial growth. Samples from pines growing along the seaside under different levels of sand burial were collected. Tree-ring width series were crossdated and detrended chronologies were established. To evaluate growth relationships with climate correlation analysis was performed. Release/suppression analysis was performed to evaluate burial effect. Burial affected radial growth both in unburied and buried parts of stem. Under deep burial (more than 0.6 m) the occurrence of missing tree-rings increased. Radial growth since storms of 1967 - 1969 declined in pines blown over with sand. No major release periods were observed. Unburied pines also showed growth suppression dominating over release, especially during the last forty years, which might be related with erosion of the Kolka coast, changing the abiotic factors. Late winter and early spring temperatures were the main climatic factors affecting Scots pine growth of unburied trees, but buried trees (parts of stems) showed weaker reaction to extreme temperatures. Precipitation had an insignificant influence, presumable due to a well-drained soil and sufficient available moisture.

Key words: dendroecology, *Pinus sylvestris*, radial growth, sand burial in costal dunes, Scots pine.

Introduction

Wooded seacoast dunes are characterized by environmental factors changing in time and space (Moreno-Casasola 1986). Also they are a protected habitat in the EU (92/43/EEC 2180). Wind-induced coastal erosion and moving sand often causes complete or partial burial of plants (including trees) under certain conditions, even causing plant death (Moreno-Casasola 1986; Maun 1998). The burial effect can be divided in two types: high frequency with low intensity and catastrophic burial. A low intensity burial event is common for sandy coastal habitats, mainly affecting plants (mostly grasses) growing on the beach, foredunes and primary dunes (Moreno-Casasola 1986; Maun 1998; Dech, Maun 2006). Occasionally sand drift can reach secondary dunes, where pine and other woody plants are present causing their burial (Moreno-Casasola 1986; Maun 1998; Eberhards

2003), although these burials are still low intensity. Catastrophic burial events occur with low frequency, on occasions when larger quantities of released sand are available and strong wind forces drifts and deposites the sand material deeper inland into secondary dunes. Such situations are seen at the seacoast dune habitats during severe storm periods when dune vegetation is damaged, thus releasing sand material, and in wandering dunes where sand is weakly fixed (Marin, Filion 1992; Ulsts 1998; Eberhards 2003). Usually catastrophic burial events result in a thick layer of sand deposits. Burial effect in coastal dunes overall also depends on relief. Moving dunes (coastal or inland) that bury trees with a thick layer of sand often cause a deficit of water or abundance of soil moisture (if climate and microrelief are rich in water) resulting in reduction of photosynthesis, even resulting in a burial-intolerant plant death (Alestalo 1971; Schweingruber 1996; Maun 1998).

Scots pine does not form adventitious roots and should be considered as intolerant to burial. The buried parts of the stem maintain transport functions from roots, but radial growth can decrease depending on depth of burial through stem respiration and oxygen available for the root system (Alestalo 1971; Dech, Maun 2006).

Burial changes soil physical, physicaly-chemical, chemical (Jury, Horton 2004) and ecological characteristics: decreases soil oxygenation (influencing cambium during growth period), decreases deeper soil layer temperature (also making it more constant), increases or decreases moisture depending on site specifics, affects biotic factors such as mycorrhizal relations and the influence of pathogenic organisms, resulting in physiological stress and a decrease of growth in burial-intolerant species such as Scots pine (Alestalo 1971; Lavigne 1996; Schweingruber 1996; Maun 1998; Hartmann et al. 2000; Wimmer 2002; Larcher 2003; Mancuso, Marras 2003). Burial can change tree-ring formation in stems, as burial influences location of the stem bending point, resulting in reaction wood formation in different sections of stem. With low water stress and temperate climate conditions (temperatures), competition factors should play the main role in overall growth variation with burial as an additive effect occurring occasionally (Schweingruber 1996; Kuuluvianen et.al. 1998; Larcher 2003). Nevertheless, sometimes in intolerant woody plants under burial growth improvement can be observed in relation to release from competition after forest fire or forest clearing (also medium intensity natural disturbance) (Marin, Filion 1992).

Burial may also affect wood anatomy. Growth in buried parts of the stem becomes more similar to root growth as larger vessels are produced, despite strong reduction of tree ring size, observed in coniferous trees (*Picea glauca*) and common oak (*Quercus robur*) (Cournoyer, Filion 1994; den Ouden et al. 2007). Thus, in addition to effect on tree ring width, wood anatomy might also change due to drift sand and dune activity study.

Under strong burial (up to 4.2 m or 80 % of height) Scots pine was observed to form narrow or no tree-rings and produce significantly less biomass (Alestalo 1971; Dech, Maun 2006). The burial effect is not permanent: after sand deposit removal (erosion) growth rate can increase to normal (Alestalo 1971). Another coniferous tree species – white spruce (*Picea glauca*), on subarctic dunes in Hudson Bay, Quebec, Canada reacted similarly by strongly reduced stem radial growth under burial and showed normalization after erosion (Marin, Filion 1992; Cournoyer, Filion 1994), indicating that growth patterns can be a useful tool for determining past dune activity. Dech and Maun (2006) investigated burial effect in a dune habitat on several artificially planted woody plant species, and concluded that burial-tolerance differs among species and is directly connected with species and adventitious root formation ability. The authors suggested Scots pine as a burial-intolerant

species, which linearly decreases biomass formation (growth) as the sand deposit layer thickens.

A strong storm in January 2005 strongly eroded the coastal dunes along the Baltic sea coast at the Cape Kolka, uncovering buried parts of stems of pines, making it possible to estimate burial depth and obtain samples at different height above the base of stem from parts of stems that were previously buried. The majority of pines were completely washed out and fallen. The main catastrophic burial events in Kolka should be related to storms, because sand material normally is fixed by vegetation and usual wind force doesn't transport it very deep into land (Moreno-Casasola 1986; De Raeve 1989; Maun 1998; Eberhards 2003). A catastrophic burial event in the last hundred years at Kolka coast is thought to have occurred in a severe storm in the period of 1967 - 1969, when coasts (foredunes) were severely eroded, coastal habitats were strongly degraded and significant quantities of sand material released and drifted into land burying part of coastal forests (Eberhards 2003)

The aim of the study was to determine the effect of sand burial on radial growth of Scots pine at Cape Kolka. The goals of the study were to compare tree ring chronologies obtained from buried and unburied trees, compare chronologies obtained from buried trees at different heights above the base of stem, and to compare the influence of climatic factors on growth of trees buried at different depths. Release and suppression analysis was also used to suggest when major burial events might have occurred.

Materials and methods

Study area and sampling plots

The study was carried out in northwestern Latvia, Slītere National park, Cape Kolka (Fig. 1). The sampling territory is mostly covered with boreal dry pine forests. Microrelief is formed by dune ridges and interdune depressions, with height 4 to 10 m above sea level

Fig. 1. Sampling territory.

(Eberhards 2003). The soil is sandy, poor in nutrients. In the former USSR regime, the territory was a restricted border zone with a very low anthropogenic influence (only military personal and few local villagers). Forest logging for the last hundred years has remained at a very low level.

High frequency low intensity burial at Kolka was common during the entire last century (Eberhards 2003). Nowadays the effect of burial still remains, only it is not lasting, as sea mostly erodes the Kolka coast forming a bluff, also slowing sand drift into land and forest burial (Ulsts 1998). Woody plants in wooded seacoast dunes in Kolka do not suffer a water deficit or abundance, because groundwater is available (Eberhards 2003) and soil drainability avoids abundance of water in shallower horizons and the sea moderates the microclimate. Moderate burial levels in the study site allow photosynthesis (branches and top of trees are not buried). Nowadays erosion processes still remain uncovering previously buried pines (mostly dead for a long time).

Three sampling plots were established: two along the beach (250 × 10 m) with trees buried at different depth and a control sampling plot (20 × 20 m) approximately 200 m away from the beach, where no burial effect on trees was observed. All sampling plots were covered with pine forest. Sampling plot coordinates are shown in Table 1.

Sampling and measurement

At the control site dominant trees were cored using a Pressler increment corer. In sites along the beach all trees were cored or stem discs were taken, depending on stem diameter (trees with diameter more than 5 cm were cored). Increment cores were taken at 0.3 m height above stem base (closest possible position to base of stem) from all trees and additional two or three cores were taken from strongly buried (burial depth more than 0.6 m) trees 1.3 m above stem base. Stem discs from smaller trees were obtained 0.3 m above stem base. We ensured that at least one core from each tree had a direct hit into stem pith. Increments and stem discs were collected in summer periods of 2005 and 2006 (control tree group). In the control sampling plot cores were taken from living trees, in sampling plots near the beach mostly dead trees lying on sand were cored.

For every buried tree burial depth was measured according to the margin where epiphyte or soil organism presence and sand debris were visible (margin was clearly visible in the field).

In the laboratory cores were dried and glued in a fixation plank, gradually sandpapered (sandpaper roughness from 150 to 400) and cleared from sawdust. Prepared cores were scanned using a digital scanner (HP Scanjet 8200) with resolution 1200 dpi in 16-bit color depth (RinnTech 2002). Tree ring widths were measured using the program Lignovision v. 1.36, manually placing tree ring borders for the best quality. In the study the whole tree ring widths (summing early and late wood widths) were used.

Table 1. Coordinates of sampling plots

Sampling plots	Coordinates (center of the plot) LKS92(x; y)
Sampling plot 1 (slightly buried trees)	57°45'30.4"N; 22°35'46.8"E
Sampling plot 2 (strongly buried trees)	57°45'25.9"N; 22°34'52.6"E
Control plot (unburied trees)	57°45'14.8"N; 22°34'52.5"E

Mathematical processing

Tree ring series were divided into four groups according to burial depth and sampling height: (i) control group – unburied trees cored at 0.3 m above stem base; (ii) slightly buried (burial depth less than 0.3 m) – trees cored at 0.3 m above stem base; (iii) strongly buried cored at stem base (0.3 m above stem base, burial depth more than 0.6 m); (iv) strongly buried cored 1.3 m above stem base (burial depth more than 0.6 m). Tree ring series with minimum length of 40 years were used in further analysis.

The COFECHA program was used for measurement quality control and crossdating with segment length of 40 years and lag 20 (Holmes et al. 1986; Cook, Briffa 1990; Grissino-Meyer 2001). Tree ring series were detrended and chronologies were calculated with ARSTAN. In further analysis mean tree ring widths and residual chronologies were used (Holmes et al. 1986; Cook, Krusic 2005).

Signatures of relationships of climatic factors to chronologies were determined with Pearson linear correlation analysis (Sokal, Rohlf 1981; Fritts 2001) and also using the program Dendroclim2002 for the whole available reference period (Biondi, Waikul 2004).

To evaluate growth dynamics before and after storms of 1967 - 1969 linear regression lines based on tree ring widths for 30-year periods before and after storms of 1967 - 1969 were constructed. Slopes of the regression lines were compared using the "comparison of regression lines analysis" method in the Statgraphics plus v.2.1 program (Sokal, Rohlf 1981; Manugistics 1996).

To compare radial growth tendencies and synchronicity among groups Gleichläufigkeit (GLK) indices were calculated (Esper et al. 2001). To evaluate abrupt growth changes in the stand that were maintained for a longer period release/suppression analysis was conducted (Baker, Bunyavejchewin 2006). Growth changes with relative values more than 25 % were included in the analysis. We considered as significant those relative values of release and suppressions that exceeded 20 % of stand (group) tree number.

Climatic data was obtained from the Latvian Environment, Geology and Meteorology Agency for the Kolka Meteorological Station, [missing data for the Second World War period (1941 - 1945) was replaced by modeled estimates based on Riga Station data]. Absolute minimal, maximal and average temperatures for months and seasons, and precipitation sums for months and seasons were used. October, November and December climatic data were considered and used as next year parameters.

Results

In the study 177 samples from 128 trees were collected; after crossdating and quality verification 105 samples from 73 trees were selected for further analysis. Numbers of samples collected and used for building chronologies are shown in Table 2.

Crossdating showed that many samples had missing tree rings and growth within groups was variable. For chronology construction data series showing at least $r = 0.25$ correlation with the COFECHA master series were included. Reference periods for groups with first five years cut are shown in Table 2. Minimal reference period was 103, maximal 142 years. Samples taken from strongly buried trees from the base of stem showed the shortest reference period due to wood rot.

For each group mean tree ring widths were calculated (Fig. 2). To evaluate changes in

Table 2. Numbers of samples suitable for further analysis and reference periods

	Control (burial absent)	Slightly buried	Strongly buried at stem base	Strongly buried 1.3 m above stem base	Other samples/ trees	Total
Burial depth (m)	0	< 0.3	> 0.6	> 0.6	[0.3; 0.6]	
Number of samples	42	37	25	54	19	177
Number of trees	15	37	25	32	19	128
Reference period	145 (2006-1862)	112 (2005-1894)	105 (2005-1901)	107 (2005-1899)	110 (2005-1896)	
Number of samples after crossdating and quality control	36	17	18	34	0	105
Number of trees after crossdating and quality control	13	17	18	25	0	73
Reference period after crossdating and quality control	142 (2004-1863)	109 (2004-1896)	103 (2004-1902)	106 (1899-2004)	0	

growth of sample groups after storms of 1967 - 1969 linear regression lines for periods of 1935 - 1964 and 1965 - 1994 were constructed (Fig. 3) and trend line slopes were compared (Table 3) (slopes differ when p-values < 0.05). The slopes of regression lines did not significantly differ among sample groups in the 30-year period before the storms of 1967 - 1969. In the period after the storms trend line slopes significantly differed among sample groups, showing a decline in radial growth in strongly buried sample groups. The control group showed no decline, while the slightly buried group only non-significantly declined in radial growth after storms.

Mean tree ring width series and ARSTAN chronologies among sample groups were compared using correlation analysis. Calculated correlation coefficients shown in Table 4 are significant at a = 0.05. The highest correlations were observed between samples taken from the same trees at different heights (strongly buried sample groups). To evaluate radial growth synchronicity GLK indices were calculated for sample groups (Table 4).

To analyze relations of radial growth with climate correlation analysis was performed, based on ARSTAN residual chronologies (Fig. 4). Correlations significant at p = 0.05 are shown in Table 5. In total 23 climatic factors showed significant correlations.

Significant correlation of late winter and early spring average temperatures with radial growth was common for all sample groups. The influence of February average temperature on growth was observed in all sample groups and showed the highest correlation coefficient values among average temperature factors. The same was observed for extreme (maximal and minimal) temperatures. The strongly buried at stem base sample group overall showed weaker relations to extreme temperatures. Precipitation sums showed little influence, as one significant correlation with June precipitation in the strongly buried at stem base sample group was found.

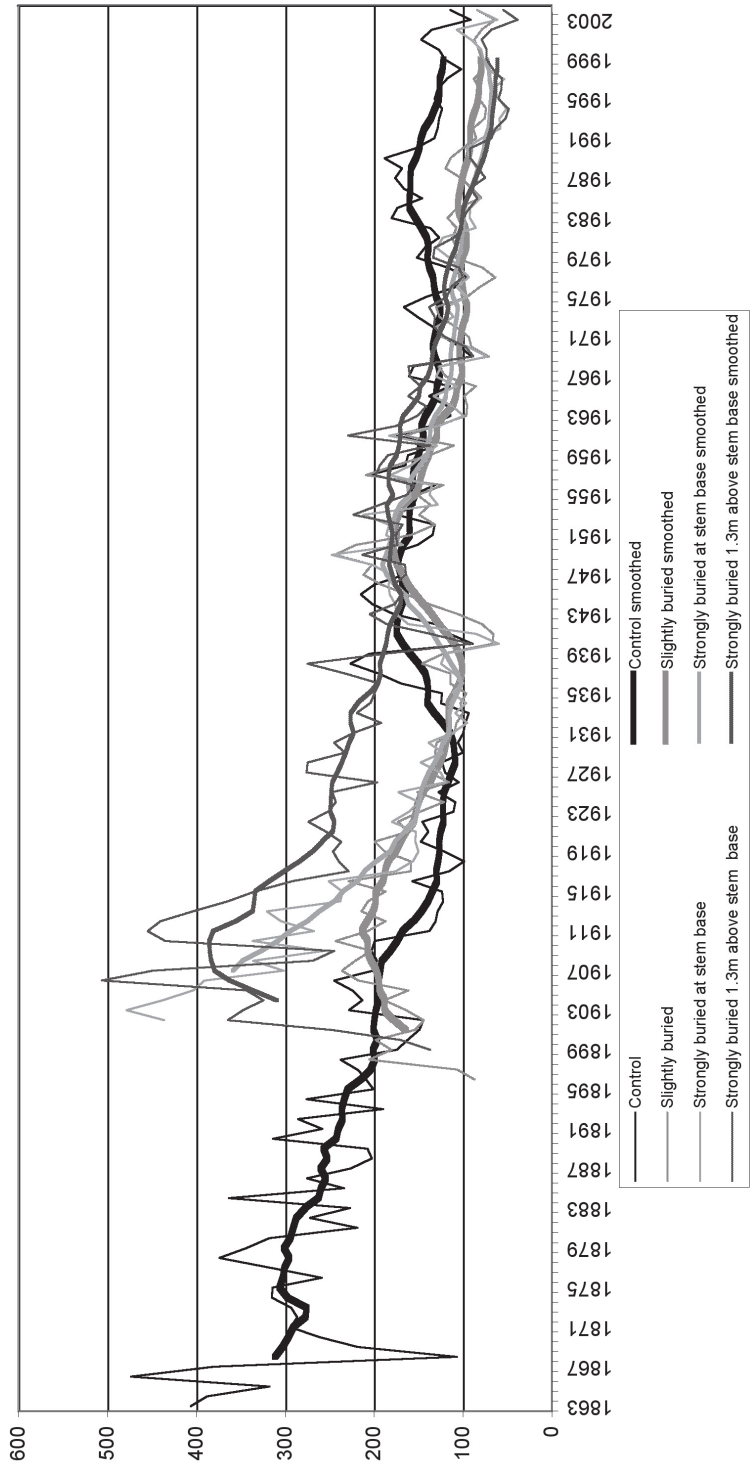

Fig. 2. Mean tree-ring width (0.01 mm) series of groups (smoothing – 11 years).

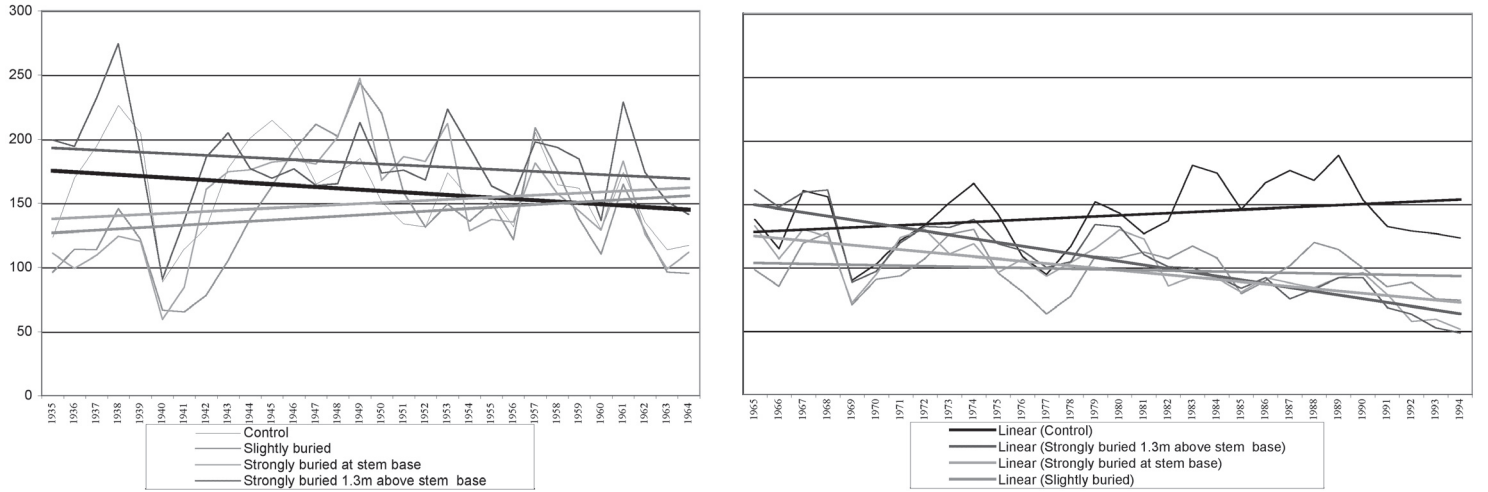

Fig. 3. Mean tree-ring widths (0.01 mm) and regression lines of sample groups for periods of 1935 - 1964 and 1965 - 1994.

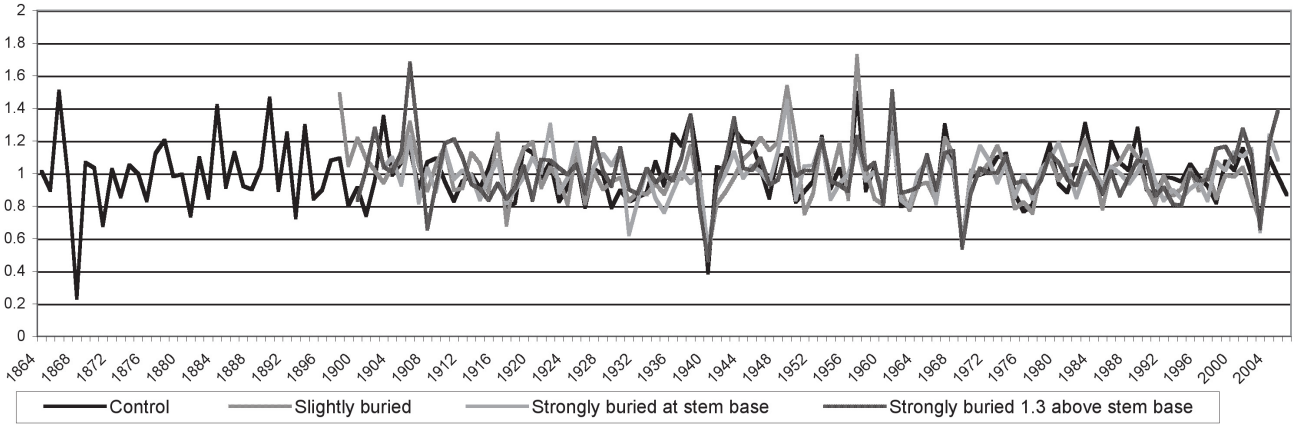

Fig. 4. Detrended (ARSTAN residual) chronologies for sample groups.

Table 3. Comparison of regression line slopes (p-values shown) among sample groups for periods 1935 - 1964 and 1965 - 1994 (before and after storms of 1967 - 1969)

	Slightly buried	Strongly buried at stem base	Strongly buried 1.3 m above stem base
Before storms of 1967 - 1969			
Control	0.0938	0.1024	0.8215
Slightly buried		0.9023	0.1378
Strongly buried at stem base			0.1378
After storms of 1967 - 1969			
Control	0.0605	0.0001	0.0000
Slightly buried		0.0067	0.0000
Strongly buried at stem base			0.0222

Table 4. Correlation coefficients (r) between sample groups for mean tree ring widths and ARSTAN chronologies, and Gleichläufigkeit (GLK) index values (mean tree ring widths compared)

Mean tree ring widths/ ARSTAN chronologies/ GLK	Slightly buried	Strongly buried at stem base	Strongly buried 1.3m above stem base
Control	0.50 / 0.66 / 0.77	0.54 / 0.57 / 0.81	0.44 / 0.55 / 0.74
Slightly buried		0.74 / 0.58 / 0.67	0.72 / 0.55 / 0.68
Strongly buried at stem base			0.89 / 0.64 / 0.83

Release/suppression analysis (Fig. 5, 6) shows that the periods of abrupt changes of radial growth (absolute relative value compared to previous 10-year period more than 25 %) differ strongly among sample groups. In general, growth suppression was more common than growth release in all sample groups. Thus, in all of the groups, 5-year periods where 20 - 40 % of trees show a 25 % or more long-term suppression of growth were quite common. Sample groups where the burial effect was low had some release events, but still suppression dominated (not shown). Strongly buried sample groups showed dominantly suppression (Fig. 6).

Discussion

The occurrence of missing tree-rings in coastal habitats (dune forest) under the influence of sand burial is related with a growth decline, when woody plants form very narrow (sometimes too narrow to identify) rings (Marin, Filion 1992). Heterogeneity of radial growth is related with environmental factor variation: topography, spatial distribution of trees with different wind influence (Maun 1998). Crossdating of control samples was less complicated (than in buried sample groups) as no burial effect was detected and abiotic factors were likely similar for trees in the sampling plot.

Growth of Scots pine in Cape Kolka area can be characterized as unstable, wavy. Growth patterns of the sample groups (Fig. 2) before storms of 1967-1969 were similar, as an aging effect was observed (growth decline with time) and fluctuation of tree-ring

Table 5. Statistically significant correlations (r) between sample group ARSTAN residual chronologies and climatic factors

		Control	Slightly buried	Strongly buried 1.3 m above stem base	Strongly buried at stem base
Average temperatures	Dec				0.19
	Jan	0.30	0.27	0.28	0.28
	Feb	0.43	0.37	0.45	0.34
	Mar	0.41	0.32	0.44	0.28
	Apr	0.27	0.24	0.35	0.33
	Jul				–0.17
Minimal temperatures	Sep			0.28	
	Dec			0.28	
	Jan	0.29	0.27	0.29	
	Feb	0.35	0.27	0.37	0.27
	Mar	0.38		0.39	
	Apr			0.34	0.28
	Winter	0.30	0.30	0.33	0.25
	Spring	0.39		0.40	
	Season	0.32	0.28	0.34	0.23
Maximal temperatures	Jan		0.26		
	Feb	0.24	0.31	0.35	0.33
	Mar		0.30	0.32	
	May	0.27	0.35		
	Autumn	–0.28			
	Winter		0.32		0.26
	Spring	0.26	0.33		
Precipitation sums	Jun				0.34

widths in a large scale was comparable. A growth decrease in all sample groups in 1941 was related with extremely low winter temperatures especially in January and February.

Wider tree-ring formation in the strongly buried sample groups at 1.3 m compared to 0.3 m above base could be explained by rapid growth in length followed by stem thickening (Schweingruber 1996). A decline of growth in buried trees after burial in storms of 1967-69 is suggested, as was also observed in other areas (Alestalo 1971; Marin, Filion 1992). For pines growing in places where burial was absent or minimal the tree-rings even showed increasing trends, maybe due to climate change (Fig. 3).

Correlation analysis and GLK values (Table 4) showed that the highest similarity between tree-ring series was for the strongly buried tree groups sampled at different heights. Thus the burial influences the whole stem radial growth, not only the buried parts. Dech and Maun (2006) conducted experimental burial on saplings of several tree species growing in dune habitats and concluded that Scots pine can not change biomass

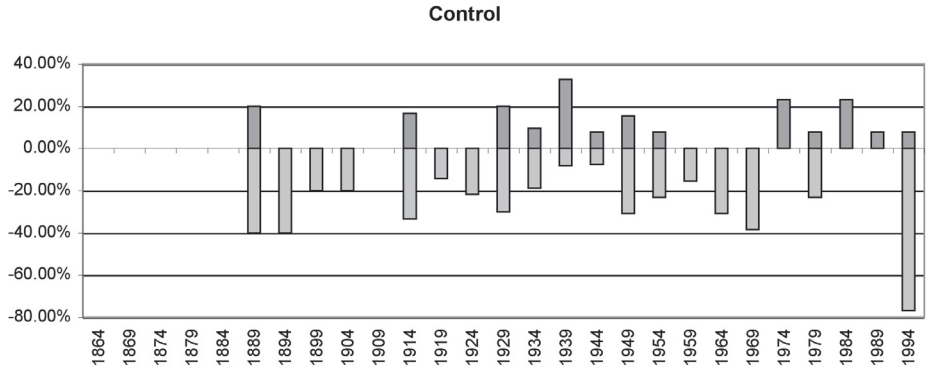

Fig. 5. Release/suppression (% of trees) of radial growth of control sample group.

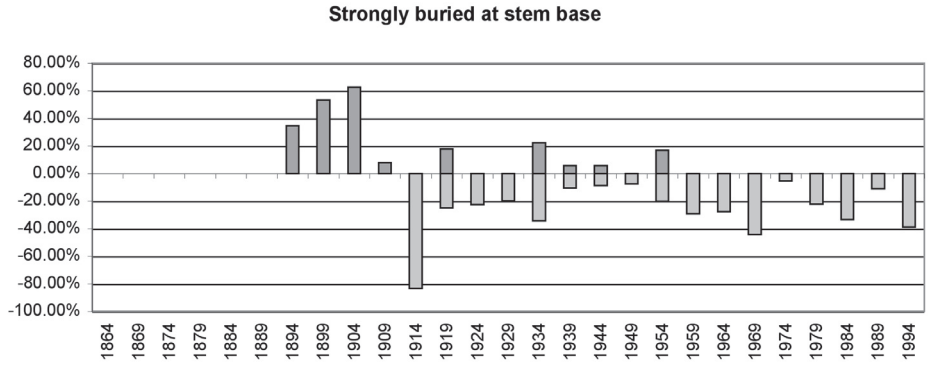

Fig. 6. Release/suppression (% of trees) of radial growth of group of strongly buried samples cored at base of stem.

allocation, thus buried parts grow at the same rates as unburied parts. Maun (1998) also suggested that burial influences the growth of the whole plant. The most differing radial growth patterns were between unburied and buried trees, which indicate the influence of burial.

Growth relations with climatic factors (Table 5) in all sample groups show the main characteristics found previously for Scots pine in Latvia on dry soils: positive correlations with winter and early spring average temperatures (Elferts 2007). The same relations with winter and spring temperatures were also observed in Poland (Sudetic mountains), for Scots pine growing on dry mountain slopes (Wilczynski, Skrzyszewski 2002). Trees with stems buried more than 0.6 m (strongly buried sample groups) show additional factors such as December, July and September temperatures and June precipitation. A relation with June precipitation is common for northwestern Latvia (Elferts 2007), which was observed only in the strongly buried group cored at stem base. We suggest that these signatures have remained from the period when growth could be considered as normal. However, the other groups did not show this relation. The observed negative effect of July temperature might occur via promotion of pathogenous organism activity, as soil temperature rises under burial conditions in July. Also higher soil temperatures in the buried part could

cause heat shock thus suppressing growth (Pichler, Oberhuber 2007).

Buried trees showed fewer relations with extreme temperatures (usually representing short periods of influence), which can be explained with sand burial reacting as a buffer softening extreme climatic expression (Maun 1998). Radial growth of strongly buried trees at stem base showed less and weaker relations compared to growth of strongly buried cored 1.3 m above stem base. Differences could be caused by expression of climatic signal under burial at various heights of stem: growth rates should remain the same in buried and unburied parts of stem (Dech, Maun 2006), but tree-ring widths might have slightly different ratios, thus effecting correlation.

Release/suppression analysis showed that in all groups, 5-year periods were common in which 20-40% of trees showed suppressed growth for at least 10 years. This suggests a generally harsh environment for the seacoast pines: wind damage, salt spray, and winter desiccation. The control sample group (Fig. 5) showed growth release and suppression during the entire reference period, but the occurrence of suppression was more common. Strong growth suppression in 1994 - 1999 was most likely caused by coastal erosion when a rather wide part of the coast was washed off (Eberhards 2003), thus changing growth conditions via salinity (salt drift from sea) and the influence of wind (Larcher 2003). Release in strongly buried sample group (Fig. 6) before 1910 can probably be explained by the young age of the trees. The strong suppression in the 1910 - 1920 in this group likely represents a growth decline after the rapid growth of saplings.

The effect of sampling height on ring width for pines buried by sand is minimal. There is rather high similarity (GLK, correlation coefficients) between strongly buried sample groups (Table 3), which agrees with Chin and Wang (2005) who found no significant differences of radial growth in samples taken at different heights above (0.3 m and 1.3 m) stem base from another coniferous tree species - white spruce *Picea glauca*.

In conclusion, radial growth in dune habitats especially under burial conditions is variable, and missing rings occur often. Growth patterns between buried and unburied trees and parts of trees are quite similar (according to GLK and correlation coefficients). The main relations with climatic factors (late winter and early spring temperatures) remain, but the reaction to extreme temperatures under burial is more moderate; precipitation in dune habitats at Kolka plays an insignificant role. The coastal environment has regular events causing suppression of pine growth, particularly severe storms.

Acknowledgements

The study was conducted as an MSc thesis at the Faculty of Biology at University of Latvia. Thanks are given to Brigita Javoiša and Zane Strikše for assistance in sampling, and Didzis Elferts for help with crossdating and ideas for data analysis.

References

Alestalo J. 1971. Dendrochronological interpretation of geomorphic processes. *Fennia* 105: 1–140.

Baker P.J., Bunyavejchewin S. 2006. Suppression, release and canopy recruitment in five species from a seasonal tropical forest in western Thailand. *J. Trop. Ecol.* 22: 521–529.

Biondi. F., Waikul K. 2004. DENDROCLIM2002: A C++ program for statistical calibration of climate signals in tree-ring chronologies. *Comput. Geosci.* 30: 303–311.

Chhin S., Wang G.G. 2005. The effect of sampling height on dendroclimatic analysis. *Dendrochronologia*

23: 47–55.
Cook E., Briffa K. 1990. Data analysis. In: Cook E.R., Kairiukstis L.A. (eds) *Methods of Dendrochgronology: Applications in the Environmental Sciences.* Kluwer Academic Publishers, Dordrecht, pp. 97–161.
Cook E.R., Krusic P.J. 2005. A tree-ring standardization program bases on detrending and autoregressive time series modeling with interactive graphics. Tree ring laboratory of Lamont Doherty Earth Observatory of Columbia University, Palisades, NY. 14 p.
Cournoyer L., Filion L. 1994. Variation in wood anatomy of white spruce in response to dune activity. *Arct. Alp. Res.* 26/4: 412–417.
De Raeve F. 1989. Sand dune vegetation and management dynamics. In: van der Meulen F. et al. (eds) *Perspectives in Coastal Dune Management*. Proceedings of the European Symposium Leiden, September 7-11, 1987, pp. 99–109.
Dech J.P, Maun M.A. 2006. Adventitious root production and plastic resource allocation to biomass determine burial tolerance in woody plants from Central Canadian coastal dunes. *Ann. Bot.* 98: 1095–1105.
den Ouden J., Sass-Klaassen U.G.W., Copini P. 2007. Dendromorphology – a new tool to study drift-sand dynamics. *Neth. J. Geosci.* 86: 355–363.
Eberhards G. 2003. *Latvian Sea-Coast.* University of Latvia, Rīga. 292 p. (in Latvian) /Latvijas jūras krasti/
Elferts D. 2007. Scots pine pointer-years in northwestern Latvia and their relationship with climatic factors. *Acta Univ. Latv.* 723: 163–170.
Esper J., Neuwirth B., Treydte K. 2001. A new parameter to evaluate temporal signal strenght of tree ring hronologies. *Dendrochronologia* 19: 93–102.
Fritts H. C. 2001. *Tree Ring and Climate.* The Blackbur Press, Candwell. 567 p.
Grissino-Meyer H.D. 2001. Evaluating crossdating accuracy: a manual and tutorial for the computer program COFECHA. *Tree-ring Res.* 57: 205–221.
Hartman J.R., Pirone T.P., Sall M.A. 2000. *Pirone's Tree Maintenence.* Oxford University Press, NY. 545 p.
Holmes. R.L., Adams. R.K., Fritts. H.C. 1986. Tree-ring chronologies of western North America: California, eastern Oregon and northern Great Basin, with procedures used in the chronology development work including user manuals for computer programs COFECHA and ARSTAN. University of Arizona, Laboratory of Tree-Ring Research, Tucson. Arizona. 111 p.
Jury W.A., Horton R. 2004. *Soil Physics.* John Wiley and Sons, Oxford. 384 p.
Kuuluvianen T., Jarvinen E., Hokkanent T.J., Rouvinen S., Heikkinen K. 1998. Structural heterogeneity and spatial autocorrelation in a natural mature *Pinus sylvestris* dominated forest. *Ecogrophy* 21: 159–174.
Larcher W. 2003. *Physiological Plant Ecology: Ecophysiology and Stress Physiology of Functional Groups*. Springer, Heidelberg. 513 p.
Lavigne M.B. 1996. Comparing stem respiration on growth of jack pine provenances from northern and southern locations. *Tree Physiol.* 16: 847-852.
Mancuso S., Marras A.M. 2003. Different pathways of the oxygen supply in the sapwood of young *Olea europaea* trees. *Planta* 216: 1028–1033.
Manugistics 1996. Statgraphics Plus: Advanced Regression. *Manugistics Inc*. 4: 1–28.
Marin P., Filion L. 1992. Recent dynamics of subarctic dunes as determined by tree-ring analysis of white spruce, Hudson Bay, Quebec. *Quaternary Res.* 38: 316–330.
Maun M.A. 1998. Adaptations of plants to burial in coastal sand dunes. *Can. J. Bot.* 76: 713–738.
Moreno-Casasola P. 1986. Sand movement as a factor in the distribution of plant communities in a coastal dune system. *Plant Ecol.* 65: 67–76.
Pichler P., Oberhuber W. 2007. Radial growth response of coniferous forest trees in an inner Alpine environment to heat-wave in 2003. *Forest Ecol. Manag.* 242: 688–699.
RinnTech. 2002. *LigoVision Scientifics: Quick reference*. Heidelberg. 10 p.

Schweingruber F.H. 1996. *Tree Rings and Environment: Dendroecology.* Swiss Federal Institute for Forest, Snow and Landscape Research, Berne. 609 pp.
Sokal R.R., Rohlf F.J. 1981. *Biometry: The Principles and Practice of Statistics in Biological Research*. 2nd ed. W.H. Freeman and Company, New York. 859 p.
Ulsts V. 1998. *Coastal Zone of the Baltic Sea*. Valsts ģeoloģijas dienests, Rīga. 96 p. (in Latvian) /Baltijas jūras krasta zona/
Wilczynski S., Skrzyszewski J. 2002. The climatic signal in tree-rings of Scots pine (*Pinus sylvestris* L.) from foot-hills of the Sudetic Mountains (southern Poland). *Forstw. Cbl.* 121: 15–24.
Wimmer R. 2002. Wood anatomical features in tree-rings as indicators of environmental change. *Dendrochronologia* 20: 21–36.

Apbēršanas ar smiltīm ietekme uz parastās priedes (*Pinus sylvestris* L.) radiālo augšanu jūras krasta kāpu mežā Kolkas raga apkārtnē Latvijā

Roberts Matisons*, Guntis Brūmelis

Botānikas un ekoloģijas katedra, Latvijas Universitātes Bioloģijas fakultāte, Kronvalda bulv. 4, Rīga LV-1586, Latvija
*Korespondējošais autors, E-pasts: robism@inbox.lv

Kopsavilkums

Parastā priede ir plaši izplatīta suga Latvijā un tai piemīt augsta stresa tolerance un spēja augt arī nabadzīgos biotopos. Tā ir dominējošā suga piekrastes kāpās. Kolkas raga apkārtnes kāpās noris smilšu pārplūde, kas ieputina pludmales tuvumā augošo priežu stumbrus. Uzskatāms, ka lielākā ieputināšana notiek spēcīgās vētrās, tādās kā bijušas 1967 - 1969 gados. Pētījuma mērķis ir novērtēt ieputināšanas smiltīs un klimatisko faktoru ietekmi uz priedes radiālo augšanu. Pētījumā ievāca paraugus no priedēm, kas auga pie pludmales un kuru stumbri bija ieputināti dažādā dziļumā. Gadskārtu platumu rindas šķērsdatēja un izveidoja detrendētas hronoloģijas. Lai noteiktu saistības ar klimatiskajiem faktoriem, veica korelācijas analīzi. Ieputināšanas ietekmes novērtējumam veica augšanas uzlabošanās un kritumu (release/suppression) analīzi. Ieputināšana smiltīs ietekmēja radiālo augšanu gan ieputinātajās, gan neieputinātajās stumbru daļās. Spēcīgas ieputināšanas gadījumā (dziļāk par 0.6 m) iztrūkstošo gadskārtu skaits palielinājās. Kopš 1967. - 1969. gada vētrām radiālā augšana ieputinātajām priedēm samazinājās, būtiski augšanas uzlabojumi netika konstatēti. Neieputinātie koki arī uzrādīja biežāku augšanas samazināšanos it īpaši pēdējo četrdesmit gadu laikā, kas iespējams saistīts ar Kolkas piekrastes eroziju un abiotisko faktoru maiņu. Ziemas beigu un pavasara sākuma temperatūras parādīja nozīmīgākās saistības ar neieputināto koku radiālo augšanu, ieputinātajos kokos (stumbru daļās) novērotas vājākas saistības ar ekstrēmajām temperatūrām. Nokrišņiem netika konstatēta būtiska ietekme viegli pieejamā mitruma un ūdens caurlaidīgās augsnes dēļ.

Acta Universitatis Latviensis, 2008, Vol. 745, Biology, pp. 145–154

Specificity of packaging mRNAs in bacteriophage GA virus-like particles in yeast *Saccharomyces cerevisiae*

Jānis Rūmnieks*, Jānis Freivalds, Indulis Cielēns, Regīna Renhofa

Latvian Biomedical Research and Study Centre, Ratsupites 1, Riga LV-1067, Latvia

*Corresponding author, E-mail: j.rumnieks@biomed.lu.lv

Abstract

Heterologous expression of RNA bacteriophage coat protein genes leads to formation of virus-like particles that encapsulate intracellular RNA. Here we packaged specific mRNA molecules into bacteriophage GA capsids *in vivo*. For specificity we employed a GA operator – a 21-nucleotide-long RNA sequence that folds into a stem-loop structure and can specifically bind to the coat protein of the phage. Several plasmids were constructed for expression in *Saccharomyces cerevisiae*, which directed synthesis of both the GA coat protein and the mRNA to be packaged. As models for packaging, three different mRNAs (GA coat protein, ENA-78 and GFP) were used, each constructed in two versions that differed by the presence of the GA operator within their sequence. RNA content analysis of the produced capsids in gel electrophoresis revealed the existence of RNAs of predicted lengths. The presence of the packaged mRNAs in the capsids was further verified by reverse transcription PCR. However, the operator had rather small effect on the specificity of capsid contents, since the mRNA of GA coat protein was also invariably detected inside the capsids.

Key words: bacteriophage GA, coat protein, mRNA, packaging, virus-like particles.

Introduction

RNA bacteriophages belonging to the Leviviridae family are small viruses that infect several Gram-negative bacteria genera. RNA phages infecting *Escherichia coli* have been divided into four groups denoted I to IV (Fiers 1979). Groups I and II are related to each other and belong to the Levivirus genus; phages from groups III and IV are also closely similar and assigned to the Allolevivirus genus. The best-known representatives are phages MS2 from group I, GA from group II, Qβ from group III and SP from group IV.

The genomic RNA of leviviruses is an approximately 3500-nucleotides-long single-stranded RNA molecule that codes for only four proteins: coat protein, lysis protein, maturation protein and a subunit of the viral replicase – an RNA-dependent RNA polymerase (for a review, see van Duin 1988). The viral genome is enclosed in a $T = 3$ quasi-equivalent icosahedral capsid with diameter about 28 nm, which consists of 180 coat protein molecules. Each virion also contains a single copy of the maturation protein, which is essential for the attachment of the phage to bacterial F-pili and successful infection.

Besides its structural role, the coat protein also functions as a specific RNA binding protein that recognizes a stem-loop structure at the very beginning of the replicase gene (Bernardi, Spahr 1973). The stem-loop is often designated a translational operator, as its binding to the coat protein effectively represses the synthesis of replicase. The operator is

also believed to be a packaging signal that initiates the assembly of the capsid and thus ensures recognition and selective encapsidation of the phage RNA (Hohn 1969a; Beckett, Uhlenbeck 1988). Although the coat protein can assemble into phage-like particles *in vitro* when mixed with the genomic RNA of the phage or unspecific RNAs of different lengths (Hohn 1969b), the presence of the operator lowers the concentration requirements for capsid assembly (Beckett et al. 1988).

The coat protein genes from numerous RNA phages have been reverse-transcribed, cloned and expressed in *Escherichia coli*, leading to assembly of virus-like particles (VLPs) without the need for any other viral components (Kastelein et al. 1983; Kozlovskaya et al. 1986; Peabody 1990; Kozlovska et al. 1993; Lim et al. 1994). Such recombinant VLPs encapsulate intracellular RNA (Pickett, Peabody 1993), but are morphologically and immunologically indistinguishable from native phages.

There has also been some interest to produce VLPs *in vivo* with a specific nucleic acid content. For this, a coexpression system that directs simultaneous production of both the coat protein and the RNA to be packaged is generally utilized. For specificity, the target RNA contains the translational operator of the replicase gene. In this way, recombinant MS2 capsids containing *LacZ* RNA were produced in *E. coli* (Pickett, Peabody 1993). A similar system was recently employed also in yeast *Saccharomyces cerevisiae* where the mRNA of human growth hormone was packaged into MS2 VLPs (Legendre, Fastrez 2005), demonstrating the potential of RNA phage capsids as carriers and possible delivery vehicles for therapeutic mRNAs. Others have made use of the remarkable stability of RNA phage capsids and engineered VLPs as containers for ribonuclease-protected RNA molecules of choice. As potential controls and standards for RT-PCR detection of RNA viruses, MS2 capsids have been produced that contain RNAs with a consensus sequence from HIV-1 *gag* gene (Pasloske et al. 1998) or, similarly, a longer RNA with sequences combined from hepatitis C virus, SARS coronavirus and avian influenza virus genomes (Wei et al. 2008).

Up to now, all efforts to encapsulate heterologous RNAs into RNA phage capsids *in vivo* have been directed towards phage MS2, a type species of group I. Since the details of molecular interactions between the coat protein and RNA operator vary among different RNA phages, the results obtained with one phage cannot be extrapolated to others. We investigated whether specific RNAs can be encapsulated *in vivo* using the coat protein from phage GA, a characteristic representative of group II.

Materials and methods

Construction of plasmids

The construction of pESC-GA has been described elsewhere (Freivalds et al. 2008). pESC-GAop was constructed by amplifying a fragment from pGACPop with primers GA_fwd and GAop_rev3 (for nucleotide sequences of primers, see Table 1), which was cloned into *Bam*HI/*Hind*III-digested pESC-URA vector (Stratagene). Note: pGACPop is an *E. coli* expression plasmid that contains the GA operator sequence downstream the GA coat protein gene, with nucleotide sequence corresponding to primers GAop_rev1, GAop_rev2 and GAop_rev3. Vectors for the two-gene coexpression plasmids were prepared by digesting pESC-GA with *Not*I and *Bgl*II (pESC-GAv1) or with *Eco*RI and *Not*I (pESC-GAv2). A short double-stranded DNA fragment containing GA operator sequence and

Table 1. Oligonucleotides used for the construction of plasmids. Restriction sites for cloning are underlined and the initiation and termination codons of genes are shown in bold

Oligonucleotide	Nucleotide sequence (5' to 3')
ENA_fwd	TCGAATTC**ATG**GCTGGTCCTGCCGC
ENA_rev	ATGCGGCCGC**TTA**GTTTTCCTTGTTTCCA
GA_fwd	CAGGATCC**ATG**GCAACTTTACGCAGTTTCGT
GA_rev	TGAAGC**TTA**CGCGTAGAAGCCACTCTG
GAop_rev1	ACATAGGTTTTCCTTATGTTTTGC**TTA**CGCGTAGAAGCCACTCTG
GAop_rev2	CATGATCAATTGACCTCCTTATCGGAACATAGGTTTTCCTTATGTT
GAop_rev3	AGAAGCTTCATGATCAATTGACCTCC
GAop1	GGCCGCAAAACATAAGGAAAACCTATGTTCCA
GAop2	GATCTGGAACATAGGTTTTCCTTATGTTTTGC
GFP_fwd	TCGAATTCC**ATG**GTGAGCAAGGGCGAGGA
GFP_rev	GAGCGGCCGCAAGC**TTA**CTTGTACAGCTCGTCCAT

*Not*I and *Bgl*II sticky ends was obtained by hybridizing GAop1 and GAop2 and ligated into pESC-GAv1. The resulting plasmid was digested with *Eco*RI and *Not*I, thus producing pESC-GAv3. A DNA fragment containing the coding sequence of ENA-78 flanked by *Eco*RI and *Not*I restriction sites was amplified from plasmid pTRC-ENA (I. Cielēns, unpublished data) using primers ENA_fwd and ENA_rev and cloned into pESC-GAv2 and pESC-GAv3, resulting in plasmids pESC-GA-ENA and pESC-GA-ENAop, respectively. In a similar manner, the sequence coding for GFP was amplified using primers GFP_fwd and GFP_rev from plasmid pA62 (kindly provided by A. Strods), which contains the gene for CXCR4-eGFP fusion protein (unpublished data). The resulting fragment was cloned into pESC-GAv2 and pESC-GAv3, thus producing plasmids pESC-GA-GFP and pESC-GA-GFPop, respectively.

Production and purification of GA VLPs

Yeast transformants were obtained, cultivated and the recombinant GA capsids purified essentially as described (Freivalds et al. 2008), with an additional last purification step of ion-exchange chromatography. After gel-filtration, the fractions containing GA VLPs in TEN buffer (20 mM Tris-HCl, pH 7.8, 5 mM EDTA, 150 mM NaCl) were loaded on a DEAE-Sephadex A50 column (V = 3.5 mL, h = 5 cm) and washed with four column volumes of TEN buffer. GA capsids were eluted in the void volume while nucleic acid contaminants remained bound to the column and were subsequently eluted with TEN buffer supplemented with 1 M NaCl. Fractions containing GA VLPs were pooled and stored frozen at –20 °C until use.

RNA extraction

An equal volume of Tris-HCl buffered phenol (pH 6.7) was added to a preparation of purified capsids, vortexed for 30 s and centrifuged at 10 000 g for 5 min. The aqueous phase was collected and repeatedly phenol-extracted until no protein band could be observed at the phase interface. The aqueous phase was then washed three times with diethyl ether and the RNA concentrated by ethanol precipitation. Finally, the RNA was dissolved in a small

volume of sterile water and aliquots stored frozen at –20 °C until use.

RNA electrophoresis

RNA samples were thawed on ice. After adding of 2X RNA loading dye (Fermentas) samples were heated at 70 °C for 10 min, cooled 2 min on ice and immediately loaded on a denaturing urea-polyacrylamide gel (8 M urea, 4 % polyacrylamide, 1X TBE). After electrophoresis, the gel was stained with ethidium bromide and RNA detected by fluorescence in UV light.

Reverse transcription PCR

Synthesis of the first strand cDNA was conducted by the RevertAid kit (Fermentas) according to manufacturer's protocol and using 1.2 μg of the extracted RNA as template and either 20 pmol of sequence-specific primer (GA_rev for all RNA samples and ENA_rev for RNA extracted from GA-ENA and GA-ENAop capsids) or 90 pmol of oligo$(dT)_{18}$ for RNA preparations from GA-GFP and GA-GFPop. The reason for using oligo$(dT)_{18}$ instead of GFP_rev was the apparent formation of a stable secondary structure of the latter, resulting in no detectable reaction products at 37 °C (data not shown). After reverse transcription, 2 μL of the mixture was used as a template for second strand cDNA synthesis, using primers GA_fwd / GA_rev, ENA_fwd / ENA_rev and GFP_fwd / GFP_rev for the amplification of GA coat protein, ENA-78 and green fluorescent protein cDNAs, respectively.

Results

Construction of the in vivo *packaging system*

To attempt to produce GA VLPs *in vivo* with a specified RNA content, we chose the expression system in yeast *Saccharomyces cerevisiae*. Although the levels of heterologous protein expression in yeast are generally lower compared to those attainable in *E. coli*, the *S. cerevisiae* system is beneficial in a number of aspects. Yeast provides a source of eukaryotic, 5'-capped and 3'-poly(A)-tailed mRNAs, which is attractive considering our further goals to test GA VLPs as RNA packaging and delivery tools to mammalian cells. Also, the absence of bacterial endotoxins in yeast preparations simplifies the capsid purification procedures for this purpose. As Legendre and Fastrez (2005) demonstrated with MS2 coat protein that such system is functional in *S. cerevisiae*, we used a similar approach for the coat protein of phage GA.

To construct the *in vivo* packaging system, we used the commercial pESC-URA plasmid, which contains divergent galactose-inducible promoters GAL1/GAL10. We have previously described the construction of pESC-GA, a pESC-URA-derived plasmid that contains the wild-type GA coat protein gene under the control of GAL1 and directs production of GA VLPs in *S. cerevisiae* cells (Freivalds et al. 2008). In order to determine the effect of GA operator on the RNA content of the VLPs, we constructed in an analogous way a plasmid pESC-GAop, which contains the GA operator sequence downstream the coat protein gene.

We proceeded to modify pESC-GA to allow the encapsidation of heterologous mRNAs of choice into GA VLPs. The system was designed in a way that any gene of interest can be inserted under the GAL10 promoter in two vectors using the same cloning sites, in which one vector (pESC-GAv3) contains the GA operator just downstream the inserted

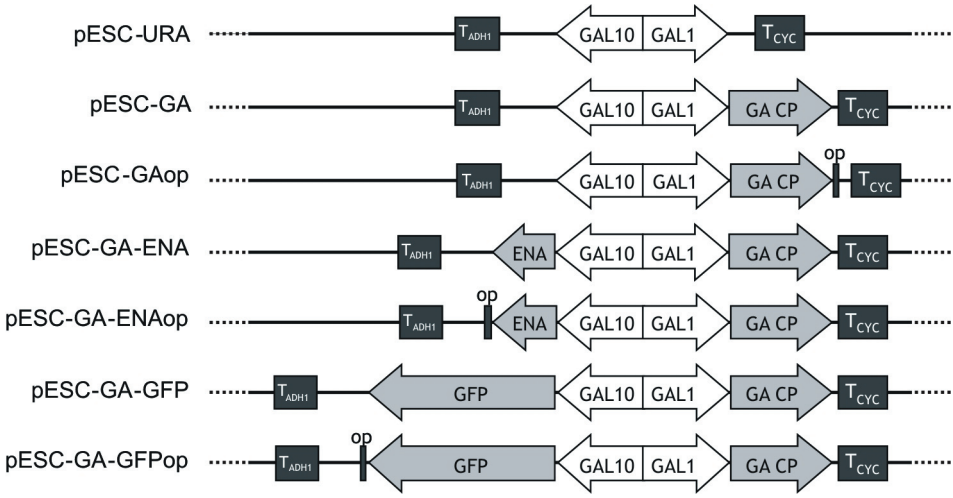

Fig. 1. Constructed plasmids for expression in S.cerevisiae. A schematic representation of the developed constructions. Genes coding for the GA coat protein (GA CP), epithelial neutrophil-activating peptide 78 (ENA) and green fluorescent protein (GFP) are indicated as well as promoters (GAL1 and GAL10), transcription terminators (T_{ADH1} and T_{CYC}) and GA operator (op).

gene, while the other (pESC-GAv2) does not and serves as a control to examine the encapsidation specificity that the operator provides. We used in the above-mentioned way two different genes to test the system: one coding for the epithelial neutrophil-activating peptide 78 (ENA-78), resulting in plasmids pESC-GA-ENA and pESC-GA-ENAop, and the other for enhanced green fluorescent protein (eGFP) with plasmids pESC-GA-GFP and pESC-GA-GFPop, respectively (Fig. 1).

Purification of GA VLPs

The purification of recombinant GA capsids from *S. cerevisiae* cells followed directly the procedures described by Freivalds et al. (2008). The fractions containing GA VLPs were remarkably pure from protein contaminants after the last step. However, electrophoretic analysis in an ethidium bromide-stained agarose gel revealed that the preparation also contains a substantial amount of free RNA that was not incorporated into capsids (data not shown). In order to adequately analyze the RNA content of the particles, removal of all other nucleic acids from the sample is of key importance. The RNA contaminants were effectively separated by introducing an additional purification step of ion-exchange chromatography on a DEAE-Sephadex A50 column. This ensured that the RNA subsequently extracted from the preparation originated only from the interior space of GA VLPs.

For convenience, the capsids produced from pESC-GA, pESC-GAop, pESC-GA-ENA, pESC-GA-ENAop, pESC-GA-GFP and pESC-GA-GFPop will further be denoted as GA, GAop, GA-ENA, GA-ENAop, GA-GFP and GA-GFPop, respectively.

Analysis of capsid RNA contents

The RNA was phenol-extracted from purified GA capsids and subjected to electrophoresis

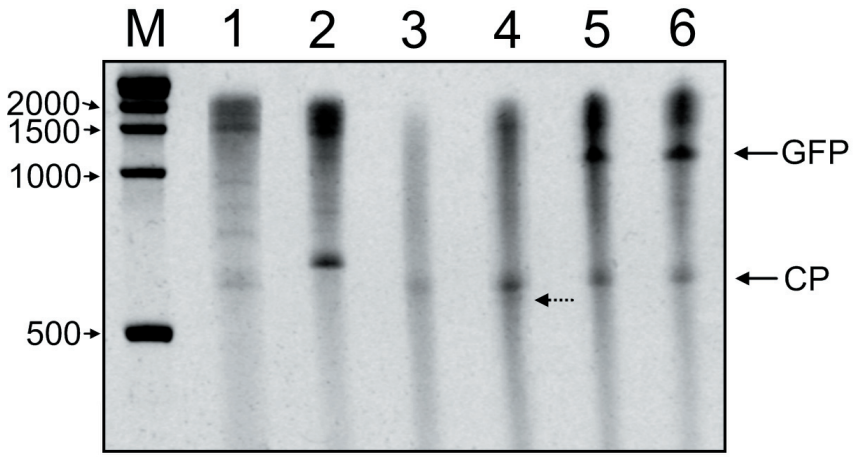

Fig. 2. Analysis of capsid RNA contents in a denaturing polyacrylamide gel. 1 μg of RNA extracted from GA (lane 1), GAop (lane 2), GA-ENA (lane 3), GA-ENAop (lane 4), GA-GFP (lane 5) or GA-GFPop (lane 6) capsids were loaded on a 4% urea-polyacrylamide gel. The positions of the GA coat protein (CP) and green fluorescent protein (GFP) mRNAs are indicated by arrows; the dotted arrow shows the supposed location of the mRNA of ENA-78. M, RNA ladder.

in a denaturing polyacrylamide gel. The RNA preparations in all cases were not homogeneous (Fig. 2). A distinct band corresponding to RNA somewhat longer than 500 nucleotides could be observed in all cases except in the preparation from GAop (lane 2), where a slightly longer RNA species was detected. Since in pESC-GAop the additional sequence with GA operator adds approximately 50 nucleotides to the 3'-untranslated region of the RNA transcript (see Table 2), this strongly suggests that the respective bands in the gel correspond to the mRNA of GA coat protein. In the case of GA-GFP and GA-GFPop (lanes 5 and 6), an additional prominent band of about 1000 nucleotides was detected, which apparently was formed by the mRNA of GFP. In the RNA preparation from GA-ENAop, a faint band could be observed just below that of the coat protein mRNA (lane 4). Further analysis in a more concentrated gel confirmed the existence of an RNA species migrating slightly faster than the mRNA of GA coat protein in preparations from GA-ENAop and also from GA-ENA, but not in those from other VLPs (data not shown). Although the sequences coding for ENA-78 and GA coat protein differ by approximately 150 nucleotides, the difference fell to about 50 nucleotides in mRNA due to unequal lengths of the untranslated regions of transcripts from GAL1 and GAL10 (Table 2). This explains the close migration and poor separation of both mRNAs and suggests that the faster-migrating band corresponds to the mRNA of ENA-78.

In order to prove unambiguously that the produced GA VLPs have packaged the expected mRNAs, the extracted RNA was analyzed by reverse transcription PCR (RT-PCR). The results (Fig. 3) showed that the mRNA of ENA-78 is present in both GA-ENA and GA-ENAop capsids (lanes 4 and 6). The mRNA of the green fluorescent protein was correspondingly present in GA-GFP and GA-GFPop capsids (lanes 8 and 10). The RT-PCR confirmed that the mRNA of the GA coat protein is present not only in GAop capsids (lane 2), but also in all other GA VLPs, regardless of the presence or absence of the operator within other mRNAs in the cell (lanes 1, 2, 3, 5, 7 and 9).

Table 2. Calculated lengths of the mRNAs packaged into the capsids. The mRNA transcription start points from GAL1 and GAL10 were determined after Johnston and Davis (1984) and the polyadenylation sites (which therefore mark the end of the 3' untranslated region) of CYC1 and ADH1 after Heidmann et al. (1992). The calculations do not include the 3' poly(A) tail, the length of which was not known but which generally spans 50-90 adenine residues in *S. cerevisiae* (Brown, Sachs 1998)

mRNA	Length of the sequence (nucleotides)			
	5'-untranslated	Protein-coding	3'-untranslated	Total
GA	66	393	126	585
GAop	66	393	178	637
ENA	12	240	280	532
ENAop	12	240	270	522
GFP	13	720	284	1017
GFPop	13	720	274	1007

Discussion

We demonstrated that it is possible to produce recombinant GA capsids *in vivo* that contain heterologous RNAs of choice. We developed a system in *S. cerevisiae* that provides a simple way to encapsulate any desired RNA sequence in GA VLPs and succeeded in packaging different model mRNAs into the particles. However, the GA operator failed to provide high encapsidation specificity of the target RNAs. This was clearly demonstrated by the incorporation of GA coat protein in mRNAs in the VLPs even in situations when other mRNAs containing the GA operator were present in the cell at the time of capsid assembly.

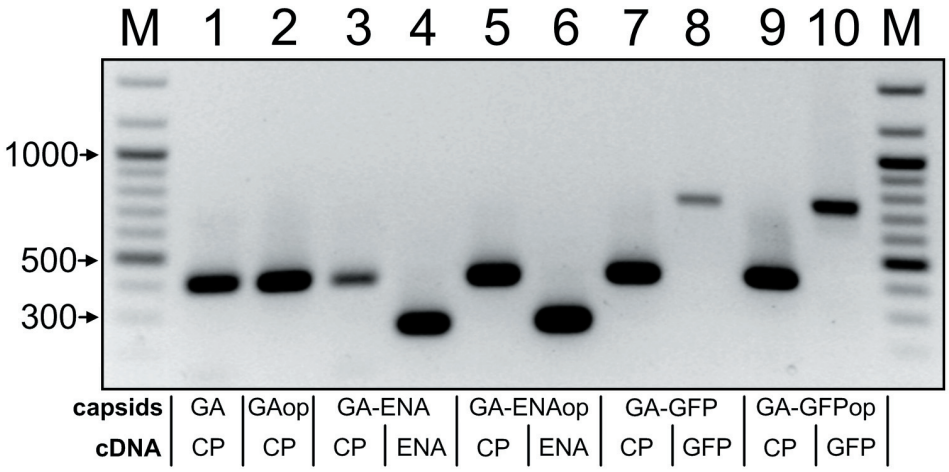

Fig. 3. Analysis of capsid RNA contents by RT-PCR. RNA was extracted from each type of the produced capsids and assayed for the presence of particular mRNAs, as indicated below. CP, cDNA of the GA coat protein; ENA, cDNA of the epithelial neutrophil-activating peptide 78; GFP, cDNA of the green fluorescent protein; M, DNA ladder.

The RNA binding properties of MS2 and GA coat proteins are slightly different. The crystal structure of the MS2 coat protein and RNA operator complex indicated that the specificity of the interaction is governed by three bases in the operator, which make direct contacts with the protein (Valegård et al. 1994). In GA this number is reduced to two, and the requirements for specific nucleotides at certain positions are also higher for MS2 than GA. MS2 coat protein only weakly binds to the GA operator, whereas GA coat protein has a similar affinity for both GA and MS2 operators (Gott et al. 1991). Consequently, GA coat protein can bind equally well to a larger pool of different RNA sequences, and the lower specificity facilitates the competition of non-operator sequences for association with the coat protein and subsequent encapsidation into the particles.

The ratio of coat protein and RNA in the cell is also important for the specificity of packaging. In a phage-infected cell, the coat protein concentration is initially low and increases gradually (Nathans et al. 1969). The high affinity of the RNA operator for the coat protein ensures specific packaging of the viral genome before the coat protein concentration reaches levels at which unspecific binding to intracellular RNA can occur (Beckett et al. 1988). The *in vivo* packaging experiments with *LacZ* mRNA showed that the specificity is indeed considerably higher at high *LacZ* and low coat protein concentrations (Pickett, Peabody 1993). The divergent GAL1/GAL10 promoters used in our system direct the production of similar levels of mRNA (Hadfield et al. 1993). In the case of MS2, this was apparently sufficient to provide a rather high specificity of packaging (Legendre, Fastrez 2005). However, to achieve high packaging specificity with GA, a higher proportion of RNA over coat protein is probably required.

For the ultimate goal to develop GA VLPs as nucleic acid delivery vehicles to eukaryotic cells, further modifications of the capsid are clearly required, which would allow to address the particles to particular types of cells. This problem might be potentially solved by chemically coupling a cell-specific peptide ligand to the surface of the capsid (Storni et al. 2004). Alternatively, chimeric RNA phage capsids can be produced by genetically fusing a foreign amino acid sequence to the coat protein (Mastico et al. 1993; Heal et al. 1999; Voronkova et al. 2002). The *in vivo* packaging system could then be used with modified coat proteins to produce chimeric capsids that contain therapeutic mRNAs or other kinds of RNA-based drugs, like ribozymes and antisense RNAs. Although the relatively low specificity of the GA coat protein-operator interaction renders the *in vivo* RNA packaging system in GA VLPs less advantageous compared to that of MS2, optimizations like adjustment of coat protein and RNA levels in the cell, the use of GA coat protein mutants that bind the operator stronger, similarly to those that are known for MS2 (Lim, Peabody 1994), and possibly other measures might significantly enhance the RNA encapsidation specificity into GA capsids in the future. Eventually, VLPs loaded with therapeutic RNAs and equipped with ligands on their surface may become powerful tools for cell-specific delivery of nucleic acid-based drugs.

Acknowledgements

We wish to thank Dr. Andris Kazāks for his support and interest in the project and Ināra Akopjana for technical assistance. This work was supported by Latvian National Research Program 07-VP-2.10.

References

Beckett D., Uhlenbeck, O.C. 1988. Ribonucleoprotein complexes of R17 coat protein and a translational operator analog. *J. Mol. Biol.* 204: 927–938.

Beckett D., Wu H.N., Uhlenbeck O.C. 1988. Roles of operator and non-operator RNA sequences in bacteriophage R17 capsid assembly. *J. Mol. Biol.* 204: 939–947.

Bernardi A., Spahr, P.F. 1973. Nucleotide sequence at the binding site for coat protein on RNA of bacteriophage R17. *Proc. Natl. Acad. Sci. USA* 69: 3033–3037.

Brown C.E., Sachs A.B. 1998. PolyA tail length control in *Saccharomyces cerevisiae* occurs by message-specific deadenylation. *Mol. Cell Biol.* 18: 6548–6559.

Fiers W. 1979. Structure and function of RNA bacteriophages. In: Fraenkel-Conrat H., Wagner R.R. (eds) *Comprehensive Virology*, vol. 13. Plenum Publishing Corporation, New York, pp. 69–204.

Freivalds J., Rūmnieks J., Ose V., Renhofa R., Kazāks A. 2008. High-level expression and purification of bacteriophage GA virus-like particles from yeast *Saccharomyces cerevisiae* and *Pichia pastoris*. *Acta Univ. Latv.* 745: 75–85.

Gott J.M., Wilhelm L.J., Uhlenbeck O.C. 1991. RNA binding properties of the coat protein from bacteriophage GA. *Nucleic Acids Res.* 19: 6499–6503.

Hadfield C., Raina K.K., Shashi-Menon K., Mount R.C. 1993. The expression and performance of cloned genes in yeasts. *Mycol. Res.* 97: 897–944.

Heal K.G., Hill H.R., Stockley P.G., Hollingdale M.R., Taylor-Robinson A.W. 1999. Expression and immunogenicity of a liver stage malaria epitope presented as a foreign peptide on the surface of RNA-free MS2 bacteriophage capsids. *Vaccine* 18: 251–258.

Heidmann S., Obermaier B., Vogel K., Domdey H. 1992. Identification of pre-mRNA polyadenylation sites in *Saccharomyces cerevisiae*. *Mol. Cell Biol.* 12: 4215–4229.

Hohn T. 1969a. Studies on a possible precursor in the self-assembly of bacteriophage fr. *Eur. J. Biochem.* 8: 552–556.

Hohn T. 1969b. Role of RNA in the assembly of bacteriophage fr. *J. Mol. Biol.* 43: 191–200.

Johnston M., Davis R.W. 1984. Sequences that regulate the divergent GAL1-GAL10 promoter in *Saccharomyces cerevisiae*. *Mol. Cell Biol.* 4: 1440–1448.

Kastelein R.A., Berkhout B., Overbeek G.P., van Duin J. 1983. Effect of the sequences upstream from the ribosome-binding site on the yield of protein from the cloned gene for phage MS2 coat protein. *Gene* 23: 245–254.

Kozlovska T.M., Cielens I., Dreilina D., Dislers A., Baumanis V., Ose V., Pumpens, P. 1993. Recombinant RNA phage Qβ capsid particles synthesized and self-assembled in *Escherichia coli*. *Gene* 137: 133–137.

Kozlovskaya T.M., Pumpen P.P., Dreilina D.E., Tsimanis A.J., Ose V.P., Tsibinogin V.P., Gren E.J. 1986. Formation of capsid-like structures as a result of expression of the cloned gene of the envelope protein of the RNA-containing bacteriophage fr. *Dokl. Akad. Nauk. SSSR* 28: 452–455. (in Russian)

Legendre D., Fastrez J. 2005. Production in *Saccharomyces cerevisiae* of MS2 virus-like particles packaging functional heterologous mRNAs. *J. Biotechnol.* 117: 183–194.

Lim F., Peabody D.S. 1994. Mutations that increase the affinity of a translational repressor for RNA. *Nucleic Acids Res.* 22: 3748–3752.

Lim F., Spingola M., Peabody D. S. 1994. Altering the RNA binding specificity of a translational repressor. *J. Biol. Chem.* 269: 9006–9010.

Mastico R.A., Talbot S.J., Stockley P.G. 1993. Multiple presentation of foreign peptides on the surface of an RNA-free spherical bacteriophage capsid. *J. Gen. Virol.* 74: 541–548.

Nathans D., Oeschger M.P., Polmar S.K., Eggen K. 1969. Regulation of protein synthesis directed by coliphage MS2 RNA. I. Phage protein and RNA synthesis in cells infected with suppressible mutants. *J. Mol. Biol.* 39: 279–292.

Pasloske B.L., Walkerpeach C.R., Obermoeller R.D., Winkler M., DuBois D.B. 1998. Armored RNA

technology for production of ribonuclease-resistant viral RNA controls and standards. *J. Clin. Microbiol.* 36: 3590–3594.
Peabody D.S. 1990. Translational repression by bacteriophage MS2 coat protein expressed from a plasmid. A system for genetic analysis of a protein-RNA interaction. *J. Biol. Chem.* 265: 5684–5689.
Pickett G.G., Peabody D.S. 1993. Encapsidation of heterologous RNAs by bacteriophage MS2 coat protein. *Nucleic Acids Res.* 21: 4621–4626.
Storni T., Ruedl C., Schwarz K., Schwendener R.A., Renner W.A., Bachmann M.F. 2004. Nonmethylated CG motifs packaged into virus-like particles induce protective cytotoxic T cell responses in the absence of systemic side effects. *J. Immunol.* 172: 1777–1785.
Valegård K., Murray J.B., Stockley P.G., Stonehouse N. J., Liljas L. 1994. Crystal structure of an RNA bacteriophage coat protein-operator complex. *Nature* 371: 623–626.
van Duin J. 1988. Single-stranded RNA bacteriophages. In: Calendar R. (ed) *The Bacteriophages*, vol. 1. Plenum Press, New York, pp. 117–167.
Voronkova T., Grosch A., Kazaks A., Ose V., Skrastina D., Sasnauskas K., Jandrig B., Arnold W., Scherneck S., Pumpens P., Ulrich R. 2002. Chimeric bacteriophage fr virus-like particles harboring the immunodominant C-terminal region of hamster polyomavirus VP1 induce a strong VP1-specific antibody response in rabbits and mice. *Viral Immunol.* 15: 627–643
Wei Y., Yang C., Wei B., Huang J., Wang L., Meng S., Zhang R., Li J. 2008. Ribonuclease-resistant virus-like particles containing long chimeric RNA sequences produced by a two-plasmid coexpression system. *J. Clin. Microbiol.* 46: 1734–1740.

mRNS iepakošanas specifiskums bakteriofāga GA vīrusveidīgajās daļiņās raugā *Saccharomyces cerevisiae*

Jānis Rūmnieks*, Jānis Freivalds, Indulis Cielēns, Regīna Renhofa

Latvijas Biomedicīnas pētījumu un studiju centrs, Rātsupītes 1, Rīga LV-1067, Latvija
*Korespondējošais autors, E-pasts: j.rumnieks@biomed.lu.lv

Kopsavilkums

RNS bakteriofāgu apvalka proteīna gēnu heterologa ekspresija izraisa vīrusveidīgo daļiņu veidošanos, kas ietver iekššūnas RNS. Šajā darbā mēs iepakojām specifiskas mRNS molekulas bakteriofāga GA kapsīdās *in vivo*. Specifiskuma nodrošināšanai izmantojām GA operatoru – 21 nukleotīdu garu RNS sekvenci, kas salokās kāta-cilpas struktūrā un var specifiski piesaistīties fāga apvalka proteīnam. Ekspresijai *Saccharomyces cerevisiae* konstruēja vairākas plazmīdas, kas nodrošināja gan GA apvalka proteīna, gan iepakojamās mRNS sintēzi. Par iepakošanas modeļiem izmantoja trīs dažādas mRNS (GA apvalka proteīna, ENA-78 un GFP), katru no tām konstruējot divos variantos, kas atšķīrās ar GA operatora klātbūtni to sekvencēs. Iegūto kapsīdu RNS satura analīze ar gēla elektroforēzi parādīja, ka ir radušās paredzētā garuma RNS. Iepakoto mRNS klātbūtni kapsīdās apstiprināja apgrieztās transkripcijas PCR. Tomēr operatoram bija samērā niecīga ietekme uz kapsīdu satura specifiskumu, jo kapsīdās vienmēr konstatēja arī GA apvalka proteīna mRNS.

Acta Universitatis Latviensis, 2008, Vol. 745, Biology, pp. 155–164

Photosynthetic performance and mycorrhizal symbiosis of a coastal marsh plant, *Glaux maritima*, in conditions of fluctuating soil salinity

Ieva Druva-Lūsīte[1]*, Andis Karlsons[2], Anita Osvalde[2], Jevgenija Ņečajeva[1], Gederts Ievinsh[1]

[1]Department of Plant Physiology, Faculty of Biology, University of Latvia, Kronvalda Bulv. 4, Rīga LV-1586, Latvia
[2]Laboratory of Plant Mineral Nutrition, Institute of Biology, University of Latvia, Miera 3, Salaspils LV-2169, Latvia

*Corresponding author, E-mail: druva@lanet.lv

Abstract

The aim of the present study was to explore the effect of seasonal fluctuations of soil salinity on chlorophyll *a* fluorescence and mycorrhizal symbiosis of *Glaux maritima* L. plants in natural conditions. Two neighboring sites with different flooding regime and putatively different soil characteristics were chosen for the investigation. The two sites significantly differed in salinity and both macronutrient and micronutrient concentrations. The relatively more sea-affected site A had higher salinity and higher concentrations of most nutrients. Potential quantum yield of photosystem II (F_V/F_M) decreased to an extremely low level in plants at site A in July indicating photoinhibition of photosynthesis. In contrast, a relatively low increase of soil salinity did not affect F_V/F_M at site B. Decreased photosynthetic performance at site A in July was reflected also by a drastic decrease both in photosystem II activity as well as in the ratio of active reaction centres. *G. maritima* plants were characterized by a low level of intensity of mycorrhizal symbiosis throughout the vegetation season while the frequency of infection in general was higher. Both parameters showed significant changes during the season. Anatomy of root colonization showed distinct patterns at the two study sites with mostly intracellular hyphae forming hyphal coils in roots of *G. maritima* at site A in contrast to site B where predominantly external hyphae were found. Mycorrhizal symbiosis could be regarded as a significant part of the adaptive mechanisms of *G. maritima*.

Key words: chlorophyll fluorescence, *Glaux maritima*, mycorrhizal symbiosis, salinity, soil mineral content

Introduction

Understanding of adaptive characteristics of wild plants from heterogeneous environments is extremely important for both conservation of plant diversity as well as for selective improvement of agriculturally important traits of cultivated plants. Soil salinity is a major concern in many regions (Pitman, Läuchli 2002). In this respect wild plants from habitats with a high natural level of soil salinity could be used as models in studies of physiological adaptations to salinity (Redondo-Gomez et al. 2006; Brown, Pezeshki 2007; Ksouri et al. 2007).

Glaux maritima L. (Primulaceae) is a perennial herb distributed on saline coastal areas of the northern hemisphere. The main natural factor causing variation in the distribution of *G. maritima* plants in coastal areas is flooding frequency, which in turn affects salinity, nutrient level, and oxygen content of the soil (Jerling 1988). *G. maritima* is characterized as a weak competitor and an opportunist. While *G. maritima* is considered to represent halophytic species having typical characteristics of a salt excluder (Rozema et al. 1978; Rozema et al. 1981) no study so far relates increased soil salinity with particular cellular adaptive mechanisms of salt tolerance besides osmotic adaptation (Rozema 1975). Protection of photosynthetic machinery in conditions of fluctuating soil salinity has recently been described as an important adaptive response for plants from heterogeneous environments (Marcile et al. 2007). Photochemistry of photosynthesis, which can be easily assessed in field conditions by means of chlorophyll *a* fluorescence measurement, is a sensitive process reflecting suboptimal changes in environmental conditions (Maxwell, Johnson 2000.).

It is generally believed that mycorrhizal symbiosis enhances plant tolerance to salinity mostly by improving uptake of mineral nutrients (Juniper, Abbott 1993; Tsang, Maun 1999). Studies with plant species native to saline environments indeed show a relatively high level of mycorrhizal colonization of halophytic plants (Hildebrandt et al. 2000).

The aim of the present study was to understand if seasonal fluctuations in soil salinity in different sites can affect photosynthetic performance of *G. maritima* in natural conditions. Changes of the performance as reflected by nondestructive chlorophyll *a* fluorescence measurements were analyzed during a growth season. In parallel both quantitative and qualitative aspects of mycorrhizal symbiosis were determined.

Materials and methods

Study area and sampling

Study area was located in western part of Latvia, on the western coast of Riga Gulf near Mersrags, Latvia (N 57°20‘ E 23°08‘). Typical habitats are coastal meadow, coastal salt marsh and coastal lagoons. Two neighboring sites with different flooding regime and putatively different soil characteristics were chosen with a 200-m distance between them. The plant community was dominated by *Festuca rubra*, *Carex nigra*, *Juncus gerardii*, *Potentilla anserina*. Site A was more affected by flooding by sea water during the season in comparison to site B. Soil and plant analysis was performed once a month during the vegetation season. As plants at the beginning of vegetation season in the middle of May were extremely small, only soil samples were taken at that time.

Measurement of chlorophyll a *fluorescence*

For continuous chlorophyll *a* fluorescence measurement, a Handy PEA (Hansatech, UK) was used. Intact leaves were dark adapted for 30 min using leaf clips provided by the manufacturer. Five measurements of individual plants were made per experimental site. The data were analyzed by appropriate software (Hansatech, UK). The ratio F_V/F_M was calculated, where F_V is the difference between the maximum fluorescence and the minimum fluorescence level F_0. Chlorophyll *a* fluorescence parameter F_V/F_M measured after a dark adaptation period reflects the potential quantum yield of photosytem II (PSII) and thus is indicative of photoinhibition (Maxvell, Johnson 2000). F_V/F_0 charaterizing the

ratio of variable fluorescence per initial fluorescence was used as an indication of PSII activity.

Performance index (PI) is a combination of the three independent parameters summing the respective responses of PSII – total number of active reaction centers per absorption, yield of primary photochemistry and efficiency with which a trapped exciton can move an electron into the electron transport chain (Appenroth et al. 2001).

To characterize energy fluxes for reaction centres, the ratio between total chlorophyll and that of antenna complexes of reaction centres could be used. The ratio Chl RC/Chl antenna can be replaced by the ratio RC/ABS, where RC is the number of active PSII reaction centres, and ABS is the quantity of light absorbed (Clark et al. 2000).

Root sampling and assessment of arbuscular mycorrhizal colonization

Root samples with soil were excavated from individual plants. Roots of at least nine individuals per site were sampled. Collected root samples were placed in a polyethylene bag and stored at 4 °C until analysis. Roots were carefully rinsed with running tap water and cut into 1-cm-long fragments. Samples for mycorrhizal assessment were prepared according to a modified method of Hayman (1970). Roots were boiled for 1 h in 10 % KOH, then washed with tap water. Staining was performed in 0.05 % trypan blue for 5 min followed by washing with tap water. Samples were stored in lactoglycerol [mixture of lactic acid, glycerol, water 1:1:1 (v/v/v)]. Root pieces were mounted on glass slides and examined under a Nicon Eclipse E200 microscope. Photographs were taken by a digital camera. Mycorrhizal colonization (abundance of hyphae, vesicles and arbuscules) was estimated after Trouvelot et al. (1986) at 400 × magnification using 10 root segments of each plant. Intensity of mycorrhizal colonization in the root system (M%) and frequency of mycorrhiza in the root system (F%) were calculated with the computer program Mycocalc (Trouvelot et al. 1986). M% was calculated according to the formulae

$$M\% = (95 \times n_5 + 70 \times n_4 + 30 \times n_3 + 5 \times n_2 + n_1)/(\text{total nb}),$$

where n_5 = number of fragments with a degree of colonization rated as "5", n_4 = number of fragments with a degree of colonization rated as "4", etc.; nb = number of eyeshots. F% was calculated according to the formulae

$$F\% = (\text{nb of fragments with mycorrhiza/total nb}) \times 100.$$

In a particular study the number of eyeshots was 100.

Measurement of soil parameters and mineral nutrients

Soil samples were taken from the root zone near *G. maritima* plants (0 - 10 cm depth). For each sample five to eight subsamples were collected and thoroughly mixed to form one sample.

Soil pH was measured in a 1 : 2.5 soil to 1M KCl volume ratio using a PB-20 pH meter (Sartorius). Soil electrical conductivity was determined in a 1 : 5 soil to deionized water volume ratio with a EC 215 conductometer (Hanna Instruments).

Soil samples were air-dried and sieved through a metal sieve (2-mm mesh size). Samples were extracted with 1M HCl in a 1:5 soil to extractant volume ratio. The levels of Ca, Mg, Fe, Cu, Zn, and Mn were measured by atomic absorption spectrophotometer AAnalyst 700 (Perkin Elmer) with an acetylene-air flame (Haswell 1991). The amount of N, P, Mo and B was assayed by colorimetry, concentration of S by turbidimetry. K and Na was measured by a flame photometer PFP7 (Jenwey) with an air-propane/butane flame.

Table 1. General soil properties and concentrations of nutrients and Na and Cl (mg L^{-1}) at two sites with *Glaux maritima*. Data are means from 5 measurements throughout the season ± SE. *, significant differences between the sites ($P < 0.01$)

Parameters / nutrients	Site A	Site B
pH*	6.2 ± 0.1	6.5 ±0.1
Electrical conductivity (dS m^{-1})*	10.8 ± 1.1	4.2 ± 0.7
N*	40 ± 3.7	21.6 ± 3.3
P*	94.6 ± 2.4	134.2 ±12.9
K*	260 ± 10	120 ± 22
Ca*	2195 ± 91	965 ± 183
Mg*	1393 ± 53	538 ± 89
S*	293 ± 61	88 ± 19
Fe	503 ± 32	507 ± 114
Mn	21.4 ± 1.8	36.7 ± 15.3
Zn*	14.8 ± 0.9	2.9 ± 0.5
Cu*	2.7 ± 0.1	0.8 ± 0.1
Mo*	0.04 ± 0.00	0.03 ±0.0
B*	7.3 ± 1.3	2.5 ± 0.5
Na*	2310 ± 163	969 ± 139
Cl*	2838 ± 280	1132 ± 200

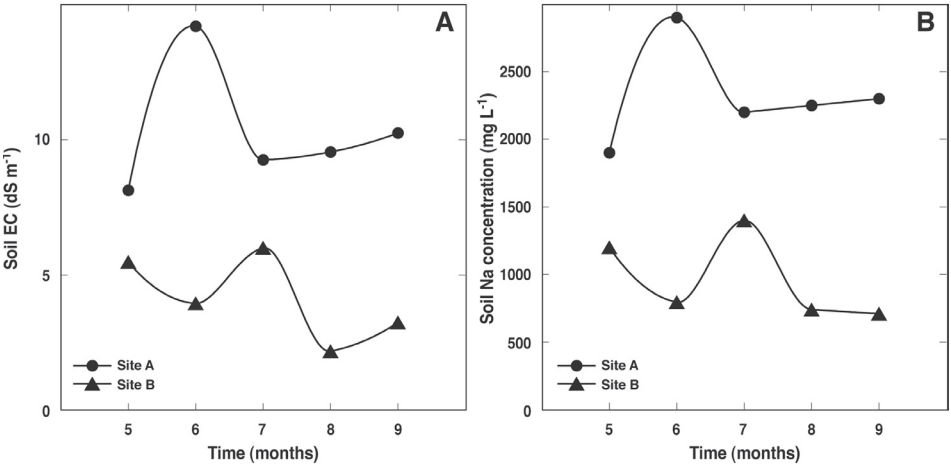

Fig. 1. Seasonal changes of soil electrical conductivity (A) and soil Na concentration (B) at two experimental sites with *Glaux maritima*.

Chloride was determined by $AgNO_3$ titration (Patnaik 1997).

Results

Differences in soil edaphic factors and fluctuations of salinity

The two study sites with *G. maritima* significantly differed in salinity and both macronutrient and micronutrient concentrations (Table 1). The relatively more sea-affected site A had

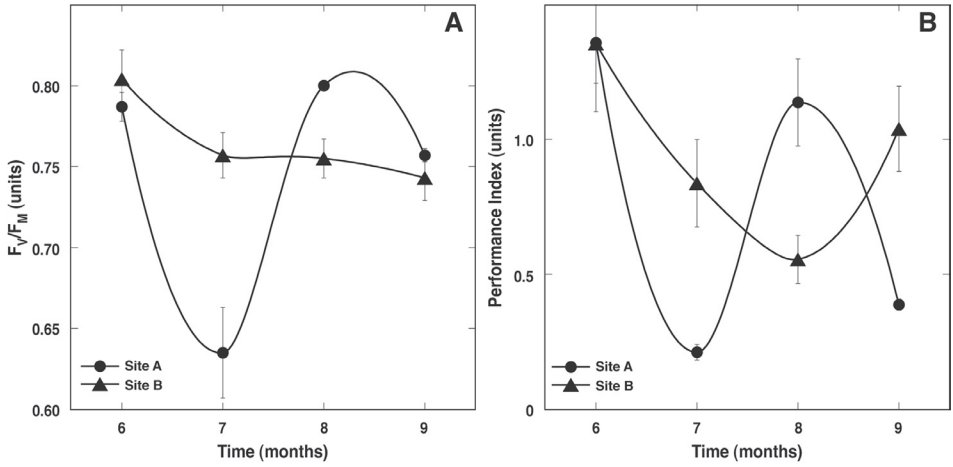

Fig. 2. Seasonal changes of potential quantum yield of photosystem II (F_V/F_M) (A) and performance index (PI) (B) of *Glaux maritima* plants at two experimental sites.

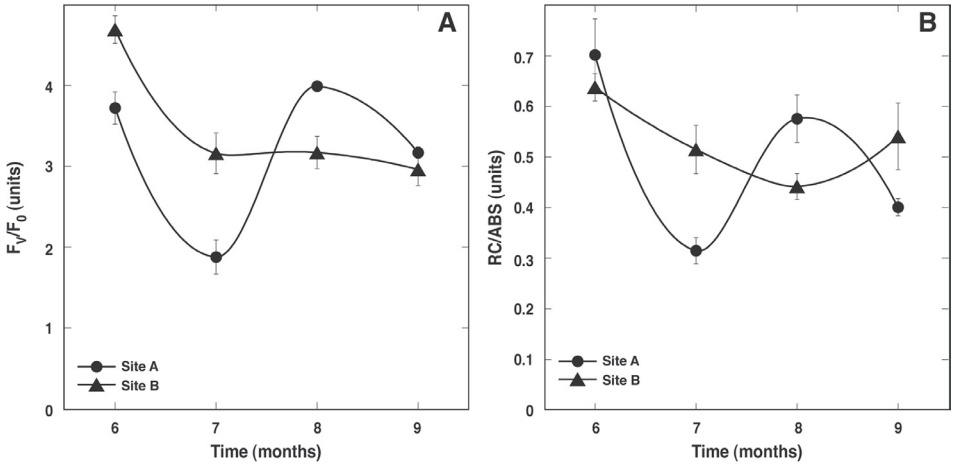

Fig. 3. Seasonal changes of photosystem II activity (F_V/F_0, A) and ratio of active reaction centres (RC/ABS, B) of *Glaux maritima* plants at two experimental sites.

higher salinity and higher concentrations of most nutrients except P, Fe and Mn. The most pronounced increase at site A was evident for Mg (< 3-fold), Zn (5-fold), Cu (> 3-fold), B (3-fold). Na and Cl concentrations at the site A was 2.4 and 2.5 times those at the site B, respectively. Higher ion content at site A was reflected by a 2.6-fold soil electrical conductivity and more acidic soil pH value.

Soil salinity at the two sites fluctuated significantly during the vegetation season as reflected by changes in the soil electrical conductivity (Fig. 1A) and Na concentration (Fig. 1B). Changes of a similar character was evident for Cl concentration (data not shown). Soil salinity at site A peaked in June while two significantly smaller peaks were evident for site B in May and July.

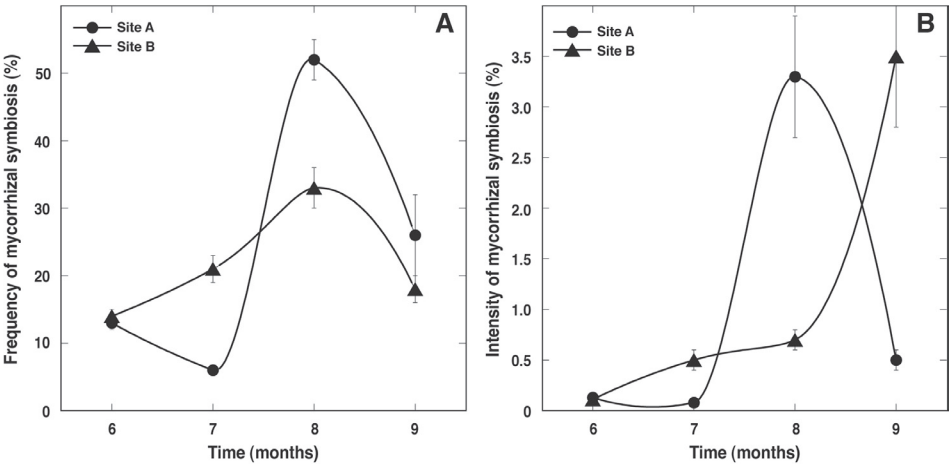

Fig. 4. Seasonal changes of frequency of mycorrhizal symbiosis (A) and intensity of mycorrhizal symbiosis (B) of *Glaux maritima* plants at two experimental sites.

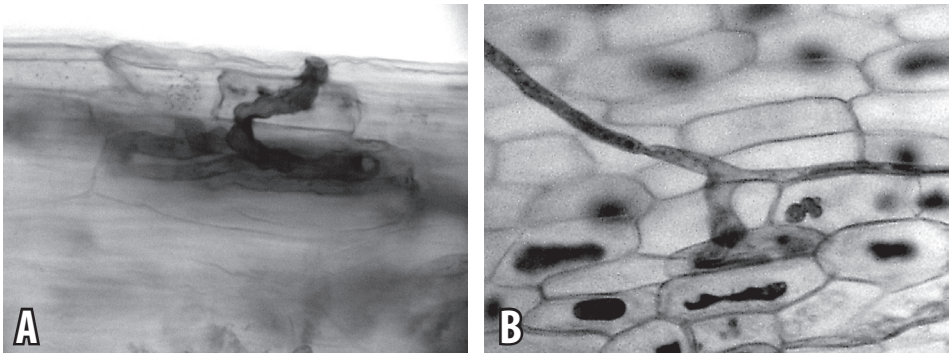

Fig. 5. Characteristic mycorrhizal fungal structures in roots of *Glaux maritima* from two experimental sites. A, intraradical hyphae forming hyphal coils at site A. B, external hyphae at site B.

Seasonal changes of chlorophyll a *fluorescence*

Potential quantum yield of PSII (F_V/F_M) decreased to an extremely low level in plants at site A in July indicating photoinhibition of photosynthesis (Fig. 2A). In contrast, a relatively low increase of soil salinity did not affect F_V/F_M at site B (Fig. 2A). However PI, which is a more complex parameter, decreased in *G. maritima* plants at site B until August followed by an increase in September (Fig. 2B) indicating that some aspects of photochemistry of PSII were affected. Indeed, a lower level of PSII activity (Fig. 3A) and decreasing ratio of active reaction centres of PSII (Fig. 3B) was evident at site B in July and August. Decreased photosynthetic performance at site A in July was reflected also by a drastic decrease both in PSII activity (F_V/F_0) and in the ratio of active reaction centres (RC/ABS; Fig. 3).

Dynamics of mycorrhizal symbiosis and anatomical differences of symbiosis

G. maritima plants were characterized by a low level of intensity of mycorrhizal symbiosis

throughout the vegetation season (Fig. 4B) while the frequency of infection in general was higher (Fig. 4A). Both parameters showed significant changes during the season. At site A lower levels of mycorrhizal symbiosis in July was followed by a drastic increase in August. In September frequency of mycorrhizal symbiosis decreased at both sites while intensity showed an opposite pattern for the two sites with a significant increase at site B and decrease at site A (Fig. 4).

Anatomy of root colonization showed a distinct pattern at the two study sites. At the sea flooding-affected site A *G. maritima* plants had mostly intracellular hyphae forming hyphal coils (Fig. 5A). In contrast plants at site B predominantly had external hyphae usually with a relatively high level of branching (Fig. 5B). No arbuscules were found in the symbiotic root cells.

Discussion

As flooding by sea water resulting in drastic increase in soil salinity is a main factor affecting distribution of *G. maritima* plants (Jerling 1988b) one may ask what is the overall effect of these environmental changes on general performance of *G. maritima*. In terms of reproduction flooding episodes have been observed to positively affect the rate of vegetative propagation of *G. maritima* (Jerling 1988a). In the present experiments fluctuation of soil salinity induced temporal changes in photochemistry of PSII of *G. maritima* plants. In the most severe situations as at site A in June photoinhibition of photosynthesis was evident in July. However, recovery of photosynthetic performance at the later stages indicates that *G. maritima* plants are indeed well-adapted to subtle changes in soil salinity.

G. maritima is known as a typical salt eliminator, which is achieved by the means of salt-secreting glands (Rozema 1975; Rozema et al. 1978). On the other hand, it has been long known that *G. maritima* is a mycorrhizal plant (Mason 1928). Mycorrhizal symbiosis of *G. maritima* has been characterized as moderate to low intensity (Hildebrandt et al. 2001). Similarly, in the present study a low level of symbiosis was found for *G. maritima*. Low mycorrhizal colonization of plants in salt marshes does not imply ineffectiveness of mycorrhizal symbiosis (Füzy et al. 2008). In spite of the relatively low intensity of mycorrhizal symbiosis in roots of *G. maritima* clear seasonal change in colonization was found (Fig. 4). In general seasonal dynamics of mycorrhizal symbiosis is a well-known phenomenon and is thought to be dependent on both climate variation as well as host phenology (Lugo et al. 2003). In temperate regions periodically fluctuating low temperature affects function of mycorrhizal symbiosis in relation to edaphic conditions (Tibbett, Cairney 2007). On the other hand this may also reflect a seasonality of mycorrhizal fungi itself (Bever et al. 2001). Usually maximum intensity of colonization is at the phase of full photosynthetic capacity (Merryweather, Fitter 1995). In our study both frequency and intensity of the symbiosis increased during the vegetation season until August in roots of *G. maritima* (Fig. 4).

Soil at both sites was characterized by an extremely high Na, Cl, B and S content. However, the amount of N, Cu and Mo can be estimated as relatively low. Together with high soil electrical conductivity and fluctuating character of changes in these parameters this indicates a direct effect of flooding by sea water. Consequently, mineral disbalance could be predicted, especially at site A. However, a high S level in the soil is one of the factors leading to higher tolerance of salt-affected plants partly through reduction of B uptake (Baker, Pilbeam 2007).

In flooded soils reduced forms of N, Mn, Fe, S are produced due to activity of anaerobic soil microorganisms (Cronk, Fennessy 2001). A decrease in redox potential can be stressful or toxic to plants. Reducing conditions also change the availability of mineral nutrients. Phosphate availability is increased due to conversion of Fe^{3+} to Fe^{2+}. In addition availability of positively charged ions e.a. K, Mg, Ca also increases in reduced conditions. Flooding also negatively affects mycorrhizal symbiosis (Carvalho et al. 2003; Šraj-Kržič et al. 2006). However, it was concluded that mycorrhizal symbiosis in salt marsh depends on soil salinity rather than on soil flooding (Carvalho et al. 2003).

Mycorrhizal plants may have a higher salt tolerance than non-mycorrhizal plants (Feng et al. 2002; Al-Karaki 2006; Sharifi et al. 2007). Improved tolerance of mycorrhizal plants vs. non-mycorrhizal in saline conditions can be related to enhanced mineral nutrition and as a result improved physiological processes (Ruiz-Lozano, Azcón 2000). In addition, potential quantum yield of PSII (F_V/F_M) is higher in plants with a higher degree of mycorrhizal colonization, especially in suboptimal conditions (Pinior et al. 2005). Consequently, in spite of a putative negative effect of high soil salinity on mycorrhizal symbiosis of *G. maritima* plants at site A in July increased frequency and intensity of the symbiosis at later stages clearly indicates an adaptive potential of mycorrhizal symbiosis. Moreover, appearance of intercellular hyphal structures (hyphal coils) in roots of *G. maritima* at site A under the effect of high soil salinity may represent inducible adaptive response. Indeed, hyphal coils have been described as exchange structures indicating intense exchange activity between the symbionts (Lugo et al. 2003).

In conclusion, photochemistry of photosynthesis of *G. maritima* plants is negatively affected by elevated soil salinity leading to significant inhibition of photosynthesis in the most severe cases. However, relatively high long-term adaptive potential of the species leads to significant recovery of physiological processes during stabilization of the salinity. Mycorrhizal symbiosis could be regarded as a significant part of the adaptive mechanisms of *G. maritima*.

Acknowledgements

The present work was supported by a grant from the University of Latvia. ESF funding for I. Druva-Lūsīte is gratefuly acknowledged. We would like to thank Brigita Laime for providing the vegetation data.

References

Al-Karaki G.N. 2006. Nursery inoculation of tomato with arbuscular mycorrhizal fungi and subsequent performance under irigation with saline water. *Sci. Hortic.* 109: 1–7.

Appenroth K.-J., Stöckel J., Srivastava A., Strasser R.J. 2001. Multiple effects of chromate on the photosynthetic apparatus of *Spirodela polyrhiza* as probed by OJIP chlorophyll *a* fluorescence measurements. *Env. Pollut.* 115: 49–64.

Bever J.D., Schultz P.A., Pringle A., Morton J.B. 2001. Arbuscular mycorrhizal fungi: more diverse than meets the eye, and the ecological tale of why. *BioScience* 51: 923–931.

Brown C.E., Pezeshki S.R. 2007. Threshold for recovery in the marsh halophyte *Spartina alterniflora* grown under the combined effects of salinity and soil drying. *J. Plant Physiol.* 164: 274–282.

Carvalho L.M., Correia P.M., Cacador I., Martins-Loucao A.M. 2003. Effects of salinity and flooding on the infectivity of salt marsh arbuscular mycorrhizal fungi in *Aster tripolium* L. *Biol. Fertil. Soils* 38: 137–143.

Clark A.J., Landolt W., Bucher J.B., Strasser R.J. 2000. Beech (*Fagus sylvatica*) response to ozone exposure assessed with a chlorophyll *a* fluorescence performance index. *Env. Pollut.* 109: 501–507.

Feng G., Zhang F.S., Li X.L., Tian C.Y., Tang C., Rengel Z. 2002. Improved tolerance of maize plants to salt stress by arbuscular mycorrhiza is related to higher accumulation of soluble sugars in roots. *Mycorrhiza* 12: 185–190.

Füzy A., Biró B., Tóth T., Hildebrandt U., Bothe H. 2008. Drought, but not salinity, determines the apparent effectiveness of halophytes colonized by arbuscular mycorrhizal fungi. *J. Plant Physiol*. 165: 1181–1192.

Hayman D.S. 1970. Endogone spore numbers in soil and vesicular-arbuscular mycorrhiza in weat as influenced by season and soil treatment. *Trans. British Mycol. Soc.* 54: 53–63.

Hildebrandt U., Janetta K., Ouziad F., Renne B., Nawrath K., Bothe H. 2001. Arbuscular mycorrhizal colonization of halophytes in Central European salt marshes. *Mycorrhiza* 10: 175–183.

Jerling L. 1988a. Clone dynamics, population dynamics and vegetation pattern of *Glaux maritima* on a Baltic sea shore meadow. *Vegetatio* 74: 171–185

Jerling L. 1988b. Population dynamics of *Glaux maritima* (L.) along a distributional cline. *Vegetatio* 74: 161–170

Juniper S., Abbott L. 1993. Vesicular arbuscular mycorrhizas and soil salinity. *Mycorrhiza* 4: 45–57.

Ksouri R., Megdiche W., Debez A., Falleh H., Grignon C., Abdelly C. 2007. Salinity effects on polyphenol content and antioxidant activities in leaves of the halophyte *Cakile maritima*. *Plant Physiol. Biochem*. 45: 244–249.

Lugo M.A., Maza M.E.G., Cabello M.N. 2003. Arbuscular mycorrhizal fungi in a mountain grassland II: Seasonal variation of colonization studied, along with its relation to grazing and metabolic host type. *Mycologia* 95: 407–415.

Marcile B.R., Lee R.W., Hellquist C.E., Kiirats O., Edwards G.E. 2007. Effects of salinity on chlorophyll fluorescence and CO_2 fixation in C_4 estuarine grasses. *Photosynthetica* 45: 433–440.

Mason E. 1928. Note on the presence of mycorrhiza in the roots of salt marsh plants. *New Phytol*. 27: 193–195.

Maxwell K., Johnson G.N. 2000. Chlorophyll fluorescence – a practical guide. *J. Exp. Bot*. 51: 659–668.

Merryweather J., Fitter A. 1995. Phosphorus and carbon budgets: mycorrhizal contribution in *Hyacinthoides non-scripta* (L.) Chouard ex Rothm. under natural conditions. *New Phytol*. 129: 619–627.

Pinior A., Grunewaldt-Stöcker G., von Alten H., Strasser R.J. 2005. Mycorrhizal impact on drought stress tolerance of rose plants probed by chlorophyll *a* fluorescence, proline content and visual scoring. *Mycorrhiza* 15: 596–605.

Pitman M.G., Läuchli A. 2002. Global impact of salinity and agricultural ecosystems. In: Läuchli A., Luttge U. (eds). *Salinity: Environment – Plants – Molecules*. Kluwer Academic Publishers, Dordrecht, pp. 3–20.

Redondo-Gomez S., Wharmby C., Castillo J.M., Mateos-Naranjo E., Luque C.J., de Cires A., Luque T., Davy A.J., Figueroa M.E. 2006. Growth and photosynthetic responses to salinity in an extreme halophyte, *Sarcocornia fruticosa*. *Physiol. Plant*. 128: 116–124.

Rozema J. 1975. An eco-physiological investigation into salt tolerance of *Glaux maritima* L. *Acta Bot. Neerl.* 24: 407–416.

Rozema J., Arp W., van Diggelen J., van Esbroek M., Broekman R., Punte H. 1986. Occurrence and ecological significance of vesicular mycorrhiza in the salt marsh environment. *Acta Bot. Neerl*. 35: 457–467.

Rozema J., Buizer D.A.G., Fabritius H.E. 1978. Population dynamics of *Glaux maritima* and ecophysiological adaptations to salinity and inundation. *Oikos* 30: 539–548.

Rozema J., Gude G. 1981. An ecophysiological study of the salt secretion of four halophytes. *New Phytol.* 89: 201–217.

Ruiz-Lozano J.M., Azcón R. 2000. Symbiotic efficiency and infectivity of an autochthonous arbuscular mycorrhizal *Glomus* sp. from saline soils and *Glomus deserticola* under salinity. *Mycorrhiza* 10: 137–143.

Sharifi M., Ghorbanli M., Ebrahimzadeh H. 2007. Improved growth of salinity-stressed soybean after inoculation with salt pre-treated mycorrhizal fungi. *J. Plant Physiol.* 164: 1144–1151.

Šraj-Kržič N., Pongrac P., Klemenc M., Kladnik A., Regvar M., Gaberščik A. 2006. Mycorrhizal colonisation in plants from intermittent aquatic habitats. *Aquatic Bot*. 85: 331–336.

Tibbett M., Cairney J.W.G. 2007. The coller side of mycorrhizas: their occurence and functioning at low temperatures. *Can. J. Bot*. 85: 51–62.

Trouvelot A., Kough J. L., Gianinazzi-Pearson V. 1986. Mesure du taux de mycorhization VA d'un système radiculaire. Recherche de mèthodes d'estimation ayant une signification fonctionnelle. In: Gianinazzi-Pearson V., Gianinazzi S. (eds) *Physiological and Genetical Aspects of Mycorrhizae*. INRA Press, Paris, pp. 217–221.

Tsang A., Maun M.A. 1999. Mycorrhizal fungi increase salt tolerance of *Strophostyles helvola* in coastal foredunes. *Plant Ecol.* 144: 159–166.

Piekrastes mitrāju auga *Glaux maritima* fotosintēzes efektivitāte un mikorizu simbioze mainīga augsnes sāļuma apstākļos

Ieva Druva-Lūsīte[1]*, Andis Karlsons[2], Anita Osvalde[2], Jevgenija Ņečajeva[1], Ģederts Ieviņš[1]

[1]Augu fizioloģijas katedra, Latvijas Universitātes Bioloģijas fakultāte, Kronvalda bulv. 4, Rīga LV-1586, Latvija

[2]Minerālās barošanās laboratorija, LU Bioloģijas institūts, Miera 3, Salaspils LV-2169, Latvija

*Korespondējošais autors, E-pasts: druva@lanet.lv

Kopsavilkums

Dotā darba mērķis bija izpētīt sezonālo augsnes sāļuma izmaiņu ietekmi uz hlorofila *a* fluorescenci un mikorizu simbiozi dabiskos apstākļos augošiem *Glaux maritima* augiem. Pētījumam izvēlējās divus tuvu izvietotus parauglaukumus ar atšķirīgu applūšanas režīmu un iespējami atšķirīgām augsnes īpašībām. Parauglaukumi būtiski atšķīrās pēc augsnes sāļuma un makroelementu un mikroelementu koncentrācijām tajā. Relatīvi vairāk jūras ietekmētajā parauglaukumā A bija lielāks sāļums un augstākas lielākās daļas minerālelementu koncentrācijas. Fotosistēmas II potenciālais kvantu iznākums (F_V/F_M) parauglaukumā A jūlijā samazinājās līdz kritiski zemam līmenim, parādot fotosintēzes fotoinhibēšanu. Pretēji tam, relatīvi nelielais augsnes sāļuma pieaugums parauglaukumā B neietekmēja F_V/F_M. Samazinātā fotosintēzes efektivitāte parauglaukumā A jūlijā bija saistīta arī ar fotosistēmas II aktivitātes un aktīvo reakcijas centru proporcijas samazinājumu. G. maritima augiem bija raksturīga zema mikorizu simbiozes intensitāte visā veģetācijas sezonas laikā, bet simbiozes frekvence kopumā bija augstāka. Abi parametri būtiski mainījās sezonas laikā. Sakņu kolonizācijas veids bija atšķirīgs divos parauglaukumos – parauglaukumā A varēja novērot pārsvarā iekššūnas hifas, kas veidoja hifu tinumus. Savukārt, parauglaukumā B dominējā ārpussaknes hifas. Mikorizu simbiozi var uzskatīt par būtisku daļu *G. maritima* adaptīvajos mehānismos.

Acta Universitatis Latviensis, 2008, Vol. 745, Biology, pp. 165–177

Changes of nutritional status of coastal plants *Hydrocotyle vulgaris* and *Aster tripolium* at elevated soil salinity

Andis Karlsons[1]*, Anita Osvalde[1], Jevgenija Ņečajeva[2], Gederts Ievinsh[2]

[1]Laboratory of Plant Mineral Nutrition, Institute of Biology, University of Latvia, Miera 3, Salaspils LV-2169. Latvia
[2]Department of Plant Physiology, Faculty of Biology, University of Latvia, Kronvalda Bulv. 4, Rīga LV-1586, Latvia

*Corresponding author, E-mail: andis_@one.lv

Abstract

The aim of the present paper was to examine the effect of increased substrate NaCl on concentration of nutrients in tissues of two coastal marsh plants *Hydrocotyle vulgaris* and *Aster tripolium*. Increased substrate salinity due to watering with NaCl solution led to accumulation of both Na and Cl ions in tissues of both species studied. In *H. vulgaris* leaf blade and leaf petiole tissues both Na and Cl concentrations were saturated. In contrast there was an increase of Na and Cl concentration in both leaf and root tissues of *A. tripolium* with increasing substrate concentration. N and P concentrations were differentially affected by increasing substrate NaCl. While both minerals increased in tissues of *H. vulgaris*, for *A. tripolium* concentration of N decreased and that of P increased in roots. The effect of NaCl on S concentration was species-specific – it increased in leaf petioles and stolons of *H. vulgaris* and decreased in both leaves and roots of *A. tripolium*. The most pronounced stimulation of mineral concentration by NaCl was found for Mn. Increase in Cu concentration was characteristic for all tissues of both species while Fe concentration increased in *A. tripolium* and leaf tissues of *H. vulgaris*. In conclusion, possible adaptive responses leading to maintenance of an optimal supply of mineral nutrients in conditions of high Na and Cl concentrations in cells can be seen.

Key words: coastal plants, *Aster tripolium*, halophytes, *Hydrocotyle vulgaris*, mineral nutrition, salinity, wild plants.

Introduction

Elevated soil salinity, which is a major concern in many regions (Pitman, Läuchli 2002) changes physico-chemical properties of the soil in turn affecting availability of minerals and their uptake (Grattan, Grieve 1993). Thus, soil salinity decreases solubility of micronutrients. In addition, ion toxicity and osmotic stress may affect transport rates and cellular concentrations of certain nutrients. These processes could lead to nutrient imbalance and changes in ion homeostasis as a result of soil salinity. Together with disturbance of cellular functions due to NaCl toxicity and osmotic stress, raised salinity may lead to suppression of vital physiological functions (Flowers et al. 1977; Hasegawa et al. 2000). Consequently plants native to habitats with fluctuating soil salinity should

possess adaptive mechanisms to compensate for consequences of nutrient imbalance.

While general aspects of mineral nutrition of wild plants have been considered (Chapin 1980; Aerts, Chapin 2000) most recent studies concentrate on several main macronutrients. However, for optimal plant growth all the essential mineral nutrients must be present in adequate levels and correct proportions, which may differ for various species and different habitats. In addition, edaphic factors have been considered as limiting, explaining species zonation in a salt marsh (Levine et al. 1998; Pennings et al. 2005). Studies on the effect of salinity on mineral nutrition of wild plants, particularly halophytes, are rare. Very few data can be found on the effect of salinity on micronutrient concentration. Therefore, the aim of the present paper was to examine the effect of increased substrate NaCl level on concentration of macronutrients and micronutrients in tissues of different organs of two coastal marsh plants *Hydrocotyle vulgaris* and *Aster tripolium*.

Materials and methods

Aster tripolium plants were propagated by tissue culture from shoot apical explants (Klavina et al. 2006). Plants representing genetically identical material with four to five leaves were transferred to plastic pots (12 × 12 cm, 15 cm deep) filled with a commercial neutralized (pH 5.5 - 6.3) peat with mineral nutrients (NPK 14-16-18).

Stock plant material of *Hydrocotyle vulgaris* was introduced in laboratory culture from one genet of naturally growing plants during summer 2005. For experiments, plants were propagated during early spring in 2007 and 2008 and represented genetically identical clonal material. As starting material, five small plants with three ramets each was planted in 30 × 40 cm plastic trays filled with a commercial neutralized peat with mineral nutrients (NPK 14-16-18).

Plants were cultivated in a growth chamber with 120 μmol m^{-2} s^{-1} of photosynthetically active radiation at the plant level provided by three fluorescent lamps, photoperiod of 16 h, temperature 20 ± 2 °C.

Plants were watered three times a week with tap water or tap water with different concentrations of NaCl. Salt was added in steps of 25 mM per day in order to avoid osmotic shock. Final NaCl concentrations in a watering solution were 0, 25, 50, 100 mM for *H. vulgaris* and 0, 25, 50, 100, 200, 400 mM for *A. tripolium*. Preliminary experiments showed that substrate Na and Cl concentration was affected not only by the concentration of the ions in the respective watering solution but also on frequency and amount of watering solution applied. Indirectly, the concentration was affected also by cultivation temperature because of increased transpiration and consequently need for more water with increasing temperature.

Plants were harvested at four weeks after the start of the treatment. *H. vulgaris* plants were separated into leaf blades, leaf petioles and stolons, *A. tripolium* plants into leaves and roots. Three separate samples per treatment were harvested for each time point. The tissues were dried in oven (60 °C), weighed and ground into a fine powder using a ball mill. The samples were dry-ashed in concentrated HNO_3 vapor and redissolved in HCl solution (HCl : deionized water 3 : 100, v/v) and analyzed for nutrient concentrations (Rinkis et al. 1987).

The levels of Ca, Mg, Fe, Cu, Zn, and Mn were measured by atomic absorption spectrophotometer AAnalyst 700 (Perkin Elmer) with an acetylene-air flame (Haswell

1991). The amount of N, P, Mo and B was assayed by colorimetry, concentration of S by turbidimetry. K and Na were measured by a flame photometer PFP7 (Jenwey) with an air-propane/butane flame. Chloride was determined by $AgNO_3$ titration (Patnaik 1997). All results were expressed on a dry mass basis.

Substrate samples for Na and Cl analysis were air-dried and sieved through a metal sieve (2-mm mesh size). Samples were extracted with 1M HCl in a 1 : 5 soil to extractant volume ratio and measured by a flame photometer (for Na) or by $AgNO_3$ titration (for Cl). Experiments were repeated two times. Only data from a representative experiment are shown.

Results

Nutrient concentration in different organs of H. vulgaris *and* A. tripolium

When cultivated in control conditions *H. vulgaris* accumulated significantly higher concentrations of N, Ca, Mg, Fe, Mn and Zn in the leaf blade tissues in comparison to leaf tissues of *A. tripolium* (Table 1). Concentrations of nutrients in tissues of *H. vulgaris* decreased in the order leaf blades > leaf petioles > stolons for N, Ca, Mg, S, Fe, Mn and Zn. In contrast, higher concentration of K was evident in leaf petioles and stolons in comparison to leaf blades of *H. vulgaris*. For *A. tripolium* leaf tissues had higher concentrations than root tissues for all the nutrients measured except Mg, Fe, Zn and Cu.

Substrate NaCl level, corresponding NaCl concentrations in tissues and plant growth

Increased substrate salinity due to watering with NaCl solution led to accumulation of both Na (Fig. 1) and Cl (Fig. 2) ions in tissues of both species studied. However contrasting trends of concentration-dependence characteristics were found for *H. vulgaris* and *A.*

Table 1. Concentration of mineral nutrients in tissues of different organs of *Hydrocotyle vulgaris* and *Aster tripolium*. Data are means from 3 measurements ± SE

	Hydrocotyle vulgaris			*Aster tripolium*	
	Leaf blades	**Leaf petioles**	**Stolons**	**Leaves**	**Roots**
Macronutrients (% DM)					
N	2.00 ± 0.06	1.35 ± 0.08	1.00 ± 0.09	1.25 ± 0.03	0.90 ± 0.02
P	0.32 ± 0.03	0.40 ± 0.02	0.36 ± 0.02	0.39 ± 0.04	0.29 ± 0.03
K	2.14 ± 0.15	6.40 ± 0.16	3.98 ± 0.10	3.24 ± 0.10	0.90 ± 0.03
Ca	4.10 ± 0.11	1.90 ± 0.14	0.39 ± 0.02	0.96 ± 0.04	0.37 ± 0.02
Mg	0.65 ± 0.03	0.28 ± 0.01	0.11 ± 0.01	0.35 ± 0.01	0.29 ± 0.02
S	0.34 ± 0.02	0.07 ± 0.01	0.10 ± 0.01	0.43 ± 0.02	0.21 ± 0.01
Micronutrients (mg kg^{-1})					
Fe	142 ± 3	56 ± 6	44 ± 4	60 ± 2	225 ± 3
Mn	90 ± 3	19 ± 1	8 ± 1	32 ± 2	11 ± 1
Zn	150 ± 4	48 ± 4	24 ± 3	26 ± 1	30 ± 2
Cu	6.2 ± 0.4	3.4 ± 0.2	4.8 ± 0.2	6.8 ± 0.2	9.0 ± 0.3
Mo	2.2 ± 0.1	0.3 ± 0.0	0.3 ± 0.0	2.7 ± 0.2	1.3 ± 0.2
B	30 ± 2	10 ± 1	14 ± 1	28 ± 2	7 ± 1

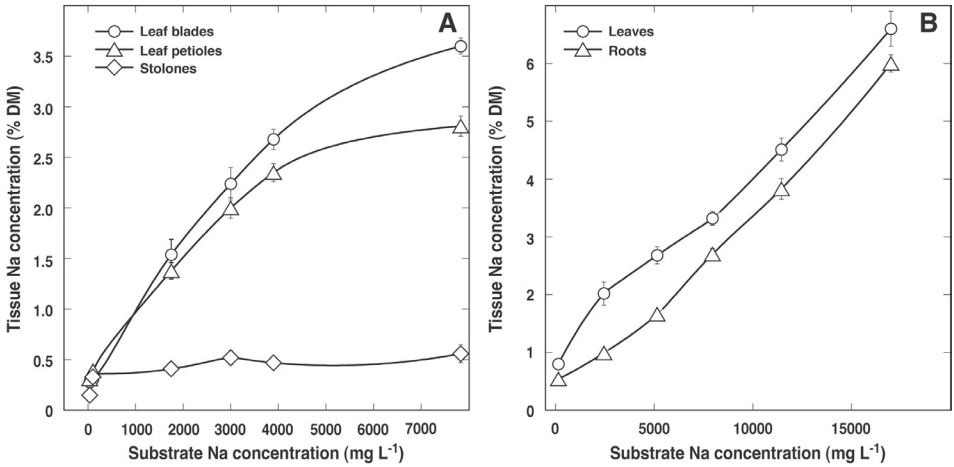

Fig. 1. Relationship between substrate Na concentration and tissue Na concentration of different organs of *Hydrocotyle vulgaris* (A) and *Aster tripolium* (B).

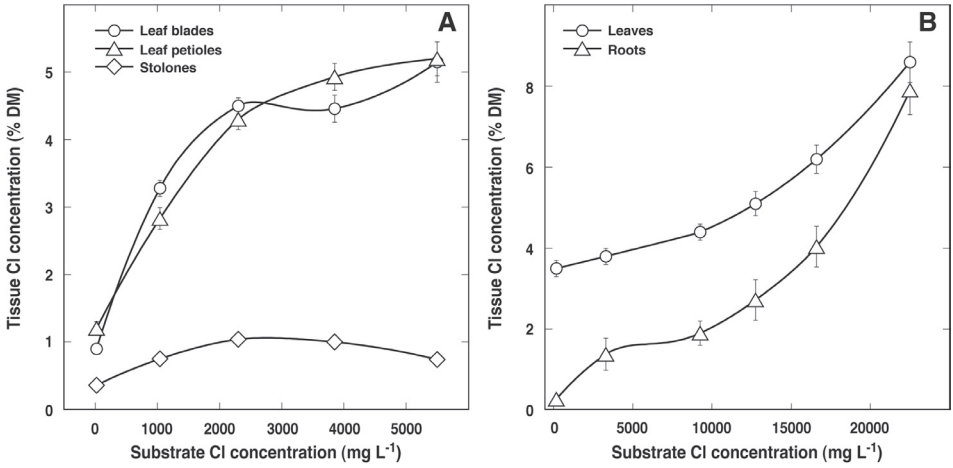

Fig. 2. Relationship between substrate Cl concentration and tissue Cl concentration of different organs of *Hydrocotyle vulgaris* (A) and *Aster tripolium* (B).

tripolium. In *H. vulgaris* leaf blade and leaf petiole tissues both Na and Cl concentrations were saturated at soil ion concentration of about 4000 mg L^{-1} (Fig. 1A, 2A). In stolon tissues of *H. vulgaris* increase of Na and Cl concentration with increasing substrate NaCl concentration was significantly lower. In contrast to *H. vulgaris* there was a linear increase of Na concentration in both leaf and root tissues of *A. tripolium* with increasing substrate concentration up to 17 000 mg L^{-1} (Fig. 1B). However tissue Cl concentration increased in a polynomial manner (Fig. 2B).

Increased salinity resulted in a near-linear decrease of dry mass of leaf blades, leaf petioles and stolons of *H. vulgaris* (Fig. 3A). In *A. tripolium* low NaCl concentration (up to 50 mM) had no effect on growth of leaves although a progressive decrease in leaf mass

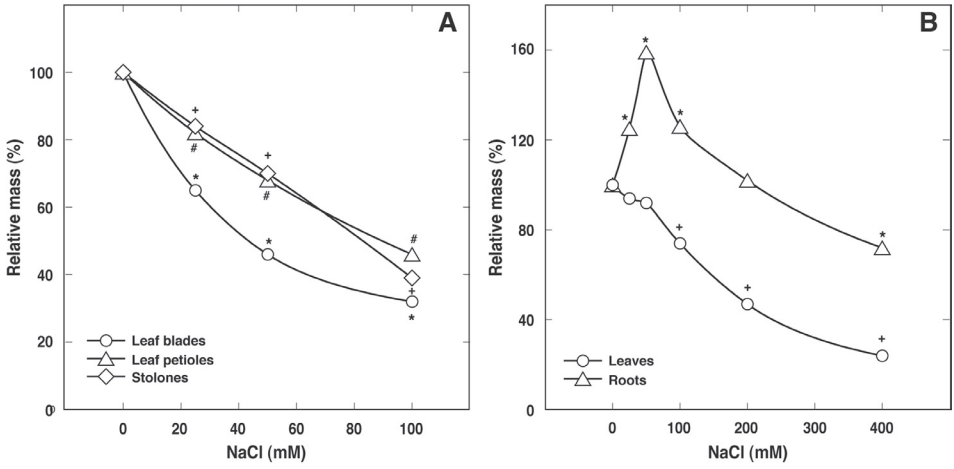

Fig. 3. Effect of different NaCl concentrations on a relative final mass of *Hydrocotyle vulgaris* (A) and *Aster tripolium* (B) organs. ⋆, #, +, statistically significant differences from control ($P < 0.01$) for a particular species and tissues.

was evident at higher concentrations (Fig. 3B). In contrast low NaCl (up to 100 mM) stimulated root growth while inhibition was visible only at 400 mM NaCl.

Effect of NaCl on nutrient concentration

Concentration of N increased in all tissues of *H. vulgaris* treated with 25 to 100 mM NaCl (Fig. 4A). However only 100 mM NaCl treatment resulted in increase of N concentration in leaves of *A. tripolium* (Fig. 4B). In contrast significant decrease of N concentration was found in roots of *A. tripolium* treated with 25 to 200 mM NaCl. Tissue P concentration of NaCl-treated *H. vulgaris* plants showed a concentration-dependent increase (Fig. 5A). In *A. tripolium* treated with NaCl P decreased in leaves (25 to 200 mM) while increased in roots (200 to 400 mM; Fig. 5B).

Response of K concentration in NaCl-treated *H. vulgaris* plants depended on the tissues analyzed. While a decrease of K was found in leaf blades, there was a stimulation of increase in the concentration in leaf petioles by NaCl and no significant changes in stolons (Fig. 6A). In tissues of both leaves and roots of *A. tripolium* 50 to 100 mM NaCl caused a small but statistically significant decrease of K concentration with a following increase at higher NaCl (Fig. 6B).

Increased substrate NaCl resulted in a small but statistically significant decrease of Ca concentration in leaf blade tissues of *H. vulgaris* and increase in leaf petiole tissues (data not shown). Only nonsignificant changes were found for both leaf and root tissues of *A. tripolium* in respect to Ca concentration. No changes in Mg concentration were observed in leaf petioles and stolons of *H. vulgaris* and both leaves and roots of *A. tripolium* (data not shown). NaCl caused significant decrease in Mg concentration only in leaf blade tissues of *H. vulgaris*.

One of most contrasting species-dependent effects of NaCl was found for changes in S concentration. There was a decrease in S concentration in leaf blades of *H. vulgaris* treated with 50 to 100 mM NaCl (Fig. 7A). However the same concentration resulted in increase

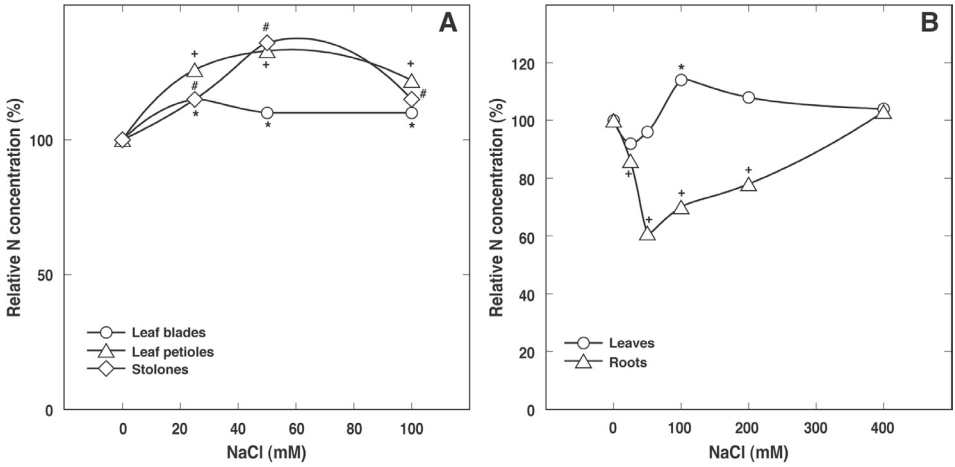

Fig. 4. Effect of different NaCl concentrations on relative tissue N concentration in different organs of *Hydrocotyle vulgaris* (A) and *Aster tripolium* (B). ⋆, #, +, statistically significant differences from control (P < 0.01) for a particular species and tissues.

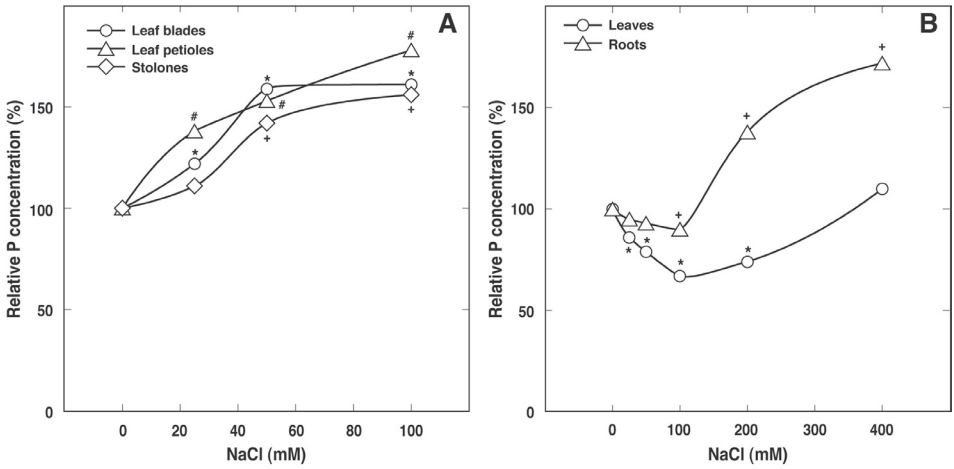

Fig. 5. Effect of different NaCl concentrations on relative tissue P concentration in different organs of *Hydrocotyle vulgaris* (A) and *Aster tripolium* (B). ⋆, #, +, statistically significant differences from control (P < 0.01) for a particular species and tissues.

of S level in stolons while in leaf petioles NaCl treatment resulted in more than a two-fold increase in tissue S concentration. In contrast, S concentration decreased in both leaf and root tissues of *A. tripolium* (Fig. 7B).

Similar to macronutrients NaCl treatment resulted in different effect in respect to concentration of various micronutrients in tissues of *H. vulgaris* and *A. tripolium*. Only minor changes due to NaCl treatment were found in Fe concentration in leaf blades and stolons of *H. vulgaris*, where 100 mM NaCl slightly stimulated it in the blades while inhibiting in stolons (Fig. 8A). However, there was linear increase of Fe concentration in leaf petiole tissues with increasing NaCl concentration. Similarly NaCl treatment resulted

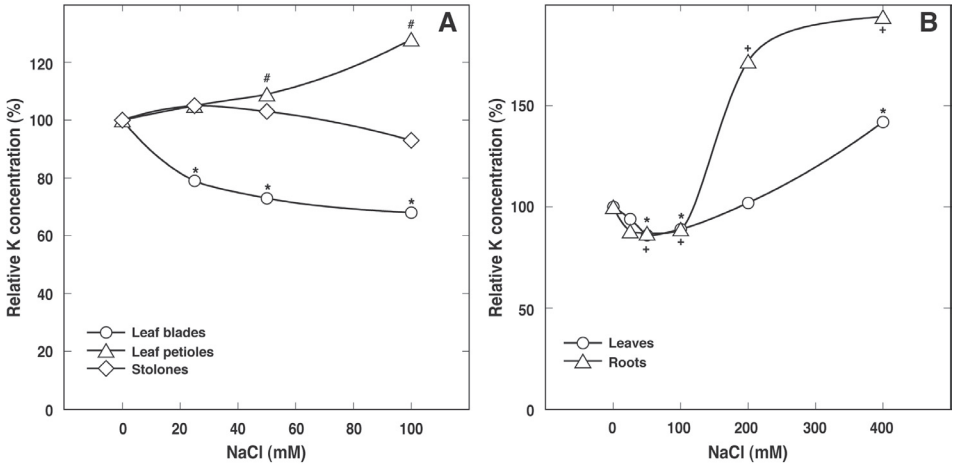

Fig. 6. Effect of different NaCl concentrations on relative tissue K concentration in different organs of *Hydrocotyle vulgaris* (A) and *Aster tripolium* (B). ⋆, #, +, statistically significant differences from control (P < 0.01) for a particular species and tissues.

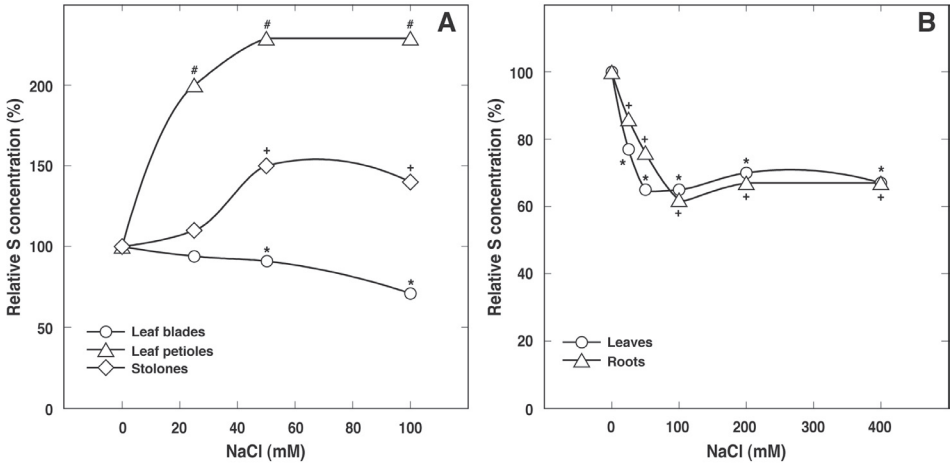

Fig. 7. Effect of different NaCl concentrations on relative tissue S concentration in different organs of *Hydrocotyle vulgaris* (A) and *Aster tripolium* (B). ⋆, #, +, statistically significant differences from control (P < 0.01) for a particular species and tissues.

in increase of Fe concentration in both leaves and roots of *A. tripolium* (Fig. 8B).

The most pronounced stimulation of mineral concentration by NaCl was found for Mn. Concentration of Mn increased in all tissues analyzed from both species (Fig. 9A, B). A maximum increase in *H. vulgaris* was more than five-fold in leaf petiole tissues treated by 100 mM NaCl. In roots of *A. tripolium* the highest increase (by four times) was observed for 200 mM NaCl treatment.

No changes in Zn concentration were caused by NaCl in tissues of both *H. vulgaris* and *A. tripolium* (data not shown).

In all tissues of both *H. vulgaris* and *A. tripolium* plants treated with NaCl there was an

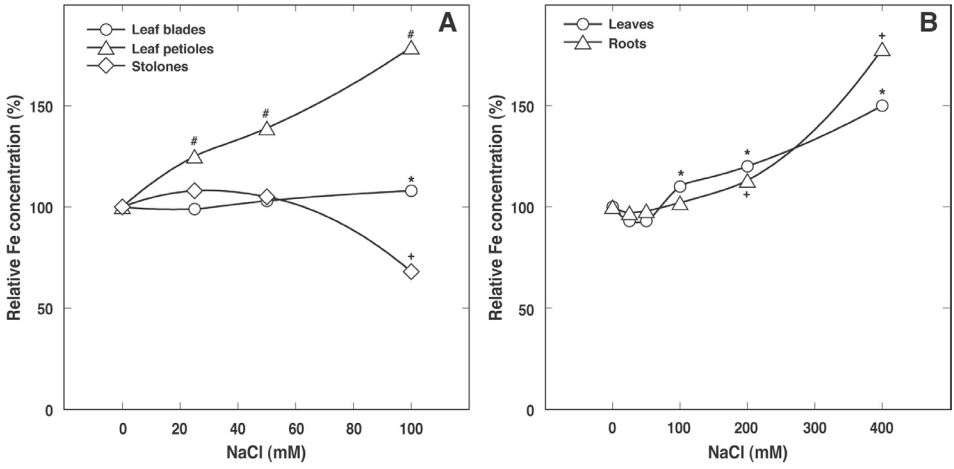

Fig. 8. Effect of different NaCl concentrations on relative tissue Fe concentration in different organs of *Hydrocotyle vulgaris* (A) and *Aster tripolium* (B). ⋆, #, +, statistically significant differences from control (P < 0.01) for a particular species and tissues.

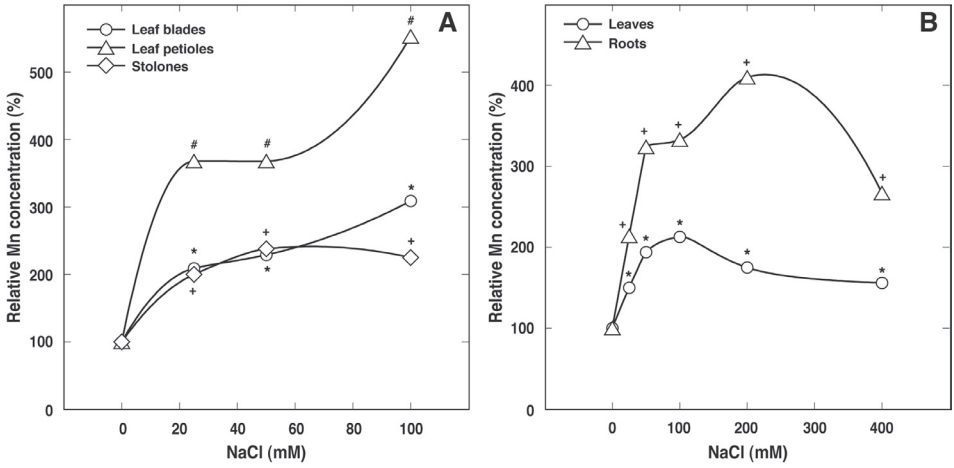

Fig. 9. Effect of different NaCl concentrations on relative tissue Mn concentration in different organs of *Hydrocotyle vulgaris* (A) and *Aster tripolium* (B). ⋆, #, +, statistically significant differences from control (P < 0.01) for a particular species and tissues.

increase in Cu concentration (Fig. 10A, B). However there were no statistically significant changes at 25 to 50 mM NaCl for leaf blades and stolons of *H. vulgaris* (Fig. 10A) and at 25 to 100 mM and 25 to 50 mM for leaves and roots of *A. tripolium*, respectively (Fig. 10B).

A slight increase in B concentration was found in *A. tripolium* leaves at 200 to 400 mM NaCl (data not shown). Tissue Mo concentration showed an increase in leaf petioles and stolons of *H. vulgaris* under the effect of NaCl while no changes were visible in *A. tripolium* (data not shown).

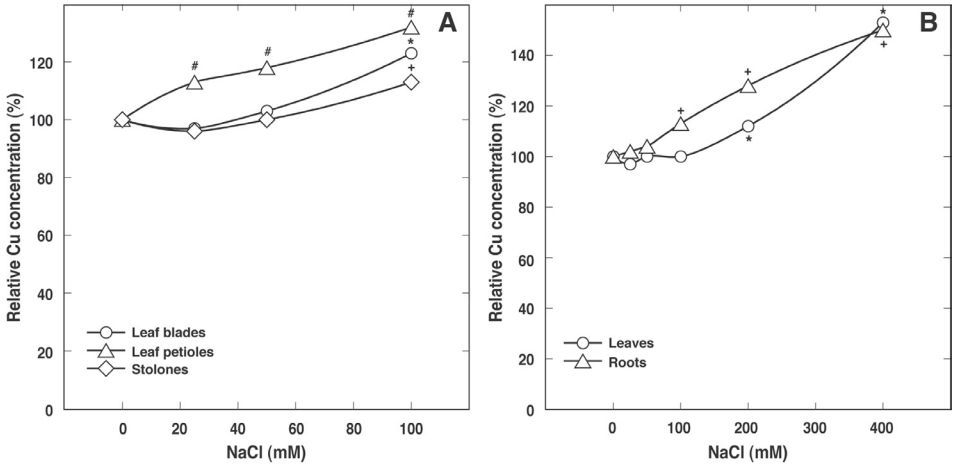

Fig. 10. Effect of different NaCl concentrations on relative tissue Cu concentration in different organs of *Hydrocotyle vulgaris* (A) and *Aster tripolium* (B). ⋆, #, +, statistically significant differences from control ($P < 0.01$) for a particular species and tissues.

Discussion

It is generally recognized that increased soil salinity differently affects concentration of different mineral elements in plant tissues (Romero, Marañón 1996). The presented data clearly show that the two species studied possess both similar and different responses of nutrient uptake in conditions of elevated salinity, thus reflecting a presence/absence of particular biochemical mechanisms of potential adaptive character. The differences in part could be due to different levels of salt tolerance in these species. *H. vulgaris* can be characterized as relatively salt-tolerant glycophyte with no increase in growth under elevated salinity (Fig. 3). *A. tripolium* is a moderately tolerant halophyte where only growth of underground parts are stimulated at moderate salinity (25 to 100 mM NaCl, Fig. 3). Consequently, some effects of elevated mineral concentrations under high salinity might be attributed to maintaining a constant uptake in a situation when growth of the organ is inhibited, resulting in increase of concentration of a particular mineral (Rinkis et al. 1989), which could be the case for *H. vulgaris* in all treatments and *A. tripolium* at NaCl higher than 200 mM. In addition, increased concentration of a particular mineral could be related to maintaining a nutrient balance at elevated Na and Cl concentrations in plant tissues (Grattan, Grieve 1993).

In respect to NaCl itself it is generally believed that more than 90 % of the Na in halophytes is located in the shoot (Flowers et al. 1977). In the present study this was the case for *H. vulgaris* but not for *A. tripolium*. At highest substrate NaCl concentration both leaves and roots of *A. tripolium* accumulated similar concentrations of both Na and Cl (Fig. 1, 2). Another difference between the species in terms of Na and Cl accumulation was related to saturability of the response in *H. vulgaris* in contrast to *A. tripolium* where no saturation was evident. However it can not be ruled out that concentration of Na and Cl in tissues of *A. tripolium* is saturable at higher substrate NaCl concentration.

In terrestrial ecosystems both N as well as P can be growth-limiting macronutrients

(Aerts, Chapin 2000). Under salt stress conditions, the uptake of N by plants is generally affected. Reports show both inhibitory (Bernstein 1974; Messedi et al, 2004) and stimulatory (Sági, Erdei 2005) effects on the plant N uptake under high salinity for different species. In contrast, only minor changes in N uptake were found in NaCl-treated plants in the present experiments (Fig. 4). While most of the studies demonstrating stimulative effect of salinity on tissue P concentration were performed in sand or solution cultures (Grattan, Grieve 1993) our results supported the idea that salinity enhances uptake of P by roots (Fig. 5). This effect was most pronounced for *H. vulgaris*. These observations were contradictory to the earlier study by Ullrich-Eberius and Yingchol (1974).

The maintenance of a high cytosolic K/Na concentration ratio is a key requirement for plant growth in salt (Glenn et al. 1999). Higher K/Na ratio can improve plant resistance to salinity (Asch et al. 2000). It is widely recognized that a high Na concentration inhibits K uptake by plants (Grattan, Grieve 1993; Dorsaf et al 2004; Fuchs et al. 2005). On the other hand, Na appeared to stimulate the K content in several species (Mahmooad 1996; Basra, Basra 1997). No difference in K uptake was evident in previous experiments with *A. tripolium* leading to significant increase in the ratio Na to K (Ramani et al. 2006). In the vacuole the amount of Na clearly increased with increasing NaCl concentration while the amount of K was relatively unaffected. In contrast, Cooper (1982) found about a three-fold decrease in K concentration in *A. tripolium* leaves together with a decline in Ca content. In the present experiments K concentration increased both in leaves and roots of *A. tripolium* and decreased in leaf blades of *H. vulgaris* under the effect of increasing NaCl concentration (Fig. 6) thus supporting the idea that a higher K/Na ratio is indeed associated with higher salinity tolerance and can be regarded as an adaptive response (Ben Hamed 2008).

Calcium is known to play a special role in tolerance under salinity. Increased concentration of Ca in cells has a certain protective effect against high NaCl concentration including minimization of leakage of cytosolic K as well as protection of membrane integrity against Na replacement of Ca and Mg (Cramer et al. 1988). In the present experiments no significant changes in Ca level were observed indicating that this was not the case. Reduced accumulation of Ca in leaves and increased in roots is a common response of halophytic species to increased salinity (Romero, Marañón 1996). In addition it was suspected that the sensitivity of *Arabidopsis* plants to 50 mM NaCl was due to inhibition of K or Ca root transport (Attia et al. 2008). A high K and Ca level could contribute to osmoprotection (Bohnert et al. 1999). However, it was shown that salinity caused a decrease in concentrations of K and Ca in wheat plants only at deficient nutrient solution macronutrient concentrations (Hu, Schmidhalten 1997)

The most striking effect of elevated substrate NaCl was found in respect to Mn concentration, which increased in all the organs of both species (Fig. 8). Increase of Mn concentration with salinity has been noted for the annual legume *Melilotus segetalis*, which is well adapted to elevated salinity (Romero, Marañón 1996) and for other halophytic plant species (Williams 1994). It could be assumed that increased uptake of Mn, Fe and Cu with increasing substrate salinity in the present study is related to equalization of ion uptake. In contrast to our results, in another study with *A. tripolium* increased substrate salinity resulted in a three-fold decrease in shoot K and Mn concentration as well as a statistically significant decrease of Ca and Fe (Cooper 1982). Surprisingly, NaCl treatment in drained conditions did not result in elevated shoot Na concentration in these experiments.

Sulfur is a key element in plant stress responses because of a well known role of glutathione in antioxidative defense (Rausch, Wachter 2005; Baker, Pilbeam 2007). A striking difference was found in the present experiments between the studied species in respect to the effect of increased substrate NaCl on tissue S concentration (Fig. 6). While a decrease in S content was found in leaves of both species and in root tissues of *A. tripolium*, a significant increase was evident both in leaf petioles and stolons of *H. vulgaris* indicating that the observed changes in the latter case of could be attributed to an indirect effect of NaCl.

While no general trend was found in the present experiments for the effect of high NaCl on mineral concentrations in tissues of *H. vulgaris* and *A. tripolium*, adaptive responses leading to maintenance of an optimal supply of mineral nutrients in conditions of high Na and Cl concentrations in cells can be seen. When the same changes of a particular nutrient were evident under the effect of elevated substrate NaCl, both in leaves and roots or in leaf blades and leaf petioles of *A. tripolium* and *H. vulgaris*, respectively, where comparable concentrations of NaCl accumulated, the direct effect of high tissue concentration of Na and Cl could be expected. In particular, this was the case with significantly decreased concentration of a particular mineral. When considering increased concentration of particular minerals in tissues at elevated substrate salinity both active equalization of ion uptake and an effect of growth inhibition-related ion accumulation should be taken in to the account.

Acknowledgements

The present study was supported by a grant from the University of Latvia.

References

Aerts R., Chapin F.S.III 2000. The mineral nutrition of wild plants revisited: a re-evaluation of processes and patterns. *Adv. Biol. Res*. 30: 1–67.

Asch F., Dingkuhn M., Miezan K., Dörfling K, 2000. Leaf K/Na ratio predicts salinity induced yield loss in irrigated rice. *Euphytica* 113: 109–118.

Attia H., Karray N., Rabhi M., Lachaal M. 2008. Salt-imposed restrictions on the uptake of macroelements by roots of *Arabidopsis thaliana*. *Acta Physiol. Plant.* 30: 723–727.

Basra A.S., Basra K.R. 1997. *Mechanisms of Environmental Stress Resistance in Plants.* CRC Press. 407 p.

Ben Hamed K., Messedi D., Ranieri A., Abdelly C. 2008. Diversity in the response of two potential halophytes (*Batis maritima* and *Crithmum maritimum*) to salt stress. In: Abdelly C. (ed) *Biosaline Agriculture and High Salinity Tolerance*. Birkhäuser, Basel, pp. 71–80

Bernstein L., Francois L.E., Clark R.A. 1974. Interactive effects of salinity and fertility on yields of grains and vegetables. *Agronomy J*. 66: 412–421.

Chapin F.S.III 1980. The mineral nutrition of wild plants. *Annu. Rev. Ecol. Syst.* 11: 233–260.

Cooper A. 1982. The effects of salinity and waterlogging on the growth and cation uptake of salt marsh plants. *New Phytol.* 90: 263–275.

Cramer G.R., Epstein E., Läuchli A. 1988. Kinetics of root elongation of maize in response to short-term exposure to NaCl and elevated calcium concentration. *J. Exp. Bot.* 39: 1513–1522.

Dorsaf M., Nehla L., Claude G., Chedly A. 2004. Limits imposed by salt to the growth of the halophyte *Sesuvium portulacastrum*. *J. Plant Nutr. Soil Sci.* 167: 720–725.

Flowers T.J., Troke P.F., Yeo A. R. 1977. The mechanism of salt tolerance in halophytes. *Annu. Rev. Plant Physiol.* 28: 89–121.

Fuchs I., Stölzle S., Ivashikina N., Hedrich R. 2005. Rice K^+ uptake channel OsAKT1 is sensitive to salt stress. *Planta* 221: 212–221.

Glenn E.P., Olsen M., Frye R., Moore D., Miyamoto S. 1994. How much sodium accumulation is necessary for salt tolerance in subspecies of the halophyte *Atriplex canescens* L. P*lant Cell Environ.* 17: 711–719.

Grattan S.R., Grieve C.M. 1993. Mineral nutrient acquisition and response by plants grown in saline environments. In: Pessarakli M. (ed) *Handbook of Plant and Crop Stress*. Marcel Dekker, New York, pp. 203–226.

Hasegawa P.M., Bressan R.A., Zhu J.-K., Bohnert H.J. 2000. Plant cellular and molecular responses to high salinity. *Annu. Rev. Plant Physiol. Plant Mol. Biol.* 51: 463–499.

Haswell S.J. 1991. *Atomic Absorption Spectrometry: Theory, Design and Applications*. Elsevier. Amsterdam.

Hu Y., Schmidhalter U. 1997. Interactive effects of salinity and macronutrient level on wheat. 2. Composition. *J. Plant Nutr.* 20: 1169–1182.

Klavina D., Gailite A., Ievinsh G. 2006. Initial responses of explants from rare and endangered coastal plants during initiation of tissue culture. *Acta Univ. Latv.* 710: 81–91.

Levine J.M., Brewer J.S., Bertness M.D. 1998. Nutrients, competition and plant zonation in a New England salt marsh. *J. Ecol.* 86: 285–292.

Mahmood K, Malik K.A., Lodhi M.A.K., Sheikh K.H. 1996. Seed germination and salinity tolerance in plant species growing on saline wastelands. *Biol. Plant.* 38: 309–31??.

Patnaik P. 1997. *Handbook of Environmental Analysis*. CRC Press. 584 p.

Pennings S.C., Grant M.-B., Bertness M.D. 2005. Plant zonation in low-latitude salt marshes: distangling the roles of flooding, salinity and competition. *J. Ecol.* 93: 159–167.

Pitman M.G., Läuchli A. 2002. Global impact of salinity and agricultural ecosystems. In: Läuchli A., Luttge U. (eds) *Salinity: Environment – Plants – Molecules*. Kluwer Academic Publishers, Dordrecht, pp. 3–20.

Ramani B., Reeck T., Debez A., Stelzer R., Huchzemeyer B., Scmidt A., Papenbrock J. 2006. *Aster tripolium* L. and *Sesuvium portulacastrum* L.: two halophytes, two strategies to survive in saline habitats. *Plant Physiol. Biochem.* 44: 395– 408.

Rausch T., Wachter A. 2005. Sulfur metabolism: a versatile platform for launching defence operations. *Trends Plant Sci.* 10: 503–509.

Rinkis G., Ramane H., Kunicka T. 1987. *Methods of Soil and Plant Analysis*. Zinatne, Riga. (in Russian)

Rinkis G., Ramane H., Paegle G., Kunicka T. 1989. *System of Optimization and Diagnostic Methods of Plant Mineral Nutrition*. Zinatne, Riga. (in Russian)

Romero J.M., Marañón T. 1996. Allocation of biomass and mineral elements in *Meliotus segetalis* (annual sweetclover): effects of NaCl salinity and plant age. *New Phytol.* 132: 565–573.

Rozema J., Blom B. 1977. Effects of salinity and inundation on the growth of *Agrostis stolonifera* and *Juncus gerardii*. *J. Ecol.* 65: 213–222.

Sági B., Erdei L. 2005. Adaptive responses to high salinity of two subspecies of *Aster tripolium* on different nitrogen sources. *Acta Biol. Szeged.* 49: 115–116.

Ullrich-Eberius C.I., Yingchol Y. 1974. Phosphate uptake and its pH-dependence in halophytic and glycophytic algae and higher plants. *Oecologia* 17: 17–26.

Williams T.P., Bubb J.M., Lester J. 1994. The occurrence and distribution of trace metals in halophytes. *Chemosphere* 28: 1189–1199.

Minerālā statusa izmaiņas piekrastes augiem *Hydrocotyle vulgaris* un *Aster tripolium* paaugstināta augsnes sāļuma ietekmē

Andis Karlsons[1], Anita Osvalde[1], Jevgenija Ņečajeva[2], Ģederts Ieviņš[2]

[1]Minerālās barošanās laboratorija, LU Bioloģijas institūts, Miera 3, Salaspils LV-2169, Latvija
[2]Augu fizioloģijas katedra, Latvijas Universitātes Bioloģijas fakultāte, Kronvalda bulv. 4, Rīga LV-1586, Latvija
*Korespondējošais autors, E-pasts: andis_@one.lv

Kopsavilkums

Darba mērķis bija izpētīt paaugstināta NaCl satura substrātā ietekmi uz minerālvielu koncentrāciju divu jūras piekrastes augu *Hydrocotyle vulgaris* un *Aster tripolium* audos. Paaugstinātais substrāta sāļums, ko panāca, laistot augus ar NaCl šķīdumu, izsauca Na un Cl jonu uzkrāšanos abu pētīto augu sugu audos. *H. vulgaris* lapu plātnēs un kātos gan Na, gan Cl koncentrācija bija piesātināma. Pretēji tam, Na un Cl koncentrācija *A. tripolium* lapu un sakņu audos pieauga, palielinoties to koncentrācijai substrātā. N un P koncentrāciju atšķirīgi ietekmēja pieaugošs substrāta NaCl daudzums: N un P līmenis palielinājās *H. vulgaris* audos, N koncentrācija samazinājās , bet P koncentrācija – pieauga *A. tripolium* saknēs. NaCl ietekme uz S saturu bija pretēja abām pētītajām sugām – tas pieauga *H. vulgaris* lapu kātos un stolonos, bet samazinājās gan *A. tripolium* lapās, gan saknēs. Visizteiktākais pieaugums NaCl ietekmē bija novērojams attiecībā uz Mn. Cu koncentrācijas pieaugums bija raksturīgs abu sugu visiem audiem, bet Fe koncentrācija pieauga *A. tripolium*, kā arī *H. vulgaris* lapās. Var secināt, ka pētāmajiem augiem piemīt iespējami adaptīvas reakcijas, kas vērstas uz optimāla minerālvielu satura nodrošināšanu augstas šūnu Na un Cl koncentrācijas apstākļos.

Acta Universitatis Latviensis, 2008, Vol. 745, Biology, pp. 179–186

Growth of tissue culture and changes in oxidative enzyme activity of *Sorbus* and tayberry cultivars during cold storage

Dace Kļaviņa[1]*, Gederts Ievinsh[2]

[1]Tissue Culture Department, National Botanical Garden, Miera 1, Salaspils LV-2169 Latvia
[2]Department of Plant Physiology, Faculty of Biology, University of Latvia, Kronvalda Bulv. 4, Rīga LV-1586, Latvia

*Corresponding author, E-mail: dace.klavina@nbd.gov.lv

Abstract

The aim of the present work was to compare the effect of different concentrations of sucrose on success of long-term cold storage of two woody plant tissue cultures – *Sorbus* and tayberry cultivars. Increased sucrose concentration significantly diminished the number of necrotic shoots for *Sorbus* explants. High sucrose concentration in the medium together with other optimal cultivation conditions allowed successful storage of *Sorbus* and tayberry cultivars without subculturing for five years. After transplanting to fresh medium at 24 °C explants completely renewed growth and development. During the period of initial growth inhibition at low temperature the activity of oxidative enzymes peroxidase and polyphenol oxidase increased, reaching a peak value when growth of the explants resumed. Increase of both peroxidase and polyphenol oxidase activity during the period of growth inhibition was positively correlated with the concentration of sucrose in the incubation medium.

Key words: cold storage, oxidative enzymes, *Sorbus*, sucrose, tayberry, tissue culture.

Introduction

Cold storage or slow growth of plant tissue cultures is widely used as a method for maintenance of *in vitro* collections of plant tissues (Blakesley et al. 1996). The cold storage success of each taxon is determined genetically (Engelmann et al. 1997; Palonen, Buszard 1998), but it also depends on storage temperature, illumination, cultivation medium composition as well as preconditioning of tissue cultures before low temperature application (Wilson et al. 1998; Jouve et al. 2000). Addition of sucrose to the medium increases dry mass and maintains overall plantlet quality during cold storage (Wilson et al. 1998; Palonen, Junttila 1999).

Transfer to cold induces expression of wide array of genes, many of which are related to adaptation to cold (Chinnusamy et al. 2006). From the first days of low temperature storage explants undergo significant biochemical change in oxidative metabolism (Jouve et al. 2000). Peroxidases and polyphenol oxidase are important constituents of enzymatic oxidative metabolism, leading to formation of bioactive phenolic compounds (Mika et al. 2004; Mayer 2006). Consequently, increased activity of peroxidase or polyphenol

oxidase in cultivated plant tissues during cold storage may be an indication of deleterious metabolic changes.

The aim of the present experiments was to compare the effect of different concentrations of sucrose on success of long-term cold storage of two different commercially important woody plant tissue cultures – *Sorbus* and tayberry cultivars. Oxidative enzyme activity was monitored as an indicator of oxidative metabolism.

Materials and methods

The *Sorbus* cultivar ‚Krasnaja Krupnaja' and tayberry cultivar ‚Medana' maintained for several years in tissue culture were used for cold storage experiments. As explants, shoot fragments (2 cm in length) from proliferating culture were planted on Murashige-Skoog medium with addition of 0.3 mg L^{-1} 6-benzylaminopurine) and different concentrations of sucrose (30, 40, 60 g L^{-1}). The cultures were adapted on the medium at 25 °C (photoperiod 16 h, PAR 40 μmol s^{-1} m^{-2}) for three weeks before transfer to low temperature (5 °C, photoperiod 16 h, PAR 20 μmol s^{-1} m^{-2}) cold storage.

Samples for enzyme analysis during the first month of cold storage were taken every two weeks, later – once a month. Enzymes were extracted from frozen explant tissues ground to fine powder with 25 mmol L^{-1} HEPES/KOH buffer (pH 7.2) containing 3 % polyvinylpolypirrolidone (w/v). Peroxidase (EC 1.11.1.7) and polyphenol oxidase (EC 1.10.3.2) activity was measured spectrophotometrically as described previously with guaiacol plus H_2O_2 and pyrocatechol as substrates, respectively (Andersone, Ievinsh 2002). Four replicates of enzyme determination for each time point were performed.

Results

Sorbus explants were successfully cultivated for 5 years in conditions of cold storage at 5 °C. Three media differing in sucrose concentration were used in the present experiments

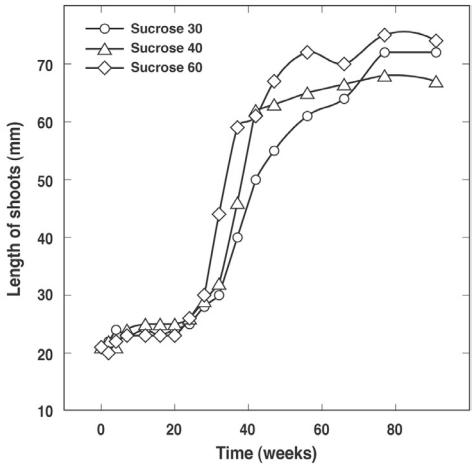

Fig. 1. Growth of shoot explants of *Sorbus* cv.‚Krasnaja Krupnaja' at different sucrose concentrations during cold storage at 5 °C.

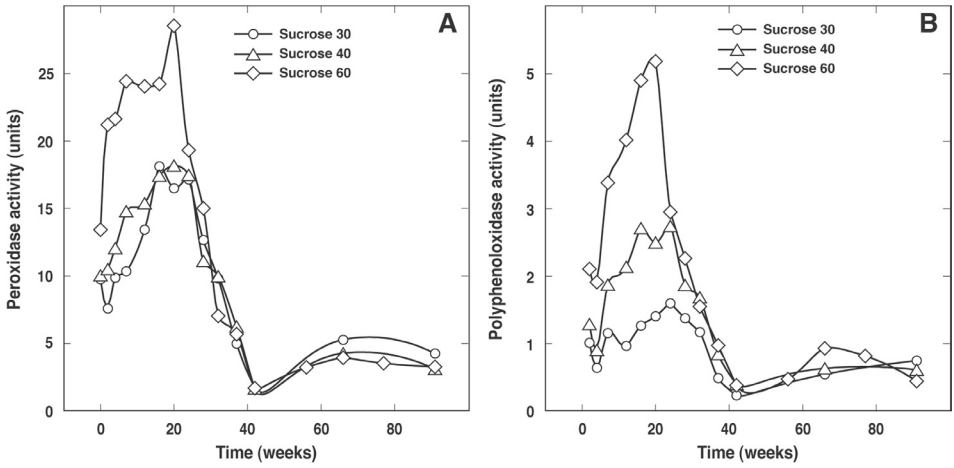

Fig. 2. Time course of peroxidase (A) and polyphenol oxidase (B) activity in explants of *Sorbus* cv. ‚Krasnaja Krupnaja' at different sucrose concentrations during cold storage at 5 °C.

for cold storage. Complete growth inhibition of *Sorbus* explants was evident at all sucrose concentrations used for cultivation from week 10 till 20 (Fig. 1). During that period activity of oxidative enzymes peroxidase and polyphenol oxidase increased reaching a peak value at the time when growth of the explants resumed (Fig. 2). The growth inhibition-related increase in oxidative enzyme activity depended on the sucrose concentration used for cultivation – the increase was highest at 60 g L^{-1} sucrose concentration. However sucrose concentration did not affect growth characteristics of *Sorbus* explants in the growth inhibition stage during cold storage. When intensive growth of explants started after 37 weeks of cultivation in cold conditions, explants grown at higher sucrose concentration (40 and 60 g L^{-1}) had a tendency to have higher growth rates (Fig. 1). However the effect was not seen at later stages. Cytokinin stimulated formation of adventitious shoots (1.3 to 1.5 per initial explant in average). Adventitious shoot formation was not affected by the sucrose concentration used. However after 91 weeks of cold cultivation, an increased concentration of sucrose in the medium diminished the amount of necrotic shoots (Table 1). The effect was more pronounced for the main shoots in comparison to adventitious shoots. At the highest sucrose concentration (60 g L^{-1}) all explants were viable after 5 years of cold storage without subcultivation. No root formation was evident on *Sorbus* explants

Table 1. Effect of sucrose concentration on the number of necrotic shoots (as % from initial explants for main shoots or % from newly formed adventitious shoots) on *Sorbus* explants after 91 weeks of cultivation at 5 °C

	Number of necrotic shoots (%)	
Sucrose concentration (g L^{-1})	**Main shoots**	**Adventitious shoots**
30	55 ± 5	32 ± 4
40	30 ± 4	28 ± 2
60	15 ± 2	17 ± 3

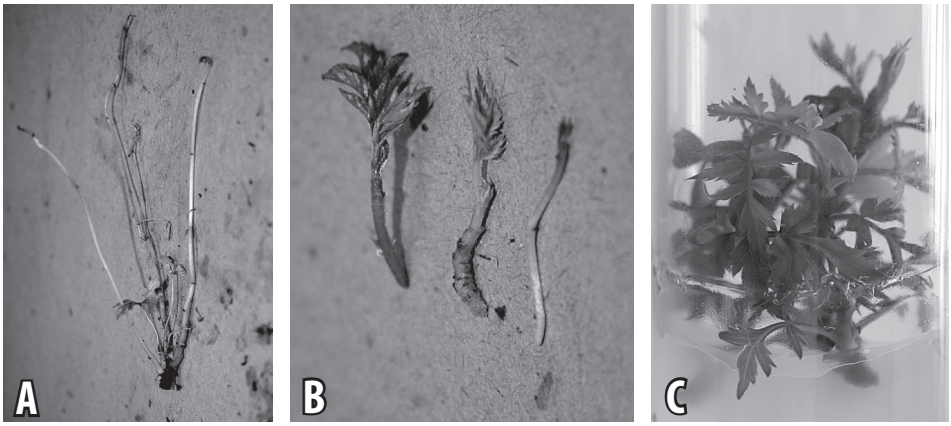

Fig. 3. A, microshoots formed from one explant of *Sorbus* cv. ‚Krasnaja Krupnaja' after 5 years of cold storage at 5 °C. B, cold-stored explants before transfer to a fresh medium. C, the same explants after one month at 24 °C.

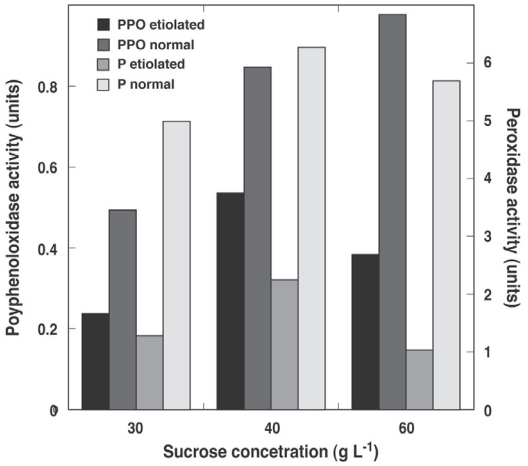

Fig. 4. Effect of morphological characteristics of shoots formed on *Sorbus* explants stored at 5 °C for 37 weeks on peroxidase and polyphenol oxidase activity during the stage of active growth.

during cultivation. In contrast, at lower sucrose concentrations all explants died after 3 to 4.5 years of cold cultivation.

Sorbus microshoots from explants cultivated 5 years in the cold were suitable for further propagation (Fig. 3A, B). After explanting to fresh medium at 24 °C they completely renewed growth and development (Fig. 3C).

After transfer from 24 °C to cold storage conditions (5 °C) the activity of both oxidative enzymes examined increased in cultivated tissues of *Sorbus*, reaching maximum values 16 to 24 weeks after the start of cold storage (Fig. 2). The increase was most pronounced at highest sucrose concentration (60 g L^{-1}), being five times and three times that of initial activity, for polyphenol oxidase and peroxidase, respectively. However the difference disappeared during the latter stages of cultivation. During activated shoot growth there

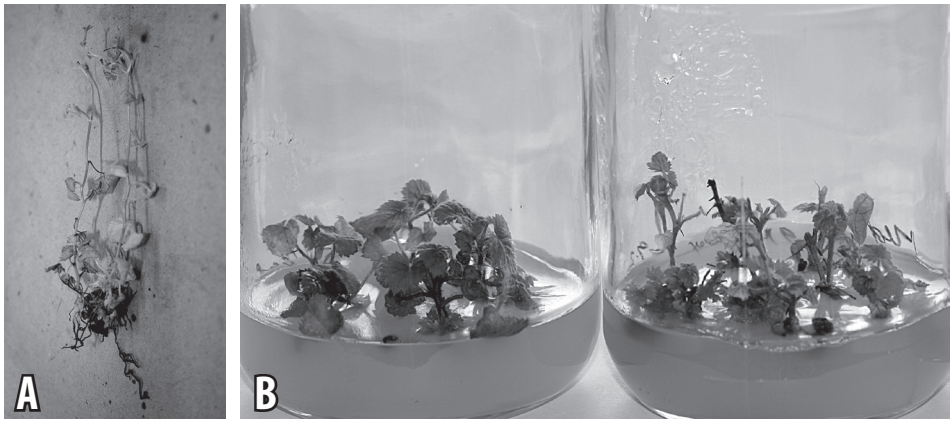

Fig. 5. A, microshoots formed from one explant of tayberry ‚Medana' stored at 5 °C for 5 years (sucrose 30 g L^{-1}). B, regrowth of new explants after transfer to a fresh medium containing sucrose 40 g L^{-1} (left) or 60 g L^{-1} (right).

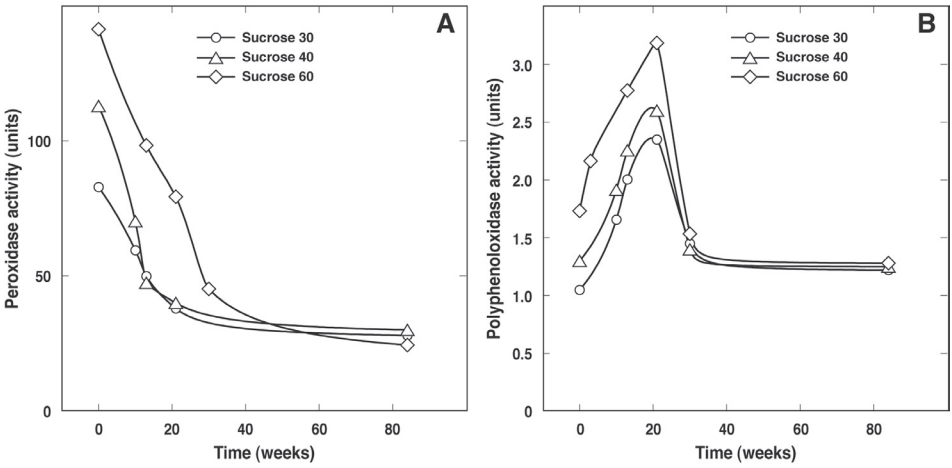

Fig. 6. Time course of peroxidase (A) and polyphenol oxidase (B) activity in explants of tayberry ‚Medana' at different sucrose concentrations during cold storage at 5 °C.

was a dramatic decrease of enzyme activities.

At the stage of growth activation from week 30 oxidative enzyme activity was analyzed separately in normal and extremely elongated etiolated shoots. Etiolated shoots had an average fresh mass of 29 ± 5 mg in contrast to 67 ± 7 for normal shoots. Elongated shoots had significantly lower activity of both polyphenol oxidase and peroxidase at all tested sucrose concentrations (Fig. 4).

Tayberry cv. ‚Medana' explants were successfully cultivated at 5 °C for 5 years. Growth of explants was less inhibited than in the case of *Sorbus* explants. In addition, in contrast to *Sorbus* where only the highest sucrose concentration (60 g L^{-1}) in the medium was suitable for long storage, tayberry explants cultivated at all sucrose concentrations (30, 40, 60 g L^{-1}) were completely viable and suitable for further micropropagation (Fig. 5A). After transfer

to a fresh medium these explants developed normally at 24 °C (Fig. 5B).

Root formation was monitored during cold storage of tayberry explants at all sucrose concentrations, during the period of low peroxidase activity (21 to 30 weeks of cultivation; Fig. 6).

Tayberry cv. ‚Medana' explants showed a similar time course of oxidative enzyme activity during cold storage as found for *Sorbus* explants (Fig. 6). However the period of cold transfer-induced increase in the activity was relatively shorter, especially for peroxidase activity. Increase of both peroxidase and polyphenol oxidase activity during the period of growth inhibition was positively correlated with the concentration of sucrose in the medium. Average peroxidase activity in tayberry explants was about 10 times that in *Sorbus* explants, while the average polyphenol oxidase activity in both cultures was in the same range.

Discussion

Successful storage without subculturing for woody plant species usually is up to two years. The longest cold storage reported so far is 60 months for *Eucalyptus grandis* shoot explants (Hausman et al. 1994). In the present work storage without subculturing of equivalent length was achieved by *Sorbus* and tayberry cultivars. The explants were suitable for further micropropagation with vigorous regrowth at 24 °C.

Growth inhibition is a necessary prerequisite for preservation of plant tissues by a slow growth technique. Thus, cold incubation-induced slow growth of plant tissue cultures resembles natural dormancy period of vegetative tissues in the temperate region. However, three phases in respect to growth processes were clearly distinguishable during cold storage of both *Sorbus* and tayberry explants in the present experiments: growth inhibition for a initial 20 weeks of cold incubation followed by a relatively rapid shoot elongation (30 to 40 weeks), and further a reduced but relatively stable growth rate. Similar to our observations, it was already described earlier that woody plant cultures grow during cold storage (Pruski et al. 2000).

During the first phase of cold incubation explant tissues undergo cold acclimation. Low temperature as a signal acts through abscisic acid-dependent signaling pathways leading to physiological and biochemical changes characteristic for „end of summer" responses (Welling, Palva 2006). Increased protection against endogenous oxidative stress is one of the prerequisites of cold acclimation (Renaut et al. 2005). Thus, growth inhibition and an increase in peroxidase activity in the present experiments is related at the level of both nonspecific antioxidative protection as well as to general oxidative metabolism together with polyphenol oxidase. A distinct relationship between a relatively high activity of oxidative enzymes and a minimum growth rate was evident during the first phase of cold storage. As sucrose stimulated both peroxidase and polyphenol oxidase activity a casual relationship between cold-induced suppression of growth and increased oxidative metabolism can be suggested. The low level of activity of both enzymes during the second and the third phase of cold storage clearly indicated the absence of any oxidative-stress related metabolic disorders for all experimental treatments in spite of shoot necrosis at lower sucrose concentration for *Sorbus* explants.

Sucrose concentration in the medium was extremely important for successful cold storage of *Sorbus* explants. An increased sucrose concentration significantly diminished

the number of necrotic shoots (Table 1), and 100 % viability after five years of cold storage was achieved. In addition, there was a positive correlation between sucrose concentration and oxidative enzyme activity during the period of growth inhibition of both *Sorbus* and tayberry explants. Significant differences in oxidative enzyme activity as noted for *Sorbus* and tayberry explants was described previously also for *Rubus* and *Cerasus* cultivars (Klavina et al. 2001).

The presence of sucrose in the medium has been shown to be of critical importance during prolonged cold storage of several plant cultures (Pruski et al. 2000). A high sucrose level during *in vitro* cultivation of olive microshoots was important for further cold tolerance (Bartolozzi et al. 2001). In cold acclimation, during the initial stage of slow growth sucrose might act both as an osmoprotectant (Nagao et al. 2005; Suzuki et al. 2006) as well as one of the signals for successful growth inhibition of explants (Rolland et al. 2002). It is well known that many stress- and abscisic acid-inducible genes are coregulated by sugars (Rolland et al. 2002).

In conclusion the present experiments clearly showed that for woody plant cultivars e.a. *Sorbus* and tayberry high sucrose concentration is of extreme importance during cold incubation-induced slow growth storage. Together with other optimal cultivation conditions, storage without subculturing for five years is successful.

References

Andersone U., Ievinsh G. 2002. Changes of morphogenic competence in mature *Pinus sylvestris* L. *in vitro*. *Ann. Bot.* 90: 293–298.

Bartolozzi F., Mencuccini M., Fontanazza G. 2001. Enhancement of frost tolerance in olive shoots *in vitro* by cold acclimation and sucrose increase in the culture medium. *Plant Cell Tissue Org. Cult.* 67: 299–302.

Blakesley D., Pask N., Henshaw G.G., Fay M.F. 1996. Biotechnology and conservation of forest genetic resources: *in vitro* strategies and cryopreservation. *Plant Growth Reg.* 20: 11–16.

Chinnusamy V., Zhu J., Zhu J.-K. 2006. Gene regulation during cold acclimation in plants. *Physiol. Plant.* 126: 52–61.

Engelmann F. 1997. *In vitro* conservation methods. In: Callow J.A., Ford-Lloyd B.V., Newbury H.J. (eds) *Biotechnology and Plant Genetic Resources*. CABI, Oxon, pp. 119–161.

Hausman J., Neys O., Kevers C., Gaspar T. 1994. Effect of *in vitro* storage at 4 °C on survival and proliferation of poplar shoots. *Plant Cell Tissue Org. Cult.* 38: 65–67.

Jouve L., Franck T., Gaspar T., Cattivelli L., Hausman J.-F. 2000. Poplar acclimation to cold during *in vitro* conservation at low non-freezing temperature: metabolic and proteic changes. *J. Plant Physiol.* 157: 117–123.

Klavina D., Ievinsh G., Megre D., Jakobsone G. 2001. Changes of physiological status during cold storage of *in vitro* cultivated plants. *Acta Hort.* 616: 425-428.

Mayer A.M. 2006. Polyphenol oxidases in plants and fungi: Going places? A review. *Phytochemistry* 67: 2318–2331.

Mika A., Minibayeva F., Beckett R., Lüthje S. 2004. Possible functions of extracellular peroxidases in stress-induced generation and detoxification of active oxygen species. *Phytochem. Rev.* 3: 173–193.

Nagao M., Minami A., Arakawa K., Fujikawa S., Takezawa D. 2005. Rapid degradation of starch in chloroplasts and concomitant accumulation of soluble sugars associated with ABA-induced freezing tolerance in the moss *Physcomitrella patens*. *J. Plant Physiol.* 162: 169–180.

Palonen P., Buszard D. 1998. *In vitro* screening for cold hardiness of raspberry cultivars. *Plant Cell Tissue Org. Cult*. 53: 213–216.

Palonen P., Junttila O. 1999. Cold hardening of raspberry plants *in vitro* is enhanced by increasing sucrose in the culture medium. *Physiol. Plant.* 106: 386–392.
Pruski K., Kozai T., Lewis T., Astakie T., Nowak J. 2000. Sucrose and light effects on *in vitro* cultures of potato, chokecherry and saskatoon berry during low temperature storage. *Plant Cell Tissue Org. Cult.* 63: 215–221.
Renaut J., Hoffmann L., Hausman J.-F. 2005. Biochemical and physiological mechanisms related to cold acclimation and enhanced freezing tolerance in poplar plantlets. *Physiol. Plant*. 125: 82–94.
Rolland F., Moore B., Sheen J. 2002. Sugar sensing and signaling in plants. *Plant Cell* S: S185–S205.
Suzuki M., Ishikawa M., Okuda H., Noda K., Kishimoto T., Nakamura T., Ogiwara I., Shimura I., Akihama T. 2006. Physiological changes in gentian axillary buds during two-step preculturing with sucrose that conferred high levels of tolerance to desiccation and cryopreservation. *Ann. Bot.* 97: 1073–1081.
Welling A., Palva E.T. 2006. Molecular control of cold acclimation in trees. *Physiol. Plant*. 127: 167–181.
Wilson S.B., Iwabuchi K., Rajapekse N.C., Young R.E. 1998. Responses of broccoli seedlings to light quality during low temperature storage *in vitro*. II. Sugar content and photosynthetic efficiency. *HortScience* 33: 1258–1261.

Pīlādžu un kazenes-avenes hibrīda augšana audu kultūrā un oksidatīvo fermentu aktivitātes izmaiņas aukstuma uzglabāšanas laikā

Dace Kļaviņa[1]*, Ģederts Ieviņš[2]

[1]Audu kultūru nodaļa, Nacionālais botāniskais dārzs, Miera 1, Salaspils LV-2169, Latvija
[2]Augu fizioloģijas katedra, Latvijas Universitātes Bioloģijas fakultāte, Kronvalda bulv. 4, Rīga LV-1586, Latvija
*Korespondējošais autors, E-pasts: dace.klavina@nbd.gov.lv

Kopsavilkums

Šī darba mērķis bija salīdzināt dažādu saharozes koncentrāciju ietekmi uz divu kokaugu kultūru – pīlādžu un kazenes-avenes hibrīda – ilgstošu uzglabāšanu pazeminātā temperatūrā. Paaugstināta saharozes koncentrācija ievērojami samazināja nekrotisko dzinumu daudzumu pīlādžu eksplantiem. Augsta saharozes koncentrācija barotnē kopā ar optimāliem kultivēšanas apstākļiem ļāva veiksmīgi uzglabāt pīlādžu un kazenes-avenes hibrīdu šķirnes piecus gadus bez pārstādīšanas. Pēc pārstādīšanas svaigā barotnē eksplanti pilnībā atjaunoja augšanu un attīstību 24 °C. Sākotnējās augšanas inhibēšanas laikā pazeminātā temperatūrā oksidatīvo fermentu peroksidāzes un polifenoloksidāzes aktivitāte paaugstinājās, sasniedzot maksimumu brīdī, kad eksplantu augšana atjaunojās. Abu fermentu aktivitātes pieaugums augšanas inhibēšanas laikā pozitīvi korelēja ar saharozes koncentrāciju barotnē.

Acta Universitatis Latviensis, 2008, Vol. 745, Biology, pp. 187–198

An alternative model of the origin of genes: quantization of intron dimensions

Gunars Chipens, Nora Ieviņa*, Ivars Kalvinsh

Latvian Institute of Organic Synthesis, Aizkraukles 21, Rīga LV-1006, Latvia
*Corresponding author, E-mail: ievina@osi.lv

Abstract

More than 30 years after the discovery of split genes the problem of intron origin is not yet completely solved. To study the possible germ of life on Earth we developed a quite different point of view – the third way of origin of genes – as an alternative to the Exon theory of genes and the Insertional theory of intron origin. In accordance to the elaborated model the precursors of primeval genes including segments of the future introns were formed by oligonucleotide multiplication and duplication reactions. The gene precursors without introns and primeval genes with the very first introns were regular periodic nucleic acids containing tandemly repeated identical in size and sequence oligonucleotides. Here we demonstrate several contemporary gene families whose members have retained regularity corresponding to oligonucleotide repeats. Regular segments of these gene structures – peculiar molecular relics – contain exons, introns and intron coordinates whose numerical parameters have identical internal regularity and can be quantized – expressed as multiples of identical size oligonucleotide repeat units. The term „gene quantum" in this case shows the number of nucleotides or base pairs in an oligonucleotide named a repeat unit.

Key words: albumin-fetoprotein gene family, globin gene family, regularity of gene structures, superfamily of carbonic anhydrases, tubulin α-1A.

Introduction

The necessity to investigate possible ways of the genetic code and gene origin as a complex problem arose for us in 1964 when at the Institute of Organic Synthesis new directions of Life Sciences were developed, including peptide chemistry and biology, with the aim to synthetize new active analogues of natural peptide bioregulators for use in medicine. Two main problems arose at once – the physico-chemical and functional (biologically tantamount) relatedness of amino acid groups and the genetic (proteomic) code structure of amino acid interaction. However, the problem of origin of the genetic code and the problem of gene and intron origin are intimately and closely connected and thus we studied both of them.

The discovery of split genes in 1977 was completely unexpected (Abate 2001), shocked scientists and promoted very intensive scientific investigation directed to understand intron origin, evolution and functions. Now internet server "Google" offers more than 504 000 files describing different models of intron emergence, thus indicating that the problem is not yet solved – for advanced models there is not yet quite enough convincing and corroborative experimental evidence. Interesting models and discussions about intron

origin can be found in articles Fedorow et al. 2003; Rogozin et al. 2005; Roy, Gilbert 2005; Koonin 2006; Roy, Gilbert 2006, and others.

During the last decade we have been interested in the way of origin of the very first gene precursors – on a day before the creation of the very first primeval genes, when only the primitive nucleic acids existed which, according to our viewpoint, were short simple structure regular and periodic polinucleotides without introns. The fundamental thesis of the supposed third way model is the regularity of gene precursor structures, which were formed of tandemly repeated oligonucleotides named repeat units (RU). Their dimensions correspond to the gene quantum Q of the future genes containing exons and introns. For studies of such a model, taking into account the very long time of evolution and a lot of different mutations, there is only one possibility – to search for regularity of exon and intron dimension numerical parameters, as well as for regularity of a gene itself, as an individual regular entity formed of a whole number of repeat units. We have revealed such a regularity in several gene families.

As an simple example can serve mouse gene tubulin alpha 1A (GenBank accession NC_000081.5; Gene ID:22142; Ensebl release 49 – Mar 2008). The sum of four exons of the coding part of this gene including iniciation and termination codons is 1356 nucleotides (nt) or base pairs (bp) (1356 = 6nt × 226 = 3nt × 454). The sum $\sum_i$ of three intron dimensions which separate the four exon row is 2064nt (2064 = 6nt × 344 =3nt × 688). The sum total of exon (E) and intron (I) dimensions $\sum_{(E+I)}$ is 3420nt (3420 = 6nt × 570 = 3nt × 1140). So, the sum total of exon and intron dimensions separately and totally include a whole number of codons (n × 3nt) where n is a whole number. Below there will be shown similar examples with pentanucleotide and heptanucleotide repeats.

Before the accumulation of a large data base of gene parametres and before elaboration of exact methods of determination of the gene precursor RU sizes we will use the minimal numerical values for the potential gene guantum Q (as a smallest unit of physical parameter). Thus, the mouse tubulin alpha 1A gene quantum Q conditionally is 6nt, but may be also 12 nt; it is necessary to analyse a large amount of the tubulin family genes (Ievina, Chipens 2003).

This gene also confirms our idea that gene exons and introns in the primeval gene were formed of identical in size RU, but a gene must be regarded as a whole regular entity (with the exception of mosaic like genes formed by exon shuffling). During evolution gene component dimensions (particularly introns) were changed, but the internal regularity of a whole gene in many cases was retained unchanged. Completely regular parameters of genes or large regular gene regions must be regarded as gene molecular „fossils" or relics.

Materials and methods

It is impossible to solve very tangled and difficult problems by using the same notions and terms that have led us to these problems. Therefore when investigating intron origin we use principles of information theory and concepts of signature and equivocation (Quastler, 1965; Chipens et al. 1979; Chipens 1980; Chipens et al. 1988; Chipens 1991) and simultaneously study also the origin of the genetic code (Chipens 1996, Chipens, Ievina 2004; Chipens, Ievina 2005), because the problem of origin of genes and introns as well as the problem of origin of genetic translational and amino acid interaction (proteomic) codes are closely connected. To solve the complex problem of gene and intron origin it was

necessary to elaborate many new analytical methods and even new principles of analysis based mainly on the symmetry and antisymmetry of the genetic and proteomic codes and codon root sequences of genes or amino acids shortly enumerated below. These methods (described in our ealier publications: Chipens, Ievina 1994; Ievina, Chipens 2003 and 2004; Chipens, Ievina 2005; Chipens 2006; Chipens et al. 2006; Ievina et al. 2006) were used also in this work.

The discovery of the covert symmetry of the 2D-genetic code, which determines the potential equifunctionality of amino acids having identical second codon letters (the codon roots) was of key significance to reveal gene regularity and intron origin and give a possibility to use widely the principially new method of gene and protein investigation – Comparative Amino Acid Codon Root Analysis (CAACRA) (Chipens 1991; Chipens, Ievina 1994; Chipens 1996). CAACRA allowed to determine and later also to calculate exon and intron internal regularity as well as led to the idea of gene quantum Q and quantization of discrete numerical parametres of genes (Chipens et al. 2005; Ievina et al. 2006).

Functionally tantamount amino acids have identical codon roots (Chipens et al. 1988; Chipens 1991), but the regularity of gene and protein sequences is determined by the translational symmetry of their codon root sequences (Chipens et al 2006). The translational symmetry can be determined only using CAACRA and repeat unit piles (RUP) because mutations change the amino acid sequences, but in many cases retain unchanged their codon roots (Chipens 1991; Chipens, Ievina 1996; Ievina, Chipens 2004).

The physico-chemical basis of CAACRA is the proteomic code, which can be demonstrated by rotational symmetry analysis of the 2D-genetic code structure in a form of a square (Chipens et al. 1988; Chipens 1996) or best of all in a form of windmill vanes (Chipens, Ievina 2004). Methodology and examples of protein and gene codon root sequence analysis using CAACRA and RUP are described in our previous publications (Chipens, Ievina 1999a; Chipens, Ievina 1999b; Ievina, Chipens 2004; Chipens et al. 2005; Ievina et al. 2006).

Results and discussion

The "Third way" model of gene and intron origin

Contrary to the well known „introns early" (Gilbert, 1987) and „introns late" (a review, Logsdon, 1998) theories according to the "third way" model primeval introns and exons are products of internal evolution of one and the same gene polynucleotide chain nucleic acid (most likely of the RNA) world. Gene precursors were highly regular periodic nucleic acids formed of identical in size and sequence oligonucleotides named repeat units (RU). Exons and introns in gene structures originated after the emergence of the very first splicing machinery. Introns in the absence of constraints imposed by the coding function as well as natural selection on the level of proteins during billions of years of evolution accumulated mutations without any limits. If the hypothesis of oligonucleotide multiplication is correct, modern gene structures could have retained some regularity of codon root and possibly also amino acid sequences.

The splicesome is the most complex macromolecular machinery of the contemporary cell (Nilsen, 2003), but independently of the biochemical mechanisms of the very first splicing machinery the splicing sites can be determined only by definite nucleotide

structures in the gene precursor nucleotide chain – the RU multimer. In accordance with our working hypothesis the splicing sites may be accidentally encoded in RU precursors or formed during multistep (the first or higher steps) multiplication reaction by interaction of RU 3'- and 5'-terminal nucleotides. In such cases potential splicing sites were distributed along the nucleotide chain – a multimer of repeats – internally regularly within the intervals n × RU(nt). Consequently, the exon dimensions (expressed by number of nucleotides, nt) as well as intron coordinates (measured by ordinal numbers of 3'-nucleotides of exon row just before introns) were internally regular determined by a whole number of RU (n × RU, nt). Each number can be expand into factors (prime number multipliers). If the numerical values of gene basic parameters have a set of common factors – they possess a comon internal regularity. This regularity is strictly determined by RU size measured by a number of nucleotides (or base pairs, bp) and marked by a special term, the gene quantum Q. According to our hypothesis the basic numerical parameters in regular regions of gene precursors were discrete and can be quantized (n × Q, where n is a whole number).

Thus, multiplication reactions of oligonucleotides form long polynucleotide chains with open reading frames (in cases when RU do not contain or form termination codons).

Oligonucleotide repeat units of the albumin and carbonic anhydrase genes

A scheme of a linear one-dimensional nucleotide chain of gene exon row can be depicted as a stright line with imaginary dots located regularly within intervals corresponding to the RU size. These dots we named the gene knot points (GKP). GKP have a key significance in analysis of regularity of the basic gene numerical parametres (exon length, intron position coordinates and total length of exon row) using as a unit of measure one nucleotide (base

Table 1. Numerical parameters expressed by number of nucleotides (E - exons, I - introns, C - intron coordinates as a sum of the preceeding E length) of the mouse albumin (Alb) in accordance with GenBank data (NC_000075.5, gene ID: 11657). The gene parameters which are multiples of 7nt are framed. *Symbol ∑ and the number denoted by asterisk show the sum of exons No 1-14 or introns No 1-13

E/I, No	E (nt)	C (nt)/phase	I (nt)
1	88	88/1	2824
2	49	137/2	206
3	133	270/0	1439
4	212	482/2	847
5	133	615/0	583
6	98	713/2	740
7	130	843/0	5018
8	215	1058/2	13680
9	133	1191/0	2307
10	98	1289/2	817
11	133	1422/0	1288
12	224	1646/2	958
13	133	1779/0	1067
14	48	$\sum_{E}$ 1827/- *	$\sum_{I\ No1\text{-}13}$ 31774nt

pair) and the size of RU. GKP show the borderlines between the neighbour RU. Position of GKP or RU in the exon row polinucleotide chain can be characterized by the corresponding coordinate – the ordinal number of RU 3'-terminal nucleotide, because conditionally each RU ends by a GKP. The reference point usually is nucleotide No. 1 of the first exon.

Theoretically gene exon nucleotide chains must consist of a whole number of RU. Introns crossing GKP split the nucleotide chains, thus forming exon row. If the intron coordinates correspond to the GKP then the exon dimensions are internally regular. It goes without saying that mutations, particularly transversions and indels, as well as intron sliding disrupt this regularity sometimes completely. Therefore it is necessary to search for molecular „fossils" – segments of contemporary genes which have retained the regularity of ancestors.

The potential sizes of RU can be calculated as products of common prime numbers (factors). Such calculation usually shows small numerical values of RU dimensions and a serious problem arises about their real existance. To answer to this important question it was necessary to test and confirm the "third way" model, which was achieved by analysis of the mouse albumine (Alb) gene (Waterston et al. 2002). This gene, if we cut off the 3'-terminal intron and nucleotide sequence of poliadenylic acid (Fig. 1, Table 1) has 14 exon/13 intron structure (GenBank accession number NC_000071.5). More than a half (64.3 %) of Alb exon dimensions can be expressed as a multiple of gene quantum Q = 7nt indicating that the primary repeat unit contains 7 nt and is a heptanucleotide. It is important to underline that some of these exon sizes can be expressed only as products of two prime numbers one of which is always seven (e.g. $49 = 7 \times 7$; $133 = 7 \times 19$) confirming the heptanucleotide size of RU.

It is interesting to note that from the time immemorial the number seven is ascribed as magnificient and lucky number having peculiar strength (Miller 1956). For us it was indeed a lucky number because it firstly introduced the idea that a gene containing exons and introns must be regarded as a whole regular entity and confirmed our idea that separate intron-molecular relic dimensions (4 and 11, Table 1) could be quantized similarly as those of exons.

The sum total (∑) of the mouse Alb gene thirteen introns (I) 1-13 is 31774 nt (Table 1 and Fig. 1) and differs from the calculated value (if Q = 7nt) only by +1 nt (possibly a nucleotide insertion). Correction of this parameter (i.e. "minus" 1 nt) gives the value 31773 nt (31773 : 3 = 10591 codons; 31773 : 7 = 4539 heptanucleotide RU) which together with

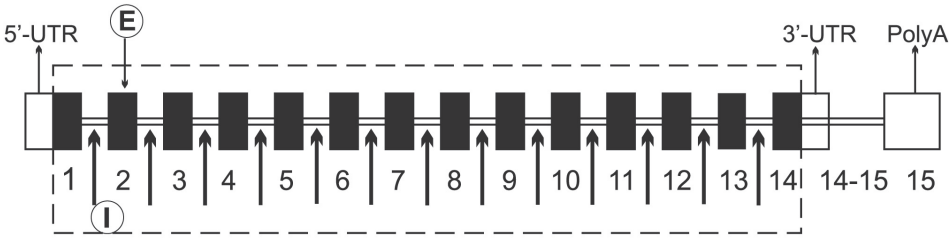

Fig. 1. A scheme of the mouse albumin (Alb) gene structure. The analyzed gene segment is framed by a dashed line. Exons (E) are designated as black boxes. Untranslated 5'-UTR and 3'-UTR of parts of the exons 1 and14 are white. The whole exon 15 – the polyadenilic acid (polyA) is shown as white box. Ordinal numbers of exons and introns (I) are shown below the corresponding gene components. The number (No) of an intron (I, shown as arrow) is the same as the exon that it follows.

Table 2. Numerical parameters of the *Arabidopsis thaliana* beta-carbonic anhydrase-2 gene coding part with introns (CA-2, TAIR: AT5G14740). Designations see Table 1. Parameters which can be expressed as multiples of Q = 5nt are framed, e.g., introns (I) No 3, 4 and 5 dimensions (nt): 135 = 5 × 27; 115 = 5 × 23; 125 = 5 × 5 × 5. The sum total of introns 1-9 is 3130 (5 × 626)

E/I, No	E (nt)	C/phase	I (nt)
1	87	87/0	752
2	118	205/1	1311
3	64	289/2	135
4	150	419/2	115
5	49	468/0	125
6	117	595/1	147
7	54	639/0	257
8	86	725/2	137
9	110	835/1	151
10	158	Σ_E993/-	Σ_I1-9
			3130

the sum of exon (E) dimensions 1-14 ($\Sigma E_{1\text{-}14}$ = 1827, Table 1) reveals the parameter $\Sigma_{(I+E)}$ = 33.600 nt, which corresponds to the whole number of codons (33 600 : 3 = 11.200) as well as the whole number of heptanucleotide repeats (33 600 : 7=4800) supporting our new hypothetical model of gene origin.

Another good idea raised by study of the bovine albumin amino acid sequence came from James Brown publication (1976) indicating that albumin-fetoprotein genes had evolved by number of internal duplications, i.e., the bovine albumine sequence could be divided into three equivalent regions of about 190 amino acids (aa) each. The sequences of two of these were more similar than either was to the third, suggesting that there had been a doubling at one point, from a molecule of about 190 aa to one of 380 aa, and then a second, incomplete, duplication that gave rise to the existing 580 aa-residue structure. There was also evidence that the fundamental macrodomain structure (ca. 190 residues) had itself evolved as the result of internal duplications from a more primitive sequence of about 77 residues (corresponding to the bovine aa sequence ~ 504-581; Brown 1976). This primitive sequence in accordance to the Brown hypothesis arose by duplication and separation of a gene segment encoding C-terminal fragment of very primitive globin family proteins similar to myoglobin and hemoglobin.

If the Brown hypothesis is correct then the primary RU of globin proteins must be 2 and 1/3 aa, i.e. 7nt. Data of our analysis, however, suggest another value – 21nt or 7aa (Chipens et al., 2006; Ievina, Chipens 2004). Therefore we reinvestigated this question once more (see chapter *Globin gene introns retained the primeval gene heptanucleotide repeats, their dimensions can be quantized*).

The superfamily of carbonic anhydrases

Another family of genes confirming the small sizes of oligonucleotide repeats are enzymes – carbonic anhydrases (CA) with a Q value 5nt. As an example can serve beta CA2 of the *Arabidopsis thaliana* (GenBank NC_003076.4, Gene ID: 831326, TAIR: AT5G14740,

NP_001031883, Table 2). The CA-family enzymes are extremely widely distributed among living organisms (Liljas, Laurberg 2000), e.g., the human genome contains 35, and the mouse – 38 different members of the CA superfamily, see for examples the PANTHER (Mi et al. 2007) classification system. Particular attention deserve firstly the revealed observations: (i) dimensions of three neighbour introns (3,4 and 5; Table 2) are multiples of 5nt and have the same internal regularity as exons 4 and 9 and many intron coordinates: 2,6,8,9, and (ii) the sum total Σ of nine introns (1-9; Table 2) can be precisely quantized (1130 : 5 = 226) once more confirming that introns were formed of the same size repeats as exons; (iii) intron drift changed the individual dimensions of introns, but the sum total in separate cases remained the same and the same internal regularity was retained for some introns – the "molecular relics".

Five nucleotides (Q = 5nt) can encode only 1⅔ of amino acids therefore most exons do not contain a whole number of codons (n × 3nt) nor a whole number of pentapeptides (n × 5nt). Not all numbers can be divided with 3 or 5nt without remainder. This is possible only if the exon dimension is a multiple of 15 (3 × 5, e.g., the exon 4; Table 2). Contrary to these arithmetical restrictions 40 % of intron coordinates C (as the sum of preceeding exons length) are multiples of pentanucleotides, i.e. the changes of E dimensions (the result of introns drift or nt insertions and deletions) compensate each other. The sum total Σ_{E+I} 993 + 3130 = 4123nt with deviation „minus" 2nt (as a result of „arithmetical restrictions") correspond to a whole number of codons (n × 3) and a whole number of pentanucleotide (n × 5) repeats : 4123 + 2 = 4125, but 4125 : 15 = 275.

Different classes (alpha, beta, gamma) of carbonic anhidrases do not possess related amino acid sequences. Completely different are also their tertiary and quarternary structures. Only their active sites show essential features of remarkable similarity (Liljas, Laurberg, 2000). According to our viewpoint pentanucleotide multiplication reactions took place before the origin of the genetic code (similarly as the heptanucleotide multiples of albumins) in accordance to the concepts of the fancyful interpretation of early evolution. The underlying assumption of this is that some contemporary processes and molecules had to appear before others and that the evolution of the information processing system involved interaction between separately evolving components (Doolittle, Brown 1994). Possibly a lot of pentanucleotide multiples without introns at first originated forming different gene nucleotide sequences without definite functions. Therefore, only after the emergence of a primitive genetic code (and splicing machinery), very different amino acid sequences were formed. According to this hypothesis introns and exons are indeed very old components of primeval genes whose precursors were formed intramolecularly and simultaneously from a simple structure regular and periodic nucleic acids. Otherwize, according to our viewpoint it is very difficult to explain the evolution of the genetic translational code within about 20 million of years in the preIsuan era about 4000 million years ago (Davis 1999). Thus, the genetic code was established soon after the formation of the Earth.

Globin gene introns retained the primeval gene heptanucleotide repeats, their dimensions can be quantized

Graphical autoscanning of the human globine primary stuctures, e.g., the human hemoglobin subunit HBA2 N-terminal amino acid sequence encoded by the exon 1 (GenBank NC_000016) strongly confirm our previously obtained data (Chipens, Ievina

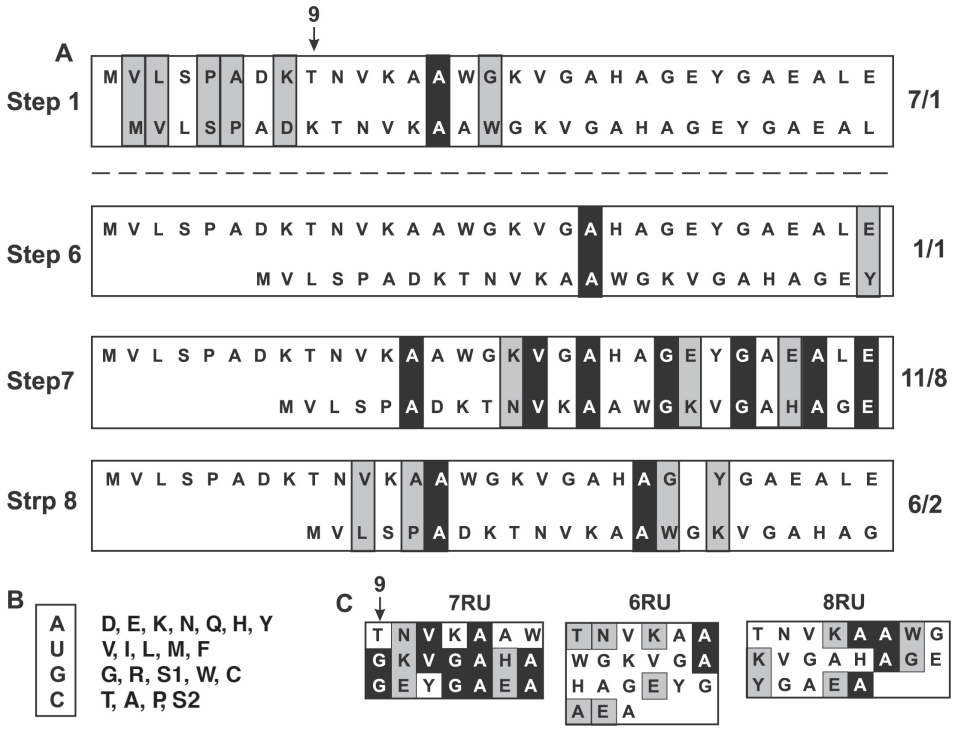

Fig. 2. Methods of analysis of the protein amino acid and the corresponding exon codon root structures using CAACRA methodology. The object of analysis – the human alpha-globin HBA2 exon 1 encoded protein fragment 1-31 (GenBank accession NC_000016). A. The "dynamic" peptide chain (the bottom line) is moved step by step (symbol-by-symbol) relatively to the idenical "static" (the top) chain. The mutual positions of separate steps (1, 6, 7, and 8) are shown. At each step of analysis in front opposite standing symbols (amino acids and corresponding codon root – the second codon letter symbols) are compared, counted and shown at the left side as a fraction of common root amino acids/identical amino acids designated as "factor" or "fraction" (f). In lines identical amino acid pairs are shown against a black background (note that at the same time they have also identical codon roots). Common root but not identical aa are shown against a grey background. B. Glossary of common-root amino acids. C. Analysis of the regularity of amino acid and codon root sequences using the method of repeat unit piles (Ievina, Chipens 2004). Amino acid symbols having an identical codon root (the second codon letter, as well as identical aa number having the same codon root) are enumerated. The highest number of identical symbols in the vertical lines (in this case the "fraction" f is expressed in percent) were when the RUP dimension corresponded to the RU size (7RU). The highest regularity is shown by the HBA2 fragment 9-29. Changes of RU size (6RU or 8RU) significantly decreased the f values (Fig. 3).

2004; Ievina, Chipens 2004) – the RU of the globin peptide chains is 7aa (or on the level of gene – 21nt; Fig. 2). However, these data do not mean that the Brown (1976) hypothesis is not correct, because according to our data of contemporary globin gene intron analysis, RU of the primeval globin genes most likely were 7nt. We find "molecular relics" – the heptanucleotide repeats (only by size, but not by sequences) in the different globin gene intron structures. For analysis we choose globin genes such as the green alga *Chlamydomonas eugametos* hemoglobins (Li637 and Li410) from the protozoan/

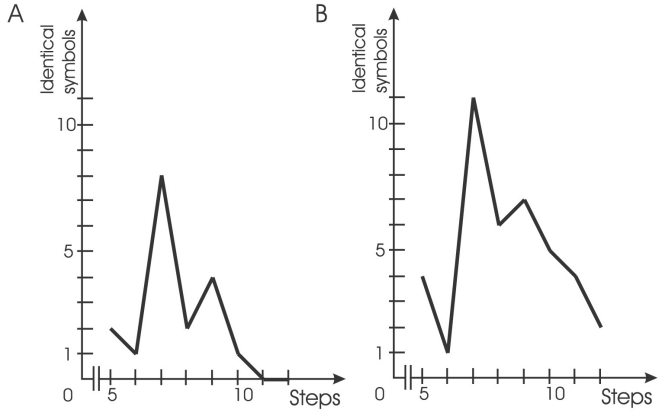

Fig. 3. A fragment of autoscanning curves of the human HBA2 amino acid sequence 1-31, (block A) and the codon root sequence of the corresponding gene exon 1. (block B). Only a fragment of the curve is shown reflecting autoscanning steps 5-12. For the CAACRA and autoscanning principles see also Fig. 2. The maximums of curves correspond to the size of HBA protein RU (7aa, A) or 7 codon roots of the HBA globin gene exons row (B).

Table 3. Intron dimensions of the globin gene family. *Deviations (Δ) are calculated relatively to the nearest GKP, e.g., for HbA-1 $\sum_i$ is 266; 266 : 7 = 38 and Δ is 0, but 266 : 21=12,66; 13 × 21 = 273 and Δ (relatively to $\sum_i$) is 7nt

Globin GenBank accession	**Intron dimensions (nt)**				**Internal regularity of the sum total $\sum_i$ and deviations (Δ, nt)***	
	No 1	**No 2**	**No 3**	**Sum total**	**Number of 7-nt repeats**	**Number of 21-nt repeats**
Homo sapiens myoglobin NC_000022	5925	6056	3440	33327	4761, Δ 0	1587, Δ 0
Homo sapiens HbA-1 NC_000016	117	149	–	266	38, Δ0	273, Δ -7
Homo sapiens HbA-2 NC_000016	117	142	–	259	37, Δ0	252, Δ +7
Homo sapiens HbB NC_000011	130	850	–	980	140, Δ0	987, Δ-7
Chlamidomonas eugametos X65870	181	296	755	1232	176, Δ0	1239, Δ -7
Glycine max U47143	101	114	240	455	65, Δ0	462, Δ-7
Ciona intestinalis AJ548500	254	123	980	1357	194, Δ+1	1365, Δ-8
Ciona intestinalis AJ548501	740	304	–	1044	149, Δ-1	1050, Δ-6

cianobacterial/globin family (Couture et al. 1994), the plant nonsymbiotic hemoglobin gene of the *Glycine max* and the *Ciona intestinalis* (class *Ascidiacea*) globins which are phylogenetically positioned at the base of vertebrates (Ebner et al. 2003). The intron structures in the globin genes family were more conservative than exons – as we supposed they retained and reflect the RU dimensions (7nt or bp) at the first step of multiplication reactions generating globin (and possibly also albumin) gene precursors. Interestingly that not only old globins, but also the sum total of the human hemoglobin gene introns are multiples of 7nt. Independently of number of introns the sum Σ_i of globins can be quantized using Q value 7nt (but not Q = 21, with the exception of myoglobin, Table 3). The human globins A1 and A2 have completely identical amino acid sequences, differing only in their intron No 2 dimension – this difference is precisely 7nt (Table 3) and seven neighbour nucleotides form a cluster before the specific nucleotide sequence of the right splice sight.

Our latest (unpublished) data of analysis of genes encoding several complex enzymes reveal their highly discrete numerical parameters containing segments of alternating neighbour exon-intron-exon-intron sequences formed of identical in size oligonucleotide RU. Biochemical unity of life and the principle biochemical universality (Dayhoff et al. 1972) allow to postulate that the "third way" of gene and intron origin described above most likely is universal for living matter in the early stage of evolution. This, of course, does not exclude other different ways of gene and intron origin and development in later stages of evolution. But according to Susumu Ohno nothing in evolution is created *de novo* – each new gene must have arisen from an already existing gene. This idea is the main motif through the famous monograph "Evolution by gene duplication" (Ohno 1970). He was also the first who postulated that early genes were oligomeric repeats (Ohno 1987).

References

Abate T. 2000. Genome discovery shocks scientists. http://www.euchromatin.org/Abate01.htm

Brown J.R. 1976. Structural origins of mammalian albumin. *Fed. Proc.* 35: 2141–2144.

Chipens G.I., Krikis A., Polevaja L.K. 1979. Physico-chemical principles of information transfer at molecular level. In: Vassileva-Popova J.G., Jensen E.K (eds) *Biophysical and Biochemical Information Transfer in Recognition*. Plenum Press, New York-London, pp. 23–48.

Chipens G. 1980. Using some principles of system analysis for investigation of peptide ligand structures and functions. In: *Structure and Function of Low Molecular Peptides*. Publishing House "Science", Riga, pp. 1–124. (in Russian)

Chipens G., Gnilomedova L.E., Ievina N., Rudzish R., Skliarova S. 1988. Equifunctionality of amino acids, the principle of signature and symmetry of the genetic code. *Proc. Latvian Acad. Sci.* 11/496: 113–116. (in Russian)

Chipens G.I. 1991. The hidden symmetry of the genetic code and rules of amino acid interaction. *Bioorgan. Khim*. 17: 1335–1346. (in Russian)

Chipens G., Ievina N. 1994. Comparative amino acid codon root analysis (CAACRA) of peptide chains. *Proc. Latv. Acad. Sci. Sect. B* 48: 50–54.

Chipens G. 1996. The second half of the genetic code. *Proc. Latv. Acad. Sci. Sect. B* 50: 151–172.

Chipens G., Ievina N. 1999a. Outlines of a nucleotide-multiplication theory of exon and intron origin. *Proc. Latvian Acad. Sci. Sect. B* 53: 65–72.

Chipens G., Ievina N. 1999b. Repeat units are the basic elements of gene and protein structural organisation. *Proc. Latvian Acad. Sci. Sect. B* 53: 54–56.

Chipens G., Ievina N. 2004. Peculiarities of the rotational symmetry of the genetic code two-

dimensional structure. *Latvian J. Chem*. 2004/1: 85–87.
Chipens G., Ievina N. 2005. Connectedness groups of codons/anticodons and origin of the genetic translational code. *Latvian J. Chem.* 2005/3: 282–290.
Chipens G., Ievina N., Kalvinsh I. 2005. A new theory of gene origin and quantisation of aspartate aminotransferase paeameters: mathematical modeling of modern gene structures. *Latvian J. Chem*. 2005/4: 311–324.
Chipens G. 2006. Symmetry and antisymmetry of the genetic code: models of the sense/antisense and the codon root code. *Latvian J. Chem.* 2006/1: 3–18.
Chipens G. Ievina N., Liepina I., Kalvinsh I. 2006. Autoscanning of codon root palindroms. *Latvian J. Chem.* 2006/4: 382–392.
Couture M., Chamberland H., St-Pierre B., Lafontaine J., Guertin M. 1994. Nuclear genes encoding chloroplast hemoglobins in the unicellular green alga *Chlamidomonas eugametos*. *Mol. Gen. Genet*. 243: 185–197.
Davis B.K. 1999. Evolution of the genetic code. *Progr. Biophys. Mol. Biol.* 72: 157–243.
Dayhoff M.O., Eck R.V., Park C.M. 1972. Model of evolutionary change in proteins. In: *Atlas of Protein Sequence and Structure* Vol. 5, Natl. Biomed. Res. Foundation, Washington, pp. 89–99.
Doolitle W.F., Brown J.R. 1994. Tempo, mode, the progenote, and the universal root. *Proc. Natl. Acad. Sci. USA* 91: 6721–6728.
Ebner B., Burmester T., Hankeln T. 2003. Globin genes are present in *Ciona intestinalis*. *Mol. Biol. Evol.* 20: 1521–1525.
Fedorow A., Roy S., Fedorova L., Gilbert W. 2003. Mystery of intron gain. *Genome Res.* 13: 2236–2241.
Gilbert W. 1987. The exon theory of genes. *Cold Spring Harbor Symp. Quant. Biol*. 52: 901–905.
Ievina N., Chipens G. 2003. A new approach to study the origin of genes and introns. *Acta Univ. Latv.* 662: 67–79.
Ievina N., Chipens G. 2004. Origin of globins and mystery of of myoglobin codon root symmetry. *Acta Univ. Latv.* 676: 97–105.
Ievina N., Chipens G., Kalvinsh I. 2006. Internal regularity and quantisation of gene parameters. *Acta Univ. Latv.* 710: 139–153.
Koonin E.V. 2006. The origin of introns and their role in eukaryogenesis: a compromise solution of the introns-early versus introns-late debate. *Biol. Direct.* 14: 22.
Liljas A., Laurberg M. 2000. A wheel invented three times. The molecular structures of the three carbonic anhydrases. *EMBO Reports* 1: 16–17.
Logsdon J.M. Jr. 1998. The recent origins of splicesomal introns revisited. *Curr. Opin. Genet. Dev.* 8: 637–648.
Mi H., Guo N., Kejerival A., Thomas P.D. 2007. PANTHER version 6: protein sequences and functions with expanded representation of biological pathways. *Nucleic Acid. Res.* 35: D247–D252.
Nilsen T.W. 2003. The splicesome: the most complex macromolecular machine in the cell? *Bioessays* 25: 1147–1149.
Ohno S. 1970. *Evolution by Gene Duplication*. Springer-Verlag, Berlin, Heidelberg. 160 p.
Ohno S. 1987. Early genes that were oligomeric repeats generated a number of divergent domains on their own. *Proc. Natl. Acad. Sci. USA* 84: 6486–6490.
Quastler H. 1965. General principles of systems analysis. In: Watterman T.H., Morowitz H.I. (eds) *Theoretical and Mathematical Biology*. Blaisdell Publ. Comp., New York, pp. 313–333.
Rogozin I.B., Sverdlov A.B., Babenko V.N., Koonin E.V. 2005. Analysis of evolution of exon-intron structure of eukariotic genes. *Brief. Bioinform.* 6: 118–134.
Roy S.W., Gilbert W. 2005. Complex early genes. *Proc. Natl. Acad. Sci. USA* 102: 1986–1991.
Roy S.W., Gilbert W. 2006. The evolution of splicesomal introns: patterns, puzzles and progress. *Nature Rev. Genet.* 7: 211–221.
Waterston R.H., et al. 2002. Initial sequencing and comparative analysis of mouse genome. *Nature* 420: 520–562.

Gēnu izveidošanās alternatīvais modelis: intronu dimensiju kvantēšana

Gunārs Čipēns, Nora Ieviņa*, Ivars Kalviņš

Latvijas Organiskās sintēzes institūts, Aizkraukles 21, Rīga LV-1006, Latvija
*Korespondējošais autors, E-pasts: nora.ievina@osi.lv

Kopsavilkums

Intronu problēmas risināšanai ir izstrādāta jauna teorija, principiāli atšķirīga no līdz šim zināmajām. Kvantitatīva gēnu parametru analīze pierāda, ka gēnu, eksonu un intronu koordinātēm piemīt iekšēja identiska regularitāte, kas liecina, ka introni ir veidojušies iekšmolekulāri gēnu priekšteču attīstības gaitā. Mūsdienu gēnu regulāro segmentu skaitliskās vērtības var izteikt ar veselu skaitļu reizinājumu ar jaunizveidotu parametru, kas nosaukts par gēna kvantu un kas izsaka bāzu pāru (nukleotīdu) skaitu gēnu polinukleotīdu virknes atkārtojuma vienībās. Iegūtie dati pierāda, ka gēnu priekšteči kā arī pirmgēni ir bijuši regulāras un periodiskas nukleīnskābes ar vienkāršu struktūru. Pirmgēnu regularitāti ir saglabājuši arī mūsdienu gēnu segmenti („molekulārie relikti") vai pat veselas kodējošo gēnu struktūras. Darbā analizēti peles tubulīns α-1A un un seruma albumīns, *Arabidopis thaliana* β-karbonilanhidrāzes-2, globīnu un hemoglobīnu ģimenes gēni.

Acta Universitatis Latviensis, 2008, Vol. 745, Biology, pp. 199–203

Cepaea vindobonensis (C. Pfeiffer, 1828) in Latvia

Arturs Stalažs[1]*, Jozef Šteffek[2], Edgars Dreijers[3]

[1]Latvian State Institute of Fruit Growing, Graudu 1, Dobele LV-3701, Latvia
[2]Faculty of Ecology and Environmental Sciences, TU in Zvolen, Institute of Forest Ecology Slovak Academy of Sciences, Štúrova 2, SK-960 53 Zvolen, Slovakia
[3]Latvian Malacological Society

*Corresponding author, E-mail: arturs.stalazs@lvai.lv

Abstract

Cepaea vindobonensis (C. Pfeiffer, 1828) is reported from one site from Riga city (Latvia). This is its only known population in Latvia. We briefly discuss information about this record and we provide historical review of the oldest collection data on this species for Latvia.

Key words: *Cepaea vindobonensis*, distribution and history, Helicidae, Latvia.

Introduction

Cepaea vindobonensis is South-East European species with a distribution from the Caucasian and Crimean territory to the Balkans. Isolated occurrence is reported from Germany, a few localities in eastern part of Austria, Czech Republic, Poland and almost the whole of Slovakia (Kerney, Cameron 1979; Wiktor 2004). For Latvia *C. vindobonensis* is mentioned by some authors in the 19th century, but this information has not been confirmed by malacologists in the 20th century. The main objective of this report, according to the historical data and newest findings, is to provide a review of *C. vindobonensis* in Latvia.

Materials

In this report *Cepaea vindobonensis* material collected in 2006 from one locality in Riga city (Latvia) and a *C. vindobonensis* shell (collected by L. Višņevska about 38 years ago) from the personal collection of A. Stalažs was used.

Results and discussion

Historical data

The first information about the occurrence of *Cepaea vindobonensis* in Latvia is found in some references from the 19th century. Krynicki (1837) mentioned this species (with names *Acavus arvensis* Ziegl. and *A. vindobonensis* Pf. – cited in the list of species, page 51) for the territory of the Russian Empire, which partly included also the present territory of Latvia. Also Krynicki (1837) did not describe the specific distribution of this species, but he mentioned possible occurrence of the species in Russia: "Locum natale talium

non est indicatum, quea magnum Rossiae spatium ocupant". Gerstfeldt (1859) in his work mentioned this species (with name *Helix* (*Tachea*) *vindobonensis* C. Pfr. = *austriaca* Mühlf., page 106) for Koknese (in Eastern Latvia) and wrote that several specimens found near Koknese have been located in collections. Ten years later Kawall (1869) included this species [as *Helix vindobonensis* Pfr. (*austriaca* Mühlf), page 4] in the list of species for Kurzeme – Northwest region of Latvia. Braun (1883) mentioned *C. vindobonensis* (with name *Helix austriaca* Mühlf., page 176) in the list of molluscs for the Eastern territories to the Baltic Sea by citing Gerstfeldt (1859).

Later Schlesch (1942) suggested that records of *C. vindobonensis* occurrence in Koknese were improbable and he mentioned that Gerstfeldt's explanation about species occurrence near Koknese is a mistake (page 311). Schlesch also rejected the possible distribution of *Cepaea nemoralis* in Koknese.

Several scientists and amateurs have consequently survived the territory near Koknese up to 1942. In papers from the 20th century *Cepaea hortensis* is mentioned only from the territory of Koknese (Pētersons 1932; Schlesch 1942). Since 1966 many habitats near Koknese have been destroyed and now are flooded by the Pļaviņu Hydroelectric Power Plant reservoir.

After the Schlesch publication in 1942, different authors listed only two snail species from the genus *Cepaea* for Latvia: *C. hortensis* and *C. nemoralis* (Sloka, Sloka 1957; Shileiko 1978; Rudzīte et al. 1996; Rudzīte et al. 1997; Spuris 1998; Rudzīte 2000). *C. nemoralis* is distributed in some sites in the Kurzeme region and two populations are found in the central part of Latvia – in the territory of Riga city (Rudzīte 2000; Dreijers, Stalažs 2000, Stalažs 2000; Stalažs 2006). *C. hortensis* is very common across Latvia and is found within various biotopes.

It is possible that in the 19th century the pale color of the shell of *C. vindobonensis* was used for identification. This could explain the former misidentifications by mentioned authors. White colored shells (generally considered as characteristic of *C. vindobonensis*) occur sporadically also in *C. hortensis* and more rarely in *C. nemoralis*. We have observed several populations of *C. hortensis* where whitish or white-yellowish shells are dominant, but also we have found whitish or dull yellowish shells for *C. nemoralis* in some individuals. The whitish-shelled *C. vindobonensis* was mentioned as similar to *C. nemoralis* also by Kerney and Cameron (1979).

There is one shell of *C. vindobonensis* in the personal collection of A. Stalažs, dated from 1998. The history of this shell is interesting because it possibly was collected from Latvia. This particular shell was collected by L. Višņevska about 38 years, ago. Višņevska provided this shell for collection (in 1998), but unfortunately she was not able to state the exact site of finding, mentioning only: "It was in Latvia near one small lake with rounded form in the vicinity of a state road. The shell was found near water". This finding cannot be used as scientific evidence; but can be interesting historical material.

Current situation

In September 2006, Jozef Šteffek found the first specimens of *C. vindobonensis* in Riga near a railway bank near Jelgavas Street (latitude 56.93841, longitude 024.09806) where it occurred together with 16 other mollusc species (Table 1). This is the first known site of confirmed occurrence of this species in Latvia.

On 24 September 2006 we collected 30 shells of *C. vindobonsnsis* from this site. We

Table 1. List of 17 mollusc species from the sampled site near Jelgavas Street (Riga, Latvia)

Species	Comments
Arianta arbustorum (Linnaeus, 1758)	
Arion cf. fasciatus (Nilsson, 1823)	
Cepaea vindobonensis (C. Pfeiffer, 1828)	non native species
Cochlicopa lubrica (O. F. Müller, 1774)	
Cochlodina laminata (Montagu, 1803)	
Deroceras sturanyi (Simroth, 1894)	
Deroceras reticulatum (O. F. Müller, 1774)	
Krynickillus melanocephalus Kaleniczenko, 1851	non native species
Laciniaria plicata (Draparnaud, 1801)	
Limax maximus Linnaeus 1758	non native species
Oxychilus draparnaudi (H. Beck, 1837)	non native species
Succinea putris (Linnaeus, 1758)	
Succinella oblonga (Draparnaud, 1801)	
Trichia hispida (Linnaeus, 1758)	
Vallonia costata (O. F. Müller, 1774)	
Vallonia pulchella (O. F. Müller, 1774)	
Vitrina pellucida (O. F. Müller, 1774)	

found altogether seven living individuals (three juvenile, four adults) and 23 empty shells, the majority of which was gnawed by small mammals. All fragmented shells occurred in the vicinity of *Acer negundo* stubs. During an additional visit on 29 September we found another 131 gnawed shells; 121 belonging to *C. vindobenesis*, seven to *Arianta arbustorum* and three to *Laciniaria plicata* shells. All were found in an area covered by *Acer negundo* shoots. *C. vindobenesis* was found in the area between Kīlevena grāvis (Kīlevena ditch) and Jelgavas street from the railway embankment to Vienības gatve, but in September 2008 the species was found also in surrounding territories. The species possibly occurs also in the nearby garden territory (it is a closed territory) on the other side of Jelgavas street and Vienības gatve.

At both sampling times shells with all five bands were found. Beside this pattern, also shells with an absent second band (10345) and shells where the first and second band was weakly apparent (1'2'345 and 12'345) occurred. Bands 3, 4 and 5 were generally dark and dominant. Only shells where the second band was absent have had light brown bands number 1, 3 and 4.

Acknowledgements

The research was funded by the VEGA grants No. 1/6007/26, 2/6007/26 and 2/5152/25.

References

Braun M. 1883. Zur Molluskenfauna der Ostseeprovinzen. *Nachrichtsbl. Deutch. Malak. Ges.* 15: 176.

Dreijers E., Stalažs A. 2000. Mollusca fauna near Kolka and at Slīteres Zilie kalni. *Raksti par dabu* 1: 22–31. (in Latvian) /Gliemju fauna Kolkas apkārtnē un Slīteres Zilajos kalnos. /

Gerstfeldt G. 1859. Aufzählung der in Est-, Liv- und Kurland beobachteten Land- und Süsswasser-Mollusken, mit besonderer Berücksichtigung der betreffenden Sammlung des Naturforschenden Vereins zu Riga. *Korresponenzblatt des Naturforscher-Verein zu Riga* 11: 106–107.

Kawall J.-H. 1869. Notice sur la Fauna malacozoologique de la Courland. *Annales de la Société Malacologique de Belgique* IV: 4.

Kerney M.P., Cameron R.A.D. 1979. *A Field Guide to the Land Snails of Britain and North-west Europe*. Collins, London. 221 p.

Krynicki A.J. 1837. Conchylia tam terrestria, quam fluviatilia et e maribus adjacentibus Imperii Rossici indigena, que pro mutua offeruntur historiae naturalis cultoribus commutatione. *Bulletin de la Société Impériale des Naturalistes de Moscou* 1: 50–51.

Pētersons H. 1932. *Notes on Mollusca of River Daugava, from Krāslava till Daugavgrīva.* Rīga. 52 p. (in Latvian) /Atzīmes par Daugavas gliemežiem, apgabalā no Krāslavas līdz Daugavgrīvai/

Rudzīte M. 2000. *Learn to Know – Latvian Landsnails.* Gandrs, Rīga. 147 p. (in Latvian) /Mācies pazīt – Latvijas zemesgliemeži/

Rudzīte M., Pilāte D., Parele E. 1996. Common Latvian names of molluscs from Latvia. *Daba un Muzejs* 6: 85–92. (in Latvian) /Latvija sastopamo gliemju sugu latviskie nosaukumi/

Rudzīte M., Pilāte D., Parele E. 1997. Molluskenfauna Lettlands. Liste der in Lettland vorkommenden Molluskenarten (Gastropoda, Bivalvia). *Mitt. Dtsch. Malakozool. Ges.* 59: 1–10.

Schlesch H. 1942. Die Land- und Süsswassermollusken Lettlands mit Berücksichtigung der in den Nachbargebieten vorkommenden Arten. *Korresponenzblatt des Naturforscher-Verein zu Riga* LXIV: 311.

Shileiko A.A. 1978. *Land Molluscs of Superfamily Helicoidea. Fauna of USSR, Mollusca.* Vol. 3. USSR Academy of Sciences, Leningrad. 384 p. (in Russian)

Sloka N., Sloka J. 1957. Mollusca. In: Tauriņa E., Ozols E. (eds) *Guide to Animals of Latvian SSR.* Vol. 1. Latvijas Valsts Izdevniecība, Rīga, pp. 732–775. (in Latvian) /Mollusca. Gliemji/

Spuris Z. (ed) 1998. *Red Data Book of Latvia, Rare and Threatened Species of Plants and Animals, Vol. 4, Invertebrates.* LU Bioloģijas institūts, Rīga. 388 p.

Stalažs A. 2000. New data on rare mollusc species in Latvia. *Raksti par dabu* 1: 21. (in Latvian) /Jaunas reto gliemju sugu atradnes Latvijā/

Stalažs A. 2006. Distribution of *Cepaea nemoralis* (Gastropoda) in Latvia. In: *Diversity and Conservation of European Molluscan Fauna*, The 1st Baltic Symposium of Malacology, September 21-23, 2006, Riga, Latvia, p. 40.

Wiktor A. 2004. *Ślimaki Lądoéwe Polski*. Wyd. Mantis, Olsztyn. 302 p.

Rievotais vīngliemezis *Cepaea vindobonensis* (C. Pfeiffer, 1828) Latvijā

Arturs Stalažs1*, Jozef Šteffek[2], Edgars Dreijers[3]

[1]Latvian Valsts augļkopības institūts, Graudu 1, Dobele LV-3701, Latvija
[2]Faculty of Ecology and Environmental Sciences, TU in Zvolen, Institute of Forest Ecology Slovak Academy of Sciences, Štúrova 2, SK-960 53 Zvolen, Slovākija
[3]Latvijas Malakologu biedrība

Kopsavilkums

Rievotais vīngliemezis *Cepaea vindobonensis* (C. Pfeiffer, 1928) ir konstatēts vienā atradnē Rīgas pilsētā. Šī ir vienīgā reāli eksistējošā sugas atradne Latvijas teritorijā. Īsumā tiek sniegta diskusija par sugas atradumu un vecākās literatūras apskats un kolekciju informācija par šo sugu Latvijā.

Acta Universitatis Latviensis **ser.** ***Biology***
PREPARATION OF MANUSCRIPTS

Manuscripts for publication should be sent to:

Prof. Gederts Ievinsh, Editor-in-Chief
Acta Universitatis Latviensis, Biology
Faculty of Biology, University of Latvia
Kronvalda bulv. 4, Rīga LV-1586
Latvia.

A final version of the accepted manuscript should be submitted electronically at gederts@lanet.lv.

Acta Universitatis Latviensis ser. *Biology* (ISSN 1407-2157) is published yearly by the University of Latvia. Original research articles covering all aspects of modern biology are welcome. Young scientists, especially PhD students in biology, are encouraged to submit their contributions.

Each manuscript submitted to *Acta Universitatis Latviensis* ser. *Biology* must be an original research report that has not been submitted as a printed article elsewhere other than as an abstract of conference presentation. Manuscripts should be submitted in triplicate on A4 paper, leaving a margin of at least 3 cm all around. Double space all typed material, including References, Tables, table titles and legends, figure legends. Use Times (12 points) font. Number all pages consecutively. Figures should be submitted on separate pages.

Manuscript should be arranged as follows.
1st page.
Title
Running title not exceeding 60 characters
Corresponding author - first name, family name, affiliation, address, phone, fax, e-mail
2nd page.
Title
Author(s)
Affiliation(s) and address(es)
E-mail of the corresponding author
Abstract
Keywords
3rd and following pages.
Introduction
Material and methods
Results

Discussion
Acknowledgements
References
Tables
Figures
Figure legends

Title should be short and informative, containing all the main key words.

Abstract. State the aim of the work, used methods and principal results. Do not exceed 600 to 1000 characters. Do not include references.

Keywords. No more than six keywords (or short phrases) characterizing the aim of the wotk should be provided. Arrange keywords alphabetically.

Introduction. Only information necessary to understand an aim of the work as well as to provide a background for performed investigations should be given here. Introduction should give an opportunity for scientists from other fields to understand the essence of the described work. Formulate the aim of the experiments at the end of the introduction.

Materials and methods or *Methods.* This section should contain all the details about performing of experimental procedures (both experimental design as well as analytical methods). The information provided must be complete enough so that results can be verified by other scientists. References to appropriate methods should be given. Include complete scientific names (genus, species, authority for the binomial, and, when appropriate, cultivar or variety etc.) for all experimental organisms. Identify the number of replications, the number of individuals, analytic replications etc. Include methods of statistical analysis. Give appropriate references on general ethic rules if necessary.

Results should be concise and objective. Use past tense. Every figure and table should be mentioned in the text.

Tables and figures should be self-explanatory without reference to text. Do not duplicate any data both in the form of tables and figures. Large bodies of primary data should not be presented.

Tables. Number tables consecutively with Arabic numerals in order of citation in the text. Provide each table with a title in a form of a complete sentence followed by a legend giving necessary explanations. Title and legend should be placed over the table. Provide a descriptive heading for each column. Avoid using large tables (more than eight columns). Place each table and its legend on a separate page. Do not use vertical lines in a table.

Figures. Number of figures should be kept to the minimum. All figures should be numbered with Arabic numerals and must be metioned sequentially in the text. Provide a caption in a form of a complete sentence followed by an explanatory legend. If a figure is composed of several parts (diagrams, graphs, pictures), label them as A, B, C etc. Place each figure on a separate A4 sheat considering reduction in printed version. Keep in mind that final dimensions of figures in the article should be no larger than 12.5 cm in width and 17 cm in height. Type size should not be less than 2 mm after reduction. For graphs prefferred symbols are closed or open circle, square, and triangle. Avoid using +, × or *. In histograms use closed, open, or striped bars. Do not use 3-D columns or different intensities of gray. Every figure should be marked with authors' names and figure number. Captions and legends should be included with the manuscript.

Style. Manuscript should be written in simple declarative sentences and must conform to accepted standards of English style and usage.

Literature citations. References should be cited in text by last names and year of publication. Cite references chronologically. When the given publication has two authors, name both authors. With

more than two authors per publication, name only a first author followed by 'et al.'. When a particular author or a group of authors has several publications for the given year, give letters 'a', 'b', 'c' etc. after the year of publication. Separate individual references by a semicolon. As an example, (Collins 1999) or (Collins, Chapper 1999) or (Collins et al. 1999) or (Collins 1999a; Collins 1999b) or (Collins 1999a; Chapper 1999b). It is possible to use also the following format 'It is important to note, that Collins (1999) already described...' As an exception, the reference to Internet may be given without including it in the list of references. Unpublished results should be cited by the name of the author only in the text, e.a., (Collins, unpublished data) or (Chapper, personal communication).

Units of measure. Temperature is expressed in degrees Celsius (°C), time in seconds (s), minutes (min), hours (h), days etc. It is appropriate to use litre (l) as a special designation for 1 dm^3. Consequently, mililitre (ml) and microlitre (µl) also can be used. In all other cases SI units must be used as much as possible. Use negative exponents to indicate units in the denominator, e.g. kg m^{-2}; m m^{-2} s^{-1}. Write out numerals one through nine, except when used with units of measure. Write out all numbers or fractions that begin a sentence, or rephrase the sentence to avoid beginning with a numeral. Use the preposition 'to' between numerals (avoid using a dash): e.g. '8 to 12 h'.

Nomenclature. In the abstract, at first mention in the text, and in *Materials and methods*, include complete biological names for all experimental organisms. Following first mentions, generic names should be abbreviated to the initial, except when confusion could arise by reference to genera with the same initial. Exceptions may be accepted in purely taxonomic papers.

Abbreviations. Use only standard scientific abbreviations accepted internationally. Abbreviations can be used if the term appears at least three times in the text. Do not use abbreviations in the abstract except if used at least three times. At first use of the term in the text or in the abstract spell it out and introduce the abbreviation parenthetically.

Discussion. Describe importance of acquired results, analysing discovered relationships in a logical sequence. References to figures and tables as well as literature sources should be given. As an exception, due to a logical sequence of performed experiments, it is possible to form a joint section *Results and discussion*.

Acknowledgements. First, provide any details on financial support received. Second, acknowledge any person you need to thank for essential help during experiments or writing your work.

References. Include only publications cited in the text. Place references in strict alphabetic order, i.e., firstly by the name of the first author, then by the name of the second author if the first author is identical for more than one reference, then by the name of the third author if the first two authors are identical, and so on. Include the names of all authors and a full title of each paper or a book. Publications by the same atuthor or the group of authors place in a chronological order. Abbreviate journal names according to ISI standards. Provide English translations for titles of all publications other than English, German, or French. The corresponding author has a full responsibility for an accuracy in citations. Citations will be edited for a format only.

The following standard form of citation should be used:

Journal articles

Enkerli J., Felix G., Boller T. 1999. The enzymatic activity of fungal xylanase is not necessary for its elicitor activity. *Plant Physiol.* 121: 391–397.

Book articles

Hammerschmidt R., Nicholson R.L. 1999. A survey of plant defense responses to pathogens. In: Agrawal A.A., Tuzun S., Bent E. (eds) *Induced Plant Defenses Against Pathogens and Herbivores*. APS Press, St. Paul, pp. 55–71.

Monographs

Fahn A. 1979. *Secretory Tissues in Plants.* Academic Press, London. 250 p.

LATVIJAS UNIVERSITĀTES RAKSTI
745. sējums, BIOLOĢIJA, 2008

Latvijas Universitātes Akadēmiskais apgāds
Baznīcas iela 5, Rīga LV-1010
Tālr. 7034535